Investigating the Formation and Utilization of Humins as a By-product of the Levulinic Acid Synthesis

Universität Hamburg

DER FORSCHUNG | DER LEHRE | DER BILDUNG

Dissertation with the aim of achieving a doctoral degree (Dr.rer.nat.)

Institute of technical and macromolecular chemistry,

Faculty of Mathematics, Informatics and Natural Sciences,

University of Hamburg

Submitted by

André Wassenberg

Hamburg, 2025

Deutsche Forschungsgemeinschaft

Biomass Catalysis Engineering

1. Evaluator: Prof. Dr.-Ing. Jakob Albert
Department of Chemistry
Institute of Technical and Macromolecular Chemistry
University of Hamburg

2. Evaluator: Prof. Dr. Wolfgang Maison
Department of Chemistry
Institute of Pharmacy
University of Hamburg

1. Examiner: Prof. Dr.-Ing. Jakob Albert
Department of Chemistry
Institute of Technical and Macromolecular Chemistry
University of Hamburg

2. Examiner: Prof. Dr. Lisa Vondung
Department of Chemistry
Inorganic and Applied Chemistry
University of Hamburg

3. Examiner: Dr. Thomas Hackl
Department of Chemistry
Scientific Service – NMR Spectroscopy
University of Hamburg

Date of Disputation: 18.07.2025

This study was conducted between October 2020 and September 2023 at the Institute of Technical and Macromolecular Chemistry of the University of Hamburg with Prof. Dr.-Ing. Jakob Albert as supervisor.

Table of Content

List of publications

Journals

- **A. Wassenberg,** T. Esser, M.J. Poller, J. Albert, Investigation of the Formation, Characterization, and Oxidative Catalytic Valorization of Humins, Materials (Basel, Switzerland) *16* (**2023**) 2864.

- **T. Esser**, A. Wassenberg, J.-C. Raabe, D. Voß, J. Albert, Catalytic Valorization of Humins by Selective Oxidation Using Transition-Metal-Substituted Keggin-Type Polyoxometalate Catalysts, ACS Sustainable Chemistry & Engineering *12* (**2024**) 543–560.

- **T. Esser**, A. Wassenberg, D. Voß, J. Albert, Selective catalytic oxidation of humins to carboxylic acids using the H4[PVMo11O40] Keggin-type polyoxometalate enhanced by alcohol doping and solubilizer, Reaction Chemistry & Engineering *9* (**2024**) 1666–1684.

- **A. Wassenberg,** T. Esser, M.J. Poller, D. Voß, J. Albert, Humin-free synthesis of levulinic acid from fructose using heteropolyacid catalysts, Biofuels, Bioproducts and Biorefining *18* (**2024**) 1585–1597.

- **T. Esser**, A. Wassenberg, D. Voß, J. Albert, Novel insights into the recovery and recyclability of homogeneous polyoxometalate catalysts applying an efficient nanofiltration process for the selective catalytic oxidation of humins, Chemical Engineering Research and Design *209* (**2024**) 311–322.

- **A. Wassenberg,** T. Esser, M.J. Poller, D. Voß, J. Albert, Valorization of Humins by Cyclic Levulinic Acid Production Using Polyoxometalates and Formic Acid, ChemSusChem (**2025**) e202401973.

Conferences

- **Wassenberg,** T. Esser, M.J. Poller, J. Albert, Valorization of waste materials resulting from the chemical conversion of biomass using tailormade polyoxometalate catalysts,
  15_{th} European Congress on Catalysis **2023**, Prague/ Czech Republic

List of abbreviations

5-HMF	5-Hydroxymethylfurfural
AA	Acetic acid
ANOVA	Analysis of variance
Approx.	Approximately
ATR	Attenuated total reflection
Ca.	Circa
C(fructose)	Fructose concentration
CO_2	Carbon dioxide
DoE	Design of Experiment
DHH	2,5-Dioxo-6-hydroxyhexanal
DMSO	Dimethyl sulfoxide
EA	Elemental analysis
FA	Formic acid
FT	Fourier transformed
gAI	Generative artificial intelligence
gKI	Generative Künstliche Intelligenz
GVL	γ-Valero lactone
H_2SO_4	Sulfuric acid
HPA	Heteropoly acid
HPAx	Vanadium substituted phosphomolybdic acid
HPW	Phosphotungstic acid ($H_3[PW_{12}O_{40}]$)
HPMo	Phosphomolybdic acid ($H_3[PMo_{12}O_{40}]$)
HPA-1	Mono vanadium substituted phosphomolybdic acid ($H_4[PVMo_{11}O_{40}]$)
HPA-2	Di vanadium substituted phosphomolybdic acid ($H_5[PV_2Mo_{10}O_{40}]$)
HPA-5	Penta vanadium substituted phosphomolybdic acid ($H_8[PV_5Mo_7O_{40}]$)
HPLC	High pressure liquid chromatography
HSiW	Silicotungstic acid ($H_3[SiW_{12}O_{40}]$)
i.e.	for example
IR	Infrared
IPA	Isopoly acid
HTC	Hydrothermal carbon
LA	Levulinic acid
MALDI-TOF	Matrix assisted laser desorption/ionization – time of flight
NMR	Nucelar magnetic resonance
OFAT	One factor-at-a-time
Ox	Oxidation
PFA	Polyfurfurylalcohol
POM	Polyoxometalate
PTFE	Polytetrafluoroethylene
pTSA	*para*-Toluene sulfonic acid
Red	Reduction

RedOx	Reduction and oxidation
SCO	Selective catalytic oxidation
Sub	Substrate
SF	Structural fragment
T	Reaction temperature
t	Reaction time
THF	Tetrahydrofuran
Wt%(acetone)	Weight percentage of acetone in solution

1. Zusammenfassung

Der Ersatz fossiler Rohstoffe ist für die chemische Industrie von großem Interesse. Die Synthese von Plattformchemikalien aus Biomasse ermöglicht die Herstellung industriell relevanter Chemikalien unter Vermeidung fossiler Rohstoffquellen. Eine der wichtigsten Plattformchemikalien ist Lävulinsäure (LA), welche industriell bislang mit dem *Biofine Prozess*, über eine saure Umsetzung mit Schwefelsäure hergestellt wird. Dieser Prozess verwendet jedoch umwelt- und reaktorschadende Katalysatoren und produziert größere Mengen Humin als Nebenprodukt. Die Entstehung dieser Feststoffe sorgt für eine starke Verringerung der Herstellungseffizienz der begehrten Plattformchemikalie, vor allem da die Weiterverwertung der Humine aufgrund deren unlöslicher Natur und unbekannter Struktur erschwert ist. Eine genauere Untersuchung und Optimierung der LA Synthese, auch hinsichtlich Entstehung, Struktur und Weiterverwertung der produzierten Humine, kann für eine effizientere und umweltfreundlicher Herstellung der Plattformchemikalie sorgen.

Zunächst wurden hierfür der Bildungsprozess und die Struktur der Humine genauer untersucht. Es wurden dafür 28 verschiedene Humine unter Variation des umgesetzten Biomasse Substrates (Fruktose, Glukose, Xylose, Saccharose), des eingesetzten Lösungsmittels (Wasser, 1:1 Mischung aus Wasser/Ethanol, 1:1 Mischung aus Wasser/ Dimethylsulfoxid (DMSO)) und des verwendeten sauren Katalysators (Schwefelsäure, *Para*-Toulolsulfonsäure (pTSA), Essigsäure (AA)) hergestellt. Die Feststoffanalytik der Humine deutete auf eine primär Furan-Ring basierte Struktur hin, die aus der Polymerisation von 5-Hydroxymethylfurfural (5-HMF) oder Furfural mit sich selbst, anderen Intermediaten in der Reaktionslösung und auch den organischen Lösungsmitteln, resultierte. Darüber hinaus konnten auch drei wiederkehrende Fragmente der größeren Huminstruktur identifiziert werden. Die hergestellten Humine wurden im Anschluss über selektive katalytische Oxidation (SCO) mit dem Polyoxometallat $H_8[PV_5Mo_7O_{40}]$ (HPA-5) zu niedermolekularen Carbonsäuren umgesetzt, um die Verwertbarkeit der produzierten Huminstrukturen zu überprüfen. Als Hauptprodukte wurden hierbei CO_2, Ameisensäure (FA) und AA erhalten. Der größte Einfluss wurde im Allgemeinen von der Wahl des Lösungsmittels ausgeübt. Die Verwendung der ethanolischen Lösung sorgte hier für eine verringerte Huminausbeute, wobei die niedrigste Ausbeute ca. 5 wt% betrug. Diese Humine konnten auch am besten über SCO umgesetzt werden, wobei Umsätze von bis zu 65 % erreicht wurden. Ein Vergleich der Feststoffanalytik vor und nach der SCO wies auf eine bevorzugte Umsetzung aliphatischer Ether- und Esterbindungen hin. Die Kombination aus AA als Katalysator und der Wasser/Ethanol Lösung produzierte die niedrigste Huminausbeute von ca. 5 wt% Kohlenstoff, wobei das Humin auch den höchsten Umsatz bei der Oxidation von 65 % erreichte, und besitzt somit ein großes Potential für die Herstellung von LA unter Vermeidung der Huminproduktion.

Anschließend wurde sich mit der Optimierung der LA Synthese beschäftigt. Hierbei wurde zunächst eine Alternative zu der herkömmlich verwendeten Schwefelsäure gesucht. Bei dem Vergleich von fünf verschiedenen Säure-Katalysatoren (Schwefelsäure, AA, $H_3[PMo_{12}O_{40}]$ (HPMo), $H_3[PW_{12}O_{40}]$ (HPW), $H_3[SiW_{12}O_{40}]$ (HSiW)) in einer Umsetzung von Fruktose wurde mit dem Polyoxometallat HSiW die höchste LA Ausbeute von ca. 61 mol% erreicht. Unter Verwendung von HSiW als saurem Katalysator wurde dann eine Optimierung der Reaktionsbedingungen der LA Synthese mittels eines Design of Experiments (DoE) (verwendete Parameter: Temperatur (T), Zeit (t), Anteil des organischen Lösungsmittels Aceton (wt%(acetone)), Substratkonzentration (c(fructose)) hinsichtlich minimaler Huminausbeute und maximaler LA Ausbeute durchgeführt, wofür ein Box-Behnken Design verwendet

wurde. Hier hing die Huminausbeute primär von der Lösungsmittelzusammensetzung und der Temperatur ab, während die LA Ausbeute primär von der Lösungsmittelzusammensetzung und der Substratkonzentration beeinflusst wurde. Im Rahmen der eingesetzten Parameter (T = 140-180 °C, t = 1-5 h, wt%(acetone) = 0-80 %, c(fructose) = 0,1-0,4 mol*L^{-1}) konnte durch Interpolation der Messergebnisse bestimmt werden, dass hohe Huminausbeuten (über 40 wt%) durch Maximierung aller verwendeten Parameter erreicht werden. Hohe LA Ausbeuten (über 60 mol%) wurden hingegen durch Maximierung von entweder Temperatur oder Zeit bei Minimierung der restlichen drei Parameter erreicht. Drei Parameterkombination wurden bestimmt, die sich auf unterschiedliche Optimierungsaspekte fokussierten. Der industriell relevanteste Parametersatz wurde anschließend erfolgreich auf eine Umsetzung der Kohlenhydrate Glukose, Xylose, Saccharose und Cellobiose angewendet, um die die Übertragbarkeit der Ergebnisse erfolgreich zu bestätigen.

Abschließend wurde, auf Basis der gesammelten Erkenntnisse, eine zyklische LA Synthese konzeptioniert, bei der FA als Katalysator für die Herstellung von LA verwendet wird und im Anschluss durch SCO das, als Nebenprodukt entstandene, Humin zurückgewonnen wird. Zunächst wurde hierfür einer der zuvor optimierten Parametersätze (T = 180 °C, t = 1 h, wt%(acetone) = 0 %, c(fructose) = 0,1 mol*L^{-1}) in einem zweistufigen Prozess für die Verwendung von FA in einem größeren Reaktionssystem angepasst. Unter Verwendung der modifizierten Reaktionsbedingungen wurde eine Huminfraktion gebildet, die anschließend in einer SCO umgesetzt wurde. Hierbei wurden optimierte Bedingungen verwendet, die mit $H_5[PV_2Mo_{10}O_{40}]$ (HPA-2) als Katalysator unter der Verwendung von Methanol, als Additiv zur Unterdrückung der CO_2 Bildung, eine hohe Ausbeute an FA (ca. 28 carbon wt%) als Hauptprodukt herstellte. Der Katalysator der SCO konnte außerdem im Anschluss über Membranfiltration abgetrennt und recycelt werden. Darauffolgend wurde die hergestellte FA über Destillation abgetrennt und aufkonzentriert, wobei eine Lösung bestehend aus 87.00 wt% Wasser, 11.65 wt% FA, 0.73 Bernsteinsäure, 0.49 wt% AA und 0.13 wt% Methylacetat erhalten wurde. Eine Reaktionslösung, deren Zusammensetzung der erhaltenen FA-Fraktion glich, konnte jedoch erfolgreich für eine erneute LA Synthese verwendet werden, wobei die zusätzlichen Produktreste keinen sichtbaren Einfluss auf die Struktur des hergestellten Humins hatten. Somit wurde der Zyklus erfolgreich geschlossen und die Grundlage für eine umweltfreundlichere und effizientere Synthese von LA geschaffen.

2. Abstract

The replacement of fossil raw materials is of great interest to the chemical industry. For this purpose, the synthesis of platform chemicals from biomass enables the production of industrially relevant chemicals while avoiding fossil raw material sources. One of the most important platform chemicals is levulinic acid (LA), which has so far been produced industrially using the *Biofine process* via an acidic reaction using sulfuric acid. However, this process uses catalysts that are harmful to the environment, as well as reactors and produces larger amounts of humins as a byproduct. The formation of these solids causes a significant reduction in the manufacturing efficiency of the sought-after platform chemical, especially as the further utilization of these humins is difficult due to their insoluble nature and unknown structure. A more detailed investigation and optimization of the LA synthesis, also regarding the formation, structure and further utilization of the humins produced, can ensure a more efficient and environmentally friendly production of the platform chemical.

First, the formation process and structure of the humins was examined in more detail. 28 different humins were produced through a variation of the converted biomass substrate (fructose, glucose, xylose, sucrose), the used solvent (water, 1:1 mixture of water/ethanol, 1:1 mixture of water/dimethyl sulfoxide (DMSO)) and the used acidic catalyst (sulfuric acid, *para*-toluene sulfonic acid (pTSA), acetic acid (AA)). The solid analysis of the humins indicated a primarily furan ring-based structure, which resulted from the polymerization of 5-hydroxymethylfurfural (5-HMF) or furfural with themselves, other intermediates in the reaction solution and also the organic solvents. In addition, three recurring fragments of the larger humin structure were also identified. The humins produced were then converted via selective catalytic oxidation (SCO) with the polyoxometalate $H_8[PV_5Mo_7O_{40}]$ (HPA-5) to form low-molecular carboxylic acids in order to determine the viability of the produced humin structures for further valorization. The main products obtained from the SCO were CO_2, formic acid (FA) and AA. In general, the greatest influence was exerted by the choice of solvent. The substrate conversion in the ethanolic solution resulted in a reduced humin yield, with a minimum humin yield of about 5 wt%. These humins also showed the best conversion rates via SCO, reaching conversion rates of up to 65 %. A comparison of solids analysis before and after SCO indicated a preferred conversion of aliphatic ether and ester bonds. The combination of AA as a catalyst and the water/ethanol solution produced the lowest humin yield of about 5 wt%, with the produced humin, while also possessing the best conversion rate of 65 %, and therefore shows great potential for the efficient production of LA.

The optimization of the LA synthesis was then addressed. The first step was to find an alternative to the conventionally used sulfuric acid. When comparing five different acidic catalysts (sulfuric acid, FA, $H_3[PMo_{12}O_{40}]$ (HPMo), $H_3[PW_{12}O_{40}]$ (HPW), $H_3[SiW_{12}O_{40}]$ (HSiW)) in an acidic conversion of fructose, the highest LA yield of about 61 mol% was achieved using the polyoxometalate HSiW. Using HSiW as an acidic catalyst, an optimization of the reaction conditions of the LA synthesis was then carried out via a design of experiment (DoE) reaction plan using a Box-Behnken design (used parameters: reaction temperature (T), reaction time (t), proportion of the organic solvent acetone (wt%(acetone)), substrate concentration (c(fructose)), which aimed at a minimized humin yield and a maximized LA yield. Here, the humin yield depended primarily on the solvent composition and temperature, while the LA yield was primarily influenced by the solvent composition and the substrate concentration. Within the parameters used (T = 140-180 °C, t = 1-5 h, wt%(acetone) = 0-80 %, c(fructose) = 0.1-

0.4 mol*L-1), it was determined by interpolation of the synthesis results that high humin yields (over 40 wt%) were achieved by maximizing all parameters used. High LA yields (over 60 mol%), however, were achieved by maximizing either temperature or time while minimizing the remaining three parameters. Three parameter combinations were determined that focused on different optimization aspects. The most industrially relevant set of parameters was then successfully applied to conversions of the carbohydrates glucose, xylose, sucrose and cellobiose in order to successfully confirm the transferability of the results.

Finally, based on the knowledge gained so far, a cyclic LA synthesis was designed in which FA is used as a catalyst for the production of LA and is then recovered via SCO from the humins formed as a by-product. First, one of the previously optimized parameter sets (T = 180 °C, t = 1 h, wt%(acetone) = 0 %, c(fructose) = 0,1 mol*L^{-1}) was adapted in a two-stage process for the usage of FA instead of HSiW in a larger reactor system. Using the modified reaction conditions, a humin fraction was formed, which was subsequently converted using SCO. Optimized conditions, using $H_5[PV_2Mo_{10}O_{40}]$ (HPA-2) as a catalyst with the addition of methanol to suppress CO_2 formation, were used here, producing a high yield of FA (about 28 carbon wt%) as the main product. The SCO catalyst could afterwards be separated and recycled using membrane filtration. The FA produced was then separated and concentrated by distillation, resulting in solution containing 87.00 wt % water, 11.65 wt% FA, 0.73 wt% succinic acid, 0.49 wt% AA and 0.13 wt% methyl acetate. However, a reaction solution whose composition was similar to the FA fraction obtained could be successfully used for a new LA synthesis, whereby the additional product residues had no visible influence on the structure of the humin produced. The cycle was thus successfully closed and the basis for a more environmentally friendly and efficient synthesis of LA was created.

3. Introduction

Fossil raw materials are of great importance in modern society, with coal, crude oil and natural gas being important sources of energy, fuels, as well as chemicals. However, fossil raw materials are non-regenerative, which results in an ever-increasing scarcity. In addition, prices and the environmental damage associated with the use of these raw materials continue to rise. Renewable resources such as wind energy, photovoltaic and biomass provide an alternative to fossil raw materials, with biomass being of particular importance for the chemical industry, as it is the only renewable source of carbon of sufficient abundance to replace fossil fuels. Furthermore, biomass is almost carbon neutral and available in large quantities. [1–8]

In 2004 a list of twelve sugar derived building block chemicals was created on behalf of the *U.S. Department of Energy* by *Werpy et al.* [9]. These compounds were intended to play a key role in the sustainable production of chemicals from biomass. Out of these twelve compounds, LA was determined to be one of the most impactful ones, due to its availability from pentoses and hexoses, as well as its high reactivity. LA can be transformed into a wide variety of other chemicals that can be applied for example as biofuels [10,11], green solvents [12] or as biobased components for the synthesis of different polyesters [13,14]. It is mainly produced through the *Biofine process* [15], in which primarily lignocellulosic biomass is converted to LA and other value chemicals such as furfural, through acid catalyzed hydrolysis using sulfuric acid. [9,15]

There are a number of challenges attached to the production of platform chemicals like LA from renewable basic materials. On the one hand, the choice of acidic catalyst is as of now suboptimal. The commonly used sulfuric acid is highly corrosive and therefore damages the reactor systems and pipings. In addition, mineral acids are generally difficult to separate from the products and not good for the environment. Several research groups have therefore tried to find suitable alternatives, with both homogeneous [16,17] and heterogenous catalysts [18–21] being applied with varying degrees of success, but to no industrial application as of yet. [22]

The creation of unwanted by-products, on the other hand, also poses a major challenge. The conversion of biomass can lead to the formation of black solids. These solids are called humins and cause major problems in industrial processes, as they are insoluble in conventional solvents and tend to clog catalysts and reactors. In addition, they represent a loss of yield. Research has shown that the formation of humins can be inhibited through methods such as the usage of organic solvents [23] or lower reaction temperatures [24]. A full suppression of their formation is however still not possible. [22,25,26]

Another point of research for increasing the profitability of LA production is the valorization of the humin by-products. Some promising results were achieved here, such as the successful production of synthesis gas [27] or the removal of antimony from waste water using humins [28]. Another possibility for humin valorization is the oxidation of the solid by-product under *OxFA* [29] conditions. Here, polyoxometalate (POM) catalysts are used to split humins with molecular oxygen into FA and other low molecular weight carboxylic acids. [30]

However, a major obstacle in the utilization of humins remains the yet unknown exact structure of the humins. Several research groups have already made big strides in trying to uncover the exact structure of humins [23,24,31–34]. It is therefore assumed that humins are made up of compounds

such as 5-HMF and 2,5-dioxo-6-hydroxy-hexanal as well as other intermediates, which are formed during the hydrolysis of sugars and their derivatives. These intermediates are assumed to polymerize by reactions such as ester- and etherification as well as aldol condensation. However, a perfect elucidation of the structure of these unwanted by-products is not yet possible but would greatly simplify their potential avoidance and industrial use, thus improving the production of the much sought-after LA. [25]

Two primary goals were pursued while working on this dissertation. One of these goals was the optimization of the process of LA synthesis. Here, the process of synthesizing LA from carbohydrates was optimized to achieve the highest possible LA yield while suppressing the formation of humins. Particular attention was paid here to the use of sustainable and environmentally friendly reaction ingredients. The other goal consisted out of an in-depth examination of humins. Here, the influences of the reaction conditions on the formation of humins, as well as the structure of the humins formed, were investigated. In addition, the valorization of humins under OxFA conditions was also investigated. Combined, the achieved results could help to make industrial synthesis more efficient and thus take an important step towards a more sustainable and environmentally friendly chemical industry.

In the theoretical part of the dissertation presented here, the different types of biomass that can be used as renewable raw materials are first presented. This is followed by an overview of the properties, applications and synthesis of LA. After this humins are introduced as the by-product of LA synthesis, including their suspected formation and research regarding their avoidance and valorization. Subsequently, the POMs, which are used in valorization methods of humins, are presented, including their properties, chemistry and applications. Lastly the *OxFA process*, which serves as the base for the humin valorization achieved during this thesis is discussed, including its applications for the conversion of humins into carbonic acids. The next chapter deals with the materials and methods used. First presented are the chemicals utilized during the presented research. This is followed by an explanation of the setup of the reactor systems, including the applied experimental procedures. Finally, there is a description of the used analytical methods, and a presentation of the calculation methods applied on the analytic results. This is followed by the cumulative and thus the main part of the dissertation. The paper, which forms the basis of the first subchapter, deals with the investigation of the influence of qualitative reaction conditions on the structure and yield of the humins during the conversion of carbohydrates to LA. In addition, the convertibility of the produced humins using POM catalysts was tested. In the second subchapter, the synthesis of LA from carbohydrates was examined for the influence of quantitative reaction parameters. This included an optimization of the reaction with regard to maximizing LA yield and minimizing humin yield using a DoE approach. The last subchapter of the cumulative part deals with the combination of the results previously obtained in the prior two subchapters to assemble a cyclic LA synthesis process, which uses the carbonic acids generated by the humin conversion for the production of more LA.

4. Theoretical background

In this chapter of the here presented dissertation, the theoretical foundations on which the publications are based are first explained. Chapter 4.1 contains the general definition of biomass and the most important plant-derived types of biomass are presented. In addition, various methods are discussed to make lignocellulosic biomass industrially processable. Chapter 4.2 deals with LA and discusses its properties, synthesis methods and uses. Additionally, the *Biofine process* [15] which is used for the commercial production of LA is explained. Humins, the byproducts of LA synthesis, are presented in Chapter 4.3. Here, particular attention is paid to the previous research concerning the elucidation of structure and mechanism of formation of said humins. In addition, previously researched strategies to avoid the formation of humins and valorization possibilities of these by-products are discussed. Chapter 4.4 deals with POMs, which were used in this work as alternative acid catalysts for the synthesis of LA and as oxidative catalysts for the valorization of humins. The properties and most common structural representatives of this class of materials are discussed here. In addition, the catalytic behavior of the structure type used in this work is explained. Chapter 4.5 is about the *OxFA process* [29], under which reaction conditions the valorization of humins was carried out. The original process for the conversion of biomass is explained, including its origins, and an overview of previous applications for the oxidative conversion of humins is given. In the final section of the theoretical background, Chapter 4.6, statistical experimental design is explained within the framework of a DoE, which was used to optimize LA synthesis. Several types of DoE are introduced, including the Box-Behnken design applied for the optimization of LA and humin yield, as well as important principles that were used in the evaluation of the collected measurement data.

4.1 Biomass: A renewable source of carbon

There are several natural sources of energy available on earth that humanity can harness. Unlike wind or hydropower, solar radiation holds a unique position as it can be transformed into organic substances, commonly known as biomass. The definition of biomass encompasses all organic (i.e. carbon-containing) substances, which includes all living plants and animals as well as their residues (excrements), non-fossilized remains and all substances produced through technical conversion or material use. [7]

Biomass can be further divided into primary, secondary and tertiary biomass. Primary biomass is created directly from the photosynthetic use of solar energy, therefore including all plants and plant residues from the agricultural sector. Secondary biomass is formed indirectly from solar energy through the breakdown or conversion of organic substances into higher organisms such as animals. All zoomass and animal residues fall under this category. The third and final category of biomass includes all products made from primary or secondary biomass by technical processing, such as chocolate and paper. [7]

Primary or plant-based biomass represents the majority of available natural biomass on earth; around 80 % of the organic carbon is bound in plants, whereas secondary or animal biomass only contribute about 0.4 % to the total organic carbon mass. The remaining organic carbon is mostly found in bacteria and fungi. Plant biomass is classified as a renewable resource as it is continually produced through photosynthesis from the carbon dioxide in the atmosphere (*Figure 1*) resulting in an almost infinite supply of organic material. [1,35]

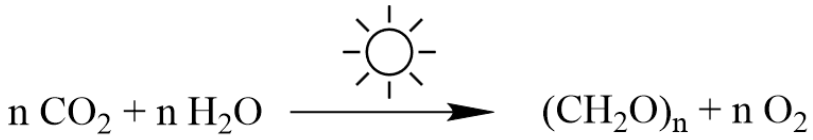

Figure 1: *General photosynthesis reaction in plants. [1]*

An important advantage that plant-based biomass possesses as a raw material is its CO_2 neutrality. The carbon released during the utilization of the biomass was previously taken from the atmosphere for photosynthesis and therefore does not promote the greenhouse effect, in contrast to the utilization of fossil raw materials such as oil or coal, which releases carbon that was "stored" in the ground for millions of years back into the atmosphere. However, the energy used to produce biomass is still largely obtained from fossil materials, resulting in the usage of biomass not yet being completely climate neutral. [1,4,7]

Plant-based biomass can be even further divided into primary and secondary plant substances. Primary substances are essential for the structure and reproductive capabilities of plants, such as triglycerides and carbohydrates. They make up the majority of the substances contained in plants. Secondary plant substances can often only be found in trace amounts in plants. They are mostly used for the pursuit of specific strategies such as the attraction of pollinators. Examples for secondary plant substances are terpenoids or dyes. [1] The more important types of plant-derived biomass are explained in more detail below.

4.1.1 Triglycerides

Triglycerides are the main component of fats and oils. They are tri-esters consisting out of one glycerol and three fatty acids, with the three fatty acids either possessing the same or different structures. Fatty acids are longer-chain carboxylic acids that are either completely aliphatic or contain additional functional groups, with the carbon chain length generally being between 8 and 22 in naturally occurring fatty acids. [1]

Triglycerides can be derived from both, animal and plant sources. The primary distinction between these sources is that animal-derived triglycerides predominantly contain saturated fatty acids, whereas plant-derived triglycerides are primarily composed of unsaturated fatty acids. Significant plant sources of triglycerides include coconut oil, palm oil, soybean oil, and rapeseed oil. For industrial applications, triglycerides are generally split into their constituent components through processes such as transesterification or hydrolysis, as illustrated in *Figure 2*. The split-up of triglycerides results in products such as fatty acids, fatty methyl esters, fatty alcohols, and glycerol. [1,36] These derivatives have wide-ranging applications, including biofuels [37], surfactants [38], cosmetics [39], and the production of materials like polyurethanes [40].

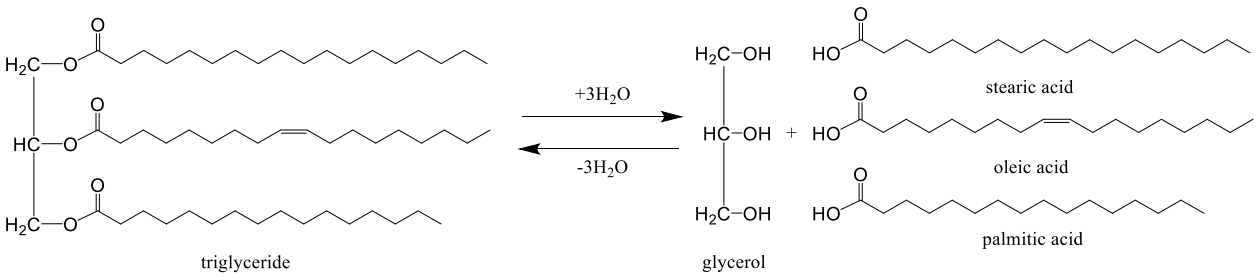

Figure 2: *Hydrolytic fat splitting of a triglyceride, adapted from Behr. [1]*

4.1.2 Carbohydrates

Carbohydrates are the primary constituents of plant cell walls. The term "carbohydrates" originated in the 19th century from the mistaken belief that these compounds were composed solely of carbon and water, with the molecular formula $C_n(H_2O)_n$. However, it is now understood that carbohydrates can also contain elements such as nitrogen and sulfur, although the term "carbohydrates" continues to be used for these compounds. [1]

Carbohydrates can be divided into the lower molecular sugars and the higher molecular polysaccharides, whereby the sugars can be further divided into oligo- and monosaccharides. Monosaccharides are aliphatic carbons with a chain length of C_3 to C_6 that also contain several hydroxyl groups. Furthermore, monosaccharides also possess either a keto or an aldehyde group with them accordingly being classified as ketoses or aldoses. The most important monosaccharides are the hexoses glucose and fructose, with glucose being an aldose and fructose being a ketose (*Figure 3*). Every saccharide possesses at least one chiral carbon atom, resulting in different enantiomeric forms of saccharides. Depending on the configuration of the chiral carbon which is furthest away from the C=O group, these are divided into *D*- or *L*-form. Carbohydrates are also able to form cyclic hemiketal and hemiacetal structures through intermolecular reactions of the keto or aldehyde groups. [1]

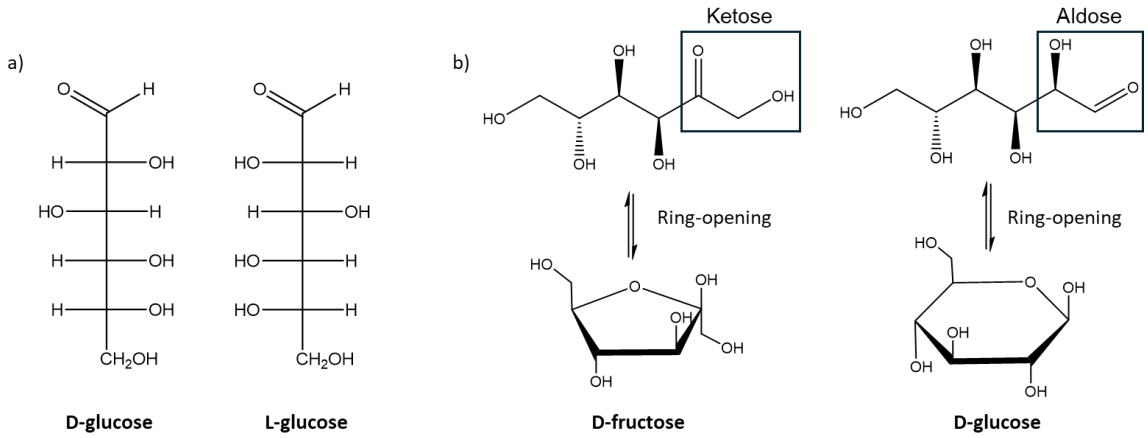

Figure 3: *Structural configuration of monosaccharides. [1] a) D-glucose and L-glucose as enantiomeric forms of hexoses; b) Hemiketal and hemiacetal forms of aldoses and hexoses exemplified by glucose and fructose.*

Monosaccharides can undergo a variety of reactions that are of industrial interest, including fermentation to lactic acid, which is essential for the production of biocompatible plastics, or gluconic acid, which is used in pharmaceuticals. Of particular importance are the dehydration reactions in

which platform chemicals such as LA or 5-HMF can be obtained from hexoses. Longer-chain oligo and polysaccharides are formed through intermolecular reactions of two or more monosaccharides. [1,7]

Oligosaccharides are saccharides made up of two to seven monosaccharide units, with the most important oligosaccharide being sucrose, which is a dimer of fructose and glucose. Polysaccharides are made up of eight or more monosaccharides. Two important polysaccharides are cellulose and starch, which are both glucose polymers with the only difference being the type of bonds between the monomers. Both possess important functions in plants, with cellulose providing stability and starch being the main energy storage of plants. Oligo and polysaccharides can be split into their constituent monosaccharides by hydrolysis. Applications of the longer-chain saccharides without prior splitting include the production of paper and hydrogels for medical uses. [1,7,41]

4.1.3 Lignocellulosic biomass

Lignocellulose makes up the main component of organic biomass. It can be derived from non-food sources such as wood or agricultural residues like corn straw and sugarcane bagasse. Lignocellulose typically consists of 40-50 % cellulose, 20-30 % hemicellulose and 10-25 % lignin, which are intermeshed and chemically bound to each other through non-covalent forces and covalent cross-linkages. The exact composition is dependent on the source. Structural examples of the three main constituents of lignocellulosic biomass can be seen in *Figure 4*. [1,7,22,42–44]

Cellulose (*Figure 4a*) the main component of lignocellulosic biomass, is a homopolymer of 1,4-glycosidically bound ring-shaped *D*-glucose in linear chains, which exist in helical formations due to their tendency to form inter- and intra-molecular hydrogen bonds. It is insoluble in water and most organic solvents. Cellulose chains possess amorphous as well as crystalline segments. Several cellulose chains together can spontaneously form microfibrils. The quasi-crystalline structure of cellulose grants the cell walls their specific stability. [1,7,45]

Hemicellulose (*Figure 4b*) is an amorphous heteropolymer which crosslinks lignin and cellulose together in the plant cell walls. It is linked to cellulose via hydrogen bonds and *van der Waals* forces. The structure and content of hemicellulose vary depending on the source, with sugars such as xylose, mannose, galactose and arabinose being its main components. Frequently occurring structures include xylan backbone chains, which are predominantly composed of xylopyranose units linked by 1,4-glycosidic bonds and often adorned with side chains formed by other saccharides. These structures are, for example, key components of softwood hemicellulose. Hemicellulose plays a crucial role in plant cells by supporting the cell wall and regulating the permeability as well as cementing of the cell membrane. [1,7,22,44,46]

Lignin is a long-chain, heterogeneous polymer which mostly consists of the phenylpropanoids *p*-coumaryl alcohol, coniferyl alcohol and sinapyl alcohol (*Figure 4c*), which are connected to each other through different binding types such as ether- or aryl-bonds and form a three-dimensional rigid network. The exact structure of lignin is undefined and can differ significantly in different parts of the same plant. It is possible, however, to characterize the lignin of certain plants by the frequency of occurrence of binding types and monolignols. In plants, lignin has several uses, including the reduction of water permeation through the cell, by using its hydrophobic character or the inhibition of the growth of microorganisms. Lignin also ensures the mechanical strength of the cell walls. [1,7,22,43,47]

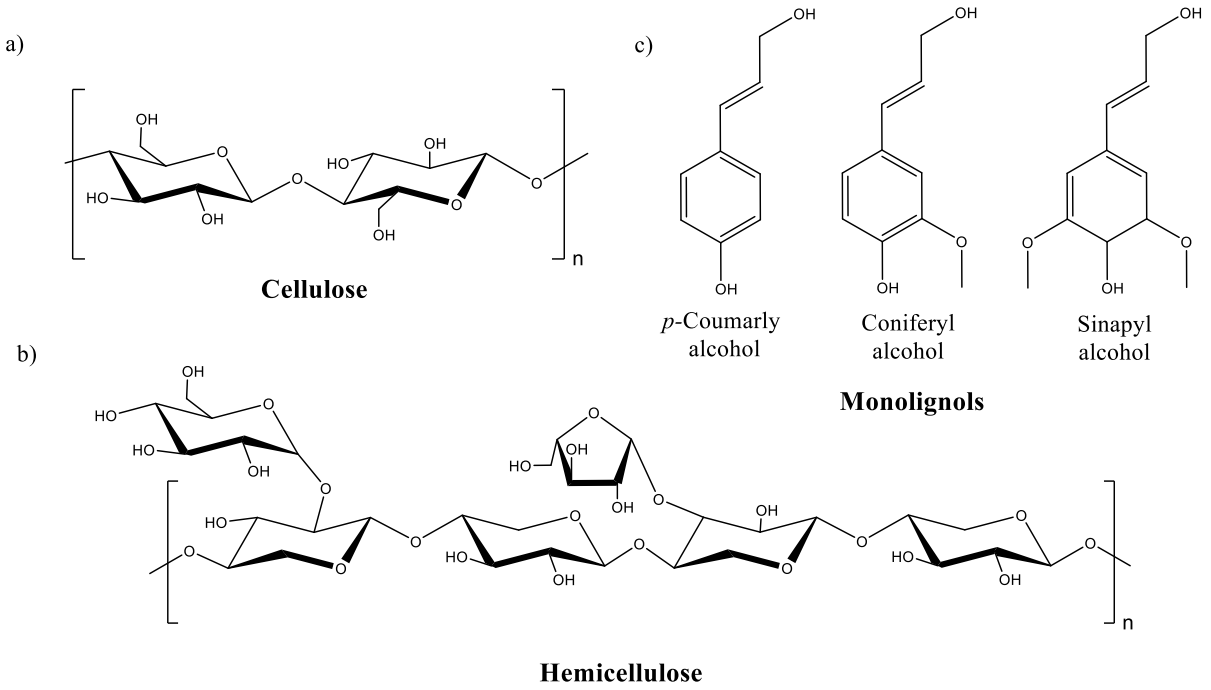

Figure 4: *Example structures of the three main constituents of lignocellulosic biomass, adapted from Ning et al.. [43] a) Cellulose. b) Cutout of a hemicellulose segment made up from a xylan back bone and D-glucose as well as L-arabinose side chains. c) Structures of the three monolignols typically found in lignin which are bound to each other through ether bonds and other types of bonds.*

The utilization of lignocellulosic biomass is hampered by its inherent recalcitrance. Pretreatments can be used to divide the chemically resistant parts of the lignocellulose and thus make them more accessible for further valorization processes. The known pretreatment methods can be divided into four categories: physical, chemical, physicochemical, and biological pretreatments. [22,48]

During physical pretreatments, the particle size of the lignocellulosic material is significantly reduced by disrupting its structure. This can be achieved through various methods: applying force through milling and grinding (mechanical pretreatment), heating (microwave pretreatment), or utilizing shear forces generated by cavitation (ultrasound pretreatment). This reduces the degree of polymerization and the crystallinity of the biomass. Physical pretreatments are particularly efficient in removing lignin from the cell walls and generate little to no toxins. One problem with these processes, however, is their high energy consumption. [22,48]

In chemical pretreatments, the structure of the biomass is dissolved by treatment with different chemicals such as acids (acid hydrolysis pretreatment), bases (alkaline hydrolysis pretreatment), organic solvents (organosolv pretreatment) and ionic liquids (ionic liquid pretreatment), with acids and bases being the most frequently used. The lignocellulosic biomass is divided through chemical reactions such as hydrolysis or saponification, which separate the components of the lignocellulosic biomass from each other and thus make them easier to process. Additionally, depending on the method employed, partial fragments of the lignocellulosic biomass are solubilized. This solubilization can facilitate an efficient fractionation of lignin, as seen with organosolv treatments. One problem of the chemical pretreatments is the usage of toxic chemicals in some of the processes, such as sulfuric acid in acid hydrolysis pretreatment. In addition, expensive solvents are often used for methods such as organosolv and ionic liquids, which necessitate their recovery from the reaction solution. [22]

In physicochemical pretreatments, the lignocellulosic biomass is processed with a combination of chemicals such as acids, bases or water and physical processes such as applications of high temperatures or pressures. This leads to an expansion of the surface area of the lignocellulosic biomass and its partial to complete hydrolysis. During the steam explosion pretreatment, for example, the hemicellulose fraction is hydrolyzed using condensed steam under high pressures (20-50 bar) and temperatures (150-250 °C) in the first step. This is followed by rapid decompression in a second step, which allows the condensed liquid to evaporate again and thus mechanically breaks up the lignocellulosic material. Other physicochemical pretreatments, such as the liquid hot water pretreatment, may employ more moderate reaction conditions (130 °C). Most pretreatment methods fall under the category of physicochemical pretreatments, with steam explosion, liquid hot water, ammonia fiber expansion and supercritical CO_2-explosion pretreatments being the main processes. These methods, however, often require expensive reaction setups. [22]

Biological pretreatments use microorganisms that produce enzymes which solubilize lignin and separate it from the biomass, resulting in the cellulose structures being made more accessible. The so-called ligninolytic enzymatic system depolymerizes the lignin through oxidative cleavage, while the hydrolytic enzymatic system breaks down cellulose and hemicellulose. An advantage of biochemical pretreatments is their low energy costs. However, these pre-treatments are very time-consuming, sometimes requiring residence times of months, which affects their industrial usability. [22]

4.2 Levulinic acid: A promising platform chemical

4.2.1 Characteristics and usage of levulinic acid

LA is a γ-ketoacid with the molecular formula of $CH_3COCH_2CH_2COOH$ (*Figure 5*). It is soluble in water, alcohols, esters, ethers as well and ketones. The keto and carboxyl group of LA are highly reactive, granting access to a wide variety of substances through chemical conversions, the position of the two functional groups even enabling intramolecular ring formation. [15,22,49]

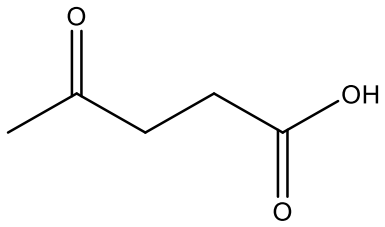

Figure 5: *Structural formula of LA.*

The first documented syntheses for LA were carried out by *Malaguti* [50] and *Mulder* [51] at the beginning of the 19th century. Both carried out reactions in which carbohydrates were converted in acidic aqueous solutions, although LA was not identified as a product in more detail. A precise characterization and naming of the substance occurred later towards the end of the 19th century by *Grote et al.* [52,53]. The potential use of LA as a basic building block for the production of other chemicals was described by *Leonard* [54] in 1956, who highlighted the high reactivity of LA and its ability to be obtained from cellulosic biomass. In 2004, *Werpy* and *Peterson* [9] came to a similar conclusion when they, on behalf of the *US Department of Energy*, compiled a list of the top twelve building block chemicals available from sugars (*Figure 6*), with the list containing substances such as maleic acid, succinic acid, and LA. While doing so, they remarked on LA possessing the potential to become a very important building in the biorefinery, citing the availability of LA from most hexoses and pentoses as one of their main reasons. [22]

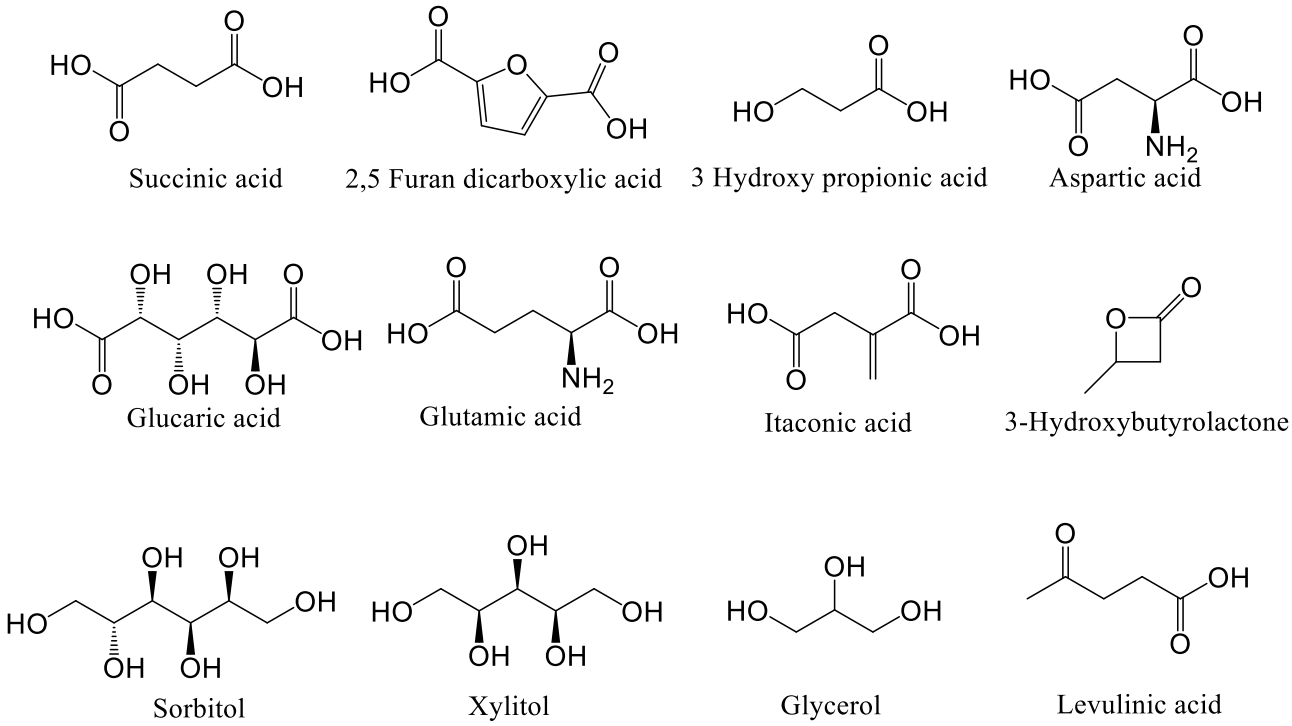

Figure 6: *Twelve important building blocks determined by Werpy et al. (succinic acid is an example for 1,4 diacids of which fumaric acid and maleic acid where also deemed to be part of the important building blocks, but were not counted themselves; similarly arabinitol is also counted among the important building blocks as an alternative to xylitol). [9]*

In accordance with the analyses by *Werpy et al.* [9] and *Leonard et al.* [54], the industrial production of LA predominantly involves the conversion of lignocellulosic biomass. The most widely adopted process for this conversion is the *Biofine Process* [15], developed in the 1990s, where lignocellulosic biomass undergoes hydrolysis using dilute sulfuric acid. Alternative synthetic routes for LA production, including the hydrolysis of acetyl succinate esters [55] and furfuryl alcohol [56] or the alkylation of nitroalkanes [57], were utilized industrially during the 20th century. However, it is noteworthy that some of these methods depend on fossil-derived feedstocks. [15,22]

LA can be converted into a variety of chemicals with various applications (*Figure 7*). Levulinates are among the more important of these chemicals. Organic levulinates, also called alkyl levulinate esters, can be produced through esterification of LA with alcohols. Alternatively, they can also be produced directly from biomass through alcoholysis. Alkyl levulinate esters such as ethyl levulinate can be used, for example, as bio-fuel additives [58] or for the production of surfactants [59]. The inorganic levulinates are also referred to as levulinate salts. They are produced by reacting LA with metal hydroxides or carbonates. Common examples of these LA derivatives include calcium levulinate, which is commercially available and can be used as a calcium supplement [60], and sodium levulinate, which can be used as a preservative [61]. Another important compound that can be derived from LA is γ-valerolactone (GVL). GVL can be synthesized through the catalytic hydrogenation of LA or α-angelica lactone which can form after internal ring closure of LA. Due to it possessing a low volatility, as well as a high boiling and flash point, GVL can be used as a green solvent. It is often used in processes involving lignocellulosic biomass, such as by *Dutta et al.* [62] during their synthesis of LA from paper waste. It can also be used as a fuel additive as an alternative to ethanol [63]. GVL can also be viewed as a platform molecule itself, as it can also be converted into several relevant chemicals such as adipic acid [64]. In addition to the examples mentioned, there are also many other chemicals that LA can be

converted into. [22] More detailed overviews of the various LA derivatives and their applications can be found in the book by *Mota et al.* [22] and the review article by *Sajid et al.* [65].

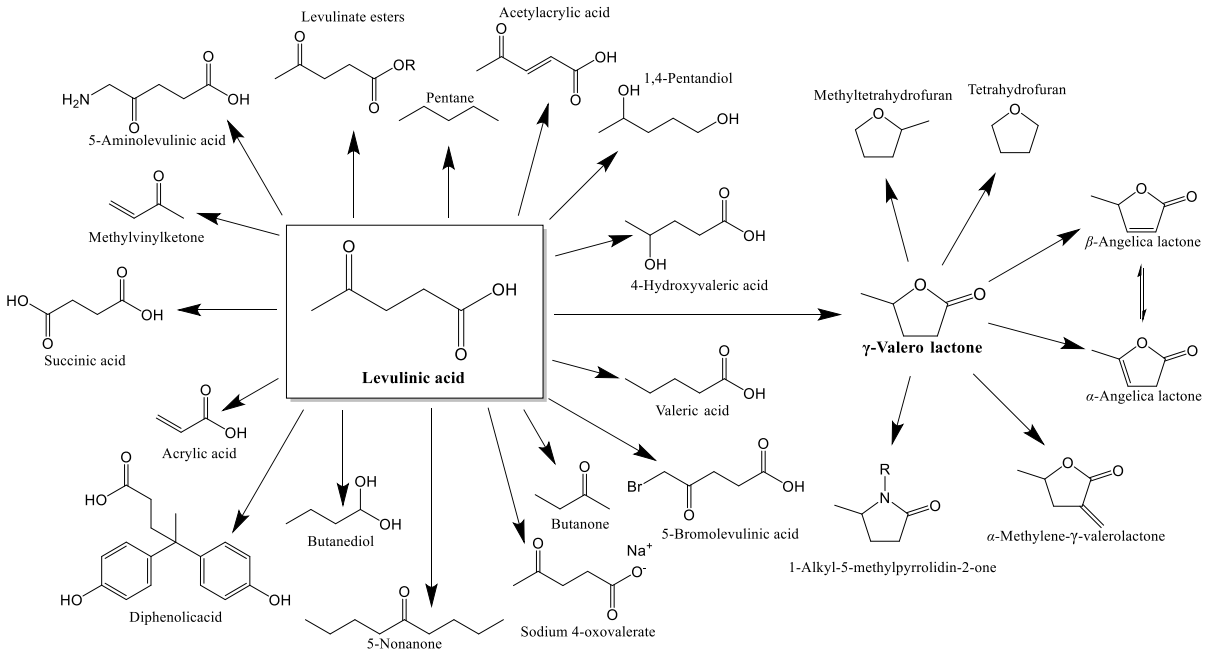

Figure 7: *Valorization products of LA and GVL, adapted from Sajid et al.. [65]*

4.2.2 Production of levulinic acid from lignocellulosic biomass

Factors such as low price, lack of impact on food production and wide availability make lignocellulose one of the most attractive starting materials for the synthesis of LA. However, pretreatments are usually necessary to prepare the lignocellulose for further conversion (see Chapter 4.1.3). The most commonly used method in LA synthesis is the acid hydrolysis, which results in the cellulose and hemicellulose portions of the lignocellulosic biomass eventually being broken down into pentoses and hexoses, which are then further hydrolyzed to LA. [22]

Pentoses and hexoses are converted to LA according to different mechanisms (*Figure 8*). The conversion for hexoses occurs with 5-HMF as an intermediate, which is first produced via several dehydrations of the hexose in an acidic medium. 5-HMF is then further dehydrated until LA is formed, with the elimination of one FA molecule. The conversion of pentoses to LA, on the other hand, occurs via the formation of furfural. Furfural is first produced by dehydrating the pentoses in an acidic medium. This is followed by a catalytic hydrogenation to form furfuryl alcohol, which is then converted again in an acidic medium to form LA. LA production can take place either in a batch reaction or in a continuous process, with continuous processes resulting in higher LA yields. [22]

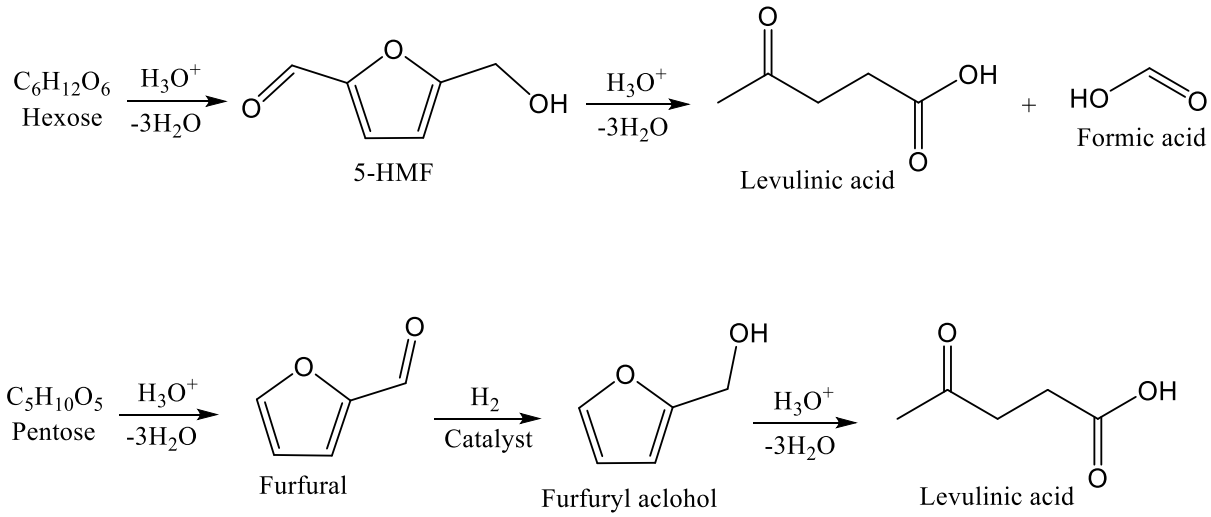

Figure 8: *Conversion mechanisms of hexoses and pentoses into LA, adapted from Mota. [22]*

The hydrolysis of biomass to LA can be carried out using both, homogenous and heterogenous acidic catalysts. The most frequently used homogeneous catalysts are mineral acids such as hydrochloric acid or sulfuric acid, which is also used in the commercial *Biofine process*. Characteristic for mineral acids are their low costs, good availability and high LA yields. However, mineral acids are difficult to recycle and can corrode reaction systems, requiring the usage of special reactors for biomass conversion. Organic acids such as AA or oxalic acid as well as Lewis acids such as aluminum chloride can be used as a less aggressive alternative, although at the cost of lower LA yields. [15,22,65]

Heterogenous catalysts such as metal oxides, zeolites or ion exchange resins have also been applied for the synthesis of LA. They are easy to separate from reaction mixtures and do not cause corrosion problems. It is also possible to adjust the selectivity of the reaction through adjustments to the acidity of the catalyst. The adsorption of reactants and products on the catalyst surface can lead to a reduction in the LA yield, however. Another issue is the deactivation of many heterogeneous catalysts during recycling due to their clogging with solid by-products formed during the reaction. In addition, longer reaction times are often necessary to achieve sufficient LA yields. [22]

The separation of LA from the product stream can proceed through several methods. In the continuous *Biofine process*, the produced LA is usually purified by first filtering off solid by-products and subsequent vacuum distillation of the liquid phase. Vacuum distillation is a simple and well-established method but also requires large amounts of energy and can result in the formation of by-products through the high temperatures employed. Solvent extraction offers an alternative in which no additional processing steps need to be used. However, the use of solvent extraction in an industrial setting requires large amounts of solvent, which can result in high costs depending on the solvent used. LA can be easily extracted with furfural, which is a cheap but also toxic solvent. Membrane separation offers another alternative due to its high selectivity and performance. During this process LA is separated due to differences in diffusivity and solubility of the resulting phases. However, the disadvantages here are the high costs and the fouling of the membranes. [22,66,67]

As an alternative to the separate production and separation of LA, it is also possible to combine the two processes in a one-pot synthesis, using biphasic systems consisting of an aqueous and an organic phase. Aprotic solvents such as tetrahydrofuran (THF), DMSO and GVL are often used as solvents for

the organic phase. Both, homogeneous and heterogeneous catalysts can be used as acidic catalysts. The reaction takes place in the aqueous phase, where carbohydrates and catalyst are dissolved. The resulting products are then extracted into the organic phase, which has a higher affinity for the products than the aqueous phase. In addition to the extraction of the products, this also reduces the number of side reactions such as cross-polymerization and rehydration that would otherwise occur in the aqueous phase. Disadvantages of this process however are long reaction times and lower yields [22].

4.2.3 The *Biofine process* and the commercial production of levulinic acid

The first industrial syntheses of LA were implemented by *Staley* [68] and *Quaker Oats* [69] in the middle of the 20th century. Both companies produced LA by converting carbohydrate-containing raw materials with hydrochloric acid. In 1990 *DSM Fine Chemicals Austria* [55] developed a process to produce LA from petrochemical derived maleic acid via acetyl succinates as intermediates, which was after some usage discontinued to switch to a biomass-based approach. [22]

In the 1990s, *Biometrics* and the *U.S. Department of Energy* collaborated with the goal of obtaining commercial grade LA from paper waste sludge [70], which resulted in the *Biofine process* being created under *Professor Steve Fitzpatrick's* leadership. The first demonstration plant was built in *the Epic Ventures Industrial Park* in *South Glens Falls New York* and successfully put into operation in 1997, with the successful production of commercial grade LA being achieved after some improvements in the purification of the produced LA. Commercial production of LA using the *Biofine process* began in 2015 in a plant built in *Caserta, Italy* with a production capacity of 10000 Mt/a [71]. Currently, the *Biofine process* is used by many companies as a basis for the production of LA from biomass, although there are some exceptions, such as *Langfang Hawk Technology & Development* in China [22], who synthesize LA from furfuryl alcohol. [22,70,71]

In the original *Biofine process* as outlined by *Hayes* and *Fitzpatrick* in 2006 [15] (*Figure 9*), lignocellulosic biomass is first shredded and then transferred by a high pressure air injection system into a mixing tank (*Figure 9, E1*), where it is mixed with dilute sulfuric acid (1.5-3 %) The resulting slurry is then passed into a plug flow reactor at a temperature of 210 to 220 °C at a pressure of 25 bar (*Figure 9, E2*), where, over a period of 12 seconds, the polysaccharides are hydrolyzed to soluble intermediates such as 5-HMF. The intermediates are then transferred to a larger reactor with milder reaction conditions of 190 to 200 °C under a pressure of 14 bar (*Figure 9, E3*), where they are converted into LA and other substances such as furfural over a timespan of approx. 20 minutes. During this stage furfural and other volatile products are usually removed, while LA and insoluble residues are transferred to a gravity separator (*Figure 9, E4*). Here, the LA is separated from the solid residues, resulting in LA yields of up to 83 % with a purity of 75 % which can be increased to 98 % through further purification. [15,22]

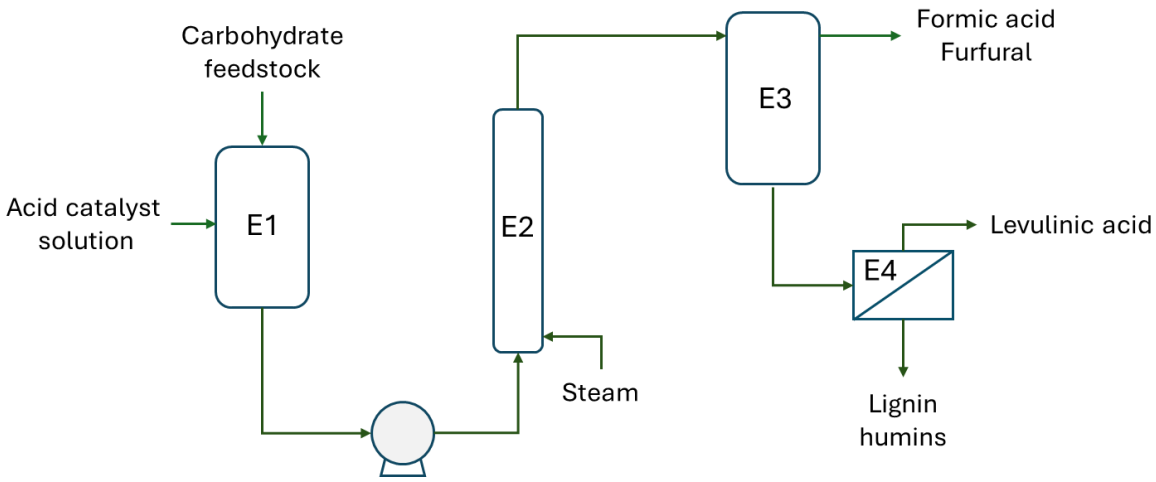

Figure 9: *Schematics of the Biofine process, reproduced from Mota. [22]*

One of the main advantages of the *Biofine process* is, that a wide range of different lignocellulosic biomass can be used as feedstock, as the hydrolysis of the biomass is not inhibited by contaminants, which would, for example, inhibit enzymatic conversions. Furthermore, high LA yields can be achieved in a relatively short amount of time. A disadvantage is, however, the usage of the hazardous sulfuric acid, which is harmful to the reactors. The difficult recovery of LA from the product stream also poses a problem. Additionally, insoluble solids are created as by-products of the process which clog the reactors and reduce the possible LA yield, the so-called humins. [15,22,25]

4.3 Humins: The by-products of sugar conversion

Humins are dark-colored solids that are generated during the catalytic conversion of cellulose and its carbohydrate derivatives. These by-products can be formed during homogeneous and heterogeneous acid catalysis, as well as in reactions without an acidic catalyst. In cases where no acidic catalyst is used, the resulting reaction products are often referred to as hydrothermal carbon (HTC). Initially, research groups differentiated between HTC and humins [72,73], however, later on, scientists stopped making that distinction [23]. Humins are almost insoluble in water, with only humin oligomers or precursors being known to be partially soluble. Organic solvents such as THF, 1,4-dioxane and DMSO can partially dissolve the solid humins, although the remaining solid residues are difficult to dissolve even through Soxhlet extraction [74]. Treatment with an alkaline solution can ensure complete water solubility of the humins. However, this occurs through a partial cleavage of the humin structure, resulting in smaller humin fragments. [23,25,72–76]

Humins are complex heterogenous polymers, whose exact structure and formation mechanism have not yet been fully revealed. The gathered research results by multiple groups however suggests a structure containing furan rings bound together through reactions such as aldol condensation, etherification and esterification, as shown in a humin structure proposed by *Shen et al*. [24] (*Figure* 10). Under milder reaction conditions, humins are formed as spherical particles (*Figure 11*). These spheres are thought to possess a hydrophobic, densely packed core and a hydrophilic, less densely packed shell. Higher temperatures, long reaction times or strong acidity however cause the sphere boundaries to disappear, resulting in the formation of amorphous agglomerates. The agglomeration of humins is also dependent on other factors such as the employed solvents as well as the pH value of the reaction solution. [24,25,72,73,75,77–79]

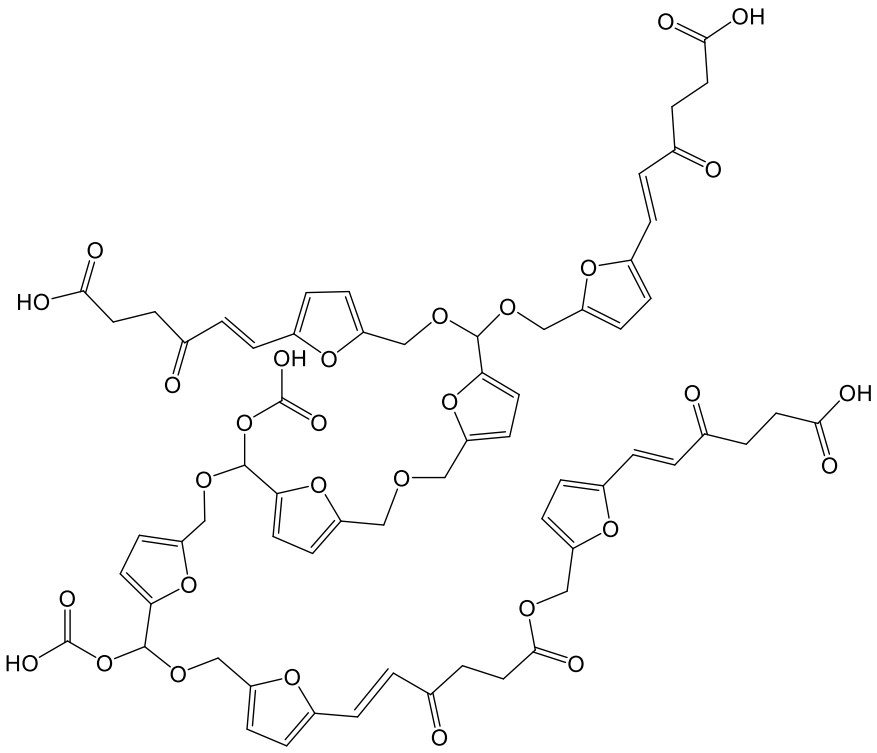

Figure 10: *Cutout of the potential substructure of humins derived from the acid catalyzed conversion of 5-HMF, reproduced from Shen et al.. [24]*

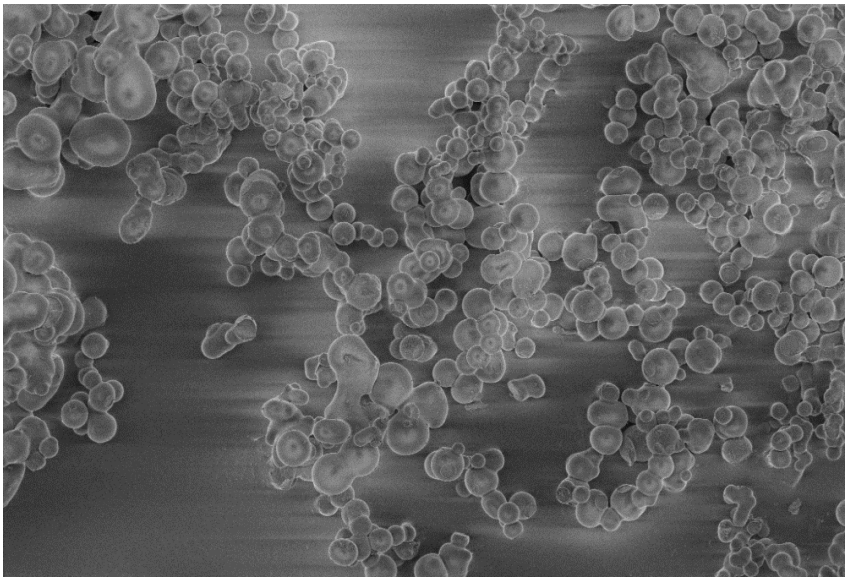

Figure 11: *Sample micrograph of a fructose humin catalyzed with sulfuric acid in water (180 °C, 6 h, pH=2).*

The formation of humins presents a significant challenge in biomass conversion processes. These by-products tend to accumulate on reactor walls and catalysts, leading to reduced catalytic activity, while being difficult to remove. Additionally, humins complicate the recycling process by adsorbing catalysts. They also absorb the formed products, further diminishing overall efficiency. [22,25,26,76]

4.3.1 Research into the formation of humins

Several noteworthy research efforts have been made for the elucidation of the structure of humins and their mechanism of formation. In the late 2000s, several groups were exploring the formation of humins without acidic catalysts. *Sevilla et al.* [72,73] postulated that humins are created through polymerization from the sugars with their decomposition products via aldol condensation and esterification. Aromatization also occurs particularly in the cores of the humin particles, which leads to the formation of hydrophobic cores. The shells of the humins would still contain oxygen-containing functional groups and would therefore be hydrophilic*. Titirici et al.* [80], on the other hand, during their comparisons of humins from various sugar and furfural derivatives, concluded that hexose-based humins, are always formed via 5-HMF. This would apply to both the formation of humins from monosaccharides as well as their formation form polysaccharides. They also postulated the same relationship about pentose humins and furfural as an intermediate, leading them to a conclusion that the formation of humins occurs through polymerization of 5-HMF or furfural. [25,72,73,80]

The incorporation of 5-HMF into the structure of humins derived from hexoses is a theory adopted by multiple research groups. *Blanksma et al.* [81] first put forward the theory in 1946 that 5-HMF was a component of humins they obtained from glucose and fructose. As proof, they stated that the elemental analysis (EA) of humins obtained from 5-HMF correspond to those of humins obtained from hexoses. Later infrared (IR) spectroscopic analysis by various research groups such as those of *van Zandvoort et al.* [31,32] and *Patil et al.* [33] confirmed the presence of furan rings in the hexose humins. [25,31–33,81]

In 2010 *Sumerskii et al.* [82] investigated the formation of humins from several carbohydrates and furfural derivates under the conditions of the industrial acid hydrolysis of wood (180 °C, 0.5 % sulfuric

acid). Their analytics concluded that humins consist out of 60 % furan rings and 20 % aliphatic fragments. Based on their experimental data, they postulated a mechanism for the formation of humins from hexoses and pentoses (*Figure 12*). Their mechanism for hexose derived humins involved polycondensation reactions between the hydroxy and carbonyl groups of 5-HMF molecules and occasionally LA (*Figure 12 A-D*), resulting in the humins also containing ether and acetal bonds. Humins derived from pentoses were instead theorized to be formed through electrophilic aromatic substitution reactions of multiple furfural molecules. Here the carbonyl groups would react with the most activated position of the furfural rings, resulting in carbon-carbon bonds between rings. The resulting oligomers would then be able to polymerize via polycondensation through the remaining carbonyl and carboxy groups to form the cross-linked polymers (*Figure 12 E*). They also postulated the absorption of incomplete dehydration products that had not yet been converted into 5-HMF or furfural and also the unreacted sugars themselves into the humin structure. [25,82]

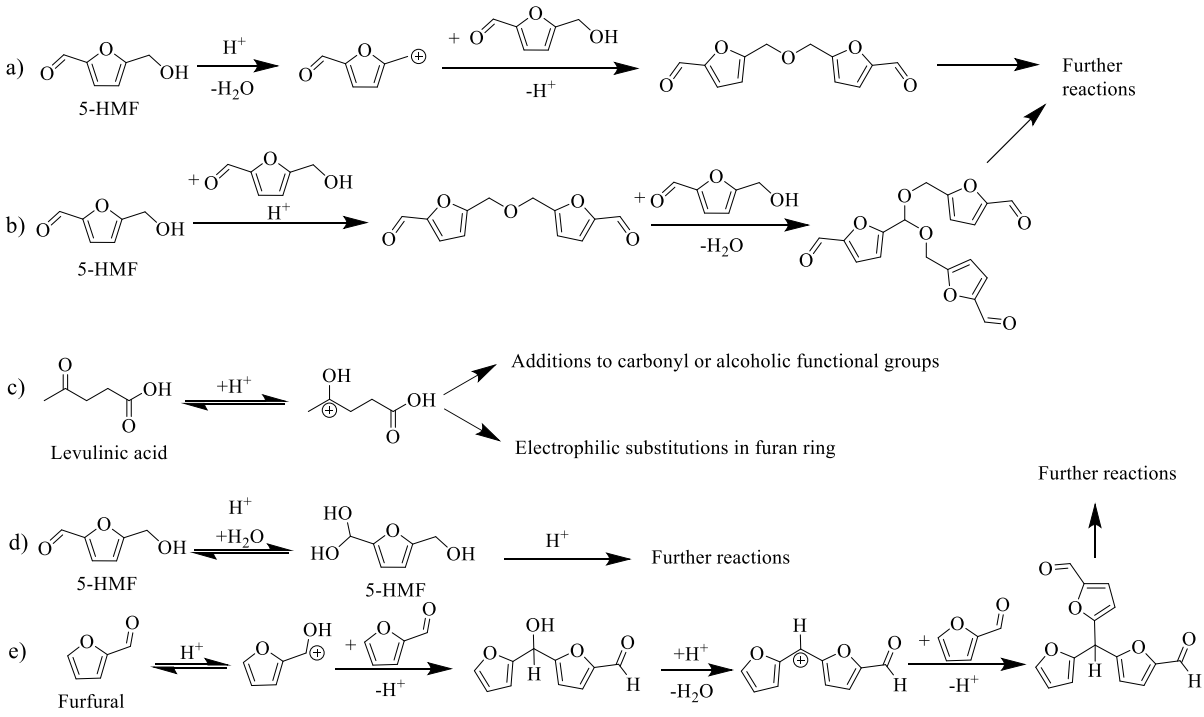

***Figure 12**: Mechanisms of humin formation from pentoses and hexoses, reproduced from Sumerskii et al.. [82] a) Etherification of two 5-HMF molecules. b) Condensation reactions of multiple 5-HMF molecules to form hemiacetals and acetals. c) Activation of LA molecule for subsequent additions to 5-HMF. d) Hydration of 5-HMF into a polyol. e) Electrophilic substitution-based mechanism of formation of furfural derived humins.*

Separately, *Patil et al.* [33,83] postulated their own mechanism of humin formation during their comparison of 5-HMF humins with those derived from fructose and glucose. They theorized that humin formation is the result of aldol condensations and additions between 5-HMF and the intermediate 2,5-dioxo-6-hydroxy-hexanal (DHH) *(Figure 13*). DHH is a theoretical intermediate of 5-HMF degradation (*Figure 14 a)*), which was first mentioned by *Blanksma et al.* [81] during their discussion of the formation of humins from 5-HMF, as a possible product of its ring-opening reaction. Later in the 1980s, *Horvat et al.* [84,85] included DHH in their breakdown of the reaction process of 5-HMF to LA as a possible intermediate, leading to the formation of polymers. However, the existence of DHH has not yet been clearly proven, which is thought to be due to its very high reactivity.

Nevertheless, DHH is accepted by a part of the research groups and is included in several models of humin formation. [25,33,81,83–85]

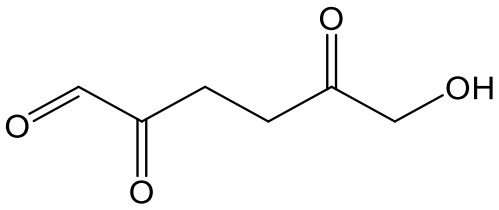

Figure 13: *Structural formula of DHH.*

Patil et al. [33,83] theorized in their research that aldol condensations with the intermediate DHH, are responsible for the lack of the vibration bands associated with the carbonyl group of 5-HMF in the IR-spectra of their humins synthesized from 5-HMF. Instead, the spectra exhibited carbonyl vibrations that matched the theoretically calculated vibration bands of DHH. Furthermore, they also proposed the possibility of humin functionalization, as they managed to incorporate benzaldehyde into the humin structure via aldol condensation. *Van Zandvoort et al.* [31,32] later built on the model proposed by *Patil et al.* [33,83] and modeled a possible humin structure based on the 5-HMF and DHH mechanism as well as their spectroscopic results (*Figure 14*). In their model, humin formation also involves nucleophilic attacks of the furan rings on the carbonyl groups of 5-HMF and the incorporation of LA. They proposed an aldol condensation of 5-HMF with the keto group of LA as the mechanism for incorporation and proved LAs incorporation through 2D solid nuclear magnetic resonance (NMR) spectra. They also proved that humin formation does not only occur via aldol condensation, as they were also able to incorporate 1,2,4-trihydroxybenzene into the humin structure. [25,31–33,83]

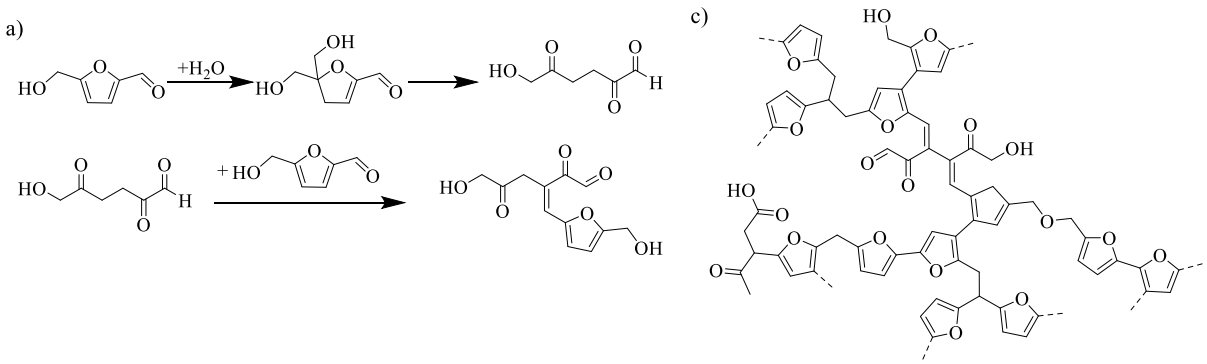

Figure 14: *Formation of humins through DHH and 5-HMF, adapted from van Zandvoort et al.. [31,32] a) Formation of DHH from 5-HMF. [31] b) Aldol condensation of DHH and 5-HMF. [31] c) Humin structure proposed by van Zandvoort et al.. [32]*

Tsilomelekis et al. [34] combined the findings of *Sumerskii et al.* [82] and *van Zandvoort et al.* [31,32] with their own results of investigating the morphology, structure and growth behavior of humins. They proposed that during the formation of 5-HMF based humins, soluble humin oligomers are initially formed by aldol condensations and ester/esterification between 5-HMF and DHH-like molecules. These then grow through the nucleophilic attacks suggested by *van Zandvoort* [31] and aggregate with further addition of 5-HMF until the insoluble humin particles are formed. They also produced humins in a solution containing DMSO, resulting in humins with smaller particle sizes, which led them to the conclusion that the aprotic solvent inhibited the nucleophilic addition and thus reduced the particle size. Later in 2018, *Tsilomelekis et al.* [76] also identified humin fragments containing DHH and 5-HMF

during their experiment for the partial dissolution of humins in various solvents. They also concluded that humins consist partially out of soluble oligomers, adsorbed onto the macromolecular structure by weak forces. [25,31,32,34,76,82]

In 2018, *Cheng et al.* [86] proposed a model for the formation of humins from pentoses. They hypothesized that the xylose humins they produced were formed by condensation reactions of furfural, its ring cleavage products and isomerized xylose. The ring cleavage of furfural was proven by the presence of FA, one of the by-products of the cleavage reaction, in the reaction solution. At the same time furan rings could be detected in the solids, which indicated the participation of furfural in the formation of humin. Different EA results of the xylose and furfural derivatives also indicated the incorporation of xylose intermediates. [25,86]

Based on their results in the hydrothermal conversion of carbohydrates and furfural derivatives in various solvents, *Shi et al.* [23] concluded that α-carbonyls, such as DHH or 2-oxopentanedial (in the case of furfural based humins) and α,β- unsaturated aldehydes, are essential components of humin formation and thus postulated their own mechanism for the formation of humins (*Figure 15*). In their research, no humins or intermediate products of the expected ring-opening reaction were formed from the thermal conversion of furfural derivatives in organic solvents. They linked this to the inhibition of the hydrolytic ring-opening reaction during which α-carbonyls such as DHH are usually formed. This was not the case when converting carbohydrates; here they suspected that the reason for the formation of humins was a β-elimination reaction in which α,β-unsaturated aldehydes are formed, which through enol-ketol tautomerism produce the α-carbonyls required for humin formation through aldol condensation. Ethanol generally suppressed humin formation, which was associated with acetalization of the ethanol and the α-carbonyls formed. [23,25]

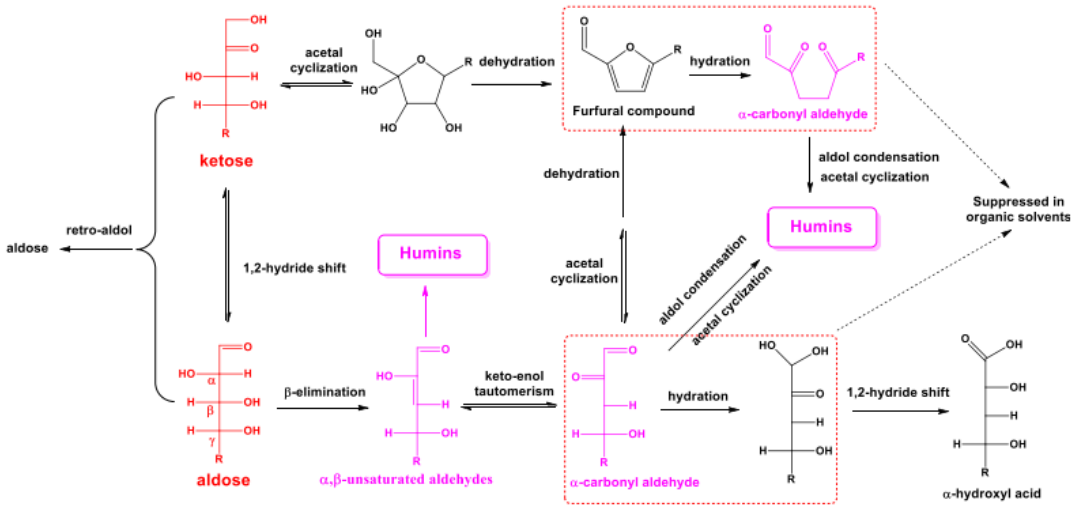

Figure 15: *Hydrothermal degradation of furfural derivatives and carbohydrates, as illustrated by Shi et al.. [23]*

Several research groups were able to identify multiple water-soluble humin oligomers during their research. During the acid-catalyzed conversion of glucose to humins, *Maruani et al.* [87] detected the formation of glucose oligomers in the aqueous phase, which, according to their statement, either act as glucose reservoirs for the continuous production of 5-HMF or react with other glucose dehydration products and were added to the humin structure. *Shen et al.* [24] performed acid-catalyzed reactions of 5-HMF for extended periods at lower temperatures. They were able to identify several water-soluble humin oligomers, which were formed through esterification, etherification, acetalization and

aldol condensation between different intermediates of 5-HMF degradation (*Figure 16*). The incorporation of LA into the humin structure could also be confirmed. They also used their findings to postulate a structure of their formed humins (*Figure 10*). In their research, *Peng et al.* [88] investigated the influence of substrate concentration on the formation of glucose humins in ethanol. They discovered structural differences in the water-soluble oligomers and solid humins that they obtained at different substrate concentrations. Water-soluble oligomers at low glucose concentrations possessed more furan rings, while the oligomers at higher concentrations contained more glycosyl bonds. However, the conversion to solid humin reversed these trends. In addition, the humin particles would be larger at the higher concentrations. Accordingly, they postulated that the formation of the water-soluble oligomers at low concentrations occurs mostly through aldol condensations and additions between 5-HMF and DHH analogues, whereby the solid humin formation leads to a degradation of the furan rings. At higher glucose concentrations however, the water-soluble oligomers consist of glycosyl units and furanic as well as aromatic fragments which are connected to one another by aliphatic compounds resulting from esterification, acetalization and aldol condensation. [24,25,87,88]

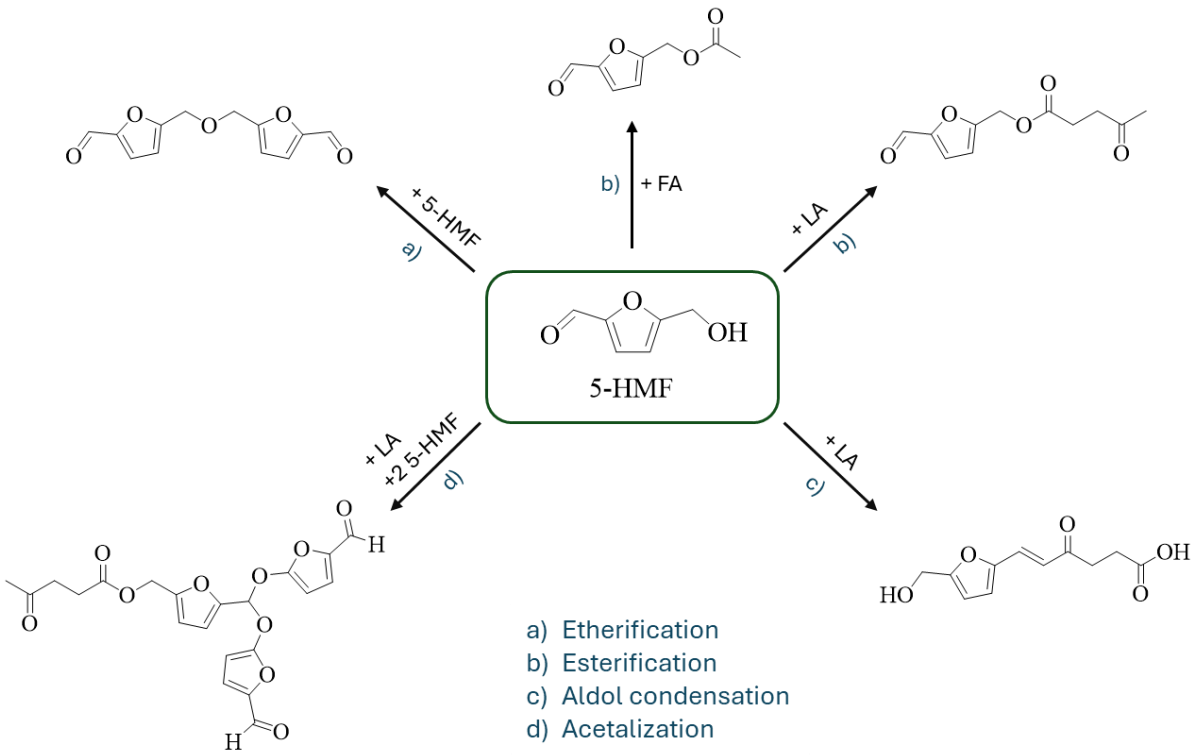

Figure 16: *Water soluble humin oligomers detected by Shen et al. [24] alongside their mechanism of formation, adapted from Liu et al.. [25]*

In their review, *Liu et al.* [75] summarized the accumulated knowledge about the formation of hexose humins in a model from cellulose to humin formation (*Figure 17*): First, the cellulose is hydrolyzed to glucose or fructose and also further converted into 5-HMF. These substances and other intermediates that also result from the cellulose hydrolysis are then cross-linked through aldol condensations, so that water-soluble oligomers are formed. The oligomers are then further combined with the original intermediates through cross-linking and nucleophilic attacks of the carbonyl groups of 5-HMF on furan rings, so that hydrophobic humin cores are formed. The hydrophilic shell of the humins, on the other hand, continues to react through esterification and etherification and thus leads to further growth of

the humin particles. This also leads to the adsorption of further molecules in solution onto the humin, which causes its size to increase further. Finally, the humin particles agglomerate and form foam-like humin cokes. [75]

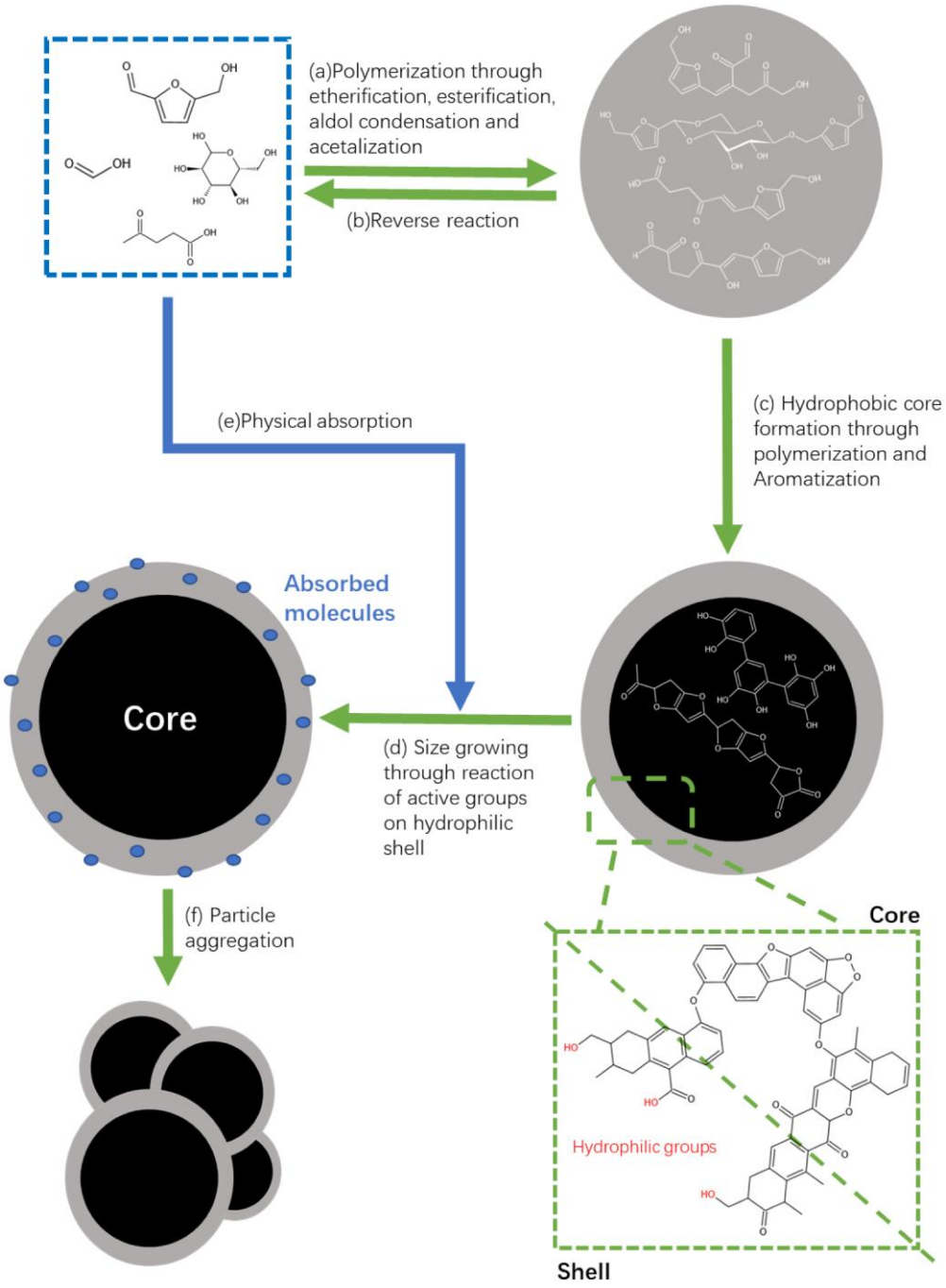

Figure 17: *Mechanism of the formation of humins based on prior research, as illustrated by Liu et al.. [75]*

Recently*, Shan et al.* [89] have put forward an alternative theory for the formation of glucose humins. They ruled out the involvement of 5-HMF and LA in the formation of humins, as adding additional amounts of the two intermediates had no influence on the formation of humins. Instead, they postulated a mechanism in which humins are formed from etherifications of cyclical intermediates produced by the dehydration of glucose. The furan signals arise from furfuryl alcohol formed from glucose, which is incorporated into the structure through electrophilic substitution. They proved this

by increasing the humin yield by adding additional amounts of kojic acid (5-Hydroxy-2-(hydroxymethyl)-4-pyron), which possesses a structure similar to the detected cyclic intermediates and furfuryl alcohol, with the spectra of the released humins also not showing any unexpected differences. Furthermore, they were able to identify some humin oligomers in the reaction solution via high-performance liquid chromatography (HPLC) coupled with a mass spectrometer, which they took as proof for their theory. Nevertheless, the exact formation of humins still remains unresolved. [25,89]

4.3.2 Suppression of humin formation

Based on the results of several research groups [33,72,79,88], reaction conditions that favor the formation of humins such as high temperatures, high concentrations and long reaction times are roughly known. Research by groups such as *Shen et al.* [24] who achieved low humin yields during their conversion of 5-HMF with low reaction temperatures have shown that the variation of these reaction parameters can reduce the formation of humins, but not completely suppress it. [24,30,88] The usage of organic solvents for the conversion of carbohydrates and furfural derivatives has shown promising results regarding the suppression of humin formation. *Shi et al.* [23] were able to completely suppress the formation of solid humins from furfural derivatives during the hydrothermal conversion in organic aprotic and protic solvents. With carbohydrates, however, solid humins still formed in the aprotic solvents. In ethanol no solid humins were formed from the conversion of aldoses, which they attributed to an acetalization reaction between ethanol and the aldehydes used in the humin formation process. *Köchermann et al.* [90] also demonstrated the potential of reducing humin yields through acetalization, during their conversion of xylose to furfural in water/ethanol mixtures. In comparison to the reaction in water, *Köchermann et al.* were able to increase the furfural yields by 40 % while reducing the yielded humin mass by 60 %. They also attributed the increased performance of the reaction to the acetalization reactions, which were presumed to be between xylose and furfural with ethanol. *Hu et al.* [79] achieved similar results of humin suppression using a water/methanol solution as solvent and usage of short reaction times and low temperatures. *Yang et al.* [91] used ethylene glycol as a solvent in their research. Using an acidic conversion of hexoses in ethylene glycol, they were able to achieve better results than during the conversions in ethanol. However, when xylose was converted, a larger amount of humins was formed, which was associated with a copolymerization of furfural and ethylene glycol. [23,79,90,91]

The use of biphasic systems was also investigated for the suppression of humin formation. For the synthesis of 5-HMF from carbohydrates, several research groups have tried to avoid side reactions and thus the formation of humins by removing the produced 5-HMF from the aqueous mixture, thus stabilizing it. *Muranaka et al.* [92] used a system consisting of phosphate buffer saline solution and 2-*sec*-butyl phenol in a ratio of 1:3, with which they succeeded in preventing the formation of solid humins. *Faba et al.* [93] achieved similar results using a biphasic system containing water and methyl isobutyl ketone with carbon nano tubes to promote the mass transfer. [75,92–96]

4.3.3 Valorization of humin waste

As a complete avoidance of the formation of humins is not yet completely feasible, research has also been carried out into the utilization of humins to increase the efficiency of biomass conversion, resulting in various applications for the solid residues (*Figure 18*). Several research groups have found humins to be viable compounds for the production of biobased thermoset materials [77,97–101].

Composite materials made from humins and poly-furfuryl alcohol have been found to possess clear advantages over comparable materials made only from polyfurfuryl alcohol (PFA), as they offer a higher tensile strength and less brittleness. Possible applications of PFA/humin resins include building materials such as plywood, boards, or flooring, with the lower cost of humins in comparison to furfuryl alcohol being an important factor. [25,99,100]

Modified humins have found applications as acidic catalysts. *Wang et al.* [102] produced sulfonated humins through a calcination and subsequent treatment of humins with sulfuric acid, with the resulting sulfonated carbons being used to produce LA from cellulose and bamboo meal with relatively high yields. They also noted a possible industrial application due to the reusability of solvent and catalyst. *Kang et al.* [103] used pTSA as acidic catalyst and sulfonating agent to convert glucose into LA and sulfonated humins. Their produced sulfonated humin showed good catalytic activity during the esterification of LA, resulting in a conversion ratio of 93 %. [102,103] Humins have also been found to possess good adsorptive properties by multiple groups. *Björnerbäck et al.* [104,105] synthesized microporous humins though a conversion of 5-HMF and carbohydrates with sulfuric acid and a following diethyl ether wash. The resulting humins exhibited high CO_2 selectivities and uptakes, enabling potential applications in gas separation processes as organic adsorbents with readily available raw materials. Humins synthesized by *Al Ghatta et al.* [28] in an ionic liquid also demonstrated a heightened affinity towards antimony ions. The humins outperformed the commercially available activated carbon, giving them a possible application in wastewater removal. The mild reaction conditions for humin formation could even save energy as no activation by steam or chemical treatment of the humins would be necessary. [28,104,105]

Beside the previously discussed applications, which leave the humin structure mostly intact, there has also been research into the valorization of humins through depolymerization. *Hoang et al.* [27,106] demonstrated a method for producing sustainable hydrogen via steam and dry reforming. They achieved almost complete conversion of humins and a good H_2 yield using sodium carbonate as a catalyst. *Agawarl et al.* [107] obtained humin oils containing aromatics such as benzene and toluene during the catalytic pyrolysis of humins with zeolites, which could be used as additives for biofuels or building blocks for polymers after separation. They also achieved similar results converting humins with a supported Pt/C catalyst in 2-propanol at milder temperatures [108]. *Maerten et al.* [30] used POM catalysts to convert humins into low molecular weight carboxylic acids via oxidative catalysis. Their process was based on the conditions of the *OxFA process*, in which biomass is converted to FA and will be discussed in a Chapter 4.5. [27,30,106–108]

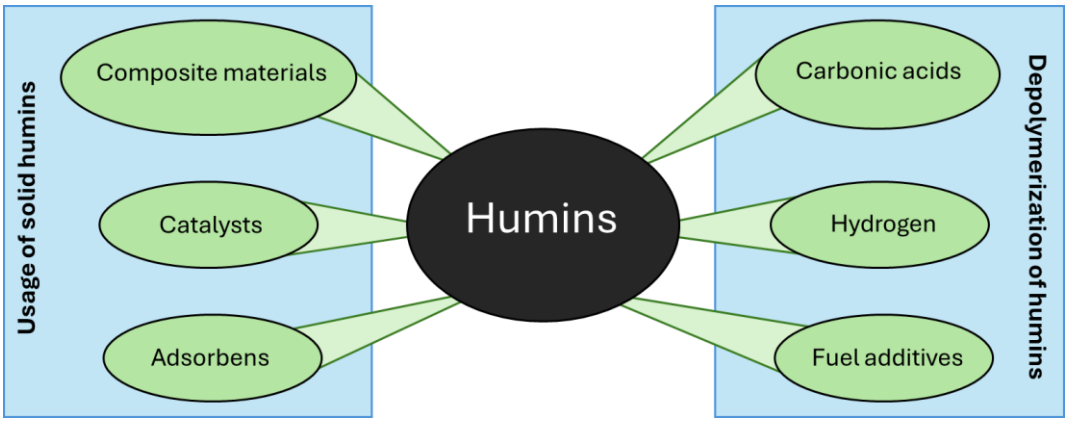

Figure 18: *Overview of different methods for the valorization of humins.*

4.4 Polyoxometalates: A promising class of catalysts

POMs are large sized (6-25 Å) and high ionic weight (ca. 1000-10000 g/mol^{-1}) poly-anionic metal oxide clusters. These clusters possess a structure based mostly on quasi-octahedrally coordinated metal atoms, which can be described as metal centered MO_x polyhedra, with MO_6 octahedra being the most frequently occurring structures. The polyhedra are connected to each other by sharing corners, edges and, rarely, faces. According to the Lipscomb principle [109], only a maximum of two oxo ligands of each polyhedron are not shared. The central metal atoms are also known as addenda atoms (M) and are early transition metals such as vanadium, niobium, molybdenum, or tungsten. The addenda atoms are generally present in their highest oxidation state in their d0 or d1 form, with coordination numbers between 4 and 7. Addenda atoms also possess a favorable combination of ionic radii as well as charges and the capabilities of forming dπ-pπ M-O bonds. Hydrogen and alkaline metals usually serve as counterions to the strongly negatively charged polyanion clusters. These counterions influence the solubility of the POM and can be replaced with other ions. POMs with smaller counter cations such as hydrogen, lithium and sodium are generally soluble in water, although the solubility can be reduced by using larger counterions such as alkylammonium. POMs possess a high stability against H_3O^+ ions, while OH^- ions in aqueous solution often led to the decomposition of the polyanionic clusters, although the pH value at which the decomposition occurs is subject to a greater variance (pH 1-14). They also possess a high thermal stability. [109–112]

4.4.1 Structure types and synthesis of polyoxometalates

Depending on their composition, POMs can be divided into isopoly anions and heteropoly anions. Isopolyo anions or isopoly acids (IPAs) consist only of addenda metals and oxygen and can be represented by the general formula $[M_m O_n]^{p-}$ (*Figure 19*). A typical IPA structure is the *Lindqvist* hexametalate structure M_6O_{19}. This structure consists of six edge-sharing MO_6 octahedra with a central oxygen atom shared by all octahedra, resulting in O_h symmetry. The *Lindqvist* structure is generally adopted by the IPAs of tantalum, tungsten, molybdenum as well as niobium and also some mixed addenda IPAs such as $[V_2W_4O_{19}]^{4-}$. [110,111,113]

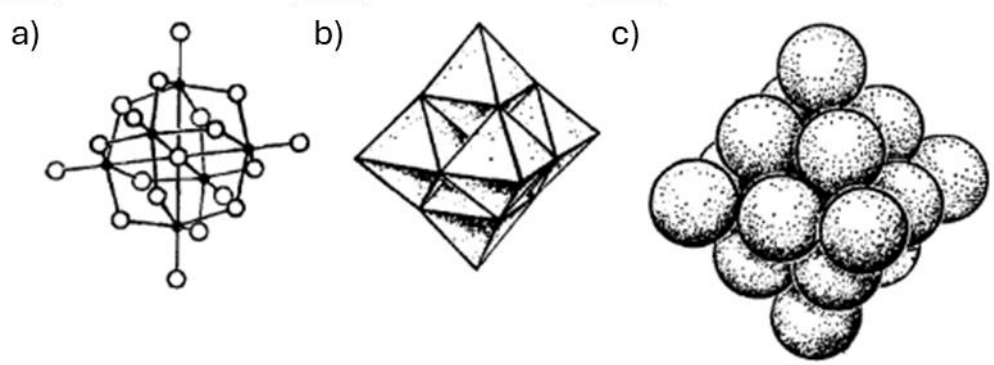

Figure 19: *Lindqvist structures, as illustrated by Pope. [111] a) Conventional atom- and bond-model. b) Coordination polyhedral model. c) Space filling model.*

In addition to addenda metals and oxygen, heteropoly anions or heteropoly acids (HPAs) contain additional elements, the so-called heteroatoms (X). HPAs can be represented using the general formula $[X_x M_m O_n]^{q-}$, whereby the number of heteroatoms cannot be higher than that of the addenda metals. The heteroatoms are generally treated as centers of the HPAs and include main

group elements such as boron, silicon, carbon, phosphorus or arsenic but also transition metals such as iron and cobalt. Over sixty-five different elements from nearly all groups of the *Periodic Table* are known to be able to occur as heteroatoms in POMs. A typical structure for heteropoly anions is the *Keggin*-structure, which is adopted by most heteropolytungstates and some heteropolymolybdates. The structure consists of a central XO_4 tetrahedron which is surrounded by twelve MO_6 octahedra. The MO_6 octahedra are divided into four groups of three edge-shared M_3O_{13} octahedra, which are connected to each other and the central tetrahedron via the corners. This arrangement results in a T_D symmetry. In addition to this arrangement, known as the α-*Keggin* structure, there exist four other isomers of the *Keggin* structure *(Figure 20*). These can be achieved through a rotation of one (β), two (γ), three (δ) and four (ε) of the M_3O_{13} trimers by 60°. The five isomers of the *Keggin* structure are also known as *Baker-Figgis* isomers, with the α and β structures being the most stable, as their M_3O_{13} trimers do not share edges. [110,111,114,115]

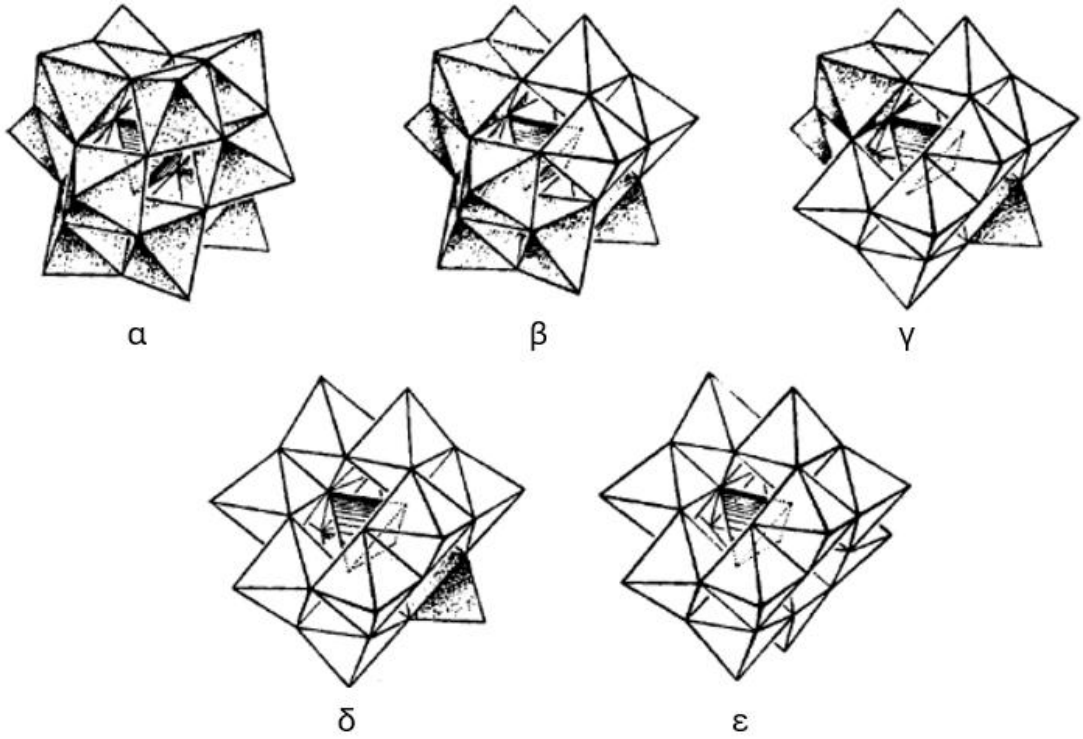

Figure 20: *Baker Figgis isomers, as illustrated by Pope. [111]*

The formation of POMs usually occurs via a self-assembly process in aqueous solution. Here, oxo anions and heteroatoms are mixed stoichiometrically in an aqueous solution, which is then acidified, leading to the formation of the POM. The polyanions are then separated from the solution by adding counterions for crystallization or extraction via diethyl ether. [111,116]

An alternative method is the synthesis via defect site containing POMs. These so-called lacunary POMs are POMs from which addenda atoms have been removed by treatment with a base, resulting in gaps in the structure of the metal oxide cluster. These gaps can be replaced by addenda atoms and other octahedrally coordinated metal atoms. It is also possible to specifically influence the properties of POMs, such as their RedOx behavior, through the insertion of appropriate atoms. [111,117–119]

POMs can be applied in a wide variety of areas such as medicine [120], magnetism [121] and photovoltaics [122]. POMs have also been successfully implemented in DNA polymerase inhibitors with potential applications as anti-AIDS drugs [123]. However, the most important application of POMs is in catalysis, which is described in more detail below.

4.4.2 Catalytic behavior of polyoxometalates

In recent years there has been a lot of research into the use of POMs as catalysts for the conversion of biomass, as can be seen in a review by *Zhong et al.* [124]. POMs possess strong acidic and oxidative capabilities, leading to POMs being used in acid and RedOx catalysis. They can be applied as homogenous and heterogenous catalysts. Several groups have achieved promising results during the conversion of cellulose and saccharides into a variety of platform molecules using different HPAs as acidic catalysts. [111,112,124–132]

A class of HPA that has been used in several oxidative conversions of biomass are the vanadium-substituted poly phosphomolybdates, here abbreviated as HPAx. HPAx-type catalysts have been successfully applied in the desulfurization and deamination of fuels [133,134], as well as delignification of wood [135]. They are also prominently featured as catalysts in the *OxFA process,* which will be discussed further below. [136,137]

HPAx-type POMs generally possess the *Keggin*-type structure of $[PV_xMo_{12-x}O_{40}]^{(3+x)-}$. They are thus strong, polybasic acids, that can release and accept electrons without changing their structure. RedOx catalysis with HPAx as a catalyst usually follows a *Mars-Van Krevelen* mechanism, by which the substrate is oxidized stoichiometrically, with the reduced catalyst being subsequently re-oxidized (*Figure 21*). For this reaction to occur the RedOx potentials of substrate oxygen and catalyst must match the following trend: E(Red) < E (HPAx) < E (O_2) = 1.23 V. HPAx catalysts with x = 2 - 6 are suitable for liquid phase oxidations at mild temperatures. [111,112,124,138–141]

$$HPAx + Sub_{Red} + yH^+ \longrightarrow H_y(HPAx) + Sub_{Ox} \quad (1)$$

$$H_y(HPAx) + \frac{1}{4}yO_2 \longrightarrow HPAx + \frac{1}{2}yH_2O \quad (2)$$

Figure 21: *Summarized mechanism of RedOx reactions of HPAx catalysts, adapted from Kozhevnikov. [141] (1) Oxidation of substrate. (2) Regeneration of catalyst.*

HPAx compounds almost dissociate completely in aqueous solutions. *Figure 22* shows the dissociation behavior of vanadium oxide species in aqueous solution in dependence of vanadium concentration and pH value. For pH values below 3.8, the vanadium ions exist in the form of VO_2^+. [111,112,124,141,142]

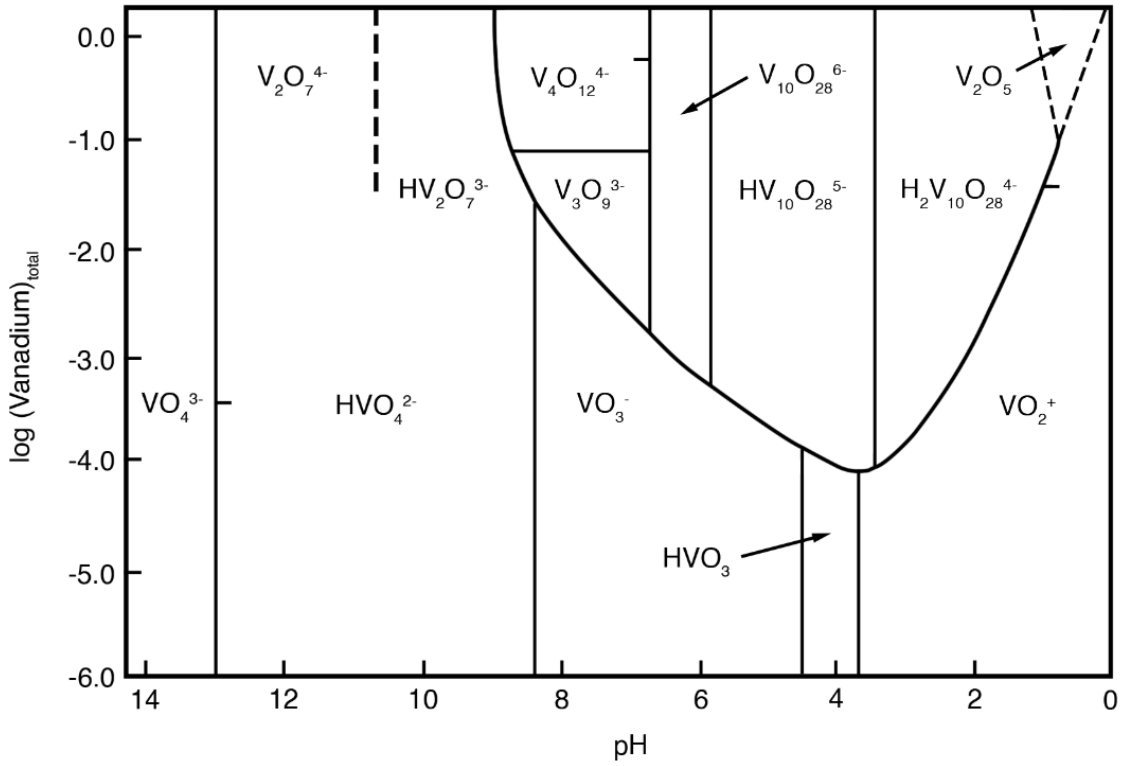

Figure 22: *Aqueous vanadium system by Murmann et al. [142], as illustrated by Huber. [143]*

These VO_2^+ ions are recognized as the active species during oxidation reactions of HPAx catalysts. The detailed process of catalysis with HPAx in aqueous solution can be seen in *Figure 23*. The HPAx catalyst first dissociates in the acidic solution and releases VO_2^+. The formed ion subsequently oxidizes the substrate, whereby V^{5+} is reduced to V^{4+} and is thus present as VO^{2+}. This reaction is assumed to be the rate-limiting step in the reaction and responsible for the RedOx properties of HPAx. The VO^{2+} ion then reacts either with an HPAx to reform a VO_2^+ species and form a reduced HPAx species or is absorbed back into the HPA(x-1) molecule with a vacancy to then generate the reduced form of HPAx. Ultimately, the catalyst is regenerated via oxidation with O_2. The free-floating VO^{2+} ions generally also do not directly react with the O_2 in an acidic solution. [139–141,144,145]

$$HPAx \longrightarrow VO_2^+ + HPA(x-1) \quad (1)$$

$$VO_2^+ + Sub_{Red} \longrightarrow Sub_{Ox} + VO^{2+} + H_2O \quad (2)$$

$$VO^{2+} + HPAx + H_2O \longrightarrow VO_2^+ + H(HPAx) + H^+ \quad (3)$$

$$VO^{2+} + HPA(x-1) + H^+ \longrightarrow H(HPAx) \quad (4)$$

$$4H(HPAx) + O_2 \longrightarrow 4HPAx + 2H_2O \quad (5)$$

Figure 23: *Detailed RedOx reaction process of HPAx catalysts in aqueous solution, adapted from Kozhevnikov. [141] (1) Dissociation of HPAx. (2) Substrate oxidation with VO_2^+ ions. (3) Reoxidation of VO^{2+} ions in solution. (4) Reincorporation of VO^{2+} into a dissociated POM. (5) Reoxidation of reduced POMs with molecular oxygen.*

4.5 The *OxFA process*: Transforming biomass into value-added chemicals

The *OxFA process* is a catalytic oxidative process in which biomass is converted into lower molecular carbon compounds. It was conceptualized in *René Wölfel's* doctoral thesis [146], and later refined by *Jakob Albert* [29,137]. The *University of Erlangen-Nuremberg* patented the *OxFA process* in 2012, and in 2015, *OxFA GmbH* was established as a joint venture between *Jbach GmbH* and *Envi Tech Biogas AG* [147,148].

The basic principle of the process is the oxidative conversion of biomass to FA in water. Molecular oxygen serves as the oxidant, with POMs being used as catalysts, due to their stability in water and low pH values, as well as their ability to catalyze the oxidative cleavage of C-C bond: The oxidative conversion can be carried out under relatively mild conditions (around 90 °C and 30 bar O_2). Separation of the produced FA is carried out via a liquid-liquid extraction with linear alcohols followed by vacuum distillation. The FA produced in this process can be used as hydrogen storage. In contrast to a direct conversion of biomass to CO_2, less energy is released during the oxidation to FA (*Figure 24*). This energy is temporarily "sacrificed" in order to obtain FA as a secondary energy storage. FA possesses several advantages as a storage molecule, as it is non-toxic and therefore environmentally friendly. In addition, the liquid state at room temperature enables uncomplicated transport and handling that can be compared with liquid fuels such as diesel. FA also has various material uses, such as in the textile industry [149]. The "sacrificed energy" can be released by subsequentially splitting the FA catalytically into H_2 and CO_2, which is also achievable at mild conditions. [29,146,150]

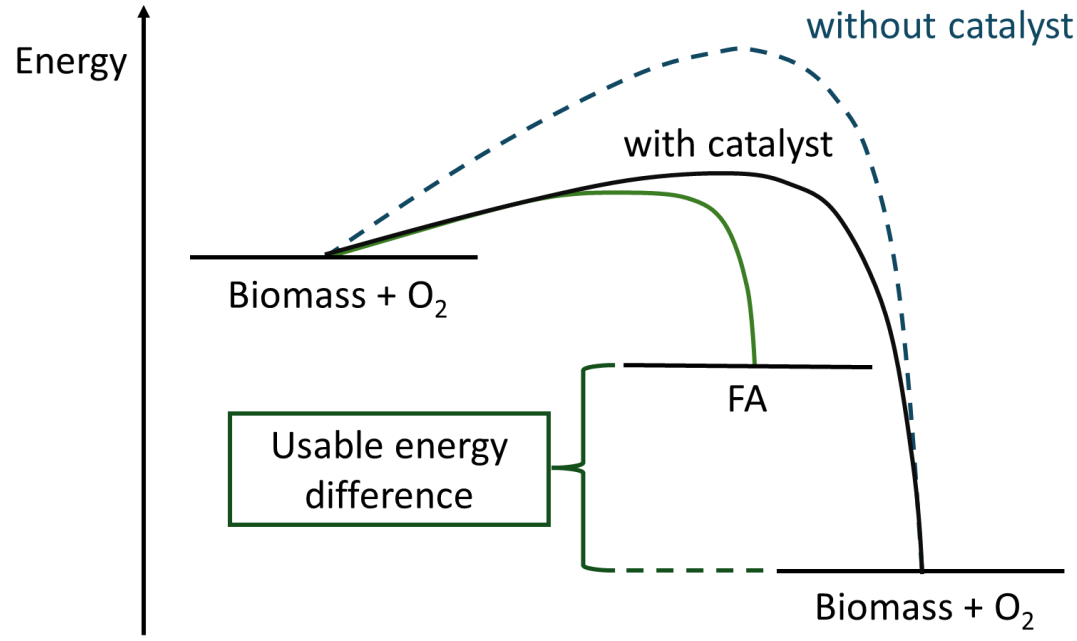

Figure 24: *Energy diagram of the production of FA through the OxFA process, adapted from Albert et al.. [29]*

A variety of biomass types have been converted to FA and other substances using the *OxFA process*. Converted substrates include multiple different sugars, molasses [151], newspapers, lignin, sugarcane bagasse [152] and also humins [30,153]. The process is very robust, as impurities such as salts or printer's ink have not shown to possess any major influences on the process. [146]

4.5.1 Catalysis of the *OxFA process*

The catalytic reactions during the *OxFA process* were investigated and illustrated by *Reichert et al.* [154]. In the first step of the POM catalyzed reaction, water-insoluble substrates are hydrolyzed by the acidic catalyst and thus solubilized. The oxidation then occurs in the liquid phase, during which the C-C bonds in the substrate are cleaved and the POM catalyst is reduced. Ultimately, the reduced catalyst is oxidized again by molecular oxygen, which starts a new cycle. The rate-determining step at low oxygen pressures is the reoxidation of the catalyst and depends on the oxygen concentration in the aqueous phase. Higher oxygen pressures result in the oxidation of the substrate being the rate-determining step instead. [154]

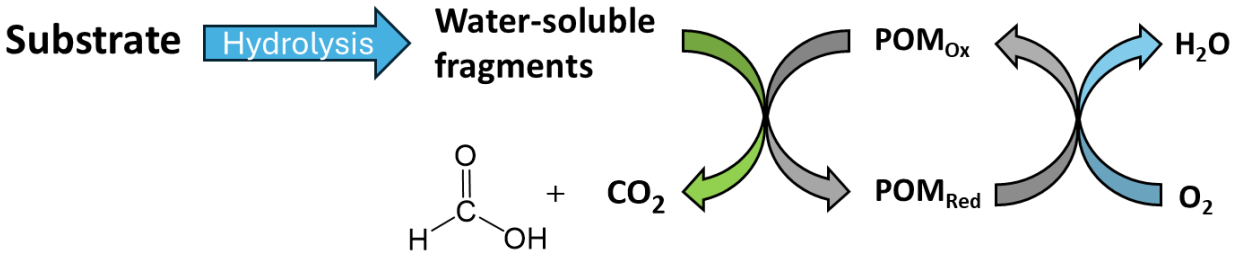

Figure 25: *Schematic of the POM catalyzed reactions during the OxFA process, modified from Reichert et al. [154]*

The process of the oxidative conversion of biomass through POMs was examined and illustrated by *Albert* [29] using the oxidation of glucose as an example (*Figure 26*). First, glucose is split down into glyoxal and erythrose, through a diol cleavage, catalyzed by the POM in acidic conditions. During this bond cleavage, a water molecule is also eliminated. The resulting erythrose is then further oxidized with another POM molecule to yield another glyoxal molecule and glycolaldehyde, which again results in the elimination of a water molecule. In a final step, the two glyoxal molecules and glycolaldehyde are catalytically converted into FA and CO_2 in a ratio of 4:2. [29]

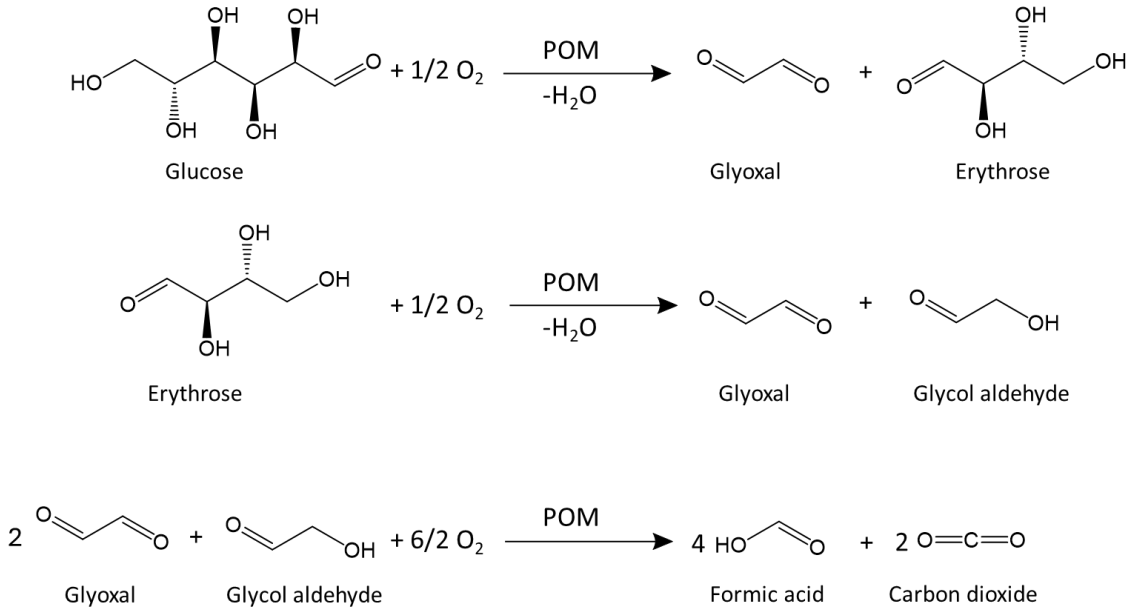

Figure 26: *POM catalyzed oxidative conversion of glucose to FA, carbon dioxide and water, adapted from Voß. [155]*

Traditionally, HPAx type catalysts are used during *OxFA* reactions, providing for the reaction a necessary strong acidity and oxidative reactiveness (Chapter 4). The original POM used by *Wölfel* [146] was the doubly vanadium-substituted $H_5[PV_2Mo_{10}O_{40}]$ (HPA-2). However, subsequent research by *Albert et al.* [156] showed that the degree of substitution of the HPAx with vanadium possesses a positive effect on the reaction rate. $H_8[PV_5Mo_7O_{40}]$ (HPA-5) was established as the catalyst of choice, as its usage resulted in the highest space-time yields and was used in most of the *OxFA* research afterwards. [30,146,151,152,156]

4.5.2 Selective catalytic oxidation of humins under *OxFA* conditions

The SCO of humins under *OxFA* conditions was first reported by *Maerten et al.* [30] in 2017. They were able to successfully convert humins derived from different feedstocks using a *Lindqvist*-type and a *Keggi*n-type POM as catalysts. The *Keggin*-type POM HPA-5 showed a higher selectivity for FA production than the *Lindqvist*-type POM, with the best results derived from the conversion of cellobiose derived humins. Large amounts of humins could be converted during the SCO of the cellobiose derived humin using HPA-5 reaching a conversion rate of 80.9 %. The maximum selectivities of FA and AA formation, which were also reached in the cellobiose humin conversion, however, remained rather low, at 12.7 % FA and 8.2 % AA, respectively. The main product of all conversions was CO_2, with a maximum yield of 62.8 % reached during the conversion of cellobiose with HPA-5. *Maerten et al.* also noted that the oxidative conversion of humins was not largely affected by the type of humin used. [30]

In 2023, *Esser et al.* [157] examined the conversion of several humin model substrates using different POM catalysts under similar conditions as *Maerten et al.* [30]. The primary objective was to investigate the oxidative conversion of compounds that share structural motifs with humins, applying these insights to the SCO of actual humins. An overview of the model substances used can be seen in *Figure 27*. Most of the model substances are furan derivatives possessing structural elements that were suspected to be part of the structure of humins through previous research, such as furan rings or ether and ester bonds (compare Chapter 4.3.). Reactions with $H_4[PVMo_{11}O_{40}]$ (HPA-1) showed best results among the SCO of the smaller, mostly water-soluble *first-generation substrates*. These conversions showed the highest selectivity towards value products and, in contrast to reactions using the more highly substituted HPA-x, showed less overoxidation of products. The subsequent conversions of the larger, insoluble *second-generation substrates* showed that HPA-1 is a good catalyst for the cleavage of ether and ester bonds, while the C-C bond cleavages proved to be more difficult. [157]

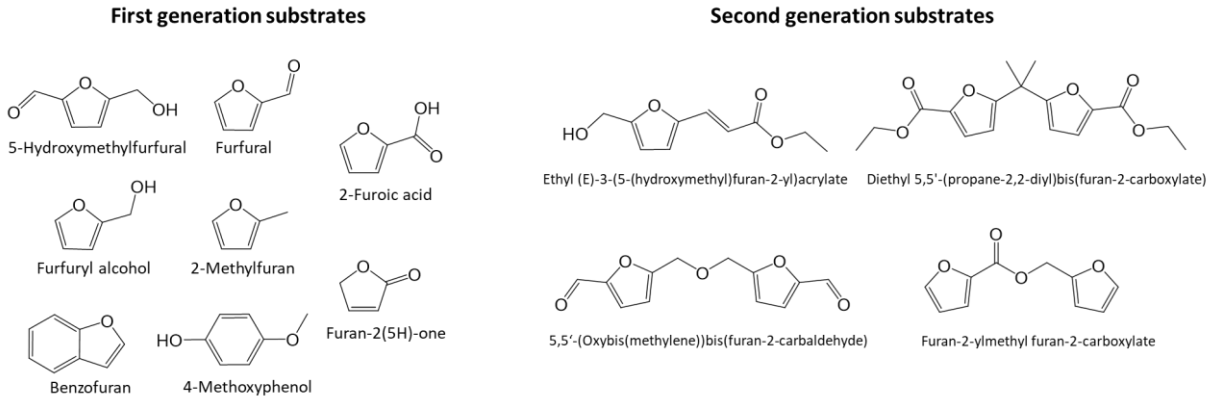

Figure 27: *First- and second-generation model substances converted by Esser et al. using different POM catalysts during their investigation. [157]*

Subsequently, in a follow-up study [158], these findings were applied to the SCO of real humins. An initial conversion using HPA-1 resulted in similar yields regarding FA and AA, compared to the previous results of *Maerten et al.* [30] using HPA-5 under the same reaction conditions. However, the conversion of humin and yield of the gas phase of the oxidations of *Esser et al.* [158] were significantly lower. For further optimization, small amounts of pTSA and methanol were used as additives. The solid acid pTSA was used as a solubilizer to grant the catalyst better access to the insoluble humins, which was successfully demonstrated by *Wölfel [146]* and *Albert [137]* during their research. Methanol was added to suppress the formation of CO_2. This usage of methanol was based on the findings of *Maerten et al.* [159], who were able to successfully suppress CO_2 formation when converting glucose under *OxFA* conditions in pure methanol. The combined usage of both additives together resulted in a drastic increase in selectivity for the formation of FA and AA. In addition, the suppression of CO_2 formation made it possible to further increase the combined yield of the value products by increasing the reaction temperature to 120 °C, without risking unwanted overoxidation. The combined yield of the value products was increased by a factor of 3.6 compared to *Maertens* [30] results, while the yield of the gas phase products was reduced by a factor of 1.6. The highest yield was achieved when converting fructose-based humins. [158]

In another follow-up study, *Esser et al.* [160] managed to further optimize the process. HPA-2 turned out to be a more suitable catalyst than HPA-1, as through the usage of the additives, the problem of over-oxidation, which prevented its use in the previous study [157], could be avoided. This also resulted in the lower temperature 90 °C being once again the optimal reaction temperature for the SCO of humins. [160]

4.6 DoE: A statistical tool for the optimization of LA synthesis

Experiments can be described as tests in which the input variables are deliberately changed, enabling the observation and recording of the reasons for the subsequent changes in the output responses. In statistical DoEs, experiments are planned in such a way that it is possible to evaluate the resulting data using statistical methods and thus determine cause-and-effect relationships. [161,162] As the synthesis of LA and the associated formation of humins are dependent on a variety of reaction conditions, such as temperature, time and concentration, the application of statistical experimental design could help to clarify the influence of these parameters on the acidic conversion of carbohydrates.

The modern approach of statistical experimental design was pioneered by *Fisher* [163] at the beginning of the 20th century during his work of analyzing data and statistics at the *Rothamstadt Agricultural Experimental Station* near *London*. DoEs have since become an important tool for statistical process control and quality improvement. During his time, *Fisher* favored the usage of factorial experiments over the commonly used one-factor-at-a-time (OFAT) experiments, where only one experimental factor (k) is varied at a time, while the others remain constant. In factorial experiments, however, the multiple factors are varied together. This results in factorial experiments requiring fewer runs to be able to estimate effects with the same precision as comparable OFAT experiments. Furthermore, this allows conclusions to be drawn about interactions between the varied input factors, which is not possible with the OFAT method. The simplest factorial design is one consisting out of two factors (k=2) and two levels (2^2), resulting in four necessary experimental runs (2^k). A disadvantage of these full factorial designs, however, is that the number of required runs increases exponentially, the higher the number of factors and levels are, which can result in an infeasibly high number of required runs. A fractional factorial design that reduces the number of required runs (2^{k-p}), can be advantageous in these circumstances. A reduction in the number of required runs is possible if it can be assumed that interactions between multiple factors (high-order) are negligible compared to low-order-interactions or main effects. However, the reduction in required runs can lead to aliasing of the effects due to the missing information about some of the factor interactions, thus reducing the resolution of the design. Fractional factorial designs are often used in research and development as well as for process optimization. [161–165]

A frequently used way to evaluate DoE data are the response surface methods, which can be used to generate 3-D rendered response maps (*Figure 28*). The basic idea of this process is that recorded data is converted into an approximate polynomial function that can be used to describe the responses in the experimental region of the design. The generation of these so-called response surfaces allows for the determination of factor-level combinations that result in an optimized response, which is important in industrial experiments. Response surfaces can be fitted using a first-order model, which assumes linearity of the factor effects or a second-order model, where the existence of quadratic factor effects is assumed. [161,162,165]

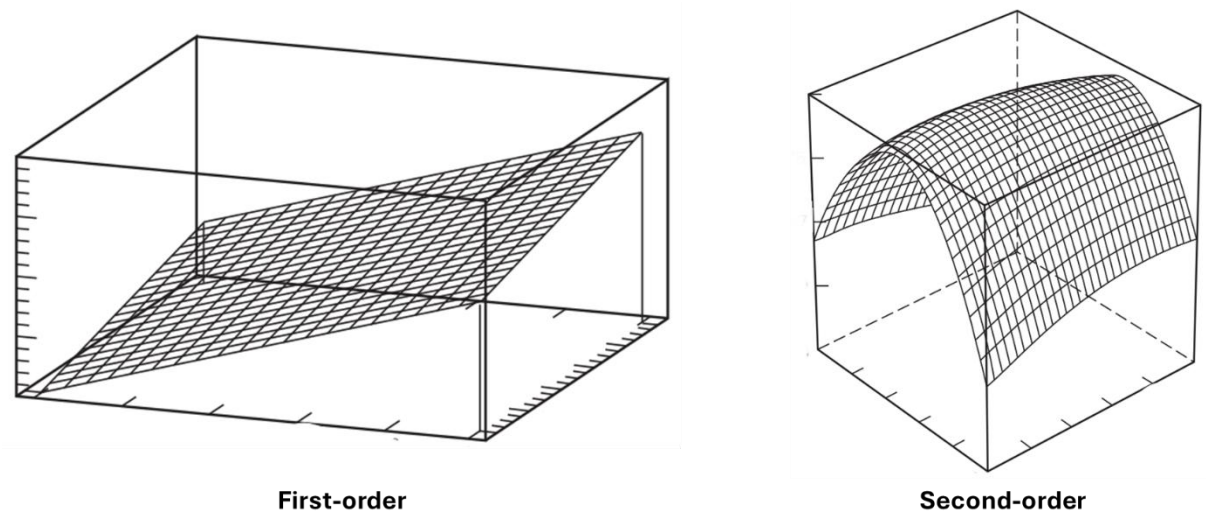

Figure 28: *Sample schematics of a first-order and a second-order response surface, as depicted by Montgomery. [161]*

Two-level designs like the 2^k design can be augmented through the addition of center points and axial points to be able to be fitted to a second-order model (*Figure 29*). The resulting design is called a central composite design (CCD) and is employed if the first-order model suffers from a lack of fit due to a significant curvature caused by nonlinearity of the factor effects. A frequently used second-order design is the *Box-Behnken* design. In contrast to other designs, the corner points of the factor space are not measured, but rather the midpoints of the edges as well as the center point. These designs are generally used when it can be assumed that the optimum lies near the center or when runs at the corner points of the factor space cannot be conducted due to limitations of the tested system. *Box-Behnken* designs are very efficient, as the number of required runs is low. Furthermore, *Box-Behnken* designs are generally rotatable, meaning the variances of all points within equal distance from the design center are equivalent. However, as these designs are not based on underlying factorial designs, they cannot be used to perform sequential experiments. [161,162,164–166]

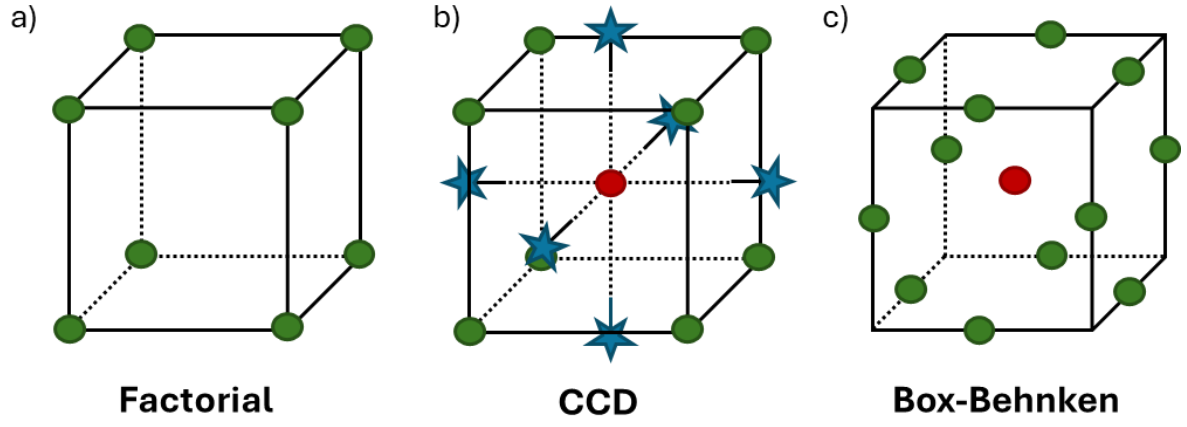

Figure 29: *Schematic visualization of the factor space of different experimental designs, according to multiple authors [162,164] a) Two-level three-factor factorial model without center points (2^3). [162] b) CCD based on a two level three-factor factorial model. [162] c) Three-factor three-level Box-Behnken design. [164]*

The statistical significance of the experimental results can be determined using an analysis of variance (ANOVA). During the ANOVA, the F-value is calculated from the mean square of the main effects and the mean square of the residual effects. This value, in combination with the p-value, indicates whether

the respective effect of the factor or factor interaction is statistically significant. Additionally, the lack of fit of the model is determined through a comparison of the error caused by excess design points with the pure error from replicate measurements. Based on the ANOVA results, a *Pareto* diagram, displaying the size of the factor effects or factor interaction effects, can then be created, in which the effects are plotted with their t-values (*Figure 30*). Plotting the t-values of the effects, instead of their absolute magnitude, counteracts possible experimental errors. The t-value is determined through the division of the numerical effects through their associated standard errors. It is also possible to insert benchmarks to assess whether the effects in the *Pareto* diagram are significant. The *critical t-value* is one of these benchmarks and is given for a specific combination of the degrees of freedom (determined by the ANOVA) and a probability value determined by the chosen threshold for risk (α-value). Another benchmark is the *Bonferroni limit*, which is named after its inventor *Carlo Emilio Bonferroni* [167]. This t-value is more conservative than the *critical t-value* and factors in the number of estimated effects by dividing it into the α-value. The use of the *Bonferroni limit* can protect against false positives but can also lead to existing effects being incorrectly disregarded as insignificant (false negatives). [161,162,167,168]

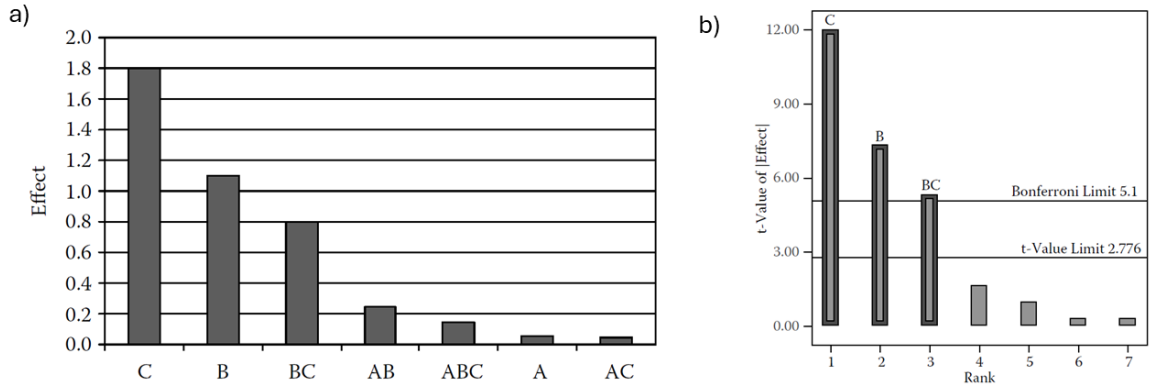

Figure 30: *Sample pareto diagrams plotting the absolute magnitude of the effects (a)) and the t-value of the effects (b)) as depicted by Anderson and Whitcomb. [162]*

5. Experimental part

5.1 Chemicals

5.1.1 Carbohydrates

All carbohydrates were purchased commercially and used without further purification. D(+)-xylose, D(+)-glucose, D(-)-fructose (all for biochemistry) were obtained from *Merck Millipore*. Sucrose (99%) was supplied by *Alfa Aesar* and D(+)-Cellobiose (>98 %) by *Carl Roth*.

5.1.2 Solvents and liquid acids

All liquid chemicals were sourced commercially and used without further purification. AA (glacial) and ethanol were obtained from VWR chemicals. Sulfuric acid (95-97 %) and DMSO were bought from *Grüssing GmbH*. FA (85 %) was obtained from *Alfa Aesar*.

5.1.3 Solid acids and catalysts

All solid acids and catalysts were used without further purification. pTSA-monohydrate was obtained from *Merck Millipore*. HPW, HPMo and HSiW were also obtained commercially from *Sigma Aldrich*. HPA-2 and HPA-5 were synthesized in our research group according to a procedure described by *Raabe et al.* [169].

5.2 Reactor setup and synthesis procedure

All reactions were carried out in high pressure reactor systems. Below is an explanation of the reactor systems and the used reaction procedures.

5.2.1 10-fold reaction setup

The screening reactions of Chapters 6.1, 6.2 and 6.3 as well as the SCO from Chapter 6.1 were carried out in a 10-fold batch reactor system. This system consisted of 10 individual autoclaves from *Parr Instruments* made of Hastelloy (C276) which had a permissible reaction volume of about 20 mL. The autoclaves were connected to the gas line via S316 stainless steel pipes, through which they could be supplied with nitrogen and oxygen. The reactors were sealed with polytetrafluoroethylene (PTFE) rings and protected against excessive reaction pressures with rupture disks made of Hastelloy (nominal pressure 100 bar ± 10 bar at 20 °C). Using a heating block made by *Horst GmbH*, the autoclaves could be heated up to 200 °C and the magnetic stirring plate from *IKA®-Werke GmbH & CO. KG* allowed stirring speeds of up to 1000 rpm. *Figure 31* shows the schematic structure of the 10-fold batch reactor setup.

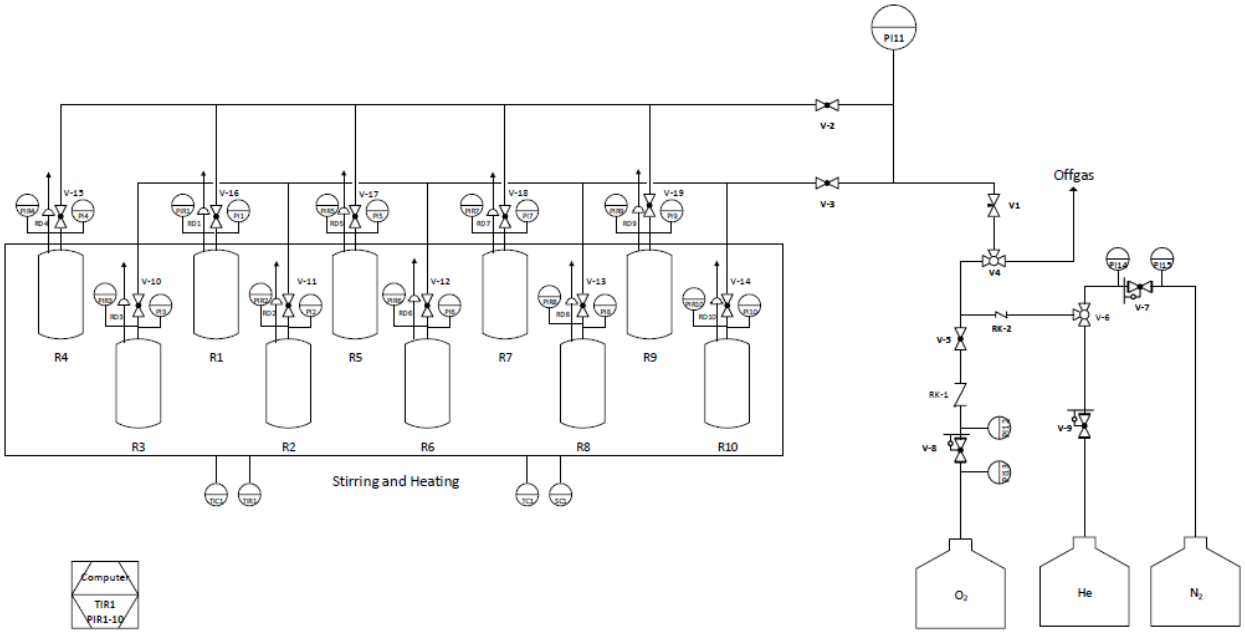

Figure 31: *Schematics of the 10-fold batch reactor system.*

The screening experiments were generally carried out following a standardized procedure. First, stock solutions of the desired solvents were prepared with the specified water/organic solvent ratios and their pH values adjusted to the desired values using the specified acidic catalyst. The stock solutions were then pipetted into 10 mL glass liners containing the respective carbohydrates to obtain solutions with the desired carbohydrate concentration. The glass inlets were then inserted into the reactors and the reactors were closed. Afterwards, the reactors were filled with the respective gas to the desired reaction pressure and heated to the respective reaction temperature. Reaching the reaction temperature marked the start of the reaction (T_0). After the respective reaction time, the reactors were removed and allowed to cool. After the reactors had cooled down, the pressure was released, and the glass liners were removed. The solids were then filtered off and the liquid phase was analyzed. The preparation of the filtered solids varied in the different chapters. In Chapter 6.1 the humins were rinsed with water, dried and ground with a mortar. The ground humins were then further purified using *Soxhlet* extraction with water as solvent and subsequently analyzed after further drying. From Chapter 6.2 onwards, the humins were only washed three times with water after filtering and then dried.

For the SCO of humins performed in chapter 6.1, each autoclave was loaded with 75 mg humin as substrate in the 10 mL glass liners. A 100 mL stock solution containing 1 g of the POM HPA-5 was prepared, with 7.5 mL of this solution being pipetted into each liner. Afterwards the glass liners were inserted into the reactors. The autoclaves were purged with 10 bar oxygen, ensuring a pure oxygen atmosphere. For the reaction, the oxygen pre-pressure was increased to about 26 bar. The autoclaves were heated to a reaction temperature of 90 °C and a stirring speed of 300 rpm was set. As a result of the temperature increase, the pressure rose to the desired reaction pressure of 30 bar and the stirrer speed was set to 1000 rpm. After 15 h, the reactors were removed from the 10-fold system and cooled down. Each phase (gas, liquid, solid) was analyzed separately. For this purpose, gas samples were collected from the reactor before depressurization via gas sampling bags, then the liquid and solid

phase were separated by filtration, with the solid residue being purified through *Soxhlet* extraction using water as a solvent.

5.2.2 600 mL batch autoclave

The upscaled experiments from Chapter 6.3 were carried out in a 600 mL autoclave manufactured by *Parr Instruments*. Similar to the autoclaves of the 10-fold batch reactor, the reactor was made out of Hastelloy (C276) and was connected to the gas inlet and outlet with stainless steel (S316) pipes. The gases available via the pipelines were nitrogen and oxygen. The reactor was also equipped with a Hastelloy (C276) stirrer, which was controlled by a three-phase motor from *Cemp International.* The reactor was sealed using a PTFE ring as well. To protect against higher pressures, a bursting disc made of Hastelloy (C276) with a bursting pressure of 100 bar ± 10 bar at 20 °C and a relief valve for pressures above 50 bars were used. A heating sleeve produced by *Horst GmbH*, which was equipped with a Pt100 thermocouple, was used to heat the reactor. There was also another Pt100 thermocouple installed in the reactor for temperature control, which was also made of Hastelloy. A *LAUDA Dr. R. Wobsder GmbH & CO. KG* RE 106 cryostat connected to a cooling coil made of Hastelloy in the reactor was used to cool the reactor. The pressure in the reactor was measured using a manual pressure gauge manufactured by *Swagelok* and an electrical sensor manufactured by *Ashcroft Inc*. Pressure and heating control was carried out via a controller from *Eurotherm Germany GmbH*. *Figure 32* shows the schematics of the 600 mL batch autoclave.

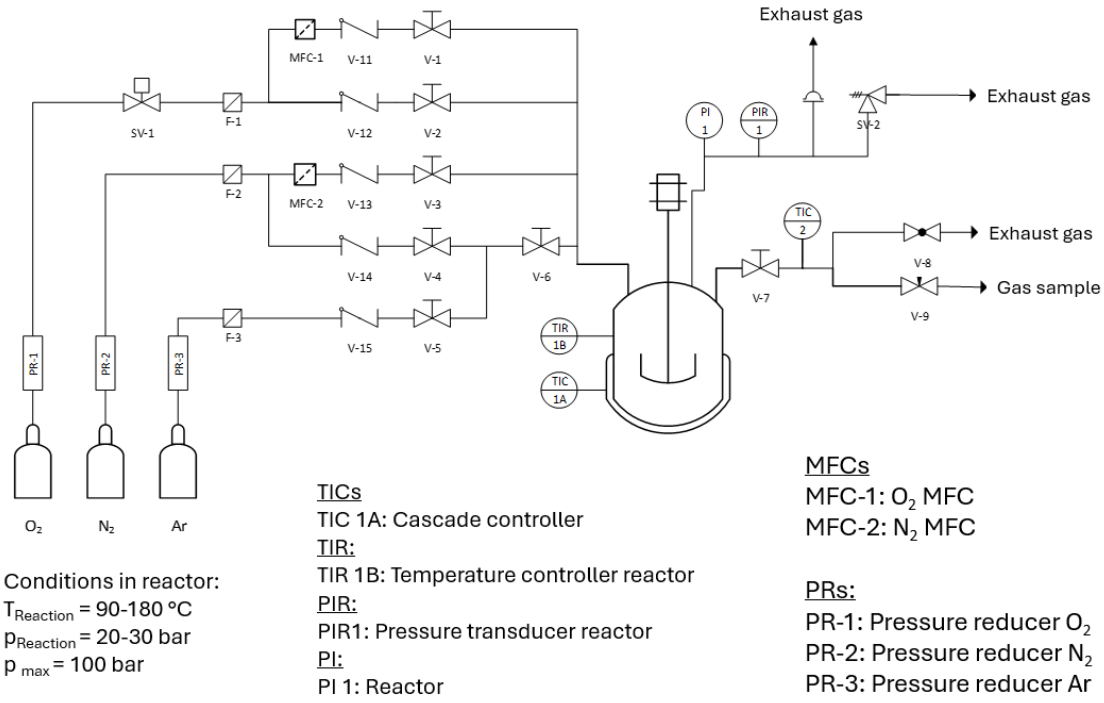

Figure 32: *Schematics of the 600 mL batch autoclave.*

The upscaled syntheses were carried out under the following conditions unless further specified: First, a stock solution of FA dissolved in water was prepared with pH 1. Afterwards 300 mL of this solution were filled into a big glass liner containing 5.4 g of fructose, to obtain a 0.1 M solution of the carbohydrate. Following this, the glass liner was inserted into the reactor, which was followed by the

sealing of the reactor. Subsequently, the reactor was filled with 40 bar of nitrogen gas and the stirrer set to 300 rpm. The reactor was then heated up to a temperature of 180 °C. After 4 hours the heating sleeve was removed and the reactor cooled down through the coolant system. Afterwards, the pressure was relieved, and the glass liner removed from the reactor. The product solution was then filtered, and the liquid phase analysed through HPLC and NMR-spectroscopy. The filtered humins were washed three times with water, dried and then analysed using IR-spectroscopy and EA.

For the upscaled SCO, 3.8 g of the POM HPA-2 were first dissolved into 150 mL of a 5 % methanol/water solution. This solution and 1.5 g of the humins produced in Chapter 6.3 during the previously described reaction procedure, were then filled into a big glass liner, which was subsequently inserted into the reactor and the reactor sealed. The reactor was then purged and filled with 26 bars of pure oxygen with the stirrer being set to 300 rpm afterwards. After a short heating period to 90 °C the stirrer was set to 1000 rpm. After 30 h the reactor was cooled down using the coolant system. This was followed by taking gas samples from the finished reaction via gas sampling bags, which were then evaluated through the usage of gas chromatography. After the pressure was released, the reactor was opened, and the glass liner removed. The reaction solution was then filtered and subsequently analysed through NMR-spectroscopy. The remaining humins were washed with water three times, dried and examined using IR-spectroscopy and EA. Subsequently, the reaction solution was further purified. This was initially done via membrane filtration according to *Esser et al*. [133]. The filtrate was then distilled at 130 °C for a period of 12 h in order to concentrate the FA contained within. NMR-samples were also taken from the filtrate as well as the fractions and analysed.

5.3 Analytical Methods

5.3.1 Gaseous phase

Gas chromatography

The composition of the gas phases after the oxidative conversions of humins was determined using a Varian GC 450 on a 2m*0,75m Shin-Carbon-column. A fifteen-minute measurement method was used to analyze the gas samples. The temperature of the column was initially held at 40°C for 2.5 minutes and then increased up to a temperature of 200 °C at a rate of 30 $K*min^{-1}$. The temperature was held at 200 °C for 7.5 minutes, and the eluting gases were detected using a thermal conductivity detector at the same temperature of 200 °C.

5.3.2 Liquid phase

High-performance liquid chromatography

For the quantitative analysis of the aqueous phases produced by the screening reactions, the oxidative humin conversion in chapter 6.1 and the upscaled LA syntheses in Chapter 6.3 a SHIMADZU HPLC system outfitted with an Aminex HPX-87H 300 mm 7.8 mm BIORAD Column and a refractive index detector was employed. The eluent used was a 5 mmol L^{-1} aqueous sulfuric acid solution. The samples were analyzed at 45 °C, 49 bars of pressure and a flow rate of 0.5 mL min^{-1}. Different sample preparation methods were used during the different chapters. In Chapter 6.1 and 6.2 the samples were first diluted with water by a factor of 10 and subsequently filtered using a 0.2 µm Micropur

syringe filter produced by *Altmann Analytik GmbH& Co. KG* before being analyzed. In Chapter 6.3 the samples were only filtered and not further diluted.

Nuclear magnetic resonance spectroscopy

Different sample preparation methods were used during the different chapters. In Chapter 6.1 the samples were prepared using a mixture of 0.4 mL of the reaction solution filtered by using a 0.2 µm Micropur syringe filter produced by *Altmann Analytik GmbH& Co. KG* and 0.2 mL of D_2O. From Chapter 6.2 onward a 0.5 mL reaction solution to 0.1 mL D2O ratio was employed instead. The NMR-samples used for quantification of the results of the humin conversion in Chapter 6.3, were produced mixing 0.6 mL of the filtered reaction solution and 0.1 mL of a 10 wt% tert-butanol/D2O solution. For the measurement of the phosphor and vanadium spectra of the used HPA-2 catalyst in chapter 6.3, 0.63 mL of a pH 1 solution containing the POM was mixed with 0.07 mL of acetone-*d6.*

For the measurements of the ^{1}H-NMR and ^{13}C-NMR samples multiple different spectrometers were used:

- *Bruker Avance III HD 400 MHz* (AVIII400): TOPSPIN 3.6.2, BBI sample head
- *Bruker Avance I 400 MHz* (AV4001): TOPSPIN 2.1, BBO sample head
- *Bruker Avance I 500 MHz* (AV500): TOPSPIN 2.1, BBI sample head
- *Bruker Avance III HD 600 MHz* (AVIII600): TOPSPIN 3.6.4, BBFO sample head

The ^{31}P-NMR and ^{51}V-NMR spectra were measured using the AVIII600 spectrometer. For the ^{31}P-NMR spectra a frequency of 242.94 MHz was employed with the number of scans being 2048 and a relaxation delay of 1 s. The ^{51}V-NMR-spectra were measured using a frequency of 157.77 MHz with the number of scans being 4096 and a relaxation delay of 0.5 s.

5.3.3 Solid phase

Infrared spectroscopy (IR)

All attenuated total reflection fourier transformed (ATR-FT) IR-spectra of the solid humins were measured using a *Shimadzu IRSpirit* with a QATR^{TM}-S single-reflection ATR in attenuated total reflection measurement mode with a diamond prism. Furthermore, the spectra were plotted in *Origin* and smoothed out using the Whitaker method.

Elemental analysis (EA)

The composition of the solid humin residues regarding carbon, nitrogen, hydrogen, sulfur and oxygen content were determined using a Model EA-3000 analyzer produced by *Eurovector.* The oxygen content was measured through pyrolysis with a *HEKAtech Analysenservice GmbH* high temperature furnace.

Scanning electron microscopy (SEM)

The SEM micrographs of the produced humins were taken using a LEO Gemini 1550 from *Zeiss* enabling acceleration voltages between 0.1 and 30 kV, as well as a minimal resolution of 1 nm. The micrographs were measured through bombardment of the solid humin samples with an electron

beam using an acceleration voltage of 2kV at 0 °C with an InLens detector collecting the secondary electrons.

Matrix-assisted laser desorption ionization time-of-flight-mass spectroscopy (MALDI-TOF)

The Matrix-assisted laser desorption ionization time-of-flight-mass (MALDI-TOF) measurements of the humins produced in Chapter 6.1 were taken with a *Bruker ultrafleXtreme* in positive reflector mode. A 2 mg*mL^{-1} solution of the humins dispersed in water and a 20 mg*mL^{-1} dihydroxybenzoic acid/TA30 (ACN/H_2O 30/70 + 0.1 % TFA) solution were prepared for the measurements. 0.7 µL of both solutions were mixed and then left to crystallize for the measurements.

5.3.4 Calculations

The sugar conversion x_i during the humin syntheses was calculated using equation (1):

$$x_i = \frac{c_{i,0} - c_i}{c_{i,0}} * 100 \quad (1)$$

$c_{i,0}$= concentration of the converted sugar before the reaction
c_i = concentration of the converted sugar after the reaction

The carbon mass yield of the humin syntheses $Y_{Cwt\%,Hi}$ was calculated using equation (2):

$$Y_{Cwt\%,Hi} = \frac{m_{Hi} * C_{Hi}}{m_{Si} * C_{Si}} * 100 \quad (2)$$

C_{Hi} = mass percentage of carbon in the produced humin H_i
m_{Hi} = mass of the produced humin H_i
C_{Si} = mass percentage of carbon in the converted sugar S_i
m_{Si} = mass of the converted sugar S_i

The yields of the different products Pi of the SCO of the humins H_i were calculated using equation (3):

$$Y_{mass,Pi} = \frac{m_{Pi}}{m_{Pi,max}} \quad (3)$$

m_{Pi}= attained mass of the products Pi

$m_{Pi,max}$ = maximum attainable mass of the products Pi

To account for deviations in the density of the reaction solution caused by the different densities of the reaction products, m_{Pi} was calculated as the product of the concentration and the molar mass of the reaction product multiplied with the measured density of the reaction solution.

$m_{Pi,max}$ was determined using equation (4):

$$m_{Pi,max} = \frac{n_{Hi,C}/N_{C,Pi}*M_{Hi}}{m_{Hi}+m_{HPAx}+m_{H_2O}} \quad (4)$$

$N_{C,Pi}$ = number of carbons contained in the reaction product

$n_{Hi,C}$ = amount of carbon contained in the humins used for conversion

$n_{Hi,C}$ was determined using equation (5):

$$n_{Hi,C} = \frac{C_{Hi}*m_{Hi}}{M_{Carbon}} \quad (5)$$

C_{Hi} = mass percentage of carbon of humin H_i determined by EA

m_{Hi} = mass of humin H_i

M_{Carbon} = mass of a carbon atom.

To determine m_{Pi} through ^{1}H-NMR-quantification the following equation (6) was used:

$$m_{Pi} = \frac{n_{Pi,q}}{V_{Rs,q}} * V_{Rs,t} * M_{Pi} \quad (6)$$

$n_{Pi,q}$= amount of product Pi contained in the reaction solution separated for quantification
$V_{Rs,q}$ = volume of the reaction solution separated for quantification
$V_{Rs,t}$ = total volume of the reaction solution
M_{Pi} = molar mass of product Pi

$n_{Pi,q}$ was determined via the following equation (7):

$$n_{Pi,q} = n_{t-but} * R_{Pi,t-but} \quad (7)$$

n_{t-but}= amount of the internal standard tert-butanol contained in the quantification sample

$R_{Pi,t-but}$ = molar ratio of product Pi in relation to the internal standard tert-butanol determined by ^{1}HNMR

6. Cumulative part

This chapter presents the published research results obtained while working on this dissertation. The publication on which Chapter 6.1 is based primarily focused on humins. Here, the influences of the reaction conditions on the structure, formation and subsequent utilization of the humins through SCO were investigated. In Chapter 6.2 the focus was more on the production of LA with a green, acidic catalyst. Here, as part of a DoE approach, ideal parameters for the synthesis of LA a) with maximum yield and b) without humin formation were determined. In Chapter 6.3, the findings from previous publications were combined to set up a cyclical process for the production of LA. The process uses FA as an acidic catalyst to produce LA, with part of the FA being recovered through SCO of the resulting humins.

Publication 1:

Investigation of the formation, characterization, and oxidative catalytic valorization of humins

André Wassenberg, Tobias Esser, Maximilian J. Poller, Jakob Albert

A. Wassenberg, T. Esser, M.J. Poller, J. Albert, Investigation of the Formation, Characterization, and Oxidative Catalytic Valorization of Humins, Materials (Basel, Switzerland) *16* **(2023).** *https://doi.org/10.3390/ma16072864*.

Publication 2:

Humin-free synthesis of levulinic acid from fructose using heteropolyacid catalysts

André Wassenberg, Tobias Esser, Maximilian J. Poller, Dorothea Voß, Jakob Albert

A. Wassenberg, T. Esser, M.J. Poller, D. Voß, J. Albert, Humin-free synthesis of levulinic acid from fructose using heteropolyacid catalysts, Biofuels, Bioproducts and Biorefining *18* **(2024)** 1585–1597. *https://doi.org/10.1002/bbb.2654*.

Publication 3:

Valorization of Humins by Cyclic Levulinic Acid Production Using Polyoxometalates and Formic Acid

André Wassenberg, Tobias Esser, Maximilian J. Poller, Dorothea Voß, Jakob Albert

A. Wassenberg, T. Esser, M.J. Poller, D. Voß, J. Albert, Valorization of Humins by Cyclic Levulinic Acid Production Using Polyoxometalates and Formic Acid, ChemSusChem **(2025)** e202401973. *https://doi.org/10.1002/cssc.202401973*.

6.1 Investigation of the formation, characterization, and oxidative catalytic valorization of humins

In this publication, the influences of different reactants on the formation and structure of humins were first investigated. Four different sugars (fructose, glucose, xylose and sucrose), three different acids (sulfuric acid, pTSA and AA), as well as 3 different solvents (water, 1:1 water/ethanol and 1:1 water/DMSO) were used in different combinations to generate humins. The choice of solvent possessed the greatest influence on the yield and structure of the humins, with the conversions performed in the DMSO/water mixture producing the largest amounts of humins and the reactions in the water/ethanol mixture producing the least amounts. It was assumed that the low yields from the conversions in ethanolic solution resulted from the formation of more soluble oligomers through the reaction of the solvent with reaction intermediates. In the investigations of the solid humins through IR, EA and SEM notable differences between the humin produced in different solvents could be seen, which could be traced back to the incorporation of the organic solvents into the humin structure. During the investigations of the humins using MALDI-TOF, three potential structural fragments of humins were also identified. Afterwards, the valorization potential of the produced humins was inspected. For this purpose, multiple humins were oxidized via SCO using HPA-5 to convert the humins into low molecular weight carbon compounds (*Figure 33*). Approximately, half of the humin mass used was converted successfully. The main products of the SCO were CO_2, FA and AA. The humin with the best conversion rate of about 65% was formed from the water/ethanol/AA system, which also possessed the lowest humin yield (about 5 wt%) during the humin formation experiment. However, the worst conversion rate (about 31 %) was achieved from the oxidation of the humin produced by the water/DMSO/sulfuric acid system. IR-spectroscopic investigations of the humins revealed an increased selectivity of the catalyst for the splitting of ether and ester bonds, as well as a decreased selectivity for the splitting of thioester and -ether bonds. As a result, it was determined that the usage of a water/ethanol/AA system could prove to be ideal for the conversion of carbohydrates to LA regarding humin yield and subsequent valorization. Further information can be found in the supporting information.

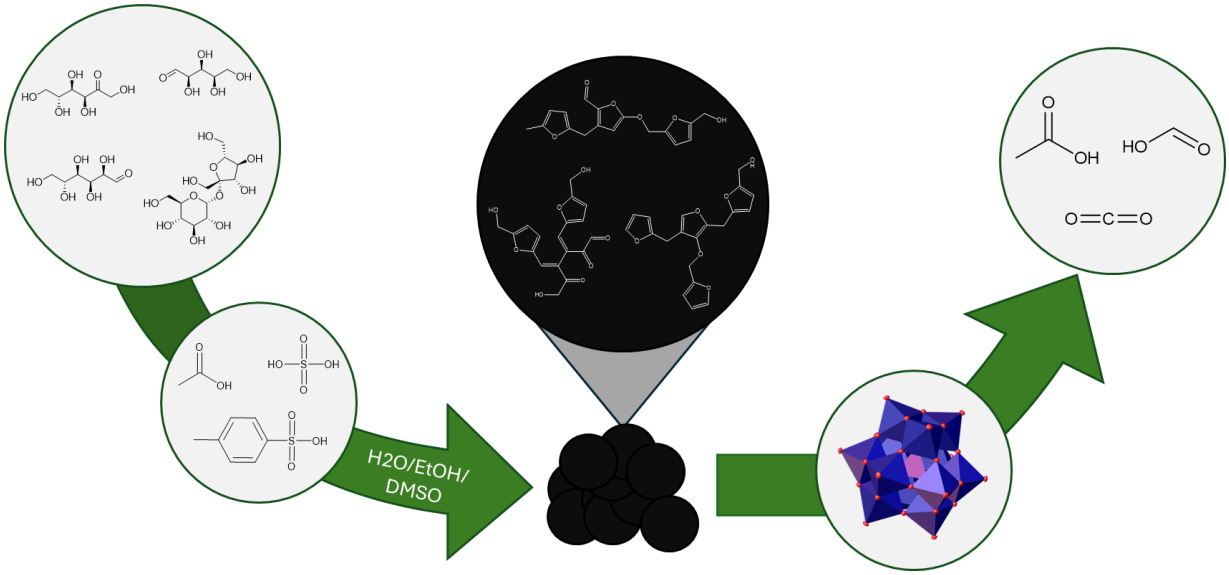

Figure 33: *Synthesis of different humins using various substrates, solvents and acidic catalysts as well as the subsequent conversions of humin into lower molecular carbon compounds via SCO using HPA-5 as catalyst.*

materials

MDPI

Article

Investigation of the Formation, Characterization, and Oxidative Catalytic Valorization of Humins

André Wassenberg, Tobias Esser, Maximilian J. Poller and Jakob Albert *

Institute for Technical and Macromolecular Chemistry, University of Hamburg, 20146 Hamburg, Germany
* Correspondence: jakob.albert@uni-hamburg.de

Abstract: The industrial use of biomass, e.g., for the production of platform chemicals such as levulinic acid, became increasingly important in recent years. However, the efficiency of these processes was reduced by the formation of insoluble solid waste products called humins. Herein, the formation of humins from various carbohydrates was investigated under different process conditions, in order to obtain information about the structure and the formation mechanism. During this process, new potential structural fragments of humins were identified. Subsequently, the produced humins were oxidatively converted to low-molecular-weight carboxylic acids with the use of polyoxometalate catalysts. The experiments showed that the use of sugars in acetic acid and ethanol only lead to the formation of a small amount of humins, which were also structurally most suitable for conversion to carboxylic acids. The main products of the oxidative valorisation of these humins were acetic acid, formic acid, and CO_2, respectively, and our results indicate that certain functional groups were converted preferentially. These findings will help to improve processes for the valorisation of biomass by enabling an overall more efficient use of thermo-sensitive feedstock such as carbohydrates.

Keywords: sustainable chemistry; green catalysis; waste valorization; humins; polyoxometalates; biomass; synthesis and characterization

Citation: Wassenberg, A.; Esser, T.; Poller, M.J.; Albert, J. Investigation of the Formation, Characterization, and Oxidative Catalytic Valorization of Humins. *Materials* **2023**, *16*, 2864. https://doi.org/10.3390/ma16072864

Academic Editors: Nikolay V. Gromov, Maria N. Timofeeva and Valentina N. Panchenko

Received: 1 March 2023
Revised: 17 March 2023
Accepted: 21 March 2023
Published: 4 April 2023

1. Introduction

Increasing global energy consumption, growing waste generation, and collective environmental awareness in our society are driving the development of sustainable processes. In addition, the current dependence of energy and chemical production on fossil raw materials and the political powers that control them lead to an increasing importance of renewable raw materials such as biomass. These materials provide the possibility of an easy access to a variety of sustainable platform chemicals and secondary energy sources through innovative processes [1]. However, to date, not many technologies exist that can convert biomass into higher value chemicals. One reason is the formation of unwanted by-products by thermal-induced reactions that make such processes inefficient and expensive. An example for such a process is the synthesis of levulinic acid from sugars (Biofine-process). In the latter, insoluble black solid polymers are formed, which are called humins [2–4]. They are formed during the acid-catalyzed conversion of carbohydrates below a temperature of 250 °C [5–9]. Humins are particularly problematic for industrial processes, as they clog up both reactor and catalyst, and signify a waste of resources into an unusable side product [10–15].

For these reasons, researchers investigated strategies to prevent the formation of humins during the conversion of biomass. Particularly, the use of different solvents [16–19] or special acidic catalysts [20–22] were the focus of such research efforts. While these methods were successful in reducing the formation of humins [16], it remains impossible to avoid them entirely. Therefore, the valorization of humins was investigated as an alternative strategy. Different approaches were investigated so far: the use of humins for the production of synthesis gas [23–25], as a precursor for porous materials [26], as a biofuel additive, or

energetic valorization by using them directly as a fuel [3]. A promising approach is the acid-catalyzed depolymerization of humins using zeolites [27,28] or polyoxometalates [4,29], as catalysts to produce humic oils as biofuel additives or low-molecular carboxylic acids. This more targeted conversion of humins into value added products showed a lot of potential for their future valorization.

In order to further develop methods for the avoidance of humin formation, it is essential to understand the mechanism behind, and to elucidate, the molecular structure of humins. Both were studied by various research groups over the past decade. The first concerted effort for their structural elucidation was made by several research groups at the beginning of the last decade [6,8]. Lund et al. first postulated a mechanism of aldol condensation between the acid-catalyzed sugar conversion intermediates 5-hydroxymethylfurfural (5-HMF) and 2,5-dioxo-6-hydroxyhexanal (DHH) [6]. This mechanism was based on prior research made by Horvat et al., who first described the reaction intermediate DHH being involved in the synthesis during the acidic conversion of hexoses [2]. Later, van Zandvoort et al. [8] expanded on these results and made a first structural proposal for more complex humins. This was also the first time it was suggested that humins are not only formed by aldol condensations, but also through other reaction types such as etherification, since substances such as levulinic acid and, additionally, added trihydroxybenzene was also incorporated into the humin structure. This was eventually confirmed by the subsequent research of multiple research groups such as Tsilomelekis et al. [13] and Shen et al. [30]. Numerous other insights were made concerning the formation of humins, resulting in the reaction mechanism for hexoses to humins by Siwei et al. in Figure 1 [9].

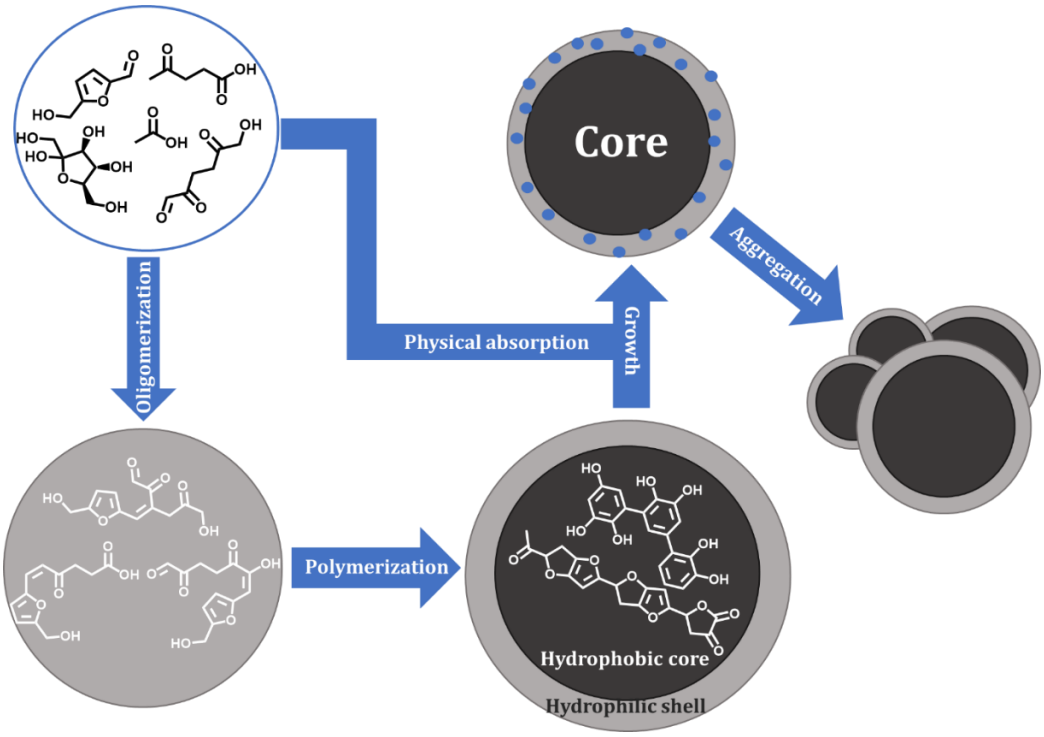

Figure 1. Process of humin formation from hexoses according to Siwei et al. [9].

First, hexoses are converted to 5-HMF and intermediates such as DHH by Brönsted-catalyzed hydrolysis. Subsequently, these intermediates react through etherification and esterification to form water-soluble oligomers, which, in turn, are connected through further reactions such as etherification, esterification, acetalization, and aldol condensations to form insoluble, hydrophobic humin cores [30–32]. These cores also possess a hydrophilic shell which is instrumental for the further growth of humins, expanding the hydrophobic core. During this process, catalysts and solvent molecules are also incorporated into the humin structure through polymerization with oligomers or through

absorption [11,13,33–35]. The resulting particles will then agglomerate step by step into a foam-like humin coke [9]. Although this research identified structural motifs of humins, details of their structure remain unknown due to their overall very complex composition. Furthermore, the influence on the formation conditions on the humin structure have not yet been thoroughly understood. We have now taken up the task to fill this gap by synthesizing humins from different sugars in various solvent/acid combinations and, subsequently, characterizing them. In contrast to previous investigations, our focus was not just the avoidance of humin formation but also the best possible valorization of the humins that are unavoidably formed. With respect to humin valorization, we took inspiration from the OxFA process, which oxidatively converts even complex biomass to formic acid using a polyoxometalate catalyst ($H_8PV_5Mo_7O_{40}$) and molecular oxygen [36,37]. This work was pioneered by Maerten et al. in 2017, who used several different polyoxometalates to convert humins to formic acid and acetic acid [29]. Similarly, we used $H_8PV_5Mo_7O_{40}$ to oxidatively convert humins that were synthesized using different sugars, solvents, and acids.

The goal of our research was to analyze the influence of the reactants on humin formation and their resulting structure to an unprecedented extent. For this purpose, we synthesized a large variety of humins through different combinations of acids and solvents. Additionally, we compared the oxidative valorization of these different humins using polyoxometalate catalysts, to identify which structural features are preferentially converted On the one hand, we aimed to identify ideal reagents for biomass conversion to avoid excessive humin formation. On the other hand, we aimed to gain the greatest value from unavoidable humin formation.

2. Materials and Methods

2.1. General Procedure for Humin Formation Experiments

For humin synthesis, all chemicals were purchased commercially and used without further purification. Acetic acid (glacial) and ethanol were obtained from VWR chemicals. Sulfuric acid (95–97%) and dimethyl sulfoxide were obtained from Grüssing GmbH. D(+)-xylose, D(+)-glucose, D(−)-fructose (all for biochemistry), and p-toluenesulfonic acid monohydrate were all obtained from Merck Millipore. Sucrose 99% was obtained from Alfa Aesar.

All experiments were conducted in a tenfold screening plant equipped with ten 20 mL Hastelloy C276 autoclaves and PTFE gaskets. All other peripheral plant components, such as valves, were made of stainless steel. This setup was able to reach reaction temperatures of up to 200 °C, and with magnetic stirring of up to 1000 rpm.

The humins formation experiments were based on the procedures of van Zandvoort et al. [6]. Several stock solutions containing either pure water or a water/organic solvent mixture in a 1:1 ratio and the chosen acidic catalyst were prepared and set to a pH of 2. Then 5 mmol of the chosen sugars were weighed into 10 mL glass liners. An amount of 5 mL of the chosen stock solution was then injected into the glass liner and the glass liner was inserted into the reactors. This acid/solvent/sugar mixture provided a molar H^+/sugar ratio of 1:100. The reactors were then heated to 180 °C at a pressure of approx. 45 bar (synthetic air) and the reaction was allowed to run for 6.5 h. After the reaction, the humins were filtered and the liquid phases sent for analysis. The humins were then rinsed with water, dried, ground in a mortar, and cleaned with water for 24 h by soxhlet extraction. The humins were then dried for 24 h at 80 °C.

2.2. General Procedure for Catalytic Oxidation of Humins

For selective catalytic oxidation experiments of humins, the polyoxometalate catalyst $H_8PV_5Mo_7O_{40}$ (HPA-5) was synthesized according to previous studies [38,39]. The molar ratio of the catalyst components was analyzed by ICP-OES. For the used catalyst, a stoichiometry of 1.2 P/5.0 V/7.0 Mo was determined.

In a typical experiment, each autoclave was loaded with 75 mg humin as substrate in a 10 mL glass liner. A stock solution containing about 28 mmol L^{-1} vanadium in the form

of a polyoxometalate catalyst was prepared. In case of $H_8PV_5Mo_7O_{40}$ catalyst, 1000 mg or 0.56 mmol of polyoxometalate, corresponding to 2.8 mmol of vanadium, was dissolved in 100 mL water. Each liner was filled with 7.5 mL of this stock solution, resulting in a carbon to vanadium ratio of about ca. 19 mol_{Carbon} $mol^{-1}{}_V$. The glass liners were then inserted into the reactors. After purging the autoclaves with 10 bar oxygen, ensuring pure oxygen atmosphere, the reactors were pressurized to a pre-pressure of about 26 bar. Subsequently, a reaction temperature of 90 °C and a stirring speed of 300 rpm for a better heat transfer were set. As a result of the temperature increase, the pressure rose to the desired reaction pressure of 30 bar and the stirrer speed was set to 1000 rpm.

After the reaction, each phase (gas, liquid, solid) was analyzed separately. For this purpose, gas samples were collected from the reactor before depressurization, and then, the liquid and solid phase were separated by filtration.

2.3. Analytical Methods

The amount of gaseous CO_2 and CO was measured using a Varian GC 450 on a 2 m × 0.53 mm (ID) Shin-Carbon-column using a TCD detector.

For the quantitative analysis of the aqueous phase (determination of soluble reaction products such as formic acid, acetic acid, and succinic acid), a SHIMADZU HPLC system outfitted with an Aminex HPX-87H 300 mm 7.8 mm BIORAD Column and a refractive index detector from SHIMADZU (Kyoto, Japan) was employed. A 5 mmol L^{-1} concentration of aqueous sulfuric acid solution was utilized as the eluent. Samples were analyzed at flow rates of 0.5 mL min^{-1}, 49 bar of pressure, and 45 °C.

A QATR^{TM}-S single-reflection ATR was used to measure AT-FT IR spectra in attenuated total reflection (ATR) measurement mode (with a diamond prism). The spectra were plotted in origin and smoothed with the Savitzky–Golay method.

The following analyses were carried out by the respective service groups in the Department of Chemistry at Hamburg University:

- The nuclear magnetic resonance (NMR) spectra were measured using a Bruker AVANCEII 600 MHz spectrometer. Samples were prepared by mixing 0.4 mL of the filtered reaction solutions with 0.2 mL of D_2O. Spectra of the reaction solutions can be found in the Supporting Information.
- Elemental analyses were carried out using the Model EA-3000 analyzer of Fa. EuroVector (Milano, Italy).
- SEM micrographs were recorded using a LEO Gemini 15505 from Zeiss (Oberkochen, Germany).
- MALDI-TOF measurements were taken with a Bruker ultrafleXtreme (Billerica, MA, USA) in positive reflector mode. A 2 mg/mL dispersion of the humic acid in water and a 20 mg/mL dihydroxybenzoic acid/TA30 (ACN/H_2O 30/70 + 0.1%TFA) solution were prepared for the measurements. A total of 0.7 µL of both solutions were then mixed and left to crystallize.

3. Results and Discussion

3.1. Influence of Sugar, Acid, and Solvent on Humin Formation, Composition, and Structure

In order to study the formation of humins, four different sugars were chosen as starting materials: fructose, glucose, xylose, and sucrose. Fructose and glucose were chosen as hexoses, allowing a comparison between aldoses and ketoses. Xylose was chosen as a pentose, because pentoses were reported to undergo a different humin formation mechanism, in which furfural is mainly involved [12]. Sucrose was used as an example for a disaccharide. These sugars were dissolved in various solvent mixtures: pure water, which is the most environmentally friendly solvent and inexpensive, as well as 1:1 mixtures of water with ethanol and with dimethylsulfoxide (DMSO). Both ethanol and DMSO are alternative polar organic solvents, with ethanol as an example of a protic and DMSO as an example of an aprotic solvent. The formation of humins is usually impeded by non-aqueous solvents [9,18,40]; therefore, we expected a molar 1:1 mixture of water and the

organic solvents to exhibit lower humin formation than pure H_2O. The sugars and solvents were combined with three different acid catalysts: sulfuric acid (pK_a of −3) was chosen as a strong inorganic acid, which is also commonly used in industrial acid catalysis [3]. Para-toluene sulfonic acid (p-TSA) (pK_a of −2.8) was used as a strong organic acid, which is also known to facilitate the solubilization of biomass [41]. Additionally, acetic acid (AA) (pK_a of 4.75) was chosen as a typical weak acid, which is also of great interest as a green acid catalyst [42]. Table 1 provides an overview of the sugar/solvent/acid combinations, and the designations for the resulting humins, which were used throughout this study.

Table 1. Matrix of the humin formation experiments.

Humin		**H_2O**			**EtOH/H_2O**		**DMSO/H_2O**
Designation	**H_2SO_4**	**p-TSA**	**AA**	**H_2SO_4**	**p-TSA**	**AA**	**H_2SO_4**
Fructose	F1	F2	F3	F4	F5	F6	F7
Glucose	G1	G2	G3	G4	G5	G6	G7
Xylose	X1	X2	X3	X4	X5	X6	X7
Sucrose	S1	S2	S3	S4	S5	S6	S7

The reaction conditions (1 mol/L sugar, pH = 2, 180 °C, 6 h reaction time) were chosen based on previous investigations by van Zandvoort et al. [8]. These conditions were shown to produce high yield of humins without the humins taking on the form of a foamy coke, which occurs when using higher temperatures or concentrations. In order to prevent the solvent from evaporating, a pressure of 45 bar of a 1:4 O_2/N_2 mixture was applied (for details, see Section 2). The initially homogeneous solutions were not stirred during the reaction time, because humin formation would have caused the stirrers to seize in the small reaction vessels.

In order to determine sugar conversion (Table 2), all reaction solutions were investigated via magnetic resonance spectroscopy (^{1}H- and ^{13}C-NMR) as well as high performance liquid chromatography (HPLC). All relevant spectra can be found in Figures S1–S16 in the Supporting Information. Most of the NMR-spectra showed no sugar signals, which corresponds to a conversion of 100%. In cases where sugar was still present, the residual amount of sugar was quantified by HPLC to determine the conversion. Fructose and xylose achieved full conversion in all reactions, while glucose and sucrose showed lower conversions in water. This confirmed van Zandvoort's results [8]. The different conversions of glucose and fructose can be explained by the fact that fructose directly forms HMF and DHH, since it possesses a more stable ring structure, while glucose must first isomerize to fructose before reacting further to HMF and DHH [5,7,43,44]. Accordingly, sucrose also has a lower conversion, being a dimer of glucose and fructose, which must first be hydrolyzed into the monomeric sugars during the conversion process, with subsequent isomerization of glucose to fructose and conversion of the latter. This interpretation is supported by the NMR spectra (Figures S1 and S2 in the Supporting Information), as the sugar signals of the glucose and sucrose reaction solutions are identical. As the other sugars are completely converted, an effect of the acid can only be observed for the conversion of glucose in the following trend: stronger acids lead to higher conversion.

Table 2. Sugar conversion in humin formation experiments.

	H_2O			**EtOH/H_2O**			**DMSO/H_2O**
X (%)	**H_2SO_4 [a]**	**p-TSA [a]**	**AA [a]**	**H_2SO_4 [b]**	**p-TSA [b]**	**AA [b]**	**H_2SO_4 [b]**
Fructose	100	100	100	100	100	100	100
Glucose	90	74	69	100	100	100	100
Xylose	100	100	100	100	100	100	100
Sucrose	90.5	94	84	100	100	100	100

Experimental Conditions: 10-fold reaction system, 180 °C, 45 bar (1:4 O_2/N_2), 5 mL substrate mixture with 1 M sugar, pH 2, 6 h. [a] Determined through HPLC (Equation (S1)). [b] Determined by ^{1}H-NMR.

The NMR spectra additionally allowed the identification of certain intermediates (Figures S1 and S2 in the Supporting Information). Large amounts of formic acid, acetic acid, and levulinic acid were found in the aqueous reaction solutions of hexoses and sucrose. In addition, small amounts of 5-HMF were found in the NMR spectra of the acetic acid-catalyzed reaction solutions. This was a remarkable observation because weaker acids usually result in lower HMF yields [45,46], but here, HMF was only found in the reaction with the weakest acid. We assumed that during the reaction catalyzed by strong acids, all 5-HMF was polymerized to humins. In the EtOH/H_2O mixtures, the same intermediates were found, next to additional compounds resulting from reactions with the solvent, such as diethyl ether, acetic acid, and ethyl acetate (Figures S7 and S8 in the Supporting Information). Using a DMSO/H_2O mixture, formic acid was the only intermediate observed. However, additional signals here indicate decomposition products of DMSO, such as dimethyl sulfide and dimethyl disulfide (Figures S15 and S16 in the Supporting Information). This also indicates that DMSO is not stable under the applied reaction conditions.

The humins formed in these experiments were washed with water by Soxhlet extraction to remove any adsorbed soluble intermediates and were, subsequently, dried at elevated temperatures, ultimately resulting in powdery solids with a brown or black color (Figure 2). The syntheses in the purely aqueous solutions and the DMSO containing solutions resulted in black humins, while the syntheses in the solutions containing ethanol resulted in brown humins.

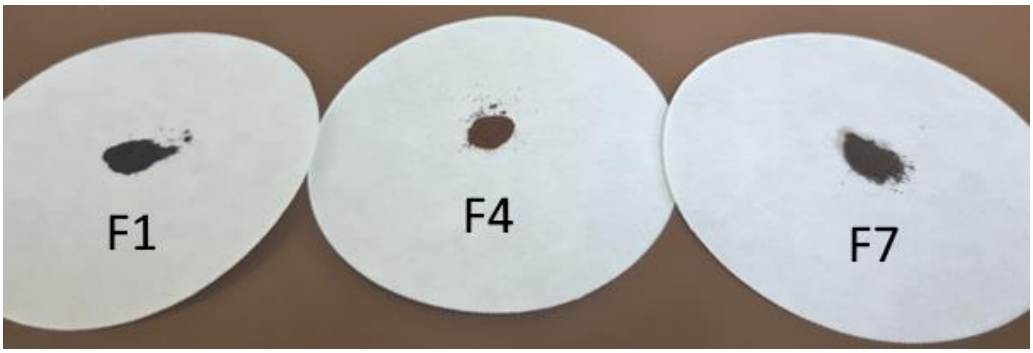

Figure 2. Humins obtained from fructose in different solvents using sulfuric acid as strong Brönsted acid.

Although the achieved conversion rates were high, the yield of humins (Figure 3) remained comparatively low, indicating that a large amount of the initial carbon remained in soluble intermediates. Generally, experiments using fructose (F1–F7) and sucrose (S1–S7) provide higher yields than glucose (G1–G7) and xylose (X1–X7), respectively. For glucose, this corresponds to the lower conversion of the sugar (Table 2). The reason for the lower humin yield resulting from xylose might be its shorter chain length, which impedes the formation of stable cyclic structures, and results in more soluble oligomeric intermediates.

This trend was not observed in reactions performed in DMSO (F7, G7, X7, and S7); however, in these cases, a substantial amount of solvent (and decomposition products) was incorporated into the humin structure (vide infra), thereby skewing the yield which was calculated relative to the initial amount of carbon in the sugar. In pure water, similar yields (approx. 45%) were obtained from sucrose (S1–S3) for all acids used. In the ethanol/water mixture, p-TSA showed a similar yield (S5), but H_2SO_4 (S4) and acetic acid (S6) formed less humin. The latter effect was also observed for glucose and fructose, whereas with xylose, all acids resulted in a higher yield in ethanol/water. In EtOH/H_2O, the yield of all sugars, with the exception of xylose, decreased significantly when acetic acid was used. This might partially be caused by esterification of acetic acid with ethanol, making the catalyst less effective. The humin yields of the reactions using the weaker acid p-TSA were generally higher than those using the stronger sulfuric acid. However, the yields of

F6, G6, X6, and S6 were all lower than those of using p-TSA and sulfuric acid. Although weaker acids should provide greater humin yields, this was the case, even though the usage of weaker acids should provide greater humin yields [45,46]. The lower yields were also consistent with the literature, as organic solvents were known to reduce the yield of humins [9,18,40]. It was, therefore, assumed that more soluble oligomers were formed by reactions of the intermediates of the sugar conversion with the resulting acetic acid and ethanol. These oligomers were then absorbed into the humin but were lost during purification and were, therefore, not considered when determining the yield. This was particularly evident with G6, where no solid was recovered in two subsequent replication attempts. The increased formation of soluble oligomers would also explain why, despite the lower humin yield, complete conversion of all sugars in the organic solvents was observed (Table 2). However, the xylose humins were excluded from this general trend, as their yields in organic solvents were greater than in pure water. Interestingly, this directly contradicted a study by Köchermann et al. which obtained lower yields from a similar mixture of xylose in ethanol and sulfuric acid than from a water/sulfuric acid mixture [47].

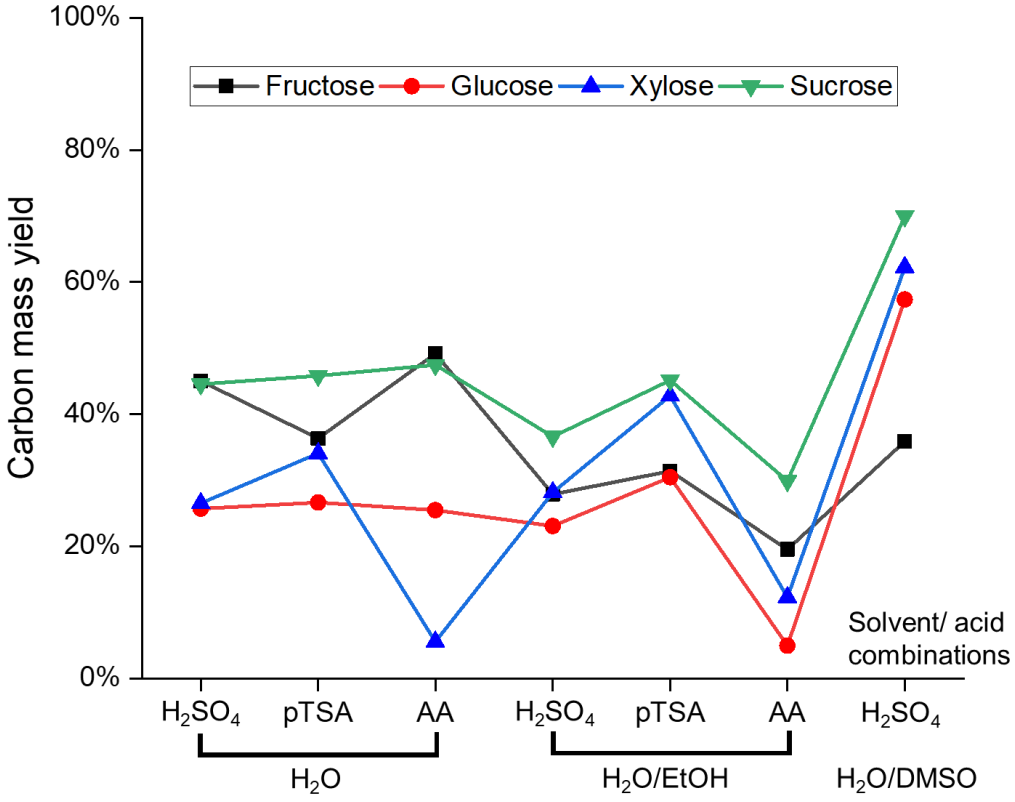

Figure 3. Overview of yields in humin formation experiments (determined with Equation (S1)).

In summary, for the goal of avoiding humin formation, the use of acetic acid in EtOH/H_2O using glucose as a substrate (G6), and the use of acetic acid in H_2O for xylose (X3), provided the best results with a humin yield of only around 5%. Aside from DMSO, which was the worst solvent of the tested selection, fructose and sucrose in neat water resulted in the highest humin formation regardless of the acid used.

With regard to the valorization of humins, their elemental composition and structural characteristics are of great importance. Therefore, we analyzed a selection of the obtained humins by elemental analysis (CHSO), electron microscopy (SEM), infrared spectroscopy (IR), and matrix-assisted laser desorption time-of-flight mass-spectrometry (MALDI-TOF MS).

The elemental composition of the synthesized humins from the different sugars was almost identical (Figure 4); only the xylose humin deviated slightly, as it possessed slightly lower H/C and O/C ratio. This confirmed the research carried out by van Zandvoort et al.

in 2013. [8]. Their investigations showed that the elementary composition of the humins obtained from fructose and glucose hardly differed from one another. It is no surprise that sucrose as a dimer of fructose and glucose produced the same result.

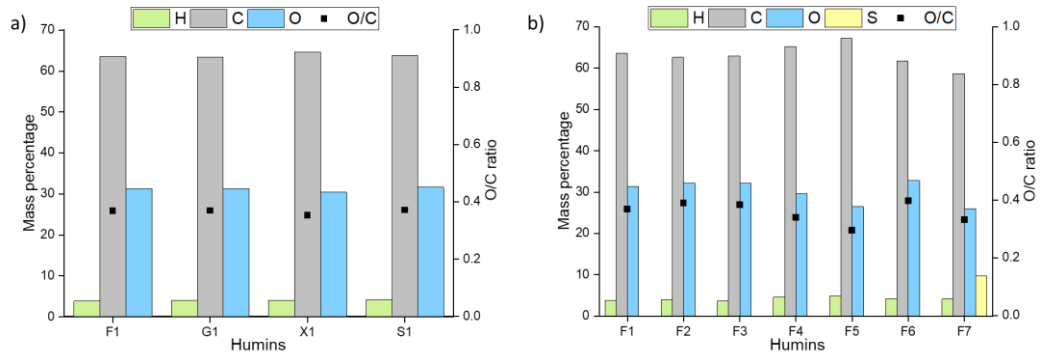

Figure 4. Elemental analysis of synthesized humins; (**a**) humins synthesized with sulfuric acid in water (**b**) humins synthesized from fructose using different acids and solvent mixtures (for elemental composition of used sugars, see Table S2).

Very interestingly, various acidic catalysts and solvents had a significant effect on the elemental composition of the resulting humins. Most notable was the presence of a significant sulfur content of about 10% for F7, which was likely due to DMSO and its decomposition products being incorporated into the humin structure. Together with the slightly lower carbon content and a hydrogen content which is similar to the other humins, this indicates the formation of thioethers/-esters in the humin structure. For humins synthesized in neat water, the oxygen content increases with decreasing strength of the acidic catalyst. This indicates that during humin formation weaker acids are more likely to catalyze esterification or etherification than aldol condensation. However, in the ethanol/water mixture, the oxygen content initially decreased sharply between sulfuric acid and p-TSA, and then, again rose up to the highest level at the weakest acid. The oxygen content of F6 here corresponded closely to that of F3. This similarity could be due to the large amount of acetic acid in both reaction solutions. Presumably, insoluble oligomers were increasingly formed here from the acetic acid and the sugars or intermediates, in which mostly ether or ester bonds were present, leading to an increased oxygen ratio. In contrast, F5 stands out due to possessing the highest hydrogen and carbon content of all fructose humins. This would indicate a high number of alkyl bonds in the humin, which could possibly indicate that, under these reaction conditions, primarily aldol condensations could be responsible for the humin formation. To a lower extent, this applies to F4 as well.

In order to further elucidate structural differences of the humins, the materials were further investigated by infrared spectroscopy (Figure 5).

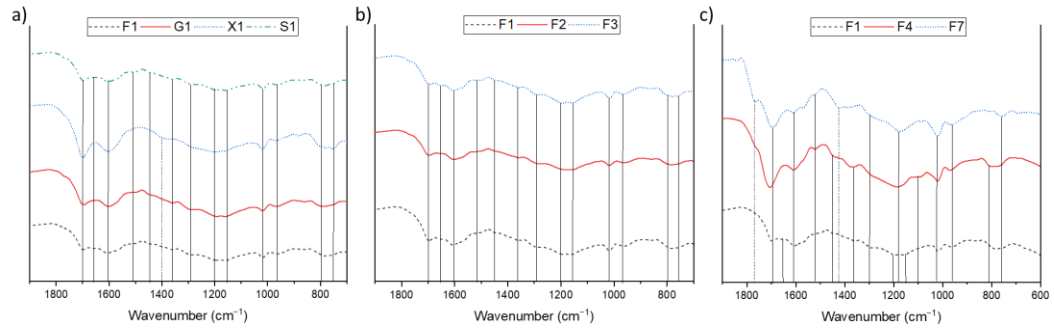

Figure 5. IR-spectra of different humins; (**a**) humins of different sugars catalyzed by sulfuric acid in neat water (**b**) fructose humins using different acids in water (**c**) fructose humins catalyzed with sulfuric acid in various solvents.

In the IR spectra of all humins, the typical signals of substituted furans (C=C vibrations at 1600 cm^{-1} and 1510 cm^{-1}, C-H out of plane vibrations at 750 cm^{-1} and 795 cm^{-1}) were observed, which are common for humins from sugars [6,8,9,13,25,48]. Additionally, ether, carbonyl, and aliphatic chains were identified (Table 3). Sulfur containing structural features, e.g., thiols, were identified for the humins formed in DMSO (Figure 5c and Figures S17–S20 in the Supporting Information).

Table 3. Assignment of IR-spectra bands.

Wavenumber [cm^{-1}]	Assignment
750 + 795	C-H Out of plane vibration substituted furan ring
965	C-H vibration furan ring
1020	C=C stretch vibration
1090	C-O-C ether vibration
1160 + 1200	C-O-C deformation vibration furan ring
1295	C-H rocking vibration
1360	C-C framework vibration (furan) C6 sugars
1395	C-C framework vibration (furan) C5 sugars
1420	C=S stretch
1460	C-H aliphatic chain vibration
1510	C=C vibration aromatic double bonds of poly substituted furans
1600	C=C stretch vibration conjugated with carbonyl
1670	C=O carbyonyl, aldehyde vibrations
1700	C=O stretch of acids, aldehydes and ketons
1775	C-S Thioester

As expected, the spectra of humins formed from the hexoses and from sucrose were all very similar (Figure 5a). The spectrum of the xylose-based humin, on the other hand, differed significantly from the hexoses in three signals: the 1700 cm^{-1} band was much more pronounced here than with the other sugars, the 1670 cm^{-1} carbonyl vibrational bands were absent, and the signal of the framework vibrations was also shifted by approx. 35 cm^{-1}. The carbonyl vibration was usually caused by the inclusion of 5-HMF into the humin structure, its absence was to be expected since humins from pentoses form via furfural and not 5-HMF [6,9]. The large difference concerning the 1700 cm^{-1} band could indicate that fewer aldol condensations were involved in the formation of xylose humins than in the formation of humins of other sugars. This different bonding pattern in the humin presumably also caused the shift in the framework vibration.

Comparing the humins formed by different acids, no major differences were observed in the IR spectra (Figure 5b). Only minor variations, such as the 1700 cm^{-1} band of F2 being slightly smaller, were identified. This suggests that the greater proportion of oxygen in this humin can be attributed to increased presence of ether bonds in the structure. The 1670 cm^{-1} band of F2 was also less pronounced. This matches the prior observation of the acetic acid catalyzed humins taking up all of the formed 5-HMF.

The biggest differences were found when comparing the humins derived from different solvents (Figure 5c). For the humin formed in DMSO (F7), two additional bands were found at 1775 cm^{-1} and 1420 cm^{-1}. The former was presumably a signal caused by thioesters, while the latter was a signal from a C=S stretching vibration. These were caused through the incorporation of decomposition products of DMSO that were taken into the humin structure, as previously discussed. In addition, the signal of the furan out of bound oscillation at 795 cm^{-1} was no longer present with F7. This indicates that the specific furan structures were not present in this specific humin in contrast to the other humins. This probably also resulted from reactions with the sulfur-containing compounds. The 1700 cm^{-1} band was significantly weaker for F1 than for F5 and F7, corresponding to an increased number of esters and carbonyls in the latter materials. This indicates a larger number of esters and ethers being formed in ethanolic solution. This also explains the more intense peak at 1090 cm^{-1} compared with the other humins, since this signal corresponded to the C-O-C ether vibration of ethyl ethers. In contrast, the 1670 cm^{-1} carbonyl vibrational

band was absent in both humins derived from partially organic solvents. This could either be due to the fact that less 5-HMF was involved in the humin formation or that the signal was overshadowed by the much larger 1700 cm^{-1} bands.

For additional structural investigations, selected humins (F1-3, G1, X1, and S1) were analyzed by MALDI-TOF MS (Figures S21–S32 in the Supporting Information). The goal was to identify common structural fragments by their m/z ratio; therefore, the main focus was the identification of similarities in the spectra. Although we were not able to detect the structural fragments postulated by Hoang et al. or Chen et al. [25,49], three fragments could be identified that repeatedly appeared in the humins (Figure 6).

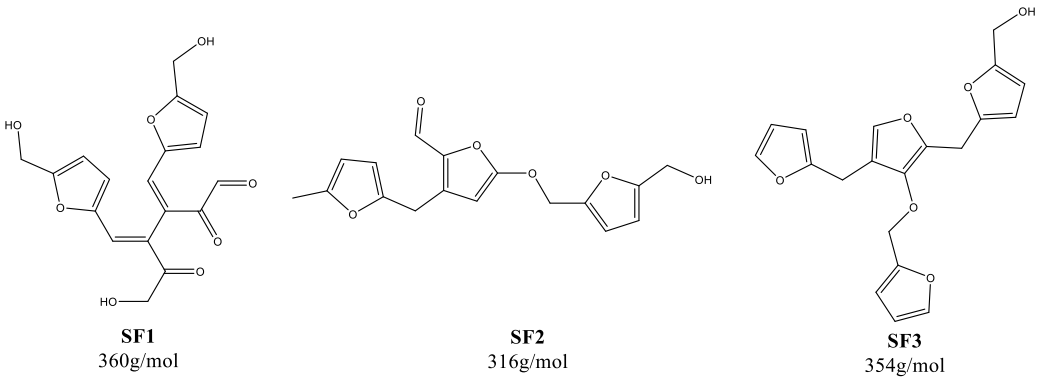

Figure 6. Postulated humin fragments based on mass spectra.

Fragment SF1 with a mass of 360 g/mol was the product of the aldol condensation of DHH with two HMF molecules. A similar fragment, consisting of DHH and HMF was previously reported by Chen et al. [49]. This interpretation was further confirmed by the fact that the relevant peak did not appear in the mass spectrum of the xylose humin, since HMF and DHH did not form the basis for humin formation here. The other two fragments with 316 g/mol and 354 g/mol, respectively, were more difficult to assign. Despite the different degradation mechanisms of hexoses and pentoses, they both appeared in humins based on hexoses as well as xylose. The proposed structures SF2 and SF3 were based on that fact and on previous analytical results.

With regard to the oxidative valorization of humins, their molecular structure and their particle morphology and size is important. Differences between humins based on different sugars were already examined by electron microscopy and were discussed sufficiently in a previous study [8]. Therefore, SEM micrographs were only taken of selected fructose-based humins (Figure 7), to investigate the influence of solvents and acid catalysts.

The fructose-based humins formed in water possess the typical humin structure of interconnected spheres, the main point of difference being the average particle sizes. Sulfuric acid-catalyzed humin particles were the smallest, while the p-TSA catalyzed ones were the largest, whereby the acetic acid resulted in an intermediate particle size. We, therefore, concluded that particle size was not related to the acid strength. The differences in particle size may also result from the erratic nature of humin formation as humin morphology itself varied greatly in the same reaction, as can also be seen on the micrographs [9]. This would indicate that the morphology of humins was unaffected by the acidic catalyst.

Exceptions in the morphology were the humins F4 (from EtOH/water) and F7 (from DMSO/water), which showed significant deviations from the spherical humin particles.

F4 seemed to consist of larger splinter-like fragments and a multitude of small amorphous particles were observed. F7 also featured splinter-like structures, although these had a slightly different appearance. The splinters of F7 did not appear as uniform as those of F4, a kind of fragmentation of the splinters was observed here.

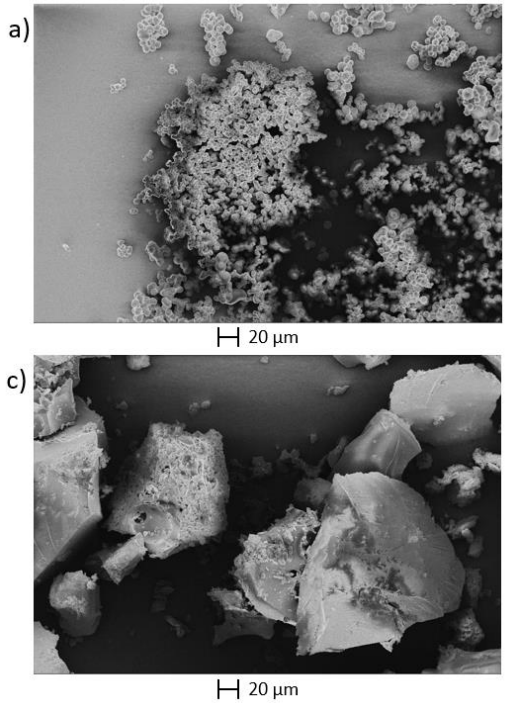

Particle size [µm]	F1	F2	F3
average	4.15	6.39	5.30
deviation	0.94	1.19	2.05

Figure 7. SEM micrographs of different humins: (**a**) F1, (**b**) F4, (**c**) F7, (**d**) average particle sizes of spherical humins.

Overall, the analysis showed that the solvent had the greatest influence on the structure of the humins formed. Sugar and acidic catalyst choice seemed to have a lesser influence.

3.2. Oxidative Conversion of Humins Using Polyoxometalate Catalysts

In the second part of our study, we investigated the potential for valorization of the synthesized humins. To this end, we chose a procedure inspired by the OxFA process [36] and previous work by Maerten et al. [29] and Raabe et al. [25]. Therefore, the humins were first dispersed in an aqueous solution containing the homogeneous polyoxometalate catalyst ($H_8PV_5Mo_7O_{40}$), and were then oxidized using molecular oxygen in a high-pressure autoclave. After reaction, the composition of the gas phase was analyzed by GC and the composition of the liquid phase was determined by HPLC. Due to the sticky nature of the used humins, the combined yield (mol% C in gas phase + mol% C in liquid phase) was used as an indicator for humin conversion.

Figure 8 shows two comparisons: on the left side (Figure 8a), humins derived from different sugars are compared with respect to the composition of their reaction mixtures after oxidation for 15 h. Hereby, only minor differences in terms of the product composition could be observed. Still, between 40% (S1 and G1) and 55% (X1) of the carbon remained in the solid residue after filtration. The main products for all humins were CO_2, acetic acid, formic acid, and succinic acid. Moreover, only traces of CO could be detected in all experiments. Table 4 gives an overview of the different product yields.

On the right hand side (Figure 8b), fructose-derived humins synthesized using different acids and solvents are compared with respect to the composition of their reaction mixtures after oxidation for 15 h. Hereby, higher differences both in combined yield as well as product composition were observed. In detail, the humins synthesized in water (F1–F3) showed a clear trend that combined yield and, therefore, conversion increases with decreasing pk_a. Therefore, using acetic acid as an acid source achieved the highest combined yield, whereby sulfuric acid showed the lowest. In terms of product composition, only minor differences could be detected (see Table 5). The humins synthesized in ethanol (F4–F6) showed a different behavior. Generally, higher carboxylic acid yields could be achieved compared to using water as a solvent (for details, see Table 5). The higher yields

of acetic acid and formic acid presumably resulted from the higher degree of etherification and esterification products of ethanol, its oxidation products, and the sugar decomposition products in the reaction solution taken up in the humins. Humin F6, therefore, showed the highest product yields of all converted humins, as the larger amount of acetic acid appeared to increase the formation of the ether and ester containing compounds in the humin. The higher yields for the liquid-phase products of the humins synthesized in ethanol could be due to alcohols absorbed in the humins, as alcohols such as methanol increase liquid-phase yields in HPA-5 catalyzed syntheses and reduce the yields gained through total oxidation of biomass such as CO_2 [50]. F5, again, showed a lower combined yield as F4 and F6. The lower O/C ratio of F5 could be a factor here, as it indicates a lower number of ether and ester bonds, although this does not explain the lower combined yield of F2 in comparison to F1 and F3. This could also be an explanation for the differences in yields between F1, G1, X1, and S1, as the humins with the highest yields (G1 and S1) showed the highest O/C ratios. The lowest combined yield of all converted humins, however, was shown by the humin F7. Interestingly, this humin showed the highest yield of carboxylic acids and, consequently, the lowest CO_2 yield. Thioesters and -ethers were only poorly converted, while aliphatic ether and ester bonds showed a better performance.

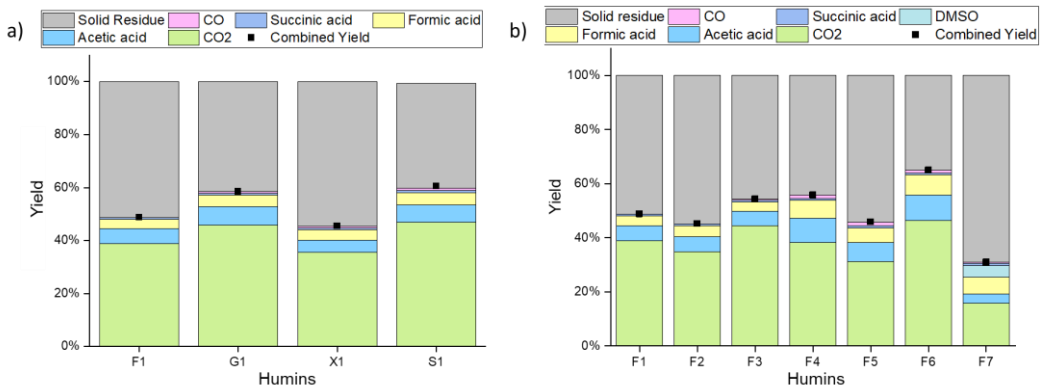

Figure 8. Oxidative conversion of humins using HPA-5 as a catalyst; reaction conditions: m (humin) = 75 mg, m(HPA-5) = 7.5 mg, T = 90 °C, t = 15 h, *p* = 30 bar O_2 in 7.5 mL water as a solvent. (**a**) humins derived from different sugars (**b**) humins synthesized using different acids and solvents (determined via Equation (S3)).

Table 4. Product yields using different sugar-derived humins; reaction conditions: m (humin) = 75 mg, m(HPA-5) = 7.5 mg, T = 90 °C, t = 15 h, *p* = 30 bar O_2 in 7.5 mL water as a solvent.

(a) Product Yields	**F1**	**G1**	**X1**	**S1**
CO_2	39%	46%	36%	47%
Acetic acid	6%	7%	5%	7%
Formic acid	4%	4%	4%	5%
Succinic acid	1%	1%	1%	1%
Combined Yield	49%	59%	45%	61%

Comparing the elemental analyses of the solids before (Tables S3–S6) with the residues after reaction (Tables S9–S11), all humins show lower carbon percentages while the oxygen percentages increased. Therefore, the oxygen to carbon ratio in the humins increased on average by a factor of 1.5. From this fact, we conclude that the residual materials have more carbonyl and hydroxy functionalities due to the catalytic oxidation. The hydrogen proportions did not change significantly. The above described trends between the humins generally remained constant.

Table 5. Product yields using fructose-derived humins using different acids and solvents; reaction conditions: m (humin) = 75 mg, m(HPA-5) = 7.5 mg, T = 90 °C, t = 15 h, *p* = 30 bar O_2 in 7.5 mL solvent.

(a) Product Yields	F1	F2	F3	F4	F5	F6	F7
CO_2	39%	35%	44%	38%	31%	46%	16%
Acetic acid	6%	6%	5%	9%	7%	9%	3%
Formic acid	4%	4%	3%	7%	5%	7%	6%
Succinic acid	1%	1%	1%	1%	1%	1%	1%
Combined Yield	52%	61%	65%	74%	53%	82%	73%

In order to confirm which structural features of the humins were preferentially broken down during the oxidative treatment, we compared the IR spectra of the humins and their solid residues after the reaction (Figure 9 and Figures S42–S49).

The comparison of the spectra before and after the oxidation process revealed significant differences: the bands corresponding to poly substituted furan rings (795 cm^{-1}, 1510 cm^{-1}), aldehydes, and ethers (1090 cm^{-1}, 1670 cm^{-1}), and aliphatic chains (1295 cm^{-1}, 1460 cm^{-1}) disappeared completely. The signals belonging to unconjugated double bonds (1020 cm^{-1}) and esters (1700 cm^{-1}) were much weaker. The band corresponding to carbonyl conjugated C=C double bonds (1600 cm^{-1}), on the other hand, became more intense and shifted to slightly lower wavenumbers. Together, this indicates that ethers and esters were converted very well in the HPA-5 catalyzed oxidation.

This also explains the decrease in the signals corresponding to substituted furan rings and aliphatic chains. If the aliphatic chains were linked via ether or ester bonds, they would consequently also be broken down. The most interesting observation here was the disappearance of the vibration band at 795 cm^{-1}, indicating substituted furan rings, which apparently were no longer present after the conversion. Therefore, it is reasonable to assume that this signal corresponded to furan rings that were connected through by ester or ether bonds which were broken down. This also indicates that in the structure of the humins that were produced in the DMSO-containing solution, these furan esters/ethers occurred little or not at all, explaining the lower conversion of F7. However, this did not explain the apparent disappearance of the band corresponding to C=C double bond vibration of substituted furans (1510 cm^{-1}). A disappearance of this band could normally indicate a splitting of the furan rings, but since all other signals of the furan rings were generally unchanged, it was assumed that the signal was swallowed up by the more intense signal of the carbonyl conjugated double bonds at 1600 cm^{-1}. The increase in this vibration band was due to the oxidation of the remaining insoluble humin residues. Together with the results from elemental analysis, which showed that the O content increased, this indicates that alkyl groups or furan rings which could not be cleaved were oxidized to form either double bonds or ketones. This would drastically increase the number of double bonds conjugated to a carbonyl compound in the humins, explaining the much more intense signal at 1600 cm^{-1}, and would simultaneously explain the loss in intensity of the band corresponding to unconjugated C=C double bonds (1020 cm^{-1}). In addition to these changes in the vibration bands, some entirely new peaks could be found in the range between 1000 and 1100 cm^{-1}. These signals most likely belonged to the catalyst HPA-5, as IR spectra of the catalyst showed asymmetric stretching vibrations of the P-O bonds in the range from 1041 to 1066 cm^{-1}. The vibrational band at 965 cm^{-1} could also have been influenced by the catalyst, since HPA-5 showed an intensive signal from the M=O bond at this wavenumber [51].

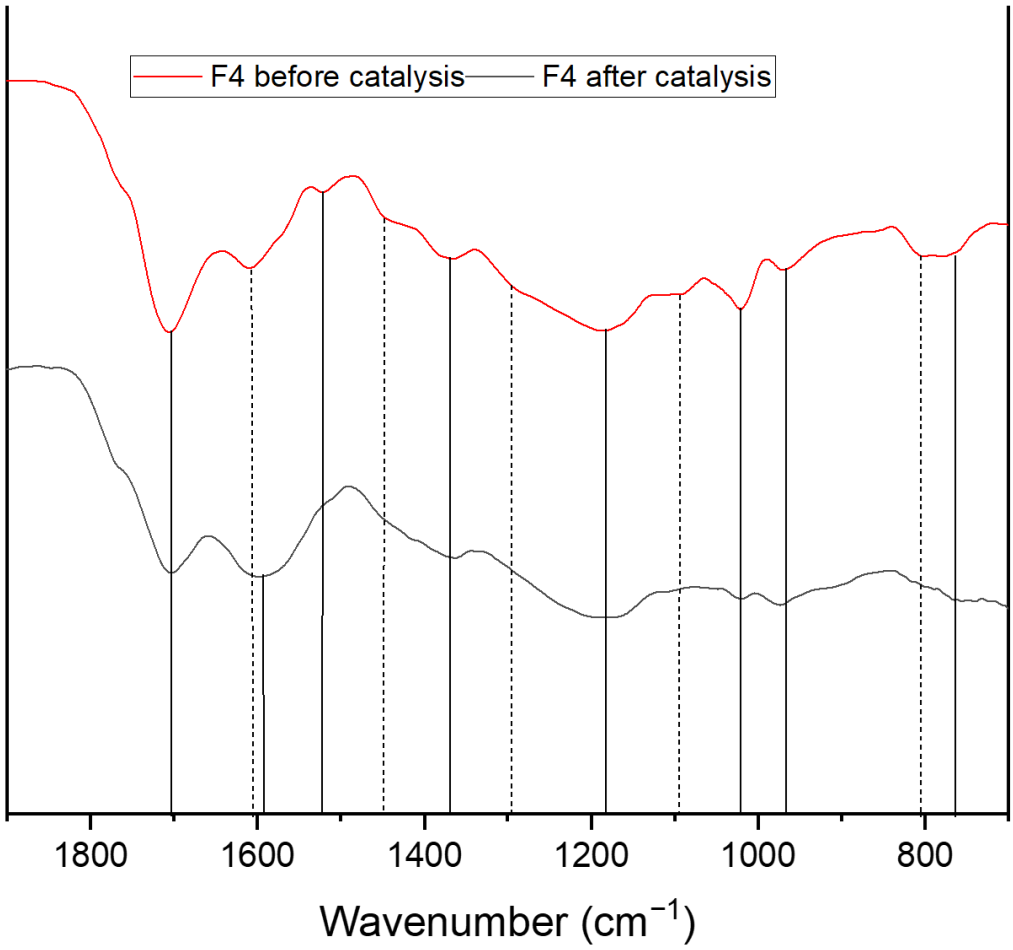

Figure 9. IR-spectra of F4 before and after the oxidative catalysis with HPA-5.

As morphological differences between the humins before the catalytic oxidation were primarily observed between humins from different solvents, F1, F4, and F7 were further studied by electron microscopy after conversion (Figure 10).

The images of F1 after the reaction (Figure 10a,b) show that the material was not comprised out of spherical particles anymore. Instead, they were fused to an amorphous cluster, as if they had melted. The particles of F4 and F7, on the other hand, appeared mostly unchanged after the oxidative treatment. The amorphous particles visible in Figure 7b,c completely disappeared from the structure and only the splinter-like particles were left, but here, they no longer had a rough surface. It seems as if primarily agglomerated oligomers were converted by the oxidative catalysis but the polymer core structures were not affected.

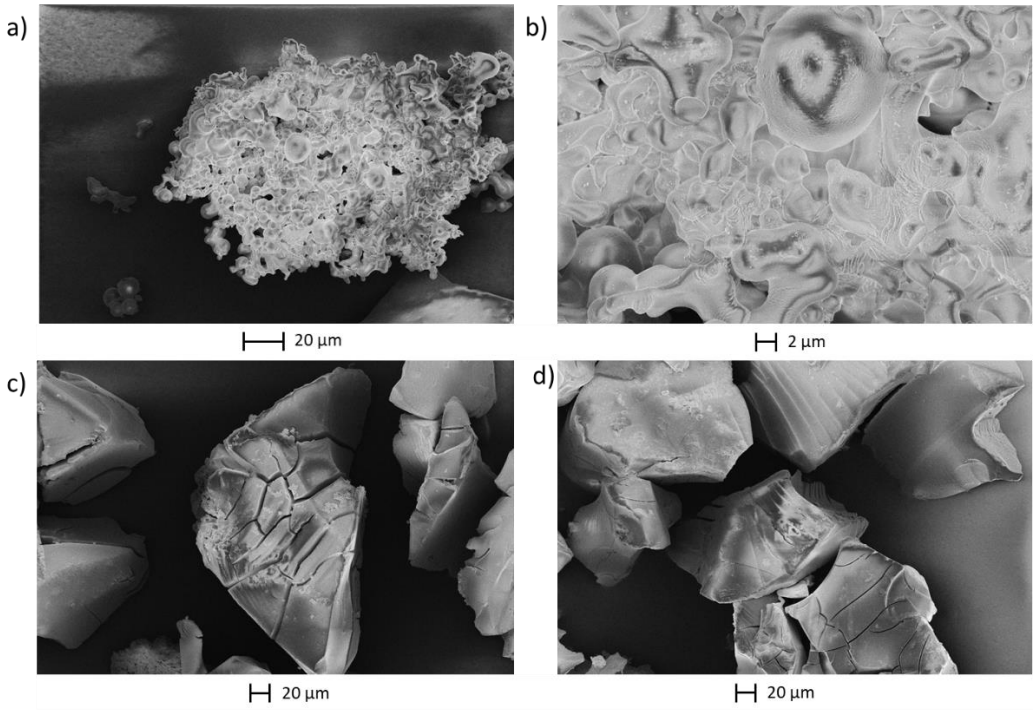

Figure 10. SEM micrographs after the oxidative catalysis with HPA-5 (**a**) F1 (**b**) F1 zoomed in (**c**) F4 (**d**) F7.

4. Conclusions

In summary, the formation of humins was studied in 28 different substrate/solvent/acid combinations. Differences between the liquid and solid phase of each experiment were analyzed by selected analytical methods. We found that the choice of solvent had the greatest influence on the molecular structure and the yield of the synthesized humins. By comparing the MALDI-TOF MS spectra and infrared spectra of the many different humins, we were able to identify various functional groups such as furan rings, ethers, and carbonyl moieties. Furthermore, we were able to identify three distinct structural fragments, with two of these fragments being found in each of the analyzed humins.

With respect to the valorization of the humins, the polyoxometalate ($H_8PV_5Mo_7O_{40}$) catalyzed oxidation was partially successful. In most cases, half of the humin mass could be converted. Unfortunately, the main product was CO_2, which only possessed limited economical applications. However, more valuable products such as acetic acid, formic acid, and succinic acid could also be obtained. Humin F6, which was formed from fructose in EtOH/H_2O using acetic acid, was converted particularly well, yielding larger quantities of acetic acid and formic acid than all other humins. From the correlation between humin structure and conversion, we conclude that ether and ester groups were converted very well by catalytic oxidation, while thioester and ether groups were only poorly converted. The furan-containing core structure of the humins remained mostly unaffected by the catalytic oxidative treatment.

Overall, the yield in the humin synthesis was the lowest for the humins with acetic acid as the catalyst and the ethanol/water solution as the solvent and F6 showed the greatest potential for valorization. Therefore, we suggest that the EtOH/H_2O/acetic acid system is the ideal choice for gaining the maximum value from sugars. These findings could potentially be used to reduce the formation of humins in a sustainable synthesis of levulinic acid and, furthermore, to convert the low amount of unavoidable humins into valuable substances.

Supplementary Materials: The following supporting information can be downloaded at: https://www.mdpi.com/article/10.3390/ma16072864/s1.

Author Contributions: Investigation, A.W. and M.J.P.; Data curation, T.E.; Writing—review & editing, J.A. All authors have read and agreed to the published version of the manuscript.

Funding: This research was funded by the Deutsche Forschungsgemeinschaft grant number AL 2130/5-1 and the APC was waived by MDPI.

Institutional Review Board Statement: Not applicable.

Informed Consent Statement: Not applicable.

Data Availability Statement: Data is provided in the Supplementary Information File.

Conflicts of Interest: The authors declare no conflict of interest.

References

1. Chheda, J.N.; Huber, G.W.; Dumesic, J.A. Liquid-Phase Catalytic Processing of Biomass-Derived Oxygenated Hydrocarbons to Fuels and Chemicals. *Cheminform* **2007**, *38*, 7164–7183. [CrossRef]
2. Horvat, J.; Klaic, B.; Metelko, B.; Sunjic, V. Mechanism of Levulinic Acid Formation. *Tetrahedron Lett.* **1985**, *26*, 2111–2114. [CrossRef]
3. Hayes, D.J.; Fitzpatrick, S.; Hayes, M.H.B.; Ross, J.R.H. The Biofine Process—Production of Levulinic Acid, Furfural, and Formic Acid from Lignocellulosic Feedstocks. In *Biorefineries-Industrial Processes and Products*; Wiley: Weinheim, Germany, 2005; pp. 139–164.
4. Maerten, S. *Humine: Bildung Und Wertschöpfung*; Rwth Publications: Aachen, Germany, 2018.
5. Corma, A.; Iborra, S.; Velty, A. Chemical Routes for The Transformation of Biomass into Chemicals. *Chem. Rev.* **2007**, *107*, 2411–2502. [CrossRef] [PubMed]
6. Patil, S.K.R.; Lund, C.R.F. Formation and Growth of Humins Via Aldol Addition and Condensation During Acid-Catalyzed Conversion of 5-Hydroxymethylfurfural. *Energy Fuels* **2011**, *25*, 4745–4755. [CrossRef]
7. Patil, S.K.R.; Heltzel, J.; Lund, C.R.F. Comparison of Structural Features of Humins Formed Catalytically from Glucose, Fructose, and 5-Hydroxymethylfurfuraldehyde. *Energy Fuels* **2012**, *26*, 5281–5293. [CrossRef]
8. Van Zandvoort, I.; Wang, Y.; Rasrendra, C.B.; Van Eck, E.R.H.; Bruijnincx, P.C.A.; Heeres, H.J.; Weckhuysen, B.M. Formation, Molecular Structure, and Morphology of Humins in Biomass Conversion: Influence of Feedstock and Processing Conditions. *Chemsuschem* **2013**, *6*, 1745–1758. [CrossRef]
9. Liu, S.; Zhu, Y.; Liao, Y.; Wang, H.; Liu, Q.; Ma, L.; Wang, C. Advances in Understanding the Humins: Formation, Prevention and Application. *Appl. Energy Combust. Sci.* **2022**, *10*, 100062. [CrossRef]
10. Kang, S.; Zhang, G.; Yang, X.; Yin, H.; Fu, X.; Liao, J.; Tu, J.; Huang, X.; Qin, F.G.F.; Xu, Y. Effects of P-toluenesulfonic Acid in The Conversion of Glucose for Levulinic Acid and Sulfonated Carbon Production. *Energy Fuels* **2017**, *31*, 2847–2854. [CrossRef]
11. Cheng, Z.; Goulas, K.A.; Quiroz Rodriguez, N.; Saha, B.; Vlachos, D.G. Growth Kinetics of Humins Studied via X-ray Scattering. *Green Chem.* **2020**, *22*, 2301–2309. [CrossRef]
12. Cheng, B.; Wang, X.; Lin, Q.; Zhang, X.; Meng, L.; Sun, R.-C.; Xin, F.; Ren, J. New Understandings of The Relationship and Initial Formation Mechanism for Pseudo-Lignin, Humins, and Acid-Induced Hydrothermal Carbon. *J. Agric. Food Chem.* **2018**, *66*, 11981–11989. [CrossRef]
13. Tsilomelekis, G.; Orella, M.J.; Lin, Z.; Cheng, Z.; Zheng, W.; Nikolakis, V.; Vlachos, D.G. Molecular Structure, Morphology and Growth Mechanisms and Rates of 5-Hydroxymethyl Furfural (Hmf) Derived Humins. *Green Chem.* **2016**, *18*, 1983–1993. [CrossRef]
14. Thapa, I.; Mullen, B.; Saleem, A.; Leibig, C.; Baker, R.T.; Giorgi, J.B. Efficient Green Catalysis for The Conversion of Fructose to Levulinic Acid. *Appl. Catal. A Gen.* **2017**, *539*, 70–79. [CrossRef]
15. Velaga, B.; Parde, R.P.; Soni, J.; Peela, N.R. Synthesized Hierarchical Mordenite Zeolites for The Biomass Conversion to Levulinic Acid and The Mechanistic Insights into Humins Formation. *Microporous Mesoporous Mater.* **2019**, *287*, 18–28. [CrossRef]
16. Dee, S.J.; Bell, A.T. A Study of The Acid-Catalyzed Hydrolysis of Cellulose Dissolved in Ionic Liquids and the Factors Influencing the Dehydration of Glucose and The Formation of Humins. *Chemsuschem* **2011**, *4*, 1166–1173. [CrossRef]
17. Chuntanapum, A.; Matsumura, Y. Char Formation Mechanism in Supercritical Water Gasification Process: A Study of Model Compounds. *Ind. Eng. Chem. Res.* **2010**, *49*, 4055–4062. [CrossRef]
18. Shi, N.; Liu, Q.; Cen, H.; Ju, R.; He, X.; Ma, L. Formation of Humins During Degradation of Carbohydrates and Furfural Derivatives in Various Solvents. *Biomass Conv. Bioref.* **2020**, *10*, 277–287. [CrossRef]
19. Hu, X.; Lievens, C.; Larcher, A.; Li, C.-Z. Reaction Pathways of Glucose During Esterification: Effects of Reaction Parameters on The Formation of Humin Type Polymers. *Bioresour. Technol.* **2011**, *102*, 10104–10113. [CrossRef]
20. Zhang, X.; Zhang, D.; Sun, Z.; Xue, L.; Wang, X.; Jiang, Z. Highly Efficient Preparation of Hmf from Cellulose Using Temperature-Responsive Heteropolyacid Catalysts in Cascade Reaction. *Appl. Catal. B Environ.* **2016**, *196*, 50–56. [CrossRef]

21. Ramli, N.A.S.; Amin, N.A.S. Kinetic Study of Glucose Conversion to Levulinic Acid Over Fe/Hy Zeolite Catalyst. *Chem. Eng. J.* **2016**, *283*, 150–159. [CrossRef]
22. Garcés, D.; Faba, L.; Díaz, E.; Ordóñez, S. Aqueous-Phase Transformation of Glucose into Hydroxymethylfurfural and Levulinic Acid by Combining Homogeneous and Heterogeneous Catalysis. *Chemsuschem* **2019**, *12*, 924–934.
23. Hoang, T.M.C.; Lefferts, L.; Seshan, K. Valorization of Humin-Based Byproducts from Biomass Processing-A Route to Sustainable Hydrogen. *Chemsuschem* **2013**, *6*, 1651–1658. [CrossRef] [PubMed]
24. Hoang, T.M.C.; Geerdink, B.; Sturm, J.M.; Lefferts, L.; Seshan, K. Steam Reforming of Acetic Acid—A Major Component in The Volatiles Formed During Gasification of Humin. *Appl. Catal. B Environ.* **2015**, *163*, 74–82. [CrossRef]
25. Hoang, T.M.C.; Van Eck, E.R.H.; Bula, W.P.; Gardeniers, J.G.E.; Lefferts, L.; Seshan, K. Humin Based By-Products from Biomass Processing as A Potential Carbonaceous Source for Synthesis Gas Production. *Green Chem.* **2015**, *17*, 959–972. [CrossRef]
26. Tosi, P.; Van Klink, G.P.M.; Celzard, A.; Fierro, V.; Vincent, L.; De Jong, E.; Mija, A. Auto-Crosslinked Rigid Foams Derived from Biorefinery Byproducts. *Chemsuschem* **2018**, *11*, 2797–2809. [CrossRef] [PubMed]
27. Agarwal, S.; Van Es, D.; Heeres, H.J. Catalytic Pyrolysis of Recalcitrant, Insoluble Humin Byproducts from C6 Sugar Biorefineries. *J. Anal. Appl. Pyrolysis* **2017**, *123*, 134–143. [CrossRef]
28. Wang, Y.; Agarwal, S.; Heeres, H.J. Catalytic Liquefaction of Humin Substances from Sugar Biorefineries with Pt/C in 2-Propanol. *Acs Sustain. Chem. Eng.* **2017**, *5*, 469–480. [CrossRef]
29. Maerten, S.G.; Voß, D.; Liauw, M.A.; Albert, J. Selective Catalytic Oxidation of Humins to Low-Chain Carboxylic Acids with Tailor-Made Polyoxometalate Catalysts. *Chemistryselect* **2017**, *2*, 7296–7302. [CrossRef]
30. Shen, H.; Shan, H.; Liu, L. Evolution Process and Controlled Synthesis of Humins with 5-Hydroxymethylfurfural (Hmf) As Model Molecule. *Chemsuschem* **2020**, *13*, 513–519. [CrossRef]
31. Sevilla, M.; Fuertes, A.B. The Production of Carbon Materials by Hydrothermal Carbonization of Cellulose. *Carbon* **2009**, *47*, 2281–2289. [CrossRef]
32. Yao, C.; Shin, Y.; Wang, L.-Q.; Windisch, C.F.; Samuels, W.D.; Arey, B.W.; Wang, C.; Risen, W.M.; Exarhos, G.J. Hydrothermal Dehydration of Aqueous Fructose Solutions in A Closed System. *J. Phys. Chem. C* **2007**, *111*, 15141–15145. [CrossRef]
33. Zhang, Z.; Liu, W.; Xie, H.; Zhao, Z.K. An Unexpected Reaction Between 5-Hydroxymethylfurfural and Imidazolium-Based Ionic Liquids at High Temperatures. *Molecules* **2011**, *16*, 8463–8474. [CrossRef]
34. Guo, H.; Qi, X.; Hiraga, Y.; Aida, T.M.; Smith, R.L. Efficient Conversion of Fructose into 5-Ethoxymethylfurfural with Hydrogen Sulfate Ionic Liquids as Co-Solvent and Catalyst. *Chem. Eng. J.* **2017**, *314*, 508–514. [CrossRef]
35. Zhang, M.; Yang, H.; Liu, Y.; Sun, X.; Zhang, D.; Xue, D. Hydrophobic Precipitation of Carbonaceous Spheres from Fructose by A Hydrothermal Process. *Carbon* **2012**, *50*, 2155–2161. [CrossRef]
36. Voß, D.; Kahl, M.; Albert, J. Continuous Production of Formic Acid from Biomass in A Three-Phase Liquid–Liquid–Gas Reaction Process. *ACS Sustain. Chem. Eng.* **2020**, *8*, 10444–10453. [CrossRef]
37. Reichert, J.; Brunner, B.; Jess, A.; Wasserscheid, P.; Albert, J. Biomass Oxidation to Formic Acid in Aqueous Media Using Polyoxometalate Catalysts—Boosting Fa Selectivity by In-Situ Extraction. *Energy Environ. Sci.* **2015**, *8*, 2985–2990. [CrossRef]
38. Albert, J.; Lüders, D.; Bösmann, A.; Guldi, D.M.; Wasserscheid, P. Spectroscopic and Electrochemical Characterization of Heteropoly Acids for Their Optimized Application in Selective Biomass Oxidation to Formic Acid. *Green Chem.* **2014**, *16*, 226–237. [CrossRef]
39. Odyakov, V.F.; Zhizhina, E.G. A Novel Method of The Synthesis of Molybdovanadophosphoric Heteropoly Acid Solutions. *React. Kinet. Catal. Lett.* **2008**, *95*, 21–28. [CrossRef]
40. Hu, Y.; Li, H.; Hu, P.; Li, L.; Wu, D.; Xue, Z.; Zhu, L.; Hu, C. Probing the Effects of Fructose Concentration on The Evolution of Humins During Fructose Dehydration. *React. Chem. Eng.* **2022**, *8*, 175–183. [CrossRef]
41. Albert, J.; Wölfel, R.; Bösmann, A.; Wasserscheid, P. Selective Oxidation of Complex, Water-Insoluble Biomass to Formic Acid Using Additives as Reaction Accelerators. *Energy Environ. Sci.* **2012**, *5*, 7956. [CrossRef]
42. Sajid, M.; Farooq, U.; Bary, G.; Azim, M.M.; Zhao, X. Sustainable Production of Levulinic Acid and Its Derivatives for Fuel Additives and Chemicals: Progress, Challenges, and Prospects. *Green Chem.* **2021**, *23*, 9198–9238. [CrossRef]
43. Divya, P.S.; Nair, S.; Kunnikuruvan, S. Identification of Crucial Intermediates in The Formation of Humins from Cellulose-Derived Platform Chemicals Under Brønsted Acid Catalyzed Reaction Conditions. *Chemphyschem A Eur. J. Chem. Phys. Phys. Chem.* **2022**, *23*, E202200057. [CrossRef] [PubMed]
44. Kang, S.; Fu, J.; Zhang, G. from Lignocellulosic Biomass to Levulinic Acid: A Review on Acid-Catalyzed Hydrolysis. *Renew. Sustain. Energy Rev.* **2018**, *94*, 340–362. [CrossRef]
45. Jung, D.; Körner, P.; Kruse, A. Kinetic Study on The Impact of Acidity and Acid Concentration on The Formation of 5-Hydroxymethylfurfural (Hmf), Humins, and Levulinic Acid in The Hydrothermal Conversion of Fructose. *Biomass Conv. Bioref.* **2021**, *11*, 1155–1170. [CrossRef]
46. Girisuta, B.; Janssen, L.P.B.M.; Heeres, H.J. A Kinetic Study on The Decomposition of 5-Hydroxymethylfurfural into Levulinic Acid. *Green Chem.* **2006**, *8*, 701. [CrossRef]
47. Köchermann, J.; Schreiber, J.; Klemm, M. Conversion of D-Xylose and Hemicellulose in Water/Ethanol Mixtures. *Acs Sustain. Chem. Eng.* **2019**, *7*, 12323–12330. [CrossRef]
48. Sumerskii, I.V.; Krutov, S.M.; Zarubin, M.Y. Humin-Like Substances Formed Under the Conditions of Industrial Hydrolysis of Wood. *Russ. J. Appl. Chem.* **2010**, *83*, 320–327. [CrossRef]

49. Chen, X.; Guigo, N.; Pizzi, A.; Sbirrazzuoli, N.; Li, B.; Fredon, E.; Gerardin, C. Ambient Temperature Self-Blowing Tannin-Humins Biofoams. *Polymers* **2020**, *12*, 2732. [CrossRef]
50. Wesinger, S.; Mendt, M.; Albert, J. Alcohol-Activated Vanadium-Containing Polyoxometalate Complexes in Homogeneous Glucose Oxidation Identified with 51 V-Nmr and Epr Spectroscopy. *Chemcatchem* **2021**, *13*, 3662–3670. [CrossRef]
51. Raabe, J.-C.; Aceituno Cruz, J.; Albert, J.; Poller, M.J. Comparative Spectroscopic and Electrochemical Study of V(V)-Substituted Keggin-Type Phosphomolybdates and -Tungstates. *Inorganics* **2023**, *11*, 138. [CrossRef]

6.2 Humin-free synthesis of levulinic acid from fructose using heteropolyacid catalysts

As part of the research for this publication, the parameters used for the synthesis of LA from sugars were to be optimized. For this purpose, an acidic catalyst was initially sought, which would represent a more environmentally friendly alternative to the conventionally used mineral acids. To achieve this, multiple acidic catalysts were first used to generate humins. Sulfuric acid was used to represent mineral acids, while FA was used as an organic acid. In addition, the three HPAs HPMo, HPW and HSiW were used as catalysts. The highest LA yields were achieved with HSiW as catalyst, while the usage of FA produced the least amount of LA. Following this the reaction parameters were optimized regarding a low humin yield and a high LA yield in the form of a DoE (*Figure* 34). Reaction time, temperature, substrate concentration and weight fraction of the organic solvent acetone served as parameters. It turned out that the LA yield depended most on the solvent composition and the temperature. The humin yield depended most on the substrate concentration and solvent composition. High LA yields were achieved with low substrate concentrations, low organic solvent contents and either long reaction times at low temperatures or short reaction times at high temperatures. High humin yields were achieved with high substrate concentrations, high organic solvent proportions, high reaction times and high temperatures. Based on these findings, it was possible to determine parameter sets for a LA synthesis without humin formation as well as a LA synthesis with a possible LA yield of up to 69 %. These two sets of parameters followed the philo$_{so}$phy of maximum LA yield through low substrate concentration, organic solvent content and temperature, as well as a high reaction time. In addition, an industrially more applicable set of parameters with a lower reaction time and higher temperature was created. Afterwards, this set of optimized parameters could also be successfully transferred to the conversion of other carbohydrates, resulting in substantial yields of platform chemicals, proving the validity of the determined parameters. More information can be found in the supporting information.

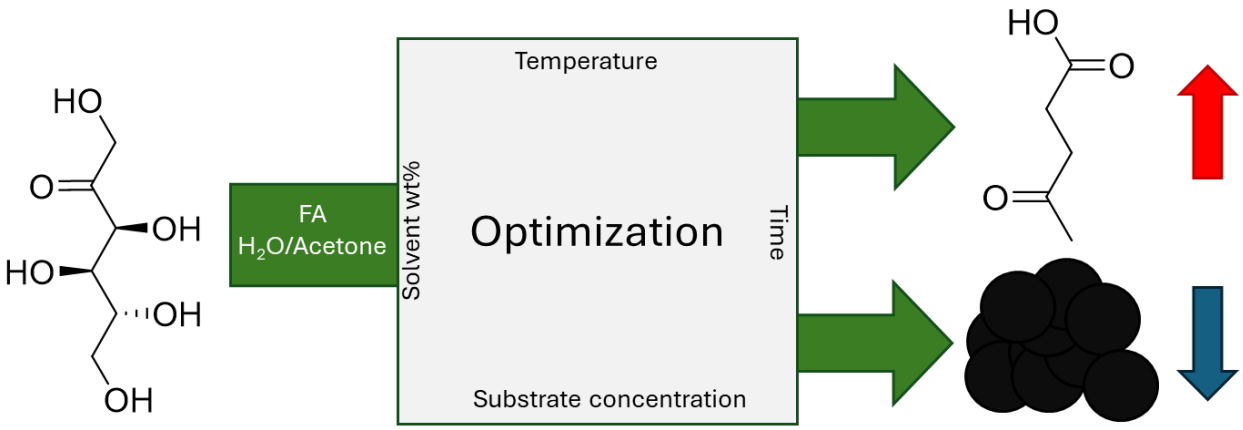

Figure 34: *Optimization of LA and humin yields during the acidic conversion of fructose using FA in an H_2O/acetone mixture through a variation of temperature, solvent wt%, time and substrate concentration.*

Original Article

Biofpr Biofuels Bioproducts & Biorefining

Humin-free synthesis of levulinic acid from fructose using heteropolyacid catalysts

André Wassenberg, Tobias Esser, Maximilian J. Poller, Dorothea Voß, Jakob Albert, Institute for Technical and Macromolecular Chemistry, University of Hamburg, Hamburg, Germany

Received April 12 2024; Revised May 14 2024; Accepted May 29 2024;
View online 28 June 2024 at Wiley Online Library (wileyonlinelibrary.com);
DOI: 10.1002/bbb.2654; *Biofuels, Bioprod. Bioref.* 18:1585–1597 (2024)

Abstract: Levulinic acid (LA) is one of the top bio-based platform molecules that can be converted into many valuable chemicals. Herein, we report the sustainable synthesis of LA acid from various sugars using heteropolyacid catalysts. By using a Box–Behnken design of experiment, both LA yield (up to 69 mol%) and complete suppression of parasitic humin formation could be achieved within a 5 h reaction time at 140°C using fructose as a substrate. The effects of various reaction parameters like temperature, sugar concentration, addition of organic co-solvent and reaction time on LA yield and humin formation were examined in a three-dimensional space. Moreover, the results could be successfully transferred to other sugars like glucose or cellobiose, paving the way for an atom-efficient and sustainable LA synthesis process. © 2024 The Author(s). *Biofuels, Bioproducts and Biorefining* published by Society of Industrial Chemistry and John Wiley & Sons Ltd.

Supporting information may be found in the online version of this article.

Key words: heteropolyacids; levulinic acid; sugars; humins; DoE

Introduction

In recent times, reducing our dependence on fossil raw materials has been an increasingly important topic. This has been made even more clear by the energy crisis of the last few years. One way to reduce the dependence on fossil raw materials in the chemical industry is to produce platform chemicals such as levulinic acid (LA) from biomass.

Levulinic acid is a γ-ketoacid which is soluble in water, alcohols, esters, ethers and ketones. Its highly reactive functional groups grant LA access to a variety of chemical transformations.[1] Levulinic acid can be used for the synthesis of several market-relevant biochemicals[2] including succinic acid,[1] γ-valerolactone,[3,4] aminolevulinic acid,[5] diphenolic esters and other commodity chemicals.[6] These LA derivates possess a wide variety of different uses. They are used as plasticizers,[7] resins,[8] polymer precursors[9] and pharmaceuticals.[7,10,11] Levulinic acid derivatives are also used in the fuel industry, for example, γ-valerolactone and 2-methyltetrahydrofuran can be mixed with petroleum products to produce clean-burning fuels.[3,12]

Since LA is such an important chemical, efficient synthesis methods are necessary to meet industrial needs. There are

Correspondence to: Jakob Albert, Institute for Technical and Macromolecular Chemistry, University of Hamburg, Hamburg 20146, Germany. E-mail: jakob.albert@uni-hamburg.de

multiple different ways to produce LA, such as fermentation or extraction from waste generated by other industrial processes or through direct synthesis.[13,14] However, at this point, LA is industrially manufactured exclusively via the Biofine Process.[7] The Biofine Process was developed in the 1990s by BioMetics and the US Department of Energy comprising a two-stage high-temperature process where sulfuric acid is used to convert lignocellulosic biomass to LA and its derivatives.[1] Although the Biofine Process is used by several companies to produce LA, the process is still not sustainable. Sulfuric acid, for example, is not an ideal acidic catalyst, as it is an environmentally harmful chemical and can also damage the biogenic feedstock through erosion and corrosion.[7,15] Other mineral acids such as HCl have proved to be effective in converting various biomasses as homogenous catalysts,[16,17] but suffer from the same problems with recovery and missing environmental sustainability.[7,18] Organic acids such as formic acid are more suitable in terms of separation and environmental safety; however, they come along with the drawback of only being able to achieve moderate yields of LA.[19–21] Heterogeneous catalysts such as TiO_2 and zeolites have also been used for the production of LA, as they possess better recovery and no separation issues, but have not yet become established in the chemical industry.[18,22–25]

An interesting alternative as an acidic catalyst are polyoxometalates, especially in their free acidic form as heteropoly acids (HPAs), a subclass having found increasing use in the valorization of biomass in recent years,[26] including the production of platform chemicals like 5-hydroxymethylfurfural and LA from cellulose and its derivatives.[27] Polyoxometalates contain anionic metal oxide clusters, whose negative charge is balanced with various counter cations able to catalyze a wide variety of reactions depending on their composition.[26,28] They can be used either as homogeneous catalysts in an aqueous solution or immobilized on a support material as heterogeneous catalysts.[29] In particular, their use as acidic catalysts in aqueous solution is of special interest, as in contrast to conventional mineral acids, HPAs are less damaging to the environment, much less corrosive and easier to recycle.[26,30–33]

Unfortunately, the choice of a suitable acidic catalyst is not the only complication that plagues industrial LA synthesis, as the undesirable formation of insoluble solid residues during synthesis also presents a considerable challenge.[7] These so-called humins are polymeric black solids that are formed during the acidic conversion of cellulosic biomass and its derivatives.[34–36] It is believed that they are formed through esterification, etherification, aldol condensation and other reactions between LA and reaction intermediates of the hydrolysis of sugars.[37] However, the exact mechanism of humin formation still remains unknown. Since they are not soluble in conventional solvents, humins cause a variety of issues in the reaction system as their formation wastes substrates[38,39] and clog reactors as well as catalysts owing to coking.[25,40,41] As the effective valorization of humins tends to be difficult, it is better to prevent humin formation in the first place. Multiple attempts were made to achieve this ambitious goal by varying reaction parameters such as acidic strength, reaction time and temperature, leading to several insights about the kinetics of the formation of LA and humins.[20,36,42–51] Besides the variation of quantifiable reaction parameters, the use of different solvents was also investigated,[39,40,47,51–57] discovering that organic solvents reduce humin formation in most cases, consequently making their usage in the synthesis of LA very attractive.

Unfortunately, these studies are not free of complications. On the one hand, the influences of individual reaction parameters are often only considered linearly or two-dimensionally. Moreover, there is no consideration of the interaction caused by changing more than two parameters so far. In addition, with a few exceptions,[44,46,58] the effects of reaction parameters are usually only examined on either LA or humin formation and not on both together. On the other hand, the results also often lack a certain degree of comparability between different studies. For example, Toif *et al.* showed that for a reaction system consisting of glucose, water and sulfuric acid, higher temperatures (approximately 180°C) are ideal for a high LA yield,[43] while in a system with fructose, water and sulfuric acid, lower temperatures (approximately 140°C) were proved to be more efficient by Fachri *et al.*[58] It seems that a separate optimization would have to be carried out for each biomass substrate in order to optimize the LA and to minimize the humin yield.

In the study presented here, a holistic optimization approach for LA synthesis in parallel with minimizing parasitic humin formation was carried out. By applying a design of experiment (DoE) for a defined acid–water–solvent system, the effects of various reaction parameters on LA yield and humin formation were examined in a three-dimensional space. To this end, a suitable acidic catalyst that meets modern industrial requirements was first selected in a preliminary test. Through the following optimization study, enhanced reaction parameters for a high LA and a low humin yield were obtained and subsequently applied in order to test their transferability to other biomass-derived substrates.

Materials and methods

Experimental procedure

All chemicals used for synthesis were purchased commercially and used without further purification. Sulfuric acid (95–97%)

was obtained from Grüssing GmbH. D(+)-xylose, D(+)-glucose and D(−)-fructose were obtained from Merck Millipore. Sucrose (99%) and formic acid (85%) were obtained from Alfa Aesar. Phosphotungstic acid hydrate (HPW), phosphomolybdic acid hydrate (HPMo) and silicotungstic acid hydrate (HSiW) were all obtained from Sigma Aldrich. D(+)-Cellobiose (>98%) was obtained from Carl Roth.

The experiments were conducted in a 10-fold screening plant consisting of 10 parallel 20 mL autoclaves made of Hastelloy C276 using Teflon based gaskets. All other plant components were made from 1.4571 stainless steel. Through a heating plate, temperatures of up to 200°C were enabled. The heating time in all experiments was approximately 15 min and was excluded from the given reaction times.

The reaction conditions were adapted to the ones used in a previous study,[52] albeit a bit modified to increase the LA yield. For the experiments to select the acidic catalyst, five stock solutions were prepared consisting of the respective acid dissolved in water to achieve a pH value of 1. Afterwards 7.5 mL of the stock solutions were filled into a glass liner together with fructose to achieve a 0.25 mol L^{-1} solution of the respective sugar. The glass liners were then inserted into the reactors and heated up to a temperature of 180 °C under a pressure of approximately 40 bar nitrogen for 3 h. After the reaction, the solution was filtered, and the liquid phase analyzed (see below).

For the DoE and the subsequent substrate variation, solutions of acetone and water were prepared with the respective mass proportions of acetone to water corresponding to the specified percentages. Silicotungstic acid hydrate was also added to the solutions in order to achieve a mass concentration of HSiW of 0.8% in the stock solutions. The reactions were carried out in the same way as described previously, with sugar concentration, reaction time, temperature and solvent proportion corresponding to the information given in Table S1.

Analysis of reaction solutions

A Shimadzu HPLC system with an Aminex HPX-87H 300 × 7.8 mm BIORAD column and a refractive index detector was used for the quantitative measurements of the aqueous product solution. The eluent was an aqueous sulfuric acid solution at a concentration of 5 mmol L^{-1}. Samples were analyzed at 0.5 mL min^{-1} flow rate, 45 bar and 45°C.

Nuclear magnetic resonance (NMR) spectra were measured using a Bruker Avance II 600 MHz spectrometer. In order to prepare samples, 0.4 mL of the filtered reaction solutions was combined with 0.2 mL of D_2O. Exemplary spectra of the reaction solutions are displayed in the Supporting Information.

To measure Fourier-transformed infrared spectra attenuated total reflection measurement (FTIR/ATR) (with a diamond prism) was employed using a QATRTM-S single-reflection attenuated total reflection from Shimadzu. The Whittaker method was used to smooth the spectra once they were plotted in origin.[59]

The elemental analyses (C, H, N, S, O) were measured using a Model EA-3000 analyzer from Fa. EuroVector.

Determination of quantitative reaction parameters

The conversion of sugars as well as the yields from the reaction intermediates and products were determined via HPLC. The general procedure for the calculation is given in the equations below. The sugar conversion (Eqn 1), LA yield (Eqn 2) and humin yield (Eqn 3) were calculated based on the concentration's determined by the HPLC analysis of the respective weight fractions.

$$X\left(sugar\right) = \frac{n\left(sugar\right)initial - n\left(sugar\right)final}{n\left(sugar\right)initial} \quad (1)$$

$$Y\left(LA\right) = \frac{n\left(LA\right)final}{n\left(sugar\right)initial} \quad (2)$$

$$Y\left(humin\right) = \frac{m(humin)final}{m\left(sugar\right)initial} \quad (3)$$

Results and discussion

Acidic catalyst selection

As mentioned previously, it is of great interest to find a sustainable and efficient acidic catalyst for the industrial conversion of biomass to LA. Five different acids were selected for a series of tests: sulfuric acid as a benchmark, formic acid, HPMo, HPW and HSiW. Sulfuric acid was used as the current industry standard in order to produce benchmark values. The other acids possess properties that potentially make them superior to sulfuric acid and other mineral acids for use in LA synthesis, with formic acid being used as a representative for strong organic acids, which are generally more environmentally friendly. HPMo, HSiW and HPW are heteropoly acids and used here to determine the suitability of polyoxometalates for the production of LA. All three HPAs are strong acids that possess acidic strengths even higher than that of sulfuric acid,[33,60] with

the relative strengths of the acids being in the following order: $pK_a(HPW) > pK_a(HSiW) > pK_a(HPMo) > pK_a(H_2SO_4) >> pK_a(FA)$.[60] HPAs are less damaging to the equipment and can be much more easily recycled than sulfuric acid as it is possible to separate the larger HPAs from the reaction solution through membrane filtration,[31,32] which would negate one of the biggest disadvantages of the current LA synthesis process. To ensure the relative comparability of all acids, the reaction solutions were adjusted to the same starting pH value of 1. The experiments were carried out simultaneously in the 10-fold reaction plant, using fructose as a feedstock. The latter was chosen as a substrate as it is a common sugar found in nature, which could result in a certain degree of transferability of the results for fructose to natural biomass. In addition, the conversion of fructose has already been investigated by other groups, which makes extensive comparisons with other research possible.[7,27,44,58] After each experiment, residual fructose concentration and LA concentration were measured by HPLC to determine the substrate conversion and LA yield (Eqns 1 and 2). Furthermore, the amount of humins formed was determined by weighing the produced humins and calculating the mass ratio from this weight and the mass of fructose used for the synthesis (Eqn 3). The results are summarized in Fig. 1, Fig. S1 and Table S2.

The LA yields (green bars) from the reactions of fructose using formic acid and sulfuric acid as acidic catalysts correspond approximately to those expected from the literature,[7,45,58] resulting in a higher LA yield (58 mol%) with sulfuric acid and a lower yield (37 mol%) for formic acid. When it comes to the humin yield (gray bars), the exact opposite was observed. Formic acid as a catalyst produced the highest humin yield with about 23 wt%, while the humin yield was lowest by using sulfuric acid (approximately 14 wt%). This agrees with previous results that weaker acids cause higher humin formation.[44,46] Moreover, the composition of various humins formed in the experiments using different acidic catalysts differed only slightly (Fig. S2).

It is expected that owing to the higher acid strengths, the yields of LA using HPAs would be higher than those using sulfuric acid. However, only the LA yield of the HSiW-catalyzed reaction (approximately 61 mol%) is higher than that with using sulfuric acid. HPW achieves a similar LA yield (58 mol%) to sulfuric acid whereas HPMo achieved the lowest LA yield of all acidic catalysts with only about 32 mol%. It would have been expected that HPW, as the strongest acid, would have shown the highest LA yield, but instead this is the case with the slightly weaker HSiW. Moreover, HPW produced a higher humin

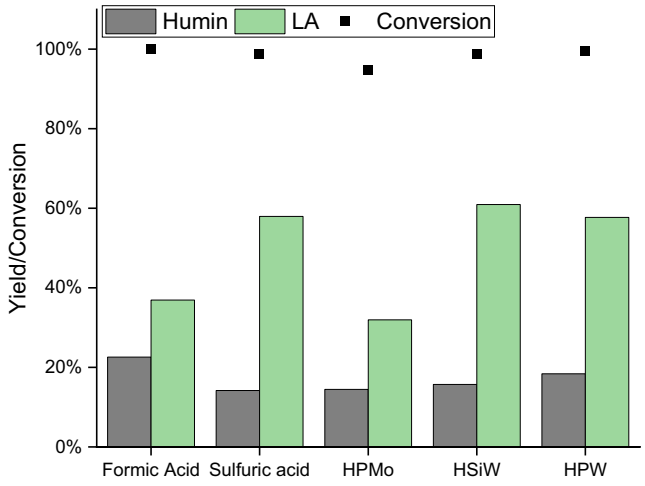

Figure 1. Acidic catalyst selection: conversion, levulinic acid (LA) yield (mol%) and humin yield (wt%) sorted by acidic strength (weakest to strongest) (0.25 mol l^{-1}, H_2O, pH = 1, 180°C, 3 h, 40 bar N_2). It is assumed that the missing biomass was converted to insoluble oligomers in concentrations too low for analytic verification. Humin yields are given in wt% as it was not possible to obtain elemental analyses from all synthesized humins owing to low yields; LA yields are given in mol% for better comparability with the literature.

yield (approximately 18 wt%) compared with the other HPAs and sulfuric acid, which all produced quite similar amounts of humin (between 14 and 16 wt%). What is most interesting, however, is the low LA yield with HPMo as an acidic catalyst. The LA yield with HPMo is significantly lower than the yield using formic acid as a much weaker acid. This cannot be explained by lower fructose conversion, as the latter is still around 95% using HPMo and the difference to the approximately 100% conversion of the other acidic catalysts would not explain the huge LA yield differences of over 30% in the case of HSiW. It seems that using HPMo primarily leads to the formation of a multitude of water-soluble humin oligomers, as the ^{1}H-NMR essentially does not differ from those of the other reaction solutions and so only formic acid, acetic acid and LA can be found (Fig. S1). A blue coloring of the reaction solution also indicates a reduction of HPMo, which could be related to the low LA yield, as the reduced catalyst would possess a much smaller acidity, therefore reducing its activity. Consequently, HPMo seems to be unsuited as an acidic catalyst for fructose conversion to LA under the applied reaction conditions.

HSiW was determined as the most promising acidic catalyst for further investigations, as it allowed for the highest

LA yield together with a small loss in carbon revealed by a moderate humin yield.

Optimizing the LA and minimizing the humin yield by DoE

With the reaction system now established, a reaction plan which would make it possible to obtain optimized parameters for a maximum LA yield with minimal production of humins had to be drawn up. It was also important that not only the effects of changes in individual factors but also those of several factors at the same time on the LA and humin yield could be revealed. A Box–Behnken design taking nonlinearity into account was chosen here as response surface designs generally allow for the effects of the changes in the factors on the response variables to be modeled, which also makes it possible to calculate optimized parameters for the conversion of fructose.[61] The Box–Behnken model is particularly suitable because it reduces the number of runs required for the model, thus saving time and money (Minitab©, https://support.minitab.com/en-us/minitab/help-and-how-to/statistical-modeling/doe/supporting-topics/response-surface-designs/response-surface-central-composite-and-box-behnken-designs/).[62] In addition, nonlinearity was taken into account as it cannot be assumed that the changes in the selected parameters had a linear effect on the response variables. Reaction time, temperature, sugar concentration and weight percentage of the organic solvent in the reaction solution were chosen as factors for the reaction plan, with the LA and humin yields being the response values. Acetone was used as the organic solvent of choice as it already has been used successfully in similar syntheses[63] and, as an aprotic solvent, should not undergo any unwanted side reactions with the produced LA unlike other protic organic solvents,[52] which should ideally result in a lower humin yield. Each of the four factors were assigned three different values, summarized in Table 1. In addition to the listed values of the factors, reactions were also carried out using 1 and 20 wt% of acetone to better determine the behavior of LA and humin yield at low organic solvent loadings. With these factor values, a total of 34 different experiments were carried out. A detailed summary of all results can be found in the Supporting Information (Table S1).

The main products in the liquid phase besides the desired LA were formic acid and acetic acid (see Figs S3 and S4). In the reactions where the solvent contained acetone, additional dimerization products of acetone could also be observed in the liquid phase. 4-Hydroxy-4-methylpentan-2-one and its elimination products 4-methylpent-3-en-2-one and 4-methylpent-4-en-2-one could be identified using ^{1}H, ^{13}C, and two-dimensional NMR spectra, with the intensity increasing with increasing acetone content and temperature (Fig. S3). However, these were not recognizable as individual substances in the HPLC chromatograms, suggesting that their peaks coincided with the larger acetone peak (Fig. S5).

The effects of changing the reaction parameters on LA and humin yield were evaluated using Design Expert and can be seen in Fig. 2 (LA yield) and Fig. 3 (humin yield). Figures 2(a) and 3(a) show the trends for the middle values of each factor. The highest LA yields were achieved at high temperatures with a short reaction time (up to 66 mol% in entry 31) or at low temperatures with a long reaction time (57 mol% in entry 2), while the LA yield becomes lower if both values are minimized or maximized, respectively. This is somewhat consistent with the results of Fachri *et al.*,[58] where the use of long reaction times and lower temperatures in a fructose–water–sulfuric acid mixture led to the highest LA yields of up to 74 mol%. They also showed that at high temperatures, the maximum LA yield could be reached in shorter reaction times, although their yields at high temperatures were significantly lower than those at lower temperatures. In Fig. 2(b,c) it can be seen that a higher acetone content has a strongly negative effect on the LA yield (17 mol% in entry 3). This effect appears to be largely linear since the trends from Fig. 2(a) are retained. The impact of the fructose concentration is not as linear. Lower concentrations seem to lead to higher yields with longer reaction times (up to 63 mol% in entry 29), while the LA yields remain approximately constant at short times and high temperatures (around 55 mol%), which also coincides with the results of Fachri *et al.*[58] The sugar concentration therefore has a much smaller effect than the acetone content of the reaction solution, which is also reflected in Fig. 4. The influence of the factors on the respective yields is shown here and the proportion of acetone clearly has the strongest effect on the

Table 1. Matrix of reaction factors and their assigned minimum, maximum and center point values for the DoE.

	Temperature [°C]	*c*(Fructose) [mol L^{-1}]	Acetone content [wt%]	Reaction time [h]
Minimum value	140	0.1	0	1
Center point	160	0.25	40	3
Maximum value	180	0.4	80	5

Parameters for all reactions: $p = 40$ bar N_2; 0.8 wt% silicotungstic acid hydrate (HSiW).

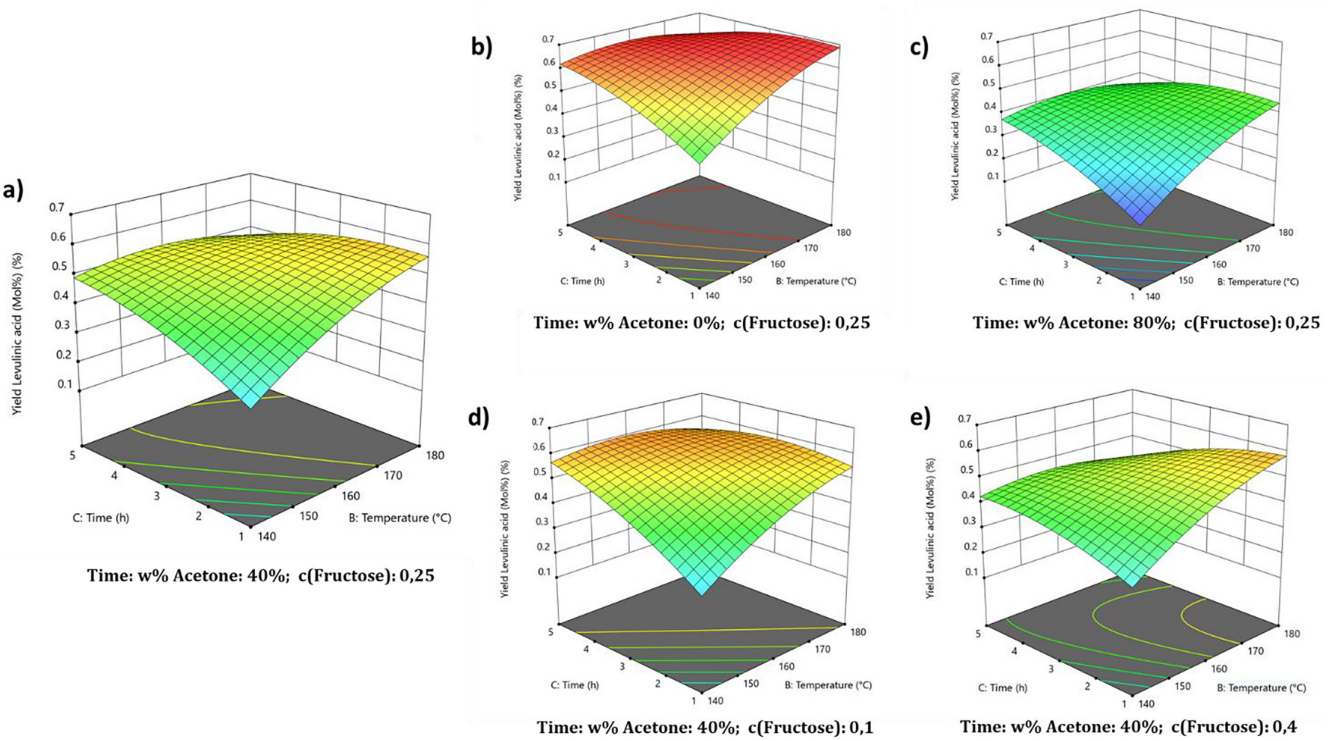

Figure 2. Surface diagrams for studying the effects of factor interactions on LA yield. Reaction conditions: T = 140–180 °C; t = 1–5 h; wt%(acetone) = 0–80; c(fructose) = 0.1–0.4 mol L^{-1}, p = 40 bar N_2; 0.8 wt% silicotungstic acid hydrate (HSiW) as a catalyst. (a) Effect of time and temperature on LA yield with wt%(acetone) = 0 and c(fructose) = 0.25 mol L^{-1}; (b) Effect of time and temperature on LA yield with wt%(acetone) = 0 and c(fructose) = 0.25 mol L^{-1}; (c) Effect of time and temperature on LA yield with wt%(acetone) = 80 and c(fructose) = 0.25 mol L^{-1}; (d) Effect of time and temperature on LA yield with wt%(acetone) = 40 and c(fructose) = 0.1 mol L^{-1}; (e) Effect of time and temperature on LA yield with wt%(acetone) = 40 and c(fructose) = 0.4 mol L^{-1}.

LA yield (Fig. 4a), while the sugar concentration has a much smaller influence.

The humin yields in Fig. 3(a) show a simpler trend compared with the LA yields. Higher temperatures and acetone contents ensure higher humin yields (up to 46 wt% in entry 16). A similar trend can also be observed with changes in fructose concentration and reaction time: maximizing the values generally provides higher humin yields (up to 30 wt% in entry 10), while minimizing the values prevents the formation of solid humins. While it is known that humin formation increases with longer reaction times, higher temperatures and sugar concentrations,[36,47,55] it is surprising that the addition of acetone as an organic solvent also leads to an increase in humin yield, as this contradicts several studies that have been carried out earlier.[47,55,56,63] An exception to this can be deduced from Fig. 3(d) where the minimization of all values except the acetone content leads to the lowest observed humin yield. However, since all yields displayed in Fig. 3(d) with a minimum reaction time are zero, this was not considered any further. All four factors appear to have a major influence on humin formation, with the influence of the sugar concentration appearing to be the highest (see Fig. 4b).

In summary, it can be concluded that high temperatures, long reaction times, high sugar concentrations and high organic solvent proportions favor undesired humin formation, whereby high temperatures, high reaction times, low sugar concentrations and low organic solvent proportions have a positive effect on the desired LA yield. However, the LA yield decreases if the temperature and time are increased at the same time, as the formation of humins is favored here. Contrary to previous assumptions, the addition of an organic solvent did not cause a general decrease in humin yield. On the contrary, a higher mass fraction in the reaction solution resulted in a significant increase in humin yield. This could possibly be due to the fact that the reaction times of one hour were already too long to be able to see a positive effect on the reaction as it was observed by Dutta *et al.*[63] Another reason could also be the combination of acetone and HSiW, which has not been investigated before. However, for the range of values examined here, it can be concluded that the addition of organic solvents is unsuitable. An ideal reaction with minimum humin yield

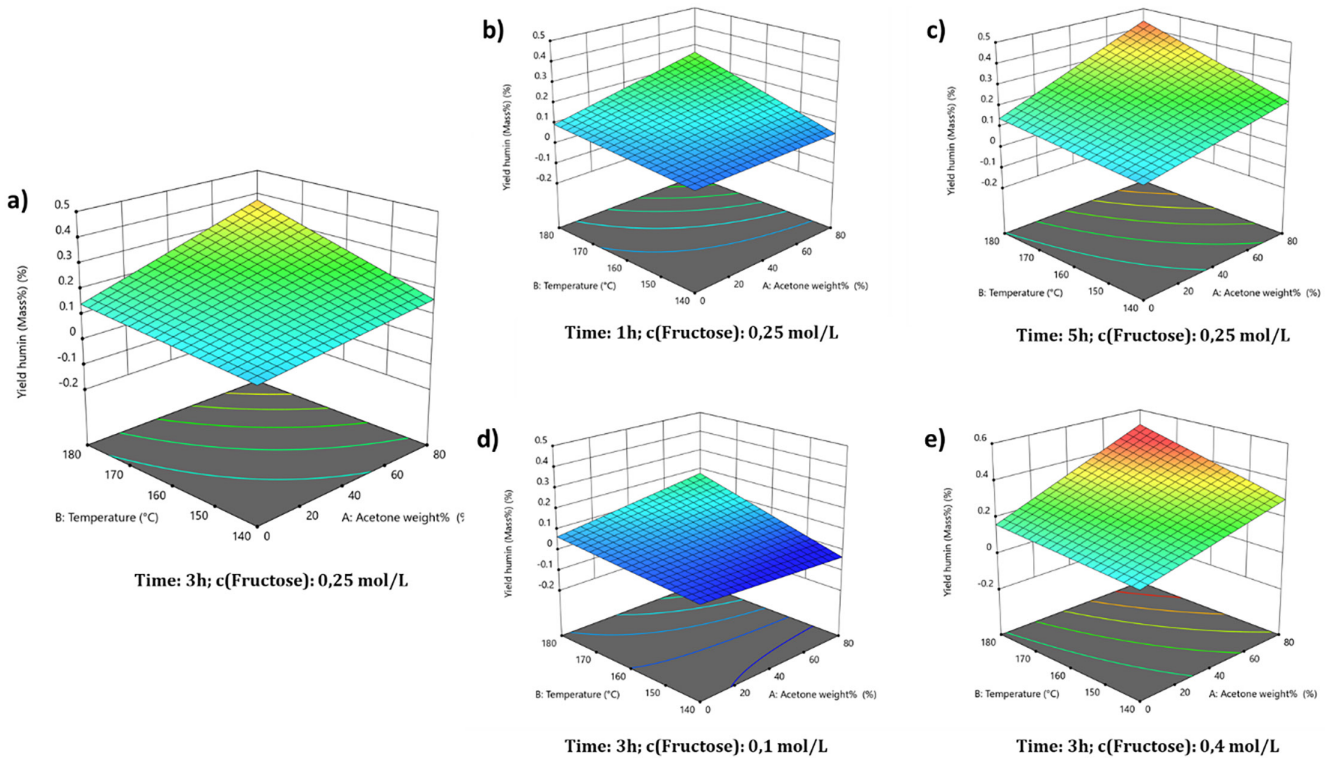

Figure 3. Surface diagrams for studying the effects of factor interactions on humin yield. Reaction conditions: T = 140–180 °C; t = 1–5 h; wt%(acetone) = 0–80%; c(fructose) = 0.1–0.4 mol L^{-1}, p = 40 bar N_2; 0.8 wt% silicotungstic acid hydrate (HSiW) as a catalyst. (a) Effect of temperature and wt%(acetone) on humin yield with t = 3 h and c(fructose) = 0.25 mol L^{-1}; (b) Effect of temperature and wt%(acetone) on humin yield with t = 1 h and c(fructose) = 0.25 mol L^{-1}; (c) Effect of temperature and wt%(acetone) on humin yield with t = 5 h and c(fructose) = 0.25 mol L^{-1}; (d) Effect of temperature and wt%(acetone) on humin yield with t = 3 h and c(fructose) = 0.25 mol L^{-1}; (e) Effect of temperature and wt%(acetone) on humin yield with t = 3 h and c(fructose) = 0.25 mol L^{-1}.

and maximum LA yield would therefore require either a high temperature with a short reaction time, or a low temperature with a high reaction time, in combination with a low sugar concentration and no addition of organic solvent.

Using the Design Expert software, two ideal sets of reaction parameters were initially created, which can be found in Table 2. Entry 1 represents a parameter combination which is expected to result in the highest possible LA yield with a relatively low humin yield, while entry 2 represents conditions under which no humin is formed at all at the expense of a slightly lower LA yield. Interestingly, the two sets of factor combinations are very similar, reinforcing that lower temperatures with longer reaction times, low organic solvent content and sugar concentrations seem to be ideal for a high LA and low humin yield. Which of the two parameter sets is preferred for an industrial application depends on the economic requirements of the synthesis: if the slightly higher yield of LA allows for the production of small amounts of humin then the parameters of entry 1 would be favorable whereby if complete avoidance of humin formation is required then the parameters of entry 2 should be applied. What is also interesting here is that at the optimum without humin formation, a non-insignificant amount of acetone is present in the reaction solution. This could indicate the results of previous studies that organic solvents do reduce humin formation under certain conditions or could be due to a calculation inaccuracy, as a large number of additional experiments would have to be carried out in order to be able to make more accurate predictions.

In this case, a higher LA yield was considered more industrially relevant. For this reason, an LA synthesis was carried out under the conditions of entry 1. It turned out that the prediction from Design Expert reflects reality rather accurately, as the obtained LA yield of 68.8 mol% and the humin yield of 1.1 wt% were relatively close to the calculated values. Although the yield achieved by these parameters is close to the 70–80% yields of the Biofine Process and produced much less humins, further challenges in the field of process engineering have to be addressed. In industrial

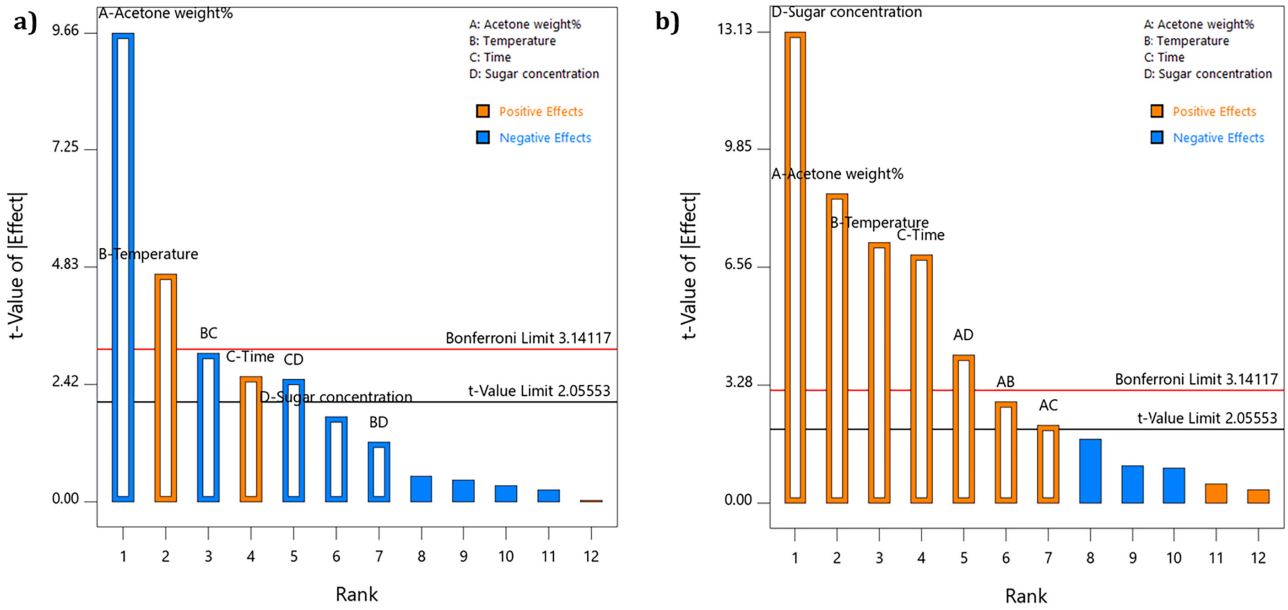

Figure 4. Pareto charts for various effects of factors on levulinic acid (LA) yield (a) and humin yield (b).

Table 2. Optimized reaction parameters calculated using Design Expert with maximal levulinic acid (LA) yield (entry 1) and complete humin supression (entry 2).

Entry	Acetone (wt%)	Temperature (°C)	Time (h)	c(Fructose) (mol L^{-1})	Humin yield* (wt%)	LA yield* (mol%)
1	0.37	140	5	0.1	1.2	69.3
2	7.86	140	5	0.1	0.0	65.1

*Predicted values.

Table 3. Reactions within 1 h reaction time sorted by levulinic acid (LA) yield.

Entry	Organic solvent (%)	Temperature (°C)	c(Fructose) (mol L^{-1})	Humin yield (wt%)	LA yield (mol%)
31	**0**	**180**	**0.1**	**1.5**	**66.1**
33	1	180	0.1	3.1	63.8
34	20	180	0.1	5.2	61.9
24	0	160	0.25	11.9	59.3
28	40	180	0.25	15.7	54.8
11	40	160	0.4	19.8	48.3
32	80	180	0.1	5.9	47.1
7	40	160	0.1	0.0	41.1
20	80	160	0.25	18.0	38.4
3	40	140	0.25	0.0	17.2

Reaction conditions: T = 140–180°C; t = 1 h; wt%(acetone) = 0–80; c(fructose) = 0.1–0.4 mol L^{-1}, p = 40 bar N_2; 0.8 wt% silicotungstic acid hydrate (HSiW) as a catalyst. The bold values are the benchmark for further investigation regarding a maximized LA yield.

processes, such as the Biofine Process, shorter reaction times are preferred as these result in much lower operating costs for the reaction plants, thus increasing their economic efficiency. This results in the parameters from Table 2 being suboptimal for use in industry owing to the long reaction times, which would make the process less efficient. For this reason, it would be better to only look at the results of the reactions with the shortest reaction times (Table 3).

When comparing the first three reactions in Table 3, the previously described trend for the acetone content is

particularly evident. Even the smallest amounts of acetone addition cause noticeable differences both in LA and humin yield under these reaction conditions. In general, it can also be seen from this table that, given the restrictions regarding the reaction time, the factor combination of 0 wt% acetone content, 1 h reaction time, 180°C reaction temperature and fructose concentration of 0.1 mol L^{-1} seems to be ideal, resulting in a LA yield of 66.1 mol%. This was further confirmed by an optimization via Design Expert that was limited to results with a 1 h response time (Table 4).

The optimal reaction parameters here match with those of reaction 31, even if the calculated yields differ slightly from the experimental results. Interestingly, another optimum can also be found among the reactions in Table 3. In Entry 7, there was no formation of solid humins at all, even though there was 40 wt% acetone present in the solution. However, the LA yield with about 41 mol% was low, resulting in further reactions with these parameters not being carried out. Instead, Entry 31 was repeated several times to examine the reproducibility of the results, leading to a standard deviation of 0.31 wt% for humin yield and only 0.12 mol% for LA yield (Table S3). Interestingly, the LA yield of 66.1 mol% is also significantly higher than that published by Fachri *et al.*, where a maximum LA yield of 52 mol% could be achieved using sulfuric acid at 180°C.[58] At higher temperatures, HSiW seems to be the superior catalyst for this reaction.

In the next set of experiments, the optimal reaction parameters were applied to other sugar substrates to demonstrate the substrate scope of the optimized LA synthesis procedure. Glucose was used as another abundant sugar that has also been frequently studied, as it is economically preferred over fructose.[7] Xylose was used as an exemple of a pentose, which possess a slightly different degradation pathway compared with hexoses.[7] Sucrose and cellobiose were used as dimeric sugars to test the transferability of the results to oligomeric biomass. These results compared with the results of the previous fructose conversion can be found in Fig. 5 and Table S4.

The LA and humin yields of the sugars differ significantly. Contrary to the acid catalyst selection, however, sugar conversions and yields seem to follow the same trends. The LA yields applying glucose and cellobiose are around 30 mol%, whereby using sucrose up to 45 mol% LA yield could be achieved. Interestingly, only little (sucrose) or almost no humin formation (glucose, cellobiose) was observed. However, ^{1}H-NMR spectra reveal also formation of several water-soluble oligomers (Figs S6 and S7).[64] Interestingly, using the pentose xylose as a substrate led to completely different results. In contrast to the other sugars tested, no LA was detected, but instead furfural (47 mol% yield) was formed, confirming previous studies documenting the acidic conversion of xylose.[7,21,56,65] Moreover, the difference between furfural yield and xylose conversion (94 mol%) is much higher compared with the other sugars, suggesting that humin formation from the conversion of pentoses leads to more water-soluble oligomers than that of hexoses and derivatives.

Conclusion

From a selection of five different acids, HSiW was determined to be the best acidic catalyst for the conversion of fructose to LA, achieving even higher yields (up to 69 mol%) than the

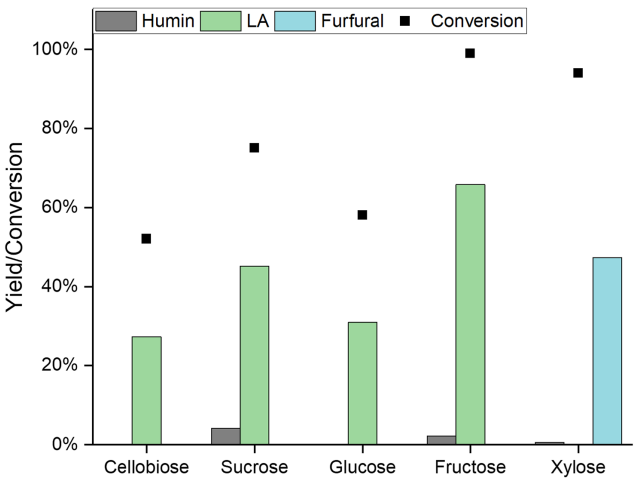

Figure 5. Substrate screening: Humin yield (wt%), levulinic acid (LA) yield (mol%) and conversion (mol%) of reactions using different sugars. Reaction conditions: T = 180°C, c(sugar) = 0.1 mol L^{-1}, t = 1 h; 0 wt% (acetone); 0.8 wt% silicotungstic acid hydrate (HSiW).

Table 4. Optimized reaction parameters calculated using Design Expert with maximal levulinic acid (LA) yield limited to a reaction time of 1 h.

Acetone (wt%)	Temperature (°C)	Time (h)	c(Fructose) (mol L^{-1})	Humin yield* (wt%)	LA yield* (mol%)
0	180	1	0.1	2.0	67.1

*Predicted values.

commonly used sulfuric acid. Subsequently, the effects of changes in temperature, reaction time, sugar concentration and proportion of organic solvent on the yields of LA and undesired humins were investigated in a DoE. Herein, the goal was to find optimized parameters for a sustainable and humin-free production of LA. It turned out that for an optimized conversion of fructose to LA using HSiW as acidic catalyst, short reaction times, low sugar concentrations, high temperature and a completely aqueous solution without the addition of acetone are ideal to completely suppress undesired humin formation. This contradicted several studies reporting that the addition of organic solvents reduces humin formation. It is assumed that the benefit of this study lies in the use of HSiW as an acidic catalyst being even very active at comparably mild reaction conditions avoiding humin formation.

Furthermore, other sugars like glucose, cellobiose and sucrose were also successfully converted to LA with only negligible humin formation using the optimized reaction parameters for fructose conversion showing the transferability of the approach to a broad range of commercially interesting substrates. Only xylose showed a completely different behavior under the reaction conditions applied leading mainly to the formation of furfural.

Therefore, especially HSiW shows interesting perspectives for applying heteropolyacids for the atom-efficient and humin-free production of LA from sugars, paving the way for more sustainable biomass valorization processes in the future.

Acknowledgements

We thank the central analytics department of the Department of Chemistry for carrying out NMR and elemental analysis measurements. J.A. and A.W. also thank the Deutsche Forschungsgemeinschaft for their financial support via the project AL 2130/5-1. Open Access funding enabled and organized by Projekt DEAL.

Conflict of interest statement

The authors declare no conflict of interest.

References

1. Hayes DJ, Fitzpatrick S, Hayes MHB and Ross JRH, The biofine process – Production of Levulinic acid, furfural, and formic acid from lignocellulosic feedstocks, in *Biorefineries-Industrial Processes and Products*, ed. by Kamm B, Gruber PR and Kamm M. Wiley-VCH Verlag GmbH, Weinheim, Germany, pp. 139–164 (2005).
2. Daniele Di Menno Di Bucchianico, Yanjun Wang, Jean-Christophe Buvat, Yong Pan, Valeria Casson Moreno, Sébastien Leveneur, Production of levulinic acid and alkyl levulinates: A process insight.
3. Bozell JJ, Moens L, Elliott D, Wang Y, Neuenscwander G, Fitzpatrick S *et al*., Production of levulinic acid and use as a platform chemical for derived products https://www.sciencedirect.com/science/article/pii/S0921344999000476 [12 April 2024].
4. Song S, Yao S, Cao J, Di L, Wu G, Guan N *et al*., Heterostructured Ni/NiO composite as a robust catalyst for the hydrogenation of levulinic acid to γ-valerolactone https://www.sciencedirect.com/science/article/pii/S0926337317305015 [12 April 2024].
5. Zai Y, Feng Y, Zeng X, Tang X, Sun Y, Lin L *et al*., Synthesis of 5-aminolevulinic acid with nontoxic regents and renewable methyl levulinate. *RSC Adv* **9**(18):10091–10093 (2019).
6. Yang F and Tang J, Catalytic upgrading of renewable levulinic acid to levulinate esters using Perchloric acid decorated nanoporous silica gels. *ChemistrySelect* **4**(4):1403–1409 (2019).
7. Sajid M, Farooq U, Bary G, Azim MM and Zhao X, Sustainable production of levulinic acid and its derivatives for fuel additives and chemicals: Progress, challenges, and prospects. *Green Chem* **23**(23):9198–9238 (2021).
8. Cousinet S, Ghadban A, Allaoua I, Lortie F, Portinha D, Drockenmuller E *et al*., Biobased vinyl levulinate as styrene replacement for unsaturated polyester resins. *J Polym Sci Part A: Polym Chem* **52**(23):3356–3364 (2014).
9. Allaoua I, Goi BE, Obadia MM, Debuigne A, Detrembleur C, Drockenmuller E *et al*., (Co)Polymerization of vinyl levulinate by cobalt-mediated radical polymerization and functionalization by ketoxime click chemistry. *Polym Chem.* **5**(8):2973–2979 (2014).
10. Rackemann DW and Doherty WOS, The conversion of lignocellulosics to levulinic acid. *Biofuels Bioprod Biorefin* **5**(2):198–214 (2011).
11. Schwartz TJ, van Heiningen ARP and Wheeler MC, Energy densification of levulinic acid by thermal deoxygenation. *Green Chem* **12**(8):1353 (2010).
12. Démolis A, Essayem N and Rataboul F, Synthesis and applications of alkyl levulinates. *ACS Sustainable Chem Eng* **2**(6):1338–1352 (2014).
13. Jeong G-T, Ra CH, Hong Y-K, Kim JK, Kong I-S, Kim S-K *et al*., Conversion of red-algae Gracilaria verrucosa to sugars, levulinic acid and 5-hydroxymethylfurfural. *Bioprocess Biosyst Eng* **38**(2):207–217 (2015).
14. Kumar A, Shende DZ and Wasewar KL, Production of levulinic acid: A promising building block material for pharmaceutical and food industry. *Mater Today Proc* **29**:790–793 (2020).
15. Rackemann D and Doherty W, A review on the production of levulinic acid and furanics from sugars. *International Sugar Journal* **115**:28–34 (2013).
16. Mascal M and Nikitin EB, High-yield conversion of plant biomass into the key value-added feedstocks 5-(hydroxymethyl)furfural, levulinic acid, and levulinic esters via5-(chloromethyl)furfural. *Green Chem* **12**(3):370–373 (2010).
17. Tarabanko VE, Chernyak M, Aralova SV and Kuznetsov BN, Kinetics of levulinic acid formation from carbohydrates at moderate temperatures. *React Kinet Catal Lett* **75**(1):117–126 (2002).
18. Antonetti C, Licursi D, Fulignati S, Valentini G and Galletti AMR, New frontiers in the catalytic synthesis of levulinic acid: From sugars to raw and waste biomass as starting feedstock. *Catalysts* **6**:196 (2016).
19. Jiang N, Huang R, Qi W, Su R and He Z, Effect of formic acid on conversion of fructose to 5-hydroxymethylfurfural in aqueous/butanol media. *Bioenergy Res* **5**(2):380–386 (2012).
20. Kupiainen L, Ahola J and Tanskanen J, Kinetics of glucose decomposition in formic acid. *Chem Eng Res Design* **89**(12):2706–2713 (2011).

21. Dussan K, Girisuta B, Lopes M, Leahy JJ and Hayes MHB, Conversion of hemicellulose sugars catalyzed by formic acid: Kinetics of the dehydration of D-xylose, L-arabinose, and D-glucose. *ChemSusChem* **8**(8):1411–1428 (2015).
22. Kuo C-H, Poyraz AS, Jin L, Meng Y, Pahalagedara L, Chen S-Y *et al*., Heterogeneous acidic TiO2 nanoparticles for efficient conversion of biomass derived carbohydrates. *Green Chem* **16**(2):785 (2014).
23. Wettstein SG, Alonso DM, Chong Y and Dumesic JA, Production of levulinic acid and gamma-valerolactone (GVL) from cellulose using GVL as a solvent in biphasic systems. *Energ Environ Sci* **5**(8):8199 (2012).
24. Upare PP, Yoon J-W, Kim MY, Kang H-Y, Hwang DW, Hwang YK *et al*., Chemical conversion of biomass-derived hexose sugars to levulinic acid over sulfonic acid-functionalized graphene oxide catalysts. *Green Chem* **15**(10):2935 (2013).
25. Thapa I, Mullen B, Saleem A, Leibig C, Baker RT, Giorgi JB *et al*., Efficient green catalysis for the conversion of fructose to levulinic acid. *Appl Catal Gen* **539**:70–79 (2017).
26. Zhong J, Pérez-Ramírez J and Yan N, Biomass valorisation over polyoxometalate-based catalysts. *Green Chem* **23**(1):18–36 (2021).
27. Zhang X, Zhang X, Sun N, Wang S, Wang X, Jiang Z *et al*., High production of levulinic acid from cellulosic feedstocks being catalyzed by temperature-responsive transition metal substituted heteropolyacids. *Renew Energy* **141**:802–813 (2019).
28. Raabe J-C, Poller MJ, Voß D and Albert J, H8[PV5Mo7O40] – A unique Polyoxometalate for acid and RedOx catalysis: Synthesis, characterization, and modern applications in green chemical processes. *ChemSusChem* **16**(16):e202300072 (2023).
29. Hombach L, Hausen N, Manjon AG, Scheu C, Kraffczyk H, Rose M *et al*., Carbon supported heteropolyacids as recyclable solid acid catalysts for the hydrolysis of Xylan. *Appl Catalysis A* **666**:119392 (2023).
30. Wang S-S and Yang G-Y, Recent advances in polyoxometalate-catalyzed reactions. *Chem Rev* **115**(11):4893–4962 (2015).
31. Raabe J-C, Esser T, Jameel F, Stein M, Albert J and Poller MJ, Study on the incorporation of various elements into the Keggin lacunary-type phosphomolybdate [PMo 9 O 34] 9– and subsequent purification of the polyoxometalates by nanofiltration. *Inorg Chem Front* **10**(16):4854–4868 (2023).
32. Esser T, Huber M, Voß D and Albert J, Development of an efficient downstream process for product separation and catalyst recycling of a homogeneous polyoxometalate catalyst by means of nanofiltration membranes and design of experiments. *Chem Eng Res Design* **185**:37–50 (2022).
33. Deng W, Zhang Q and Wang Y, Polyoxometalates as efficient catalysts for transformations of cellulose into platform chemicals. *Dalton Trans* **41**(33):9817–9831 (2012).
34. Patil SKR, Heltzel J and Lund CRF, Comparison of structural features of Humins formed catalytically from glucose, fructose, and 5-hydroxymethylfurfuraldehyde. *Energy Fuel* **26**(8):5281–5293 (2012).
35. Patil SKR and Lund CRF, Formation and growth of humins via aldol addition and condensation during acid-catalyzed conversion of 5-hydroxymethylfurfural. *Energy Fuel* **25**(10):4745–4755 (2011).
36. van Zandvoort I, Wang Y, Rasrendra CB, van Eck ERH, Bruijnincx PCA, Heeres HJ *et al*., Formation, molecular structure, and morphology of humins in biomass conversion: Influence of feedstock and processing conditions. *ChemSusChem* **6**(9):1745–1758 (2013).
37. Liu S, Zhu Y, Liao Y, Wang H, Liu Q, Ma L *et al*., Advances in understanding the humins: Formation prevention and application. *Appl Energy Combust Sci* **10**:100062 (2022).
38. Kang S, Zhang G, Yang X, Yin H, Fu X, Liao J *et al*., Effects of p-Toluenesulfonic acid in the conversion of glucose for Levulinic acid and sulfonated carbon production. *Energy Fuel* **31**(3):2847–2854 (2017).
39. Banggui Cheng, Xiaohui Wang, Qixuan Lin, Xiao Zhang, Ling Meng and Run-Cang Sun *et al*., New understandings of the relationship and initial formation mechanism for pseudo-lignin, humins, and acid-induced hydrothermal carbon.
40. Tsilomelekis G, Orella MJ, Lin Z, Cheng Z, Zheng W, Nikolakis V *et al*., Molecular structure, morphology and growth mechanisms and rates of 5-hydroxymethyl furfural (HMF) derived humins. *Green Chem* **18**(7):1983–1993 (2016).
41. Velaga B, Parde RP, Soni J and Peela NR, Synthesized hierarchical mordenite zeolites for the biomass conversion to levulinic acid and the mechanistic insights into humins formation https://www.sciencedirect.com/science/article/pii/S1387181119303610.
42. Chang C, MA X and CEN P, kinetics of levulinic acid formation from glucose decomposition at high temperature. *Chin J Chem Eng* **14**(5):708–712 (2006).
43. Toif ME and Hidayat M, Rochmadi and Budiman A, glucose to levulinic acid, a versatile building block chemical. *AIP Conf Proc* **2296**(1):20064 (2020).
44. Jung D, Körner P and Kruse A, Kinetic study on the impact of acidity and acid concentration on the formation of 5-hydroxymethylfurfural (HMF), humins, and levulinic acid in the hydrothermal conversion of fructose. *Biomass Conv Bioref* **11**(4):1155–1170 (2021).
45. Albert J and Wasserscheid P, Expanding the scope of biogenic substrates for the selective production of formic acid from water-insoluble and wet waste biomass. *Green Chem* **17**(12):5164–5171 (2015).
46. Girisuta B, Janssen LPBM and Heeres HJ, A kinetic study on the decomposition of 5-hydroxymethylfurfural into levulinic acid. *Green Chem* **8**(8):701 (2006).
47. Hu Y, Li H, Hu P, Li L, Di W, Xue Z *et al*., Probing the effects of fructose concentration on the evolution of humins during fructose dehydration. *React Chem Eng* **8**:175–183 (2022).
48. Cheng Z, Goulas KA, Quiroz Rodriguez N, Saha B and Vlachos DG, Growth kinetics of humins studied via X-ray scattering. *Green Chem* **22**(7):2301–2309 (2020).
49. Divya PS, Nair S and Kunnikuruvan S, Identification of crucial intermediates in the formation of humins from cellulose-derived platform chemicals under Brønsted acid catalyzed reaction conditions. *ChemPhysChem* **23**(11):e202200057 (2022).
50. Fu X, Hu Y, Hu P, Li H, Xu S and Zhu L, Mapping out the reaction network of humin formation at the initial stage of fructose dehydration in water. *Green Energy Environ* **9**(6):1016–1026 (2024).
51. Peng L, Tao C, Yang H, Zhang J and Liu H, Mechanistic insights into the effect of the feed concentration on product formation during acid-catalyzed conversion of glucose in ethanol. *Green Chem* **24**(13):5219–5227 (2022).
52. Wassenberg A, Esser T, Poller MJ and Albert J, Investigation of the formation, characterization, and oxidative catalytic valorization of Humins. *Materials* **16**(7):2864 (2023).
53. Bicker M, Kaiser D, Ott L and Vogel H, Dehydration of d-fructose to hydroxymethylfurfural in sub- and supercritical fluids https://www.sciencedirect.com/science/article/pii/S0896844605000859.
54. Shi N, Liu Q, Cen H, Ju R, He X, Ma L *et al*., Formation of humins during degradation of carbohydrates and furfural

derivatives in various solvents. *Biomass Conv Bioref.* **10**(2):277–287 (2020).
55. Yang H, Tao C, Peng L, Zhang J, He L, Liu H *et al*., Reactive and mechanistic insights into the acid-catalyzed conversion of concentrated C 5 /C 6 sugars in ethylene glycol. *ACS Sustain Chem Eng* **10**(5):1920–1931 (2022).
56. Köchermann J, Schreiber J and Klemm M, Conversion of d-xylose and hemicellulose in water/ethanol mixtures. *ACS Sustain Chem Eng.* **7**(14):12323–12330 (2019).
57. Dutta S, Yu IKM, Fan J, Clark JH and Tsang DCW, Critical factors for levulinic acid production from starch-rich food waste: Solvent effects, reaction pressure, and phase separation. *Green Chem* **24**(1):163–175 (2022).
58. Fachri BA, Abdilla RM, van, de Bovenkamp HH, Rasrendra CB and Heeres HJ, Experimental and kinetic modeling studies on the sulfuric acid catalyzed conversion of d-fructose to 5-Hydroxymethylfurfural and Levulinic acid in water. *ACS Sustain Chem Eng.* **3**(12):3024–3034 (2015).
59. Chen H, Ai W, Feng Q, Jia Z and Song Q, FT-NIR spectroscopy and Whittaker smoother applied to joint analysis of duel-components for corn. *Spectrochim Acta A Mol Biomol Spectrosc* **118**:752–759 (2014).
60. Kozhevnikov IV, Catalysis by heteropoly acids and multicomponent Polyoxometalates in liquid-phase reactions. *Chem Rev* **98**(1):171–198 (1998).
61. Voß D, Pickel H and Albert J, Improving the fractionated catalytic oxidation of lignocellulosic biomass to formic acid and cellulose by using design of experiments. *ACS Sustain Chem Eng* **7**(11):9754–9762 (2019).
62. Minitab©. https://support.minitab.com/en-us/minitab/help-and-how-to/statistical-modeling/doe/supporting-topics/response-surface-designs/response-surface-central-composite-and-box-behnken-designs/.
63. Esser T, Wassenberg A, Raabe J, Voß D and Albert J, Selective oxidation of mono- and difuran derivatives as model substances for humins to maleic acid and formic acid using transition metal substituted Keggin-type polyoxometalate catalysts. *ACS Sustain Chem Eng* **12**(1):543–560 (2024).
64. Corma A, Iborra S and Velty A, Chemical routes for the transformation of biomass into chemicals. *Chem Rev* **107**(6):2411–2502 (2007).
65. Choudhary V, Sandler SI and Vlachos DG, Conversion of xylose to furfural using Lewis and Brønsted acid catalysts in aqueous media. *ACS Catal* **2**(9):2022–2028 (2012).

André Wassenberg

André Wassenberg earned his bachelor's degree in business chemistry and his master's degree in chemistry at the institute of macromolecular chemistry at the Heinrich-Heine University of Düsseldorf. In 2020 he moved from Düsseldorf to Hamburg in pursuit of his doctorate. Between October 2020 and September 2023, he worked at Professor Jakob Albert's research group in the institute of technical and macromolecular chemistry at the University of Hamburg. As part of his doctoral thesis, he has researched the avoidance and valorization of humins through the usage of polyoxometalate catalysts.

Tobias Esser

Tobias Esser completed his bachelor of science degree in Applied Chemistry at the Aachen University of Applied Sciences (FH Aachen). Following this, he completed a degree in Process Engineering – Process Intensification (MSc) at the Technical University in Cologne (TH Köln). He started his PhD working in Professor Jakob Albert's research group at the Institute of Technical and Macromolecular Chemistry of the Hamburg University in 2020. As a part of his doctoral thesis, he investigated the selective catalytic oxidation of biomass, particularly humins to carboxylic acids using polyoxometalate catalysts. Another research focus was the development and optimization of the recovery of homogeneous polyoxometalate catalysts from aqueous reaction solutions by nanofiltration.

Maximilian J. Poller

Maximilian J. Poller completed his doctorate in the field of inorganic chemistry in 2019 jointly supervised by Neil Burford and Konstantin Karaghiosoff. In 2020 he joined the newly established research group of Jakob Albert at Hamburg University, where he now leads the catalyst development subgroup. His main research focus is the development of tailor-made polyoxometalates for catalytic applications.

Dorothea Voß

Dorothea Voß studied chemical engineering at the TU Dortmund. She received her master's degree in 2015 and earned her doctoral degree from the FAU Erlangen–Nuremberg in 2020. She is currently a head engineer at the Institute of Technical and Macromolecular Chemistry of the University of Hamburg. Her particular research focus is on catalytic conversion of biomass using polyoxometalate catalysts.

Jakob Albert

Jakob Albert has been Professor for Technical Chemistry and Deputy Director of the Institute of Technical and Macromolecular Chemistry at Hamburg University since 2020. He holds a Diploma (2011) and a PhD degree (2014) from FAU Erlangen-Nürnberg in Chemical Engineering. In 2021, he finished his habilitation on the Development of polyoxometalate catalysts for enhanced catalytic performance at FAU. Jakob's key activities are in the research fields of biomass valorization, power-to-X technologies and polyoxometalate catalysts, as well as scale-up and process design. He has published >75 papers and >100 conference contributions, is an inventor on 26 patents, and has received numerous scientific awards, e.g. ERC Consolidator Grant 2023.

6.3 Valorization of humins by cyclic levulinic acid production using polyoxometalates and formic acid

The aim of this publication was the creation of a cyclic process for the production of LA, in which the FA used as acidic catalyst for the synthesis can be recovered through SCO of the humin (*Figure* 35). For this purpose, a suitable substrate was initially sought amongst the five different carbohydrates fructose, glucose, xylose, sucrose and cellobiose. Here, fructose was chosen as substrate, as its conversion resulted in the highest LA yield of 38 mol%. The reaction system was then scaled up to a larger reactor size to test the scalability of the reaction and to increase the amount of humin produced. This process also entailed a modification of the reaction time, resulting in a longer reaction time and higher LA yield, thus establishing a reaction for the production of LA and humins. Afterwards, a SCO of a humin charge generated as by-product via the previously established LA production reaction was carried out. In contrast to Chapter 6.1, a further refined reaction procedure was used, utilizing HPA-2 as POM catalyst, while adding methanol as a selectivity enhancer, resulting in a significant increase of the obtained FA and other liquid products. A subsequent separation of the POM catalyst by membrane filtration was successful with a very high catalyst retention and resulted in an almost completely catalyst-free product solution. However, the complete separation of FA from the reaction solution was not possible; the boiling points of the by-products succinic acid, AA and methyl acetate prevented complete separation, which resulted in a product solution that contained these substances together with the concentrated FA and water. Following this, it was tested whether a solution with a similar composition to the FA containing fraction could also be used to efficiently produce humins and LA. It turned out that the oxidation products that were not removed had little to no effect on the LA and humins synthesized. The observed difference in yield was attributed to the lower FA concentration in the FA containing fraction. The cyclic synthesis of LA using FA as catalyst was therefore deemed as being successful. Further information can be found in the supporting information.

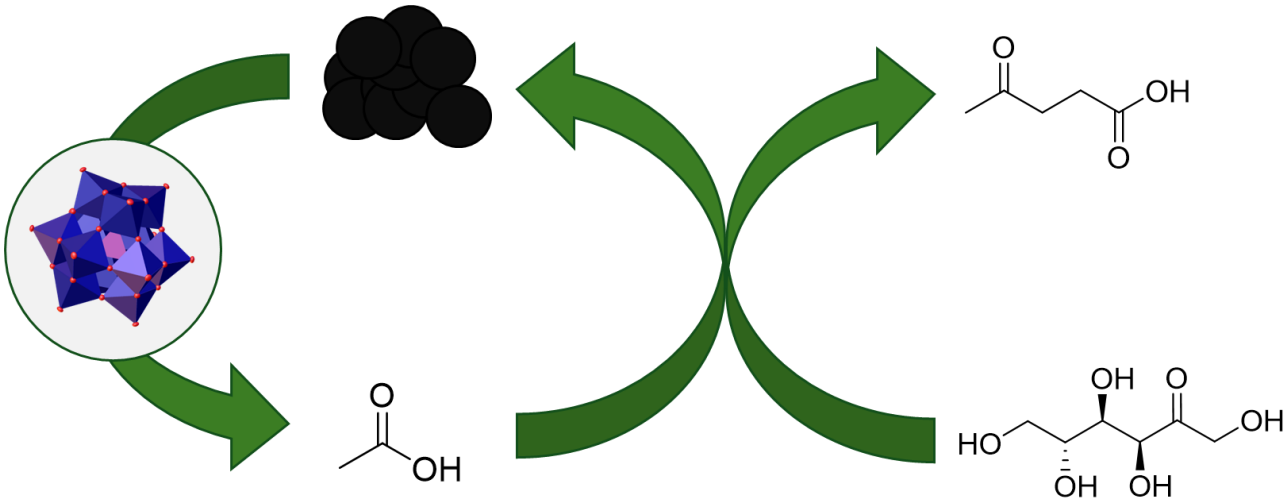

Figure 35: *Cyclic conversion of fructose to LA using FA as acidic catalyst.*

ChemSusChem

Research Article
doi.org/10.1002/cssc.202401973

Chemistry Europe
European Chemical Societies Publishing

www.chemsuschem.org

Valorization of Humins by Cyclic Levulinic Acid Production Using Polyoxometalates and Formic Acid

André Wassenberg,[a] Tobias Esser,[a] Maximilian J. Poller,[a] Dorothea Voß,[a] and Jakob Albert*[a]

At a time when increasing attention is paid to sustainability in chemistry, levulinic acid (LA) is one of the most important platform chemicals for the goal of overcoming our dependence on fossil raw materials. However, a so far limiting obstacle on the way to efficient LA production from biomass is the formation of undesirable humin byproducts. In this work, a new catalytic route for the effective utilization of these humin byproducts, enabling a cyclic synthesis of LA using formic acid (FA) as organocatalyst is proposed. Selective catalytic oxidation (SCO) of humins using the $H_5PV_2Mo_{10}O_{40}$ (HPA-2) polyoxometalate (POM) catalyst produces FA that can be isolated from the aqueous reaction mixture by using nanofiltration membranes accompanied by a complete catalyst recycling (>99%). After concentration of FA by distillation, the latter can be used as organocatalyst for LA production from sugars, whereby the formed humins can in turn be separated and used as substrates for further FA production via SCO to close the catalytic cycle. By using FA as a green and sustainable acidic organocatalyst, relatively high yields of LA (up to 42 mol%) could be achieved. In the future this can potentially lead to the creation of a closed cycle for an environmentally friendly and efficient production of green LA without undesired humin formation.

Introduction

Elimination of environmental pollutants is one of the biggest challenges in the chemical industry of the 21st century. Currently, over 90% of chemical intermediates are made from crude oil resulting in a need for new sustainable alternatives to replace finite fossil resources in the industry as well as the energy sector.[1] Platform chemicals such as levulinic acid (LA), which can be produced from lignocellulosic biomass, are promising alternatives, as they provide a renewable source of carbon both for energy and environmental applications.[2]

LA is an important platform chemical, as it provides highly reactive functional groups granting access to a variety of chemical transformations.[3] The latter can be further processed into commodities, such as γ-valerolactone,[4,5] ethyl levulinate[6–8] or methyl tetrahydrofuran.[9] Moreover, this includes the production of polymers,[10] pharmaceuticals,[11,12] resins,[13] or fuel additives.[6,14] While there are different ways to obtain LA such as fermentation of algae or extraction from waste materials,[15,16] the most widespread industrially used method is the direct synthesis through the biofine process,[17] where LA is produced together with other chemicals through the acid-catalyzed conversion of lignocellulosic biomass. Although this process achieves very high LA yields of up to 70%, it still faces several challenges.[2] One of the primary issues is the use of sulfuric acid as acidic catalyst for the biomass hydrolysis, as it is a strong mineral acid that is difficult to recycle, harmful to the environment, and corrosive to the reaction system.[2,18] For this reason, there has been a lot of research into alternative acidic catalysts. For example, acidic resins or zeolites have been investigated as solid acid catalysts as they are easier to separate and less harmful to the reaction systems.[5,19–22] However, despite some progress, none of these processes have been implemented industrially. A more promising strategy would be to use an alternative homogeneous catalyst, that would have to be relatively easy to separate and harmless to the reaction system. Strong organic acids such as formic acid (FA) fit this requirement profile perfectly, but FA-catalyzed LA synthesis have so far shown far too low yields to be industrially compatible.[23–25]

Another challenge for the sustainable production of LA is the formation of solid humin residues during the reaction process. Humins are sticky, water-insoluble by-products that form during the acidic conversion of cellulose and its derivatives (e.g. glucose, fructose, 5-hydroxymethylfurfural (5-HMF)) at temperatures above 140 °C.[26–29] They are dark-colored spherical particles that are insoluble in conventional solvents,[30] causing problems during industrial processes, as the formation of humins tends to clog up reactors and catalysts.[22,31,32] It is assumed that the process of humin formation begins with 5-HMF, an intermediate that is mainly formed during the acidic conversion of hexoses on the way to LA, and its hydrolyzation product 2,5-dioxo-6-hydroxyhexanal. These further react through esterification, etherification, acetalization, and aldol condensation so that the polymeric humins are formed, whereby other substances such as LA are also incorporated into the humins through polymerization or absorption.[26,32–34] However, the exact process of humin formation and the exact structure of

[a] Institute for Technical and Macromolecular Chemistry, University of Hamburg, Hamburg, Germany

Correspondence: Jakob Albert, Institute for Technical and Macromolecular Chemistry, University of Hamburg, 20146 Hamburg, Germany.
Email: jakob.albert@uni-hamburg.de

Supporting Information for this article is available on the WWW under https://doi.org/10.1002/cssc.202401973

humins remain unclear to date. What is certain, however, is that the formation of humins is accompanied by a significant loss of carbon, leading to a low atom efficiency.[33,35] For this reason, several studies have been carried out to avoid humin formation, for example through the usage of organic solvents.[32,36–39] Although humin formation could be successfully reduced, it has not yet been possible to completely avoid it. Therefore, efforts have been carried out to make sensible use of the humins produced, in order to reduce waste of material, thus increasing the resource efficiency. Humins have been used, for example, for the production of synthesis gas,[40,41] as a biofuel additive[17,42] or for the production of porous materials.[43] One of the most promising strategies, however, is the conversion of humins into value added chemicals, as the other methods mainly do not attempt to make meaningful use of the more complex organic structures in the humins. The best result would be the recovery of platform chemicals such as 5-HMF or LA from humins, although this is made difficult by the complex and largely unknown structure of the solids. However, visible progress has already been made in the catalytic depolymerization of the humin structure. Maerten et al.[44] were able to achieve excellent results in 2017 by oxidatively converting humins into FA and acetic acid. FA is an interesting product chemical as, in addition to its synthetic uses, it can also serve as a hydrogen (H_2) storage medium, with H_2 being considered as a promising renewable energy source that could replace fossil fuels.[45] Maerten et al. based their work on the commercialized OxFA process,[46] in which polyoxometalate (POM) catalysts are used to produce FA from biomass residues. POMs are inorganic metal oxide clusters whose properties can be adapted to the specific reaction and can catalyze both acid/base and redox reactions.[47] Due to their versatility, they can be used in various catalytic reactions such as the redox reactions in lithium-sulfur batteries[48,49] or the photo-catalytic oxidation of toluene.[50] POMs are also often used in other green catalytic reactions such as the synthesis of heterocycles[51] or the conversion of biomass into value added products.[47,52,53] Out of the different types of POMs, the vanadium containing HPAs have proven to be the most suitable for the conversion of humins, which was shown in a study by Esser et al.[54] During this study the authors determined that the active vanadium species of the HPA-type POM catalyzes the breakdown of oxygen-functionalized bonds such as ether and ester groups particularly well. Esser et al. also further refined the selective catalytic oxidation (SCO) of humins introduced by Maerten et al. in multiple studies,[54–56] resulting in higher carboxylic acid yields and improved atom efficiency.

Herein, an innovative cyclic LA production route from humins is proposed using the $H_5PV_2Mo_{10}O_{40}$ (HPA-2) POM catalyst for the SCO of humins to FA (**CH**),[56] followed by an efficient downstream separation of FA using nanofiltration,[57] coupled with FA-catalyzed LA production (**LP**)[39] and recycling of the humin waste (**H**) back into step 1 (**CH**), which would result in a more efficient use of resources (Figure 1).

Materials and Methods

Chemicals

Without any additional purification, most of the synthesis-related compounds were obtained through commercial purchases. Merck Millipore provided the D(+)-xylose (99%), D(+)-glucose (99%), and D(−)-fructose (99%, for biochemistry). Formic acid (>98%) and sucrose (99%) were obtained from Alfa Aesar. The source of D(+)-Cellobiose (>98%) was Carl Roth. Methanol (99.8%) was purchased from VWR Chemicals. The HPA-2 catalyst was synthesized according to a literature-known synthesis procedure.[58]

Catalyst Characterization

Inductively coupled plasma-optical emission spectroscopy (ICP-OES) was used to determine the stoichiometry of the HPA-2 catalyst using a *Fa. Spectro Arcos (Ametek) ICP-OES spectrometer*. A stoichiometry of 1.12 P/1.96 V/10 Mo was determined. The integrity of the Keggin-structure was verified using attenuated total reflection Fourier-transform infrared spectroscopy (ATR-FTIR) using a *QATRTM-S single-reflection ATR* from *SHIMADZU* (Figure S13), as well as using Nuclear Magnetic Resonance

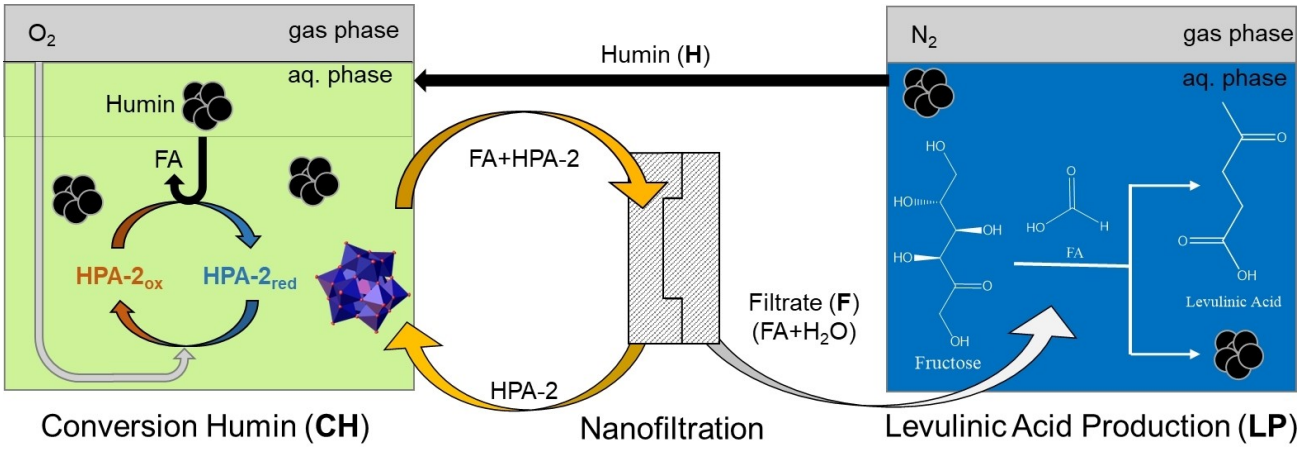

Figure 1. Cyclic LA production from humins for the catalytic elimination of environmental pollutants.

(NMR) ^{51}V NMR and ^{31}P NMR spectroscopy with a *BRUKER AVANCE II 600 MHz spectrometer* (Figures S14–15). To measure the reaction samples, 0.5 mL of the filtered reaction solutions were combined with 0.1 mL of D_2O. The used HPA-2 catalyst was tested for its structural integrity by FT-IR (Figure S16) as well as its reactive stability by Esser et al. during their previous work using ^{51}V-NMR spectroscopy (Figure S17).[56]

Experimental Setup & Procedure for SCO of Humins (CH)

The SCO experiments were carried out in a 600 mL Hastelloy C276 autoclave with a glas inlet and a gas entrainment stirrer. A method according to Esser et al.[56] was used for the SCO of the produced humins. For this purpose, 1.5 g of the humin was dispersed in 150 mL of a 95 % water/5 % methanol solution and oxidized using 1 mmol of HPA-2 as a catalyst and 30 bar of pure oxygen as oxidant for 30 h at 1000 rpm.

Experimental Setup & General Method for Nanofiltration Experiments

The membrane system used was previously described elsewhere.[57] The core of the system is a membrane cell and a HPLC pump from *Bischoff Analysentechnik u. -geräte GmbH*, which enables flow rates of up to 40 mL min^{-1} at a pressure of up to 100 bar and is therefore responsible for the pressure build-up. A special feature of the membrane system is the membrane cell with an active membrane area of 33 cm^2, which has a stirrer integrated into the cell. The stirrer allows high flow across the membrane and high turbulence regardless of the pump flow rate enabling high concentration factors even with small membrane areas. This reduces phenomena such as concentration polarization. The special design of the membrane cell was developed and patented by PS *Prozesstechnik GmbH*, where the membrane cell is also commercially available.[59] More details on the development, design and optimization of the membrane system for POM separation after SCO of humins can be found in literature.[56,57]

The XN45 membrane used is commercially available from *Mann + Hummel*. Before use, the membrane cutout was pre-wetted inside the membrane cell. For this purpose, the installed membrane was rinsed with water for 5 minutes at a flow rate of 15 mL min^{-1} and a stirrer speed of 1100 rpm. Subsequently, the membrane was rinsed for additional 115 minutes at a pressure of 30 bar. After storage in the flooded cell for 24 hours without pressure, the membrane could be used, as sufficient wetting and swelling could be assumed.[57]

In a typical separation, the membrane system was rinsed with the product solution at a flow rate of 15 mL min^{-1} and a stirring speed of 1100 rpm without applying transmembrane pressure for 5 minutes recycling all streams back into the feed storage. Afterwards, the system was rinsed at a pressure of 30 bar for 15 minutes. Subsequently, the purified permeate containing FA was withdrawn into an individual vessel and the catalyst-rich retentate was recycled back into the feed storage. At the beginning of this process, a sample of the feed solution was taken, and the time measurement was started. The retentate was circulated until half of the original feed solution was drawn off as catalyst-poor permeate. Finally, the membrane system was cleaned by rinsing with water and air. The sample of the feed solution, retentate and permeate was analyzed using ICP-OES, NMR, and HPLC. Based on the analyses, the rejection R of a respective component i could be calculated according to Equation (1). The rejection results from one minus the ratio of the measured mass concentration $ß_{Per(Com\ i)}$ of a component i in the permeate to its original mass concentration $ß_{Feed(Com\ i)}$ in the feed.

$$R_{Com\ i} = 1 - \frac{\beta_{Per}(Com\ i)}{\beta_{Feed}(Com\ i)} \quad (1)$$

The permeate flux J is defined as the mass of permeate m_{Per} withdrawn over the used membrane area A_{Mem} during the experimental period t, as shown in Equation (2).

$$J = \frac{m_{Per}}{A_{Mem} \cdot t}\ [kg \cdot h^{-1} \cdot m^{-2}] \quad (2)$$

Experimental Setup & Procedure for Levulinic Acid Production (LP)

For the conversion of several sugars to LA, a 10-fold screening plant consisting of ten 20 mL autoclaves made of Hastelloy C276 with PTFE gaskets in batch mode were used. Valves, fittings, and pipes were manufactured of stainless steel 1.4571. The plant was equipped with a heating plate, allowing reaction temperatures up to 200 °C and a magnetic stirrer. All reactors were connected to an oxygen supply line. The reaction times provided did not include the approximate 15 minute heating period.

The conditions used during the reactions in the autoclave were modelled after the ideal reaction parameters were determined in a previous study:[39] First, a stock solution of FA dissolved in water was prepared and set to a pH of 1. Then, 7.5 mL of the stock solution were pipetted into a glass liner containing the respective sugar to achieve a 0.1 mol L^{-1} solution. Afterwards, the glass liners were inserted into the reactors and pressurized with nitrogen to prevent the evaporation of the solvent during the reaction. The reactors were heated up to a temperature of 180 °C under a pressure of 40 bar for 1 hour. After reaction, the solution was filtered, and the liquid phase analysed through High Performance Liquid Chromatography (HPLC) and NMR spectroscopy.

Analysis of Substrates and Reaction Products

The Elemental analyses of the produced humins were performed using a *EURO VECTOR analyzer model EA-3000.*

A *SHIMADZU HPLC system* equipped with an Aminex HPX-87H 300 mm×7.8 mm BIORAD column and a refractive index detector from SHIMADZU was used for the quantitative analysis of the aqueous phase (determination of soluble reaction products such as LA, FA and acetic acid). The eluent used was an aqueous sulfuric acid solution with a concentration of 5 mmol L^{-1}. The samples were subjected to analysis at 45 °C, 49 bar pressure, and a flow rate of 0.5 mL min^{-1}.

The CO_2 and CO produced during the conversion of humin in the gas phase were measured with a TCD detector of a *VARIAN 450-GC* on a 2 m×0.75 mm Shin-Carbon-column.

For the NMR samples used for quantification of the results of the humin conversion, 0.6 mL of the filtered reaction solution and 0.1 mL of a 10 wt% tert-butanol/D_2O solution were used.

Results and Discussion

In order to establish a cyclic LA production route from humins, the first step is the SCO of humins to FA using the HPA-2 POM catalyst.[56] HPA-2 was used as the catalyst of choice, as it was found to be the best catalyst for oxidatively converting humins into FA among the catalysts tested during previous studies.[55,56] Other HPA catalysts resulted in poorer conversion rates of the humins or over-oxidation of the humins into CO_2. The application of an optimized reaction procedure using methanol as selectivity enhancer efficiently supresses the over-oxidation of the carbon skeleton to CO_2 and allows for a higher FA yield as well as selectivity.[55]

SCO of Humins for FA Production Using HPA-2 as a Catalyst (CH)

First of all, a significant amount of humin was produced using the procedure described in the supporting information (Table S1, Figures S1 & S2). The as-synthesized humin was converted by SCO using the HPA-2 catalyst in the 600 mL autoclave (Figure 2). In contrast to previous research,[60] SCO was not carried out in a pure aqueous solution, but applying an optimized reaction procedure shown by Esser at al.[56] using 5 vol% methanol as an additive to efficiently supress the formation of carbon dioxide.

During the reaction, a conversion of 95.5% of the solid humin could be achieved, with 4.5 wt% of the humin mass remaining as solid residue. The main product was the desired FA with a yield of 28.4 wt% of the initial carbon. In addition, acetic acid (5.7 wt%), methyl acetate (2.4 wt%), methyl formate (1.6 wt%), and succinic acid (1.2 wt%) were detected in the liquid phase via ^{1}H-NMR (Figure S3). The methyl esters were presumably produced via esterification of the carboxylic acids formed during SCO with the additive methanol. In the gas phase, CO_2 (21.8 wt%) and CO (1.7 wt%) were found. The total carbon content of the liquid phase was 38.4 wt% while that of the gas phase was 23.5 wt%, respectively, which is a noticeable improvement compared to previous studies.[44,60] As no further compounds were detected in the NMR spectra, it is assumed

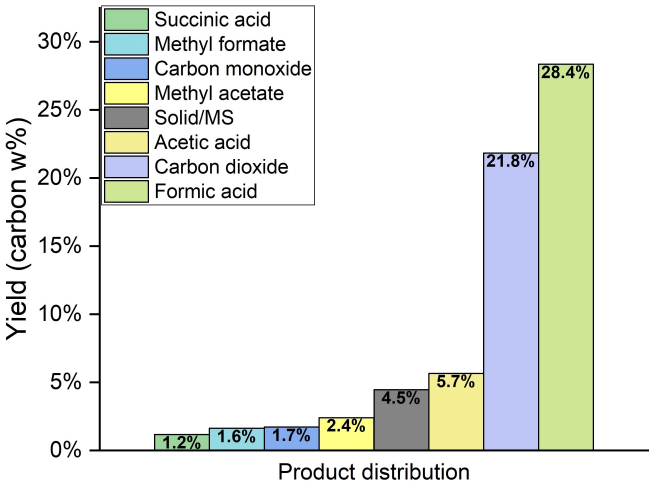

Figure 2. Results for the SCO of humin (90 °C, 30 h, 1 wt% humin in 95:5 H_2O/MeOH solution, p = 30 bar O_2, 2.5 wt% HPA-2, carbon yields determined by ^{1}H-NMR (Table S5), GC-MS and using equation S2).

that a large number of smaller carbon compounds were formed that were present in too low amounts to be detectable or were overshadowed by other larger signals, such as the water peak, as it was the case with methanediol and methoxymethanol.

The remaining solid humin was also structurally changed. Elemental analysis and infrared spectra indicate, analogous to previous research, primarily a breakdown of the ether and ester bonds inside and outside the furan rings (Figure S4 and Table S2).[60]

Nanofiltration for HPA-2 Recycling and FA Isolation Via Distillation

A nanofiltration system, which has already been described in detail in previous studies[56,57] was used to separate the HPA-2 catalyst from the aqueous reaction products. Therefore, the selected membrane must have a different resistance for the components to be separated. Ideally, one component cannot and the other can almost unhindered penetrate the membrane. The resistance of the membrane for a component is described by the rejection for a respective component, whereby a rejection of 100% means that the membrane is completely impermeable to the respective component. Since the HPA-2 catalyst should be recycled in the oxidation process, it is desirable that it is completely rejected by the membrane and enriched in the retentate. The acid-stable nanofiltration membrane XN45 proved to be very promising in previous studies[56,57] due to its high selectivity with rejections for the catalyst components of over 99% as well as low rejection of FA of close to 0% and thus enables efficient separation of HPA-2 and product. A detailed description of the experimental methodology for nanofiltration can be found in the corresponding section of the experimental part. Figure 3 shows the results for the rejections of the catalyst and therefore the membrane's ability to separate the catalyst. Since the HPA-2 dissociates in the aqueous medium, the catalyst components phosphorous

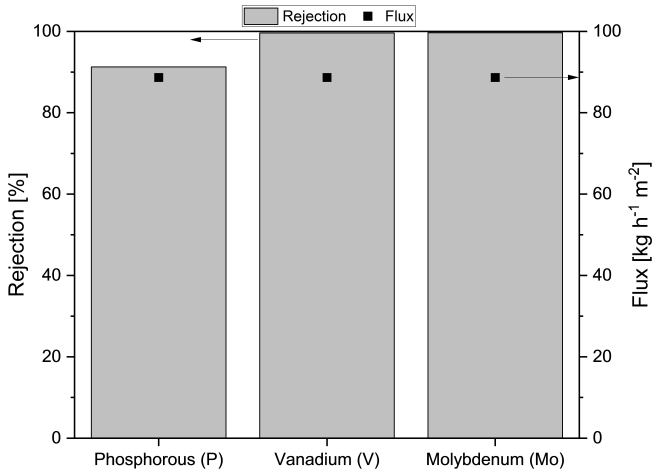

Figure 3. Rejection for catalyst components P, V and Mo in nanofiltration experiments for the product solution of the SCO of humins using HPA-2 in aqueous-methanolic solution (95 : 5). Experimental conditions: pre-wetted membranes, ambient temperature, 30 bar transmembrane pressure, 15 mL min^{-1} flow rate, 1100 rpm stirring speed.

(P), vanadium (V) and molybdenum (Mo) were analyzed individually giving the rejection for each component.

As shown in Figure 3, the XN45 membrane in the nanofiltration system enabled high rejections for V and Mo of over 99% in the present separation and therefore enables the enrichment of the catalyst in the retentate as well as the production of an almost catalyst free filtrate. The comparatively lower rejection for phosphorous is due to the excess phosphate incurred during the synthesis of the catalyst.[61]

Figure S5 shows the changes in composition for the organic compounds. In addition to its high selectivity, the XN45 membrane is also characterized by a high flux of almost 90 kg h^{-1} m^{-2}, enabling a fast and efficient downstream processing. By using nanofiltration, the initial catalyst concentration in the product solution could be significantly decreased, resulting in a purified product solution. More specifically, the initial concentration was decreased from over 25 mmol L^{-1}to 0.1 mmol L^{-1} for V and from over 127 mmol L^{-1} to 0.4 mmol L^{-1} for Mo, yielding the mostly catalyst free filtrate. Overall, the promising results of the previous studies were reproducible.[56] Furthermore, in these studies it was also successfully demonstrated that the catalyst is recyclable using nanofiltration and the selected XN45 membrane.

After nanofiltration, the filtrate was additionally separated using distillation to achieve a pure FA solution, as the membrane treatment did not remove all impurities from the reaction solution. Additionally, the measured pH value (2.1) of the permeate was deemed too high for the consecutive **LP** reaction for LA synthesis which would have to be carried out under a pH value of almost 1. The reaction solution was therefore distilled over 12 hours at up to 130 °C under atmospheric pressure in order to separate the obtained FA from the rest of the reaction solution and to further concentrate it to the distinguished acidity required for the **LP** reaction. After distillation, the highest concentration of FA could be found in the last fraction, which was left at the bottom of the flask, which is referred to hereafter as FA-fraction (Figure 4). While it was possible to completely remove most of the volatile compounds such methanol or methylformate, it was not possible to remove all other reaction products from the FA-fraction (Figures S6 & S7) due to their higher boiling points like succinic acid.

After distillation, the FA-fraction consisted of 87.00 wt % water, 11.65 wt% FA, 0.73 wt% succinic acid, 0.49 wt% acetic acid and 0.13 wt% methyl acetate. The pH value of the reaction solutions for **LP** was approx. 1 while the pH value of the fraction reached about 1.3.

Levulinic Acid Production (LP) Using FA as Organocatalyst

In order to establish a cyclic levulinic acid production (**LPC**) from humins, a suitable carbohydrate source for the initial LA synthesis using FA as an organocatalyst must be found. Similar to previous work,[39] five different sugar derivatives were selected as substrates: Cellobiose and sucrose as hexose-based disaccharides, their monomers fructose and glucose as well as the pentosic monosaccharide xylose. The results are summarized in Figure 5 and Table S3.

Fructose achieved the highest LA yield of 38% followed by sucrose with 23%. Glucose and cellobiose, however, only achieved LA yields of 9% and 8%, respectively. This might be due to the fact that glucose requires an additional isomerization step to fructose before it can be hydrolyzed to LA.[62] Contrasting to previous research,[39] significant amounts of 5-HMF (around 8% for all hexoses) could also be detected in the reaction solutions, although this can be attributed to the relatively lower acid strength of FA as an acidic catalyst compared to $H_4SiW_{12}O_{40}$, resulting in a lower conversion of 5-HMF to LA within the short reaction time of 1 hour. Interestingly, only in the conversion of sucrose and fructose a measurable amount of solid humins (around 4 wt%) was formed. When glucose and cellobiose were converted, almost no solid humins were formed. As no further substances were

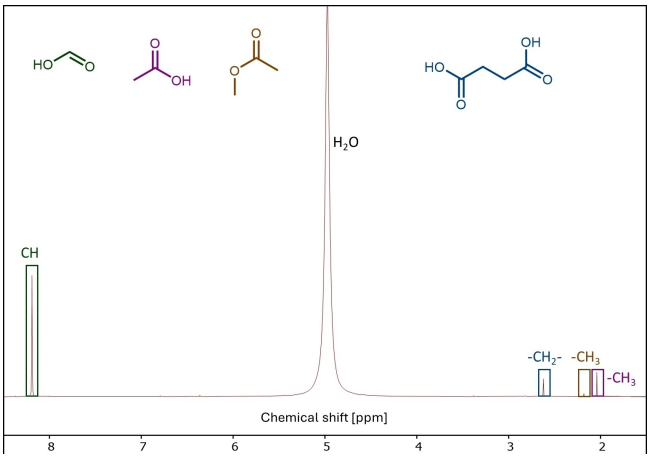

Figure 4. ^{1}H-NMR of the FA-fraction after atmospheric distillation.

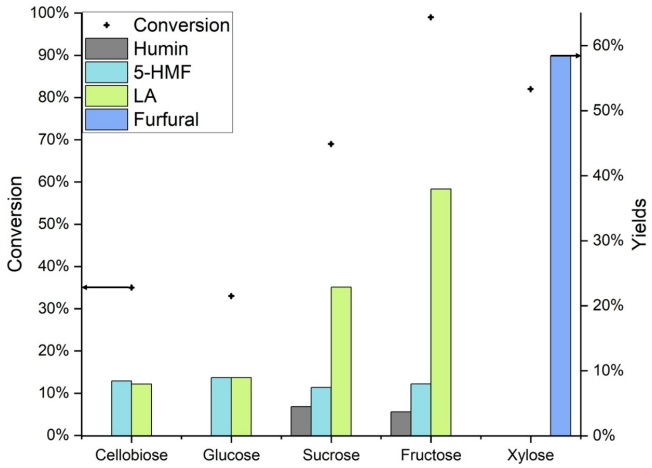

Figure 5. Conversion of various sugars using FA as an organocatalyst. Yields of LA (mol%), 5-HMF (mol%), furfural (mol%) and humin (wt%). Reaction conditions: 0.1 mol L^{-1} sugar, 7.5 mL H_2O, pH = 1 (FA), 180 °C, 1 hour, p = 40 bar N_2, yields determined by HPLC.

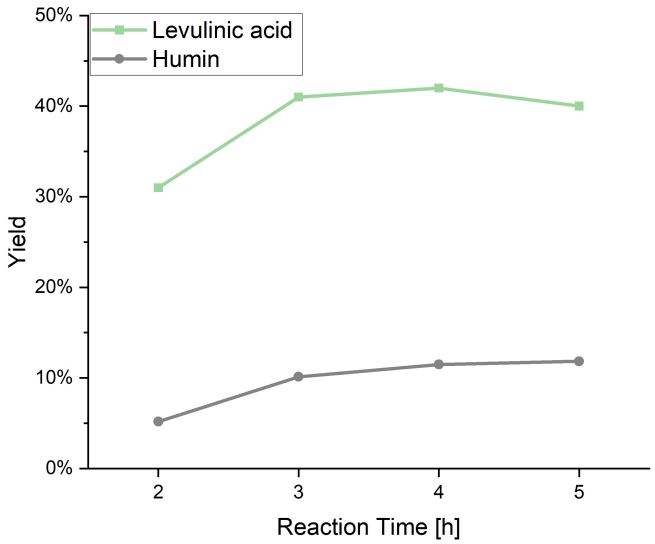

Figure 6. Course of the reaction for the upscaled LA synthesis from fructose in the 600 mL autoclave. LA yields (mol%) and humin yields (wt%) at different reaction times. Reaction conditions: 0.1 mol L^{-1} fructose, 300 mL H_2O, pH = 1 (FA), T = 180 °C, p = 30 bar N_2.

detected in the NMR spectra and the HPLC chromatograms (Figures S8 & S9) for all sugars, it is assumed that, as already postulated by Tsilomelekis et al.,[32] multiple water-soluble oligomers are formed from the remaining converted sugar, with the relative proportion of oligomers formed being greatest in fructose, the only sugar which was converted completely within the reaction time of 1 hour.

Xylose as the only pentose tested here shows a completely different behavior as it neither produces HMF nor LA or any solid residues. In contrast, only furfural with a yield of 59% is formed. The formation of furfural from xylose was expected, as xylose is known to form furfural when hydrolyzed under similar conditions.[63,64] A formation of LA did not occur as the catalytic hydrogenation of furfural to furfuryl alcohol that is necessary for the formation of LA from furfural was not possible under the conditions applied. Therefore, fructose was chosen as the substrate for initial LA synthesis catalyzed by the organocatalyst FA, as it showed the highest yield of LA.

After selecting an appropriate substrate, the reaction was scaled up from 20 mL reactors to the larger reactor system (600 mL) in order to test the scalability of the reaction and to produce the necessary amounts of material for the desired cyclic LA production. The synthesis conditions could therefore not be adopted exactly from the previous test, as the larger reactor had a different heating profile. For this reason, an additional series of tests was carried out to adapt the reaction time for the larger scale reactor and to obtain the maximum LA yield. The course of the reaction in the up-scaled LA synthesis from fructose in the 600 mL autoclave can be seen in Figure 6 and Table S4.

It can be seen that the optimal LA yield is not achieved within 1 hour reaction time, as the LA yield increases up further to reach its maximum with 42 mol% at a reaction time of 4 hours, whereas afterwards it slightly drops down. This drop in LA yield can be traced back to an increasing incorporation of the LA into the humin structure the longer the reaction proceeds. The achieved LA yield at a reaction time of 4 hours is also significantly higher than the highest value achieved during the substrate selection within 1 h reaction time. The fact that larger amounts of 5-HMF, similar to the previous reaction, were found only in the liquid phase of the reaction at the shortest reaction time (Figure S10), confirms the previous suspicion, which is also further reinforced by an examination of the solid humins produced. Within the first 3 h, the humin yield increases continuously up to 10.1 wt%, whereas from 3 h onwards only a slight increase in yield up to 11.8 wt% could be observed. Elemental analysis (Table S5) and infrared spectroscopy (Figure S11 & Table S6) show strong differences between the humins produced after 2 hours and the other humins after 3 hours onwards, all being very similar to each other, indicating that the solid humins formed undergo several structural modifications during reaction.

With longer reaction times, however, LA could be detected as the sole reaction product in liquid phase confirming the effectiveness of FA as an organocatalyst for selective LA production. Consequently, the ideal reaction time for establishing a cyclic LA production where the organocatalyst FA is directly produced from the humin residue of the original LA synthesis from fructose is considered to be 4 hours, as this reaction resulted in the highest LA yield. Moreover, significant amounts of humin were also produced, allowing for their use as substrate in the SCO, with this reaction hereinafter being referred to as **LP**. In a future industrial process, it would also become relevant to separate the LA from the rest of the solution after the successful synthesis. This is generally achieved through distillation or extraction.[65] Additionally, it could also be advisable to further optimize the FA-catalyzed LA synthesis in a follow-up study. The different reaction behaviour of FA compared to the POM catalyst used in the previous study,[39]

shows a potential for improvement to increase the FA yield through a further variation of the reaction parameters.

Cyclic Levulinic Acid Production (LPC) Using a Closed Reaction Cycle

In the next step, reaction **LPC** was carried out, which was intended to emulate a new LA production using the FA obtained from the SCO, thus starting a new cycle. For this purpose, a reaction solution was prepared that corresponded to the composition of the FA-fraction, as the amount of solution obtained after distillation was not sufficient to carry out the reaction on the same scale as the original LA synthesis **LP**. **LPC** was then carried out according to the parameters of **LP**. In addition, another reaction was carried out with a pure FA/water solution, whereby the FA to water ratio was the same as the ratio of the two substances used in **LPC**. This was intended to serve as a comparison to check what influence the additional substances left in the final fraction had on the reaction and will be referred to as **LPC-2**. The results compared to the averages of the **LP** reactions can be seen in Table 1.

It can be seen that there are only minor differences between the **LPC** and **LPC-2**. The LA and humin yields differed slightly, but these differences were still within the range of variance that could already be seen during **LP**. No major differences can be seen in the ^{1}H-NMRs either, apart from the presence of the extra substances in the reaction solution of **LPC** and some additional methanol (Figure S11). The same also applies to the comparison of the spectra of **LP** with **LPC** and **LPC-2**. The only difference here is the slightly lower LA yield, although this is presumably caused by the lower FA concentration, as the LA formation is known to increase with higher concentrations of the acidic catalyst.[39]

Table 1. Comparison of pH values of reaction solutions and average yields of **LP** with **LPC** and **LPC-2** pH values and yields (180 °C, H_2O, 0.1 mol L^{-1} fructose, t = 4 h, p = 30 bar N_2).

	LA yield mol%	Humin yield wt%	pH [−]
LP (avg)	40.7	11.5	1.0
LPC	37.0	11.4	1.3
LPC-2	36.0	12.6	1.3

The infrared spectra of the humins do not show any discernible differences (Figure S12). It seems like the lower acid concentration and the added substances had no significant impact on the humin formation to significantly alter the humin composition. It can therefore be assumed that it is possible to convert humins in a similar way to SCO and thus making a continued cycle possible.

Due to the additional step required during purification, the original planning of the cycle from Figure 1 had to be slightly modified. The reworked cycle is displayed in Figure 7.

The original LA synthesis through **LP** was successful. Yields of an average of 40.7 mol% (1.2% standard deviation) were achieved in several reactions, with an average humin yield of about 11.5 wt% (0.2% std. dev.) showing a higher LA and lower humin yield than a comparable experiment from previous research,[39] which underlines the successful optimization of the reaction parameters for LA synthesis. In this case, however, a higher humin yield could be acceptable as long as the LA yield does not suffer, as it would result in more material to be recycled into FA. A higher sugar concentration could possibly be beneficial for future studies. The experiment also had to be carried out several times in order to produce a sufficient amount of humin **H** for further reactions. In the following SCO of humin, FA could be obtained as the main product with a carbon weight content of 28.4%. This confirmed the previous results of Esser et al.[56] Moreover, the membrane could completely retain the HPA-2 catalyst and retain its structure (Figure S15). An additional distillation of the permeate had to be carried out in order to increase the FA concentration and to remove additional low-molecular by-products. Finally, a cyclic LA production **(LPC)** using a reaction solution whose composition was equivalent to that of the FA-fraction from distillation

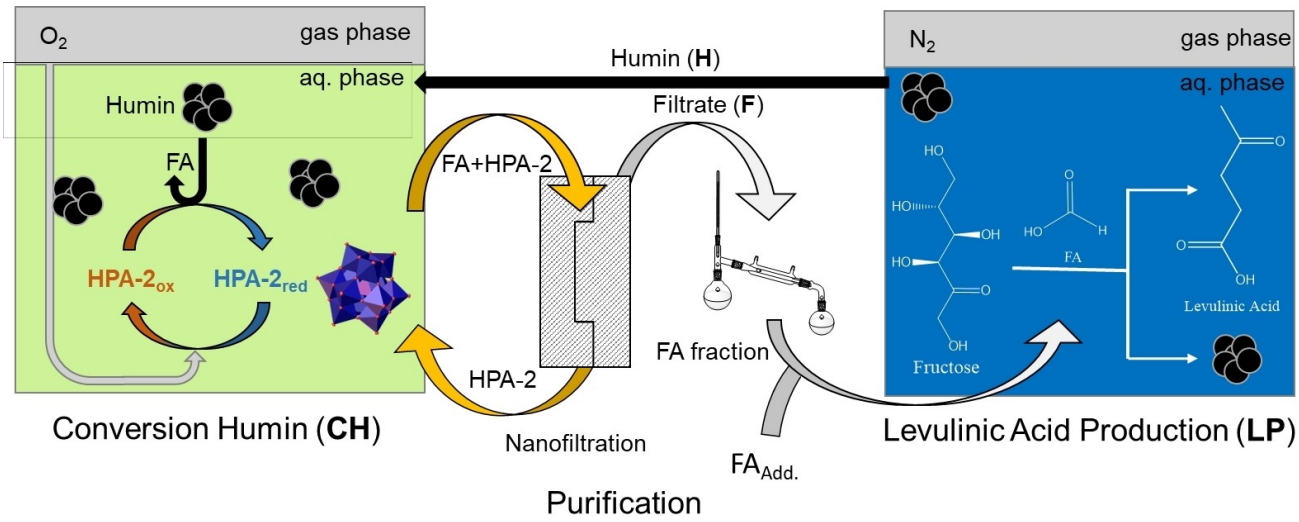

Figure 7. Modified schematics for the cyclic LA production route as performed during this study.

was then carried out successful. Although the LA yield of **LPC** was slightly lower with 37 mol%, due to the higher pH value compared to **LP**, it proved the possibility of a continued cycle, as the humins from both reactions showed no discernible differences, despite the additional substances in the reaction solution of **LPC**.

An additional **LPC-2** with the same pH value but without the low molecular weight impurities in the FA-fraction did not show any major differences compared to **LPC**. A better distillation would therefore mostly increase the recovery efficiency of the produced FA resulting in a more precise re-creation of the reaction conditions of **LP**, which should then result in similar results and make the further cyclic process possible. A cyclic synthesis of LA recycling the by-product into new catalysts is therefore certainly possible, even if some small hindrances have to be eliminated in order to increase the overall efficiency.

Conclusions

From a selection of five different sugars, fructose was confirmed to be the best substrate for FA-catalysed LA production. While xylose showed by far the highest conversion, the resulting platform chemical was furfural instead of LA. This combined with a lack of measurable humin residue made xylose unsuitable for the proposed process. Upon subsequent transfer to a larger reactor system, it was proven that the results were scalable to bigger reactors, although the results indicated higher reaction times being beneficial. Further studies into the optimal reaction conditions for the upscaled LA synthesis could also potentially result in even higher LA yields. With the modified reaction parameters multiple reactions were carried out, resulting in a sufficient amount of humin being produced, which was successfully converted by SCO using HPA-2 to form a larger amount of FA. The subsequent separation from the catalyst via nanofiltration was carried out successfully, although further purification of the permeate by distillation was necessary. In a final step, by using a reaction solution of the same composition as the solution obtained at the end of the distillation, it was proven that a new LA synthesis is possible using the FA-fraction. It was also confirmed by an additional experiment that the impurities of the FA-fraction had no noticeable influence on product formation. It could therefore be shown that the formation of a cyclic LA synthesis process using FA as an organocatalyst produced from humin residues from the initial LA synthesis from sugars is chemically possible, even if the process shown here needs to be further optimized. In follow-up studies, it would also be advisable to carry out a life cycle as well as a technoeconomic analysis of the process in order to examine its economic viability. We believe that these results show a lot of potential and that through improvements in efficiency, for example during the separation, could lead to the production of LA through FA in an environmentally friendly, cyclic system being a potential economical alternative.

Author Contributions

A. Wassenberg: methodology (main), conceptualization (equal), writing (main); M. J. Poller: methodology (supporting), conceptualization (supporting), supervision, writing – review & editing; T. Esser: methodology (supporting), conceptualization (equal), writing – description of the nanofiltration system and process; D. Voß: project administration (supporting), supervision, writing – review & editing; J. Albert: project administration (main), funding acquisition, resources, writing – review & editing

Acknowledgments

J. A., T. E., and A. W. thank the Deutsche Forschungsgemeinschaft (DFG) for their financial support via the project AL 2130/5-1. We also would like to thank the central analytical services of the Department of Chemistry at the University of Hamburg for carrying out NMR spectroscopy and elemental analysis. Open Access funding enabled and organized by Projekt DEAL.

Conflict of Interests

The authors declare no conflict of interest.

Data Availability Statement

The data that support the findings of this study are available from the corresponding author upon reasonable request.

Keywords: Environmental catalysis · Levulinic acid · Humins · Nanofiltration · Polyoxometalates · Formic acid

[1] J. Albert, A. Jess, C. Kern, F. Pöhlmann, K. Glowienka, P. Wasserscheid, *ACS Sustainable Chem. Eng.* **2016**, *4*, 5078–5086, https://doi.org/10.1021/acssuschemeng.6b01531.
[2] M. Sajid, U. Farooq, G. Bary, M. M. Azim, X. Zhao, *Green Chem.* **2021**, *23*, 9198–9238, https://doi.org/10.1039/D1GC02919C.
[3] J. J. Bozell, L. Moens, D. Elliott, Y. Wang, G. Neuenscwander, S. Fitzpatrick, R. Bilski, J. Jarnefeld, *Resour. Conserv. Recycl.* **2000**, *28*, 227–239, https://doi.org/10.1016/S0921-3449(99)00047-6.
[4] S. Song, S. Yao, J. Cao, L. Di, G. Wu, N. Guan, L. Li, *Appl. Catal. B* **2017**, *217*, 115–124, https://doi.org/10.1016/j.apcatb.2017.05.073.
[5] S. G. Wettstein, D. M. Alonso, Y. Chong, J. A. Dumesic, *Energy Environ. Sci.* **2012**, *5*, 8199, https://doi.org/10.1039/c2ee22111j.
[6] A. Démolis, N. Essayem, F. Rataboul, *ACS Sustainable Chem. Eng.* **2014**, *2*, 1338–1352, https://doi.org/10.1021/sc500082n.
[7] D. Di Menno Bucchianico, Y. Wang, J.-C. Buvat, Y. Pan, V. Casson Moreno, S. Leveneur, *Green Chem.* **2022**, *24*, 614–646, https://doi.org/10.1039/D1GC02457D.
[8] Q. Luan, L. Liu, S. Gong, J. Lu, X. Wang, D. Lv, *Process Saf. Environ. Prot.* **2018**, *117*, 341–349, https://doi.org/10.1016/j.psep.2018.05.015.
[9] V. Pace, P. Hoyos, L. Castoldi, P. Domínguez de María, A. R. Alcántara, *ChemSusChem* **2012**, *5*, 1369–1379, https://doi.org/10.1002/cssc.201100780.
[10] I. Allaoua, B. E. Goi, M. M. Obadia, A. Debuigne, C. Detrembleur, E. Drockenmuller, *Polym. Chem.* **2014**, *5*, 2973–2979, https://doi.org/10.1039/C3PY01505J.

[11] D. W. Rackemann, W. O. S. Doherty, *Biofuels Bioprod. Biorefin.* **2011**, *5*, 198–214, https://doi.org/10.1002/bbb.267.
[12] T. J. Schwartz, A. R. P. van Heiningen, M. C. Wheeler, *Green Chem.* **2010**, *12*, 1353, https://doi.org/10.1039/c005067a.
[13] S. Cousinet, A. Ghadban, I. Allaoua, F. Lortie, D. Portinha, E. Drockenmuller, J.-P. Pascault, *J. Polym. Sci. Part A* **2014**, *52*, 3356–3364, https://doi.org/10.1002/pola.27397.
[14] M. J. Climent, A. Corma, S. Iborra, *Green Chem.* **2014**, *16*, 516, https://doi.org/10.1039/c3gc41492b.
[15] G.-T. Jeong, C. H. Ra, Y.-K. Hong, J. K. Kim, I.-S. Kong, S.-K. Kim, D.-H. Park, *Bioprocess Biosyst. Eng.* **2015**, *38*, 207–217, https://doi.org/10.1007/s00449-014-1259-5.
[16] A. Kumar, D. Z. Shende, K. L. Wasewar, *Mater. Today: Proc.* **2020**, *29*, 790–793, https://doi.org/10.1016/j.matpr.2020.04.749.
[17] D. J. Hayes, S. Fitzpatrick, M. H. B. Hayes, J. R. H. Ross, in: *Biorefineries-Industrial Processes and Products*, B. Kamm, P. R. Gruber, M. Kamm (Eds.), Wiley-VCH Verlag GmbH, Weinheim, Germany, **2005**, pp. 139–164.
[18] D. Rackemann, W. Doherty, *Int. Sugar J.* **2013**, *115*, 28–34.
[19] C. Antonetti, D. Licursi, S. Fulignati, G. Valentini, A. Raspolli Galletti, *Catalysts* **2016**, *6*, 196, https://doi.org/10.3390/catal6120196.
[20] C.-H. Kuo, A. S. Poyraz, L. Jin, Y. Meng, L. Pahalagedara, S.-Y. Chen, D. A. Kriz, C. Guild, A. Gudz, S. L. Suib, *Green Chem.* **2014**, *16*, 785, https://doi.org/10.1039/c3gc40909k.
[21] P. P. Upare, J.-W. Yoon, M. Y. Kim, H.-Y. Kang, D. W. Hwang, Y. K. Hwang, H. H. Kung, J.-S. Chang, *Green Chem.* **2013**, *15*, 2935, https://doi.org/10.1039/c3gc40353j.
[22] I. Thapa, B. Mullen, A. Saleem, C. Leibig, R. T. Baker, J. B. Giorgi, *Appl. Catal. A* **2017**, *539*, 70–79, https://doi.org/10.1016/j.apcata.2017.03.016.
[23] N. Jiang, R. Huang, W. Qi, R. Su, Z. He, *BioEnergy Res.* **2012**, *5*, 380–386, https://doi.org/10.1007/s12155-011-9141-7.
[24] L. Kupiainen, J. Ahola, J. Tanskanen, *Chem. Eng. Res. Des.* **2011**, *89*, 2706–2713, https://doi.org/10.1016/j.cherd.2011.06.005.
[25] K. Dussan, B. Girisuta, M. Lopes, J. J. Leahy, M. H. B. Hayes, *ChemSusChem* **2015**, *8*, 1411–1428, https://doi.org/10.1002/cssc.201403328.
[26] S. Liu, Y. Zhu, Y. Liao, H. Wang, Q. Liu, L. Ma, C. Wang, *Appl. Energy Combust. Sci.* **2022**, *10*, 100062, https://doi.org/10.1016/j.jaecs.2022.100062.
[27] I. van Zandvoort, Y. Wang, C. B. Rasrendra, E. R. H. van Eck, P. C. A. Bruijnincx, H. J. Heeres, B. M. Weckhuysen, *ChemSusChem* **2013**, *6*, 1745–1758, https://doi.org/10.1002/cssc.201300332.
[28] S. K. R. Patil, C. R. F. Lund, *Energy Fuels* **2011**, *25*, 4745–4755, https://doi.org/10.1021/ef2010157.
[29] S. K. R. Patil, J. Heltzel, C. R. F. Lund, *Energy Fuels* **2012**, *26*, 5281–5293, https://doi.org/10.1021/ef3007454.
[30] I. van Zandvoort, E. J. Koers, M. Weingarth, P. C. A. Bruijnincx, M. Baldus, B. M. Weckhuysen, *Green Chem.* **2015**, *17*, 4383–4392, https://doi.org/10.1039/C5GC00327J.
[31] B. Velaga, R. P. Parde, J. Soni, N. R. Peela, *Microporous Mesoporous Mater.* **2019**, *287*, 18–28, https://doi.org/10.1016/j.micromeso.2019.05.049.
[32] G. Tsilomelekis, M. J. Orella, Z. Lin, Z. Cheng, W. Zheng, V. Nikolakis, D. G. Vlachos, *Green Chem.* **2016**, *18*, 1983–1993, https://doi.org/10.1039/C5GC01938A.
[33] Z. Cheng, K. A. Goulas, N. Quiroz Rodriguez, B. Saha, D. G. Vlachos, *Green Chem.* **2020**, *22*, 2301–2309, https://doi.org/10.1039/C9GC03961A.
[34] H. Shen, H. Shan, L. Liu, *ChemSusChem* **2020**, *13*, 513–519, https://doi.org/10.1002/cssc.201902799.
[35] S. Kang, G. Zhang, X. Yang, H. Yin, X. Fu, J. Liao, J. Tu, X. Huang, F. G. F. Qin, Y. Xu, *Energy Fuels* **2017**, *31*, 2847–2854, https://doi.org/10.1021/acs.energyfuels.6b02675.
[36] H. Yang, C. Tao, L. Peng, J. Zhang, L. He, H. Liu, *ACS Sustainable Chem. Eng.* **2022**, *10*, 1920–1931, https://doi.org/10.1021/acssuschemeng.1c07807.
[37] S. J. Dee, A. T. Bell, *ChemSusChem* **2011**, *4*, 1166–1173, https://doi.org/10.1002/cssc.201000426.
[38] N. Shi, Q. Liu, H. Cen, R. Ju, X. He, L. Ma, *Biomass Convers. Biorefin.* **2020**, *10*, 277–287, https://doi.org/10.1007/s13399-019-00414-4.
[39] A. Wassenberg, T. Esser, M. J. Poller, D. Voß, J. Albert, *Biofuels Bioprod. Biorefin.* **2024**, *18*, 1585–1597, https://doi.org/10.1002/bbb.2654.
[40] T. M. C. Hoang, E. R. H. van Eck, W. P. Bula, J. G. E. Gardeniers, L. Lefferts, K. Seshan, *Green Chem.* **2015**, *17*, 959–972, https://doi.org/10.1039/C4GC01324G.
[41] T. M. C. Hoang, L. Lefferts, K. Seshan, *ChemSusChem* **2013**, *6*, 1651–1658, https://doi.org/10.1002/cssc.201300446.
[42] S. Agarwal, D. van Es, H. J. Heeres, *J. Anal. Appl. Pyrolysis* **2017**, *123*, 134–143, https://doi.org/10.1016/j.jaap.2016.12.014.
[43] P. Tosi, G. P. M. van Klink, A. Celzard, V. Fierro, L. Vincent, E. de Jong, A. Mija, *ChemSusChem* **2018**, *11*, 2797–2809, https://doi.org/10.1002/cssc.201800778.
[44] S. G. Maerten, D. Voß, M. A. Liauw, J. Albert, *ChemistrySelect* **2017**, *2*, 7296–7302, https://doi.org/10.1002/slct.201701553.
[45] J. Eppinger, K.-W. Huang, *ACS Energy Lett.* **2017**, *2*, 188–195, https://doi.org/10.1021/acsenergylett.6b00574.
[46] J. Reichert, J. Albert, *ACS Sustainable Chem. Eng.* **2017**, *5*, 7383–7392, https://doi.org/10.1021/acssuschemeng.7b01723.
[47] J. Zhong, J. Pérez-Ramírez, N. Yan, *Green Chem.* **2021**, *23*, 18–36, https://doi.org/10.1039/D0GC03190A.
[48] L. Ni, J. Gu, X. Jiang, H. Xu, Z. Wu, Y. Wu, Y. Liu, J. Xie, Y. Wei, G. Diao, *Angew. Chem. Int. Ed. Engl.* **2023**, *62*, e202306528, https://doi.org/10.1002/anie.202306528.
[49] L. Ni, G. Yang, Y. Liu, Z. Wu, Z. Ma, C. Shen, Z. Lv, Q. Wang, X. Gong, J. Xie, G. Diao, Y. Wei, *ACS Nano* **2021**, *15*, 12222–12236, https://doi.org/10.1021/acsnano.1c03852.
[50] F. Wang, C. Jing, J. Ping, D. He, W. Shang, M. Zeng, N. Wang, Z. Jia, *Polyoxometalates* **2024**, *3*, 9140067, https://doi.org/10.26599/POM.2024.9140067.
[51] G. Dai, Q. Li, D. Zang, Y. Wei, *Green Chem.* **2023**, *25*, 6263–6269, https://doi.org/10.1039/D3GC00951C.
[52] C. Fan, H. Guan, H. Zhang, J. Wang, S. Wang, X. Wang, *Biomass Bioenergy* **2011**, *35*, 2659–2665, https://doi.org/10.1016/j.biombioe.2011.03.004.
[53] Y. Song, X. Wang, Y. Qu, C. Huang, Y. Li, B. Chen, *Catalysts* **2016**, *6*, 49, https://doi.org/10.3390/catal6040049.
[54] T. Esser, A. Wassenberg, J.-C. Raabe, D. Voß, J. Albert, *ACS Sustainable Chem. Eng.* **2024**, *12*, 543–560, https://doi.org/10.1021/acssuschemeng.3c06539.
[55] T. Esser, A. Wassenberg, D. Voß, J. Albert, *React. Chem. Eng.* **2024**, *9*, 1666–1684, https://doi.org/10.1039/D3RE00672G.
[56] T. Esser, A. Wassenberg, D. Voß, J. Albert, *Chem. Eng. Res. Des.* **2024**, *209*, 311–322, https://doi.org/10.1016/j.cherd.2024.08.007.
[57] T. Esser, M. Huber, D. Voß, J. Albert, *Chem. Eng. Res. Des.* **2022**, *185*, 37–50, https://doi.org/10.1016/j.cherd.2022.06.045.
[58] J. Albert, D. Lüders, A. Bösmann, D. M. Guldi, P. Wasserscheid, *Green Chem.* **2014**, *16*, 226–237, https://doi.org/10.1039/C3GC41320A.
[59] P. Schirg, Verfahren und Vorrichtung zur Filtration von Produktgemischen, PS Prozesstechnik GmbH, **2009**.
[60] A. Wassenberg, T. Esser, M. J. Poller, J. Albert, *Materials* **2023**, *16*, https://doi.org/10.3390/ma16072864.
[61] J.-C. Raabe, T. Esser, F. Jameel, M. Stein, J. Albert, M. J. Poller, *Inorg. Chem. Front.* **2023**, *10*, 4854–4868, https://doi.org/10.1039/D3QI00937H.
[62] P. S. Divya, S. Nair, S. Kunnikuruvan, *ChemPhysChem A Eur. J. Chem. Phys. Phys. Chem.* **2022**, *23*, e202200057, https://doi.org/10.1002/cphc.202200057.
[63] C. J. A. Mota, A. L. de Lima, D. R. Fernandes, B. P. Pinto, *Levulinic Acid: A Sustainable Platform Chemical for Value-Added Products*, Wiley, Hoboken NJ, **2023**.
[64] W. Yang, P. Li, D. Bo, H. Chang, *Carbohydr. Res.* **2012**, *357*, 53–61, https://doi.org/10.1016/j.carres.2012.05.020.
[65] M. Errico, R. P. Stateva, S. Leveneur, *Processes* **2021**, *9*, 490, https://doi.org/10.3390/pr9030490.

Manuscript received: September 9, 2024
Revised manuscript received: December 16, 2024
Accepted manuscript online: January 15, 2025
Version of record online: ■■, ■■

7. Discussion of results

LA is an important platform chemical for replacing fossil raw materials in the chemical industry. However, the sustainable production of this substance possesses some efficiency problems. One of the goals of this work was therefore to optimize the LA synthesis in terms of efficiency while maintaining the core requirement of sustainability. In the same sense, the formation of humins during the synthesis of LA was to be examined and better understood in order to either avoid their formation or valorize the produced humins, thus further increasing the efficiency of LA synthesis.

Influences of the reaction conditions on formation, structure and valorization of humins

In order to minimize humin formation it is necessary to study the conditions that lead to humin formation and the impact these conditions possess on the yield and structure of the generated solids. To achieve this, several different humins were generated through an acidic conversion of carbohydrates using different reaction parameters. The varied reaction parameters were acid strength, used solvent and converted substrate. The hexoses fructose and glucose, the pentose xylose, as well as the dimeric sugar sucrose were used as substrates and the strong acids H_2SO_4 and pTSA, as well as the organic acid AA, were used as acidic catalysts. Water and 1:1 mixtures of water/ethanol and water/DMSO were used as solvents. The choice and variation of solvents was of particular interest, as various research groups had already noted positive results regarding an inhibition on the formation of humins through the usage of these organic solvents [23,34,79]. From the results of these conversions, it could be seen that all inspected parameters had a sizable influence on the amount of formed humins, resulting in greatly varying humin yields from as low as a carbon mass yield of about 5 % (glucose/AA/ethanol) up to a yield of about 70 % (sucrose/ H_2SO_4/DMSO) (*Figure 36*).

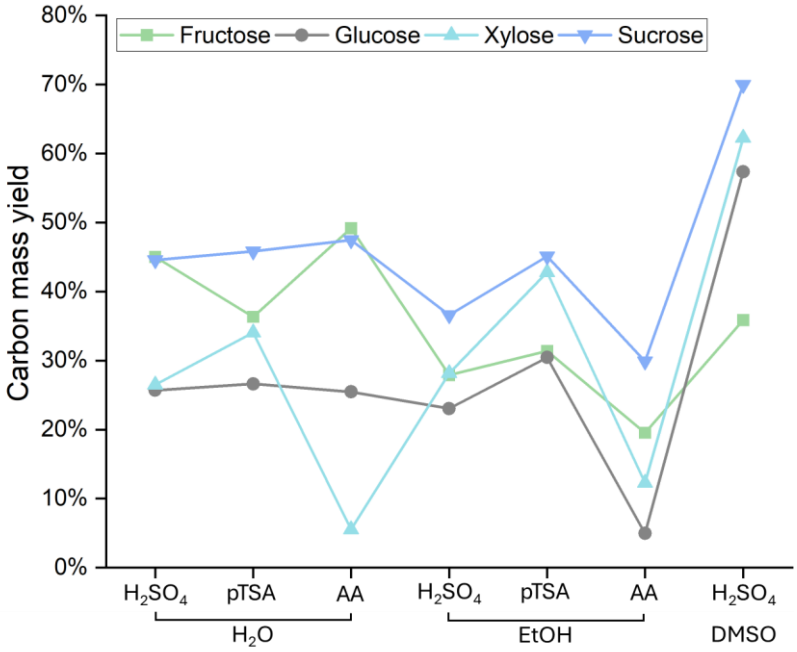

Figure 36: *Carbon mass yields of the different humins generated through the variation of substrate, solvent and acidic strength. [170]*

The use of ethanol as a co-solvent had the effect expected from previously published literature [23,79] and resulted in generally lower humin yields. This effect is attributed to the formation of water-soluble oligomers through reactions of the humin precursors with the organic solvent. The ethanol acted as a protective group and thus prevented the formation of larger humin structures [171]. A similar behavior could also be attributed to the AA used as acidic catalyst. Normally it would be expected that reactions with weaker acids would result in a higher humin yield [172,173], yet the reactions using AA as acidic catalyst generally generated the least amount of humins, especially in the water/ethanol mixture. The acetalization with AA and subsequent generation of more water-soluble oligomers would provide an adequate explanation for this occurrence. This effect was particularly pronounced with xylose, where, even in water, very little humin was formed during the reaction with AA. The inhibition of the formation of stable cyclic structures due to the shorter chain length of the pentose could have, in tandem with the acetalization with AA, almost completely prevented the formation of humins. Contrary, however, to the results using ethanol and those of *Tsilomelekis et al.* [34], the usage of the water/DMSO mixture resulted in a much higher humin yield rather than inhibiting the formation of the solid byproducts. A reason for that could be the much higher reaction temperature of 180 °C than the 140 °C that were used by *Tsilomelekis et al.* [34]. The higher reaction temperature may have caused a breakdown of DMSO, as indicated by signals of dimethyl sulfide and dimethyl disulfide found in the NMR-spectra of the corresponding reaction solution and thus resulting in an increased generation of the insoluble humin structures.

Afterwards, the structures of the generated humins were examined using solid phase analysis. Here, IR-spectroscopy and MALDI-TOF were used to determine specific structural fragments or motives of the humins, while EA was carried out to determine the element distribution in the humins and the macroscopic structure of the humins was examined using SEM. By comparing the results of different humins with each other, conclusions could also be drawn about the effects of the reaction parameters on the humin structure. The IR-spectra of the humins generally showed the ether, ester, carbonyl, aldehyde, aliphatic chain and furan ring signals that are frequently mentioned in the literature and are characteristic of humins [27,33]. Little to no differences could be seen between the spectra with different acidic catalysts and substrates. However, strong differences could be seen in the humins from different solvents: In addition to the general signals found in all the prepared humins, when compared to the humins generated in only water, the solids generated in the water/ethanol mixture showed more intense ether and carbonyl signals, while the humins prepared in the water/DMSO solutions showed additional signals indicating the presence of thioesters. These differences between the IR-spectra are attributed to a partial incorporation of the organic solvent molecules into the humin structure through etherification and esterification, thus resulting in the additional signals. This theory is also supported by the results of the EA, as substantial amounts of sulfur were found in the humins produced in DMSO, which indicate an assimilation of the solvent into the humin structure. Interestingly, the EA also shows clearer differences between humins from different acids. The results of the electron microscopy, on the other hand, are similar to those of the IR-spectroscopy; significant differences can only be seen between the humins generated in different solvents. However, these humins differ greatly in their morphology, determined by SEM: Humins produced in water are present in the spherical form known from literature [72,73], while humins produced in the ethanol mixture are more fragment-shaped with an amorphous content and humins produced in DMSO only consist of fragmented splinters. Using MALDI-TOF, three furan ring containing structural elements of the solid humins were also discovered (*Figure 37*). These structural fragments lend credence to the theory, that

humins are formed through aldol condensations between 5-HMF and DHH, as well as through esterification between furan rings.

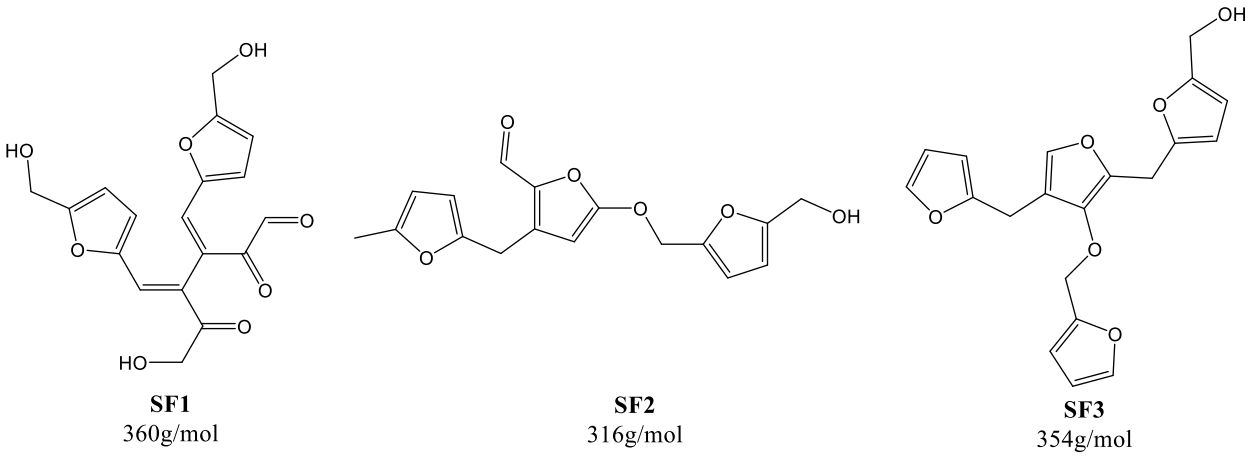

Figure 37: *Humin structural fragments (SF) postulated from MALDI-TOF data. [170]*

As it was not possible to avoid the formation of humins given the used parameter variations, the next step was to try to increase the efficiency of the conversion of carbohydrates through valorization of the generated by-products. For this purpose, several of the previously prepared humins were converted via SCO using HPA-5 as catalyst under *OxFA* conditions, based on the preliminary work by *Maerten et al.* [30], who were able to successfully convert humins into lower molecular carbonic acids. The main products of this process were CO_2, FA and AA, with the CO_2 yields being the highest (Figure 38). As the previously generated humins were converted, it was also possible to determine the influence of their structural differences, and thus the parameters used for their generation, on the valorization of the humins via SCO. Here, all reaction parameters were determined to possess at least a modicum of influence on the amount of humins converted, although the greatest variations in terms of humin conversion and product spectrum were found to result from using different solvents. Humins produced in the ethanol mixture were converted best and also showed larger proportions of low molecular weight carboxylic acids in the product spectrum, while the humins produced in DMSO were only very poorly converted. It is also interesting that the pTSA-catalyzed humins were more difficult to convert than those produced with the other acids. This is particularly surprising, as the solid phase analyses of these humins did not reveal any evidence of significant incorporation of the acid, nor other examinable differences that could explain this phenomenon. pTSA does not seem to be a good acid catalyst to obtain easily convertible humins.

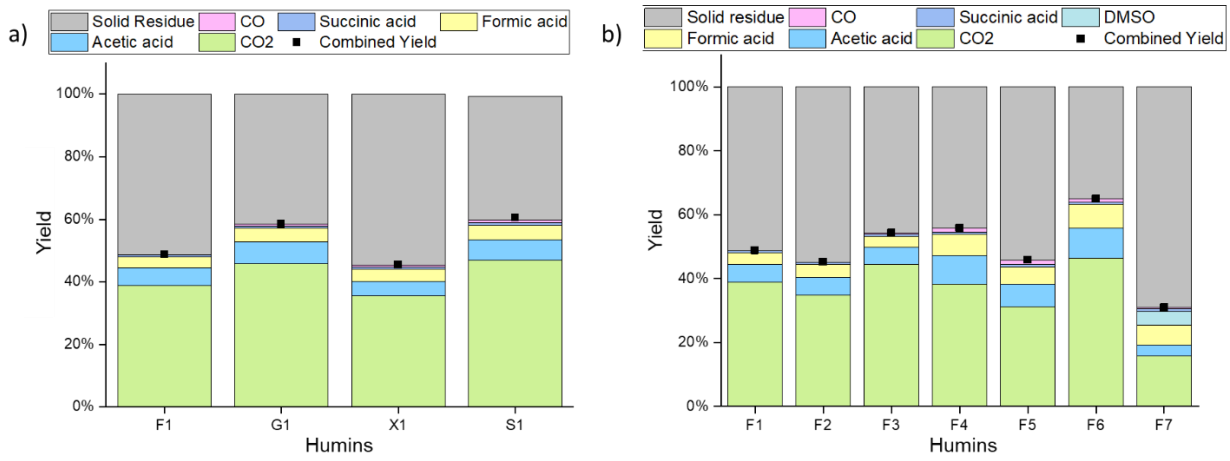

Figure 38: *Yields of the SCO performed on humins synthesized through the variation of the parameters solvent, substrate and acidic strength. [174]*

As full conversion could not be achieved in any of the reactions, it was also possible to subsequently analyze the humins after the oxidation in order to examine the trends that were observed in the yield in more detail. The comparison of the IR-spectra before and after SCO showed a clear lack of the spectral bands corresponding to poly substituted furan rings, aldehydes, ethers and aliphatic chains in the spectra obtained after the oxidative conversion. This indicated that the breaking of ether and ester bonds which are connected to the furan rings in aliphatic chains in the humin structure is especially favored by SCO. This also explains the higher conversion rates of the humins generated in ethanol and with AA respectively as these would possess a larger number of these structural motifs through reactions with solvent or acidic catalyst. The furan rings however remained unchanged in their integrity, as the spectra after SCO still indicated the presence of unsubstituted furan rings. The thioester and ester signals of the humin generated in DMSO also remained unchanged, indicating an inhibited conversion of these bonds and thus explaining the low conversion of this humin. However, the EA and SEM analyses provided less interesting results. The EA revealed an increase in the oxygen content and a decrease in the carbon content for all humins, which can be attributed to the oxidation of the remaining humins with oxygen. This can also be seen in the IR-spectra via an increase in the bands associated with carbonyl conjugated C=C double bonds. In the micrographs, the spherical structure of the humins produced in water had become a rather amorphous structure that seems to be somewhat melted, while the humins produced in organic solvents only show splinter-like fragments after SCO. In summary, the use of AA as an acidic catalyst with ethanol as an organic solvent additive provided the best results regarding humin yield and humin conversion. The combination of organic acid and organic solvent seems to be very suitable for obtaining a low humin yield from the acidic conversion of carbohydrates, while at the same time the low amount of humin produced can be easily converted for further valorization.

Optimization of the reaction parameters for LA synthesis using acidic catalysts

Having determined reaction parameters for acidic carbohydrate conversion with a low humin yield, the focus of the research was now shifted from the humin by-product to the main product LA. Similar to the preceding research, influence of the reaction parameters on the synthesis of the platform chemical was investigated. An additional goal was also the determination of optimal reaction parameters for a carbohydrate conversion with a maximal LA yield, while producing a minimal amount of humin. First, however, an alternative acidic catalyst was sought to possibly provide an industrially superior alternative in comparison to the usually used, environmentally problematic, sulfuric acid. For this purpose, fructose was hydrolyzed using FA, a stronger representative for the environmentally green organic acids than AA, which performed well during the previous research, as well as HSiW, HPMo and HPW as representatives for acidic POM catalysts, which can be separated from reaction solutions easily by membrane filtration [133] and possess high acidic strength, potentially resulting in a high LA yield. Additionally, H_2SO_4 was used to provide benchmark values. During these reactions the highest LA yield of 61 mol% was achieved using the POM HSiW, while also generating only a moderate amount of humin by-product, resulting in the POM outperforming the commercially used H_2SO_4 during these experiments. The use of the organic acid FA resulted in the highest humin yield of 23 wt%. This is consistent with the preceding results (Figure 36), where the usage of AA in water also provided higher humin yields and only decreased humin yield in the water/ethanol solution. As the results of using HSiW set an ideal baseline for further proceedings, the POM was used as the acidic catalyst for the subsequent optimization. For the optimization of the reaction an experimental plan was drafted using a Box-Behnken design, which took nonlinearity into account, as it was not certain that the change in the reaction factors had a linear influence on the output variables. The use of the response surface design allowed the modeling of the influence of the reaction parameters on the response values in order to enable the calculation of optimal reaction parameters. For this purpose, a set of reaction factors was determined, which included the variation of the parameters temperature, substrate concentration, weight fraction of an organic solvent and reaction time, using a set of three different values *(Table 1*). Acetone was used as the organic solvent of choice, despite the previously discussed results with ethanol, in order to prevent the esterification of the produced LA with the solvent. Consequently, the LA and humin yield were used as response values. The influences of the reaction factors on the response values as calculated using the experimental results can be seen in *Figure 39.*

Table 1: *Matrix of the reaction factors used for the optimization of LA and humin yield. [174]*

	Temperature [°C]	c(fructose) [mol*L-1]	Acetone content [wt%]	Reaction time [h]
Minimum value	140	0.1	0	1
Center point	160	0.25	40	3
Maximum value	180	0.4	80	5

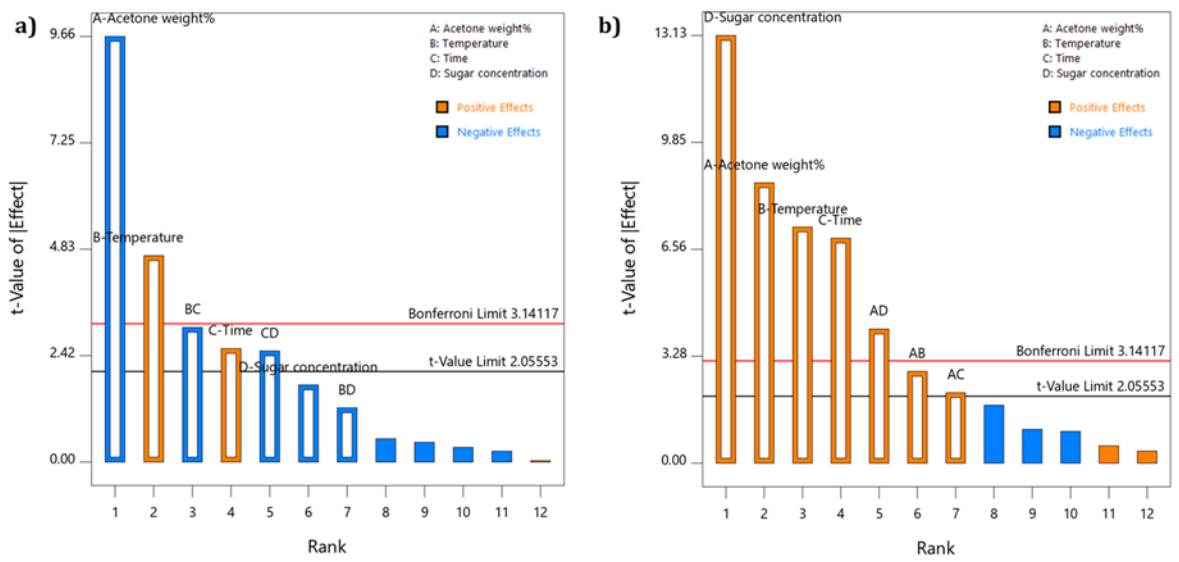

Figure 39: *Pareto charts of the effect of the reaction factors on LA (a)) and humin yields (b)). [174]*

Summarized, the experimental data shows that the formation of humins is promoted by long reaction times, high temperatures, high sugar concentrations and high organic solvent content. LA formation, on the other hand, is increased by long reaction times, high temperatures and low sugar concentrations and organic solvent proportions, although the formation decreases with a simultaneous increase in temperature and reaction time, as this combination favors the formation of humins more. This also shows that the addition of the organic solvent had a negative impact on the synthesis, contradicting the previous research results during the examination of humin formation. This effect can either be attributed to the interaction between acetone and HSiW that has not yet been researched or documented before or may be related to a missing reaction potential between LA and acetone, as the acetalization reactions between the intermediates and the solvents, which presumably are the cause of the reduced humin yield are impossible with acetone. However, it is also possible that the low humin amount of humins, generated by the reactions in the ethanol mixture during the preceding research, is caused by lower LA yields, as the NMR-spectra recorded from the reaction solutions of the carbohydrate conversions carried out in the partially organic solvents showed lower relative LA signals. Additionally, the very low humin yields resulting from the conversions using AA in the ethanol mixture could also have been caused by a lowering of the acidic strength in the reaction solution through esterification between solvent and acidic catalyst, thus reducing the carbohydrate conversions and subsequently the humin yield.

Through usage of the *Design Expert* software, two sets of parameters were created from the data (*Table 2*) which were produced with different weightings regarding the maximization of LA yield and the avoidance of humins. Both cases, however, showed that long reaction times at lower temperatures are necessary for the highest possible LA yield and a low humin yield. The small amounts of acetone specified in both optimizations could be attributed to a calculation inaccuracy resulting from the amount of data points or show that small amounts of acetone can indeed be helpful in achieving an optimal synthesis, for example through the dissolution of some of the produced humins. However, in an industrial setting, short reaction times are advantageous. Therefore, an optimized synthesis with a reaction time of one hour was developed, combining a maximized LA and minimized humin yield, while keeping the reaction time low (*Table 2, Entry 3*). A subsequent conversion of

fructose using these reaction conditions resulted in a LA yield of around 66 mol%, which deviated from the postulated synthesis by only approx. 3 %. Afterwards the reaction conditions were also applied successfully to the carbohydrates glucose, xylose, sucrose and cellobiose to test the transferability of the results to other substrates. All in all, the transfer was successful; The other sugars could all be converted into larger quantities of platform chemicals with little humin formation, with the yield being highest during the conversion of fructose. In the case of xylose, however, furfural was the product instead of LA, which was to be expected, as the reaction conditions would not enable the catalytic hydrogenation to convert furfural into furfuryl alcohol, which is necessary for the subsequent formation of LA [22]. In summary, the optimization of the conversion of carbohydrates to LA was successful, even if the lower yields for the sugars other than fructose might indicate that the reaction parameters for other substrates could still require slight improvements.

Table 2: *Optimal reaction parameters calculated with Design Expert using different weighting of result values. [174]*
Entry 1: Maximum LA yield. Entry 2: Complete suppression of humin formation.
Entry 3: Maximum LA yield at 1 h reaction time.

Entry	Acetone [wt%]	Temperature [°C]	Time [h]	c(Fructose) [mol*L^{-1}]	Humin yield* [wt%]	LA yield* [mol%]
1	0.37	140	5	0.100	1.20	69.3
2	7.86	140	5	0.100	0.00	65.1
3	0.00	180	1	0.100	2.00	67.1

*Predicted values

Cyclical production of LA using green catalysts

The preceding results show that a complete avoidance of humin formation does not necessarily result in the most efficient LA generation. As the formation of humins cannot be completely avoided, while aiming to achieve a maximal LA yield, it could prove to be more optimal to focus on an efficient valorization of the produced humins. Therefore, the aim of the final part of this research was to design a LA synthesis procedure, alternative to the conventionally used synthesis with mineral acids, which takes into account the results from the previous research on LA and humin formation and also efficiently valorizes the produced humins. The approach chosen here was the creation of a cyclic process for LA synthesis with FA as an acidic catalyst. The process would take advantage of the fact that FA can be obtained from the by-product humins via SCO, resulting in the acidic catalyst necessary for carbohydrate conversion being reformed and able to be used in a new LA synthesis. While the LA yield would be lower than through the usage of mineral acids; the increased efficiency through utilization of the by-products and the advantages of the usage of a green catalyst could make up for this disadvantage. The higher humin yield resulting from the usage of the organic acid would also be a net positive under these circumstances. This process was made possible to a large extent by the optimization of the SCO by *T. Esser* [160]. Where the relatively low FA yields of the previously applied SCO would have made the recycling of FA from the humins inefficient, the optimization by *Esser et al.* resulted in much larger FA yields after oxidation. Key factors of the optimized procedure are the suppression of the overoxidation to CO_2 through the usage of methanol as an additive and the usage of the less oxidative HPA-2 catalyst. However, to create the reaction cycle, a suitable substrate first had to be found in order to ensure the highest possible LA yield. For this purpose, the reaction conditions resulting from the optimization in the previous section *(Table 2; Entry 3)* were used here to

investigate the conversion of different carbohydrates, although the previously used HSiW was substituted with FA in this case. Fructose, glucose, xylose, sucrose and cellobiose were once again chosen as the substrates to be investigated. The results of the conversion can be seen in *Figure 40*.

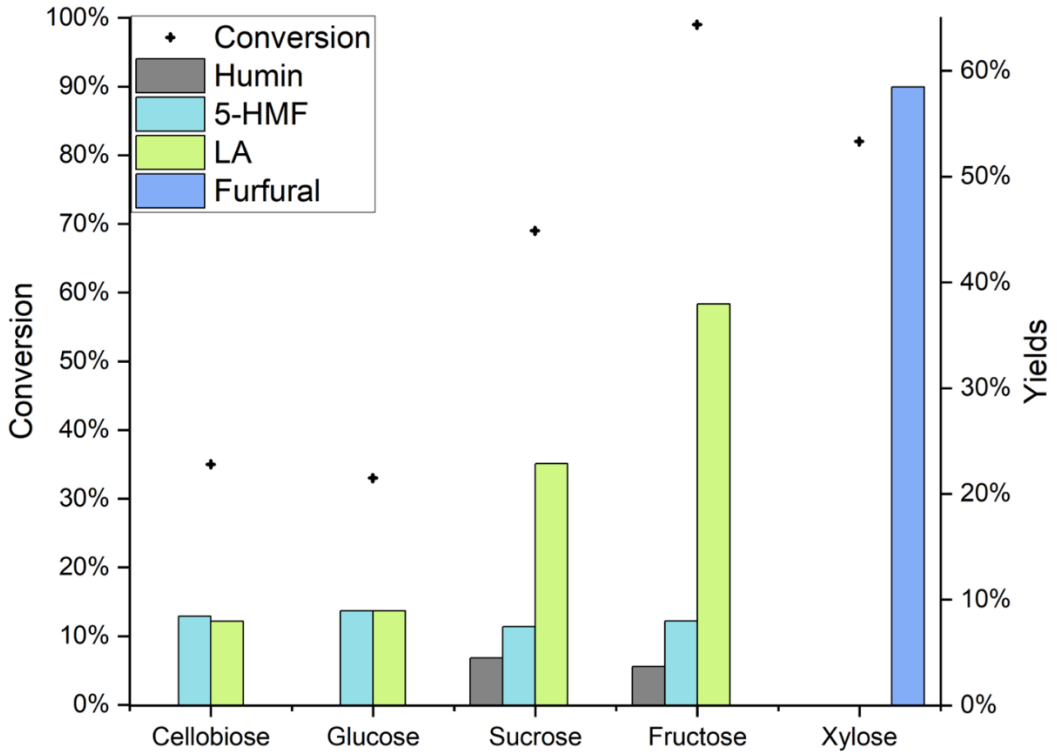

Figure 40: *Results of the conversion of different carbohydrates using the optimized reaction parameters for LA synthesis with FA as catalyst of choice. [175]*

Surprisingly, the highest yield of approx. 59 mol% was achieved through the conversion of xylose, however, the derived product was furfural and not LA. As no solid humins were formed, this result possesses potential application for the sustainable production of furfural. For the setup of the cyclic synthesis, fructose was chosen as the substrate, as its conversion resulted in the highest LA yield of 38 mol%. In order to better simulate industrial conditions, the reaction setup was scaled from the previously used 30 mL 10-fold batch reactors to a 600 mL single reactor. The reaction conditions also had to be slightly changed due to the different heating profile of the larger reactor. A series of fructose conversions using different reaction times was therefore conducted in the upscaled reaction system. This resulted in the reaction time of 4 h being recognized as the most optimal, as this time resulted in the highest LA yield of 42 mol%. However, such a large change compared to the previous reaction time cannot only be explained by the different heating profile; the presence of 5-HMF in the solution of the reaction performed with the shortest time of 2 h and its absence in the other reaction solutions indicate, that the fructose conversion is still incomplete at the time. It can therefore be assumed that the previously optimized reaction parameters do not completely conform to the usage of acids much weaker than HSiW, with the weaker acids requiring longer reaction times. In future research a further optimization using FA as acidic catalyst could also lead to potentially even higher yields LA. Here, the yield 42 mol% was deemed sufficient for the continuation of the research without further optimization. Multiple fructose conversions using these upscaled reaction parameters with a time of

4 h were performed to generate the humin necessary to perform the SCO under the conditions determined by *Esser et. al* [160] (*Figure 41*). Under these new and optimized conditions, the humin could be converted almost completely, with only sparse amounts of the humin remaining, while yielding FA as the main product, showing a huge increase in value products when compared to the previously performed SCO (*Figure 38*). The HPA-2 used as catalyst was subsequently separated from the reaction solution through a membrane separation process also developed by *T. Esser* [133,160], resulting in a rejection of 99 % of the catalyst and an almost catalyst free reaction solution after filtration. Afterwards, the filtered reaction solution was distilled, in order to separate and concentrate the synthesized FA.

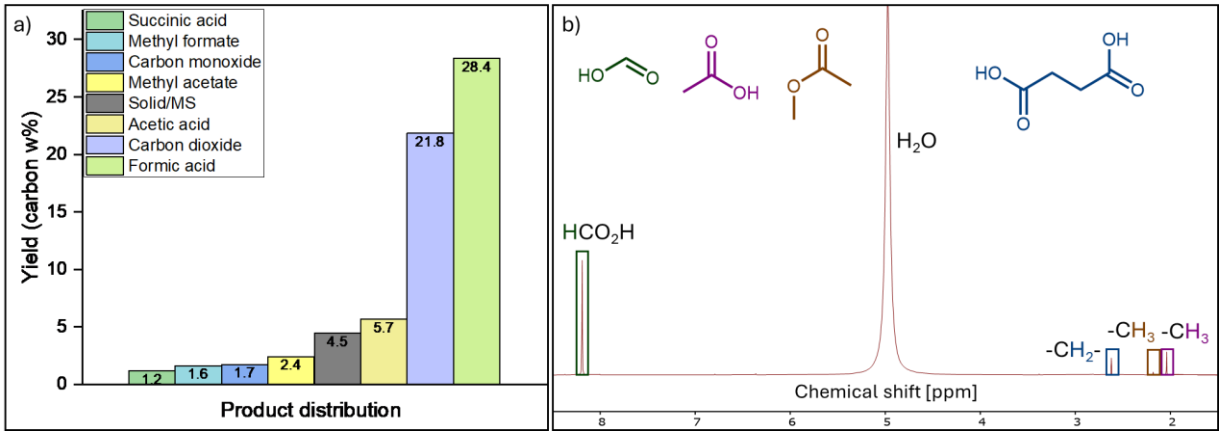

Figure 41: *a) Product spectrum of the SCO of the humin generated through the FA catalyzed fructose conversion. [175] b) ^{1}H- NMR-spectrum of the FA containing fraction after distillation. [175]*

However, due to the relatively low differences in boiling points of water and FA, as well as suboptimal distillation systems, the FA could only be concentrated in the bottom of the column, resulting in an incomplete separation from some of the other products of the SCO, such as AA, methyl acetate and succinic acid. Furthermore, the amount was not sufficient for another reaction on the same scale. During a new synthesis with an acidic catalyst whose composition was similar to the bottom fraction that remained after the distillation, however, it was possible to achieve a LA yield of 37 mol%, despite the higher pH value of 1.3 in comparison to the pH of 1 of the solution used for the original synthesis of LA. A comparison with a conversion of fructose using pure FA at a pH of 1.3 also showed that the additional products possessed no measurable influence on the result of the LA synthesis, thus resulting in the cyclic synthesis of LA being achieved (*Figure 42*). It was therefore possible to conceptualize and successfully implement a cyclic reaction system for the conversion fructose to LA using FA as acidic catalyst, while recycling the unwanted by-products into new FA. Although an optimization of the purification process is still necessary in order to increase the efficiency. A lower FA concentration could also be considered, as the differences in yields were relatively small and would result in higher catalyst efficiency. Another point of interest would also be the application of the cycle to real biomass such as paper waste or agricultural residues. After further research into its optimization, however, this cycle could potentially be a viable alternative for the industrially used carbohydrate conversions using mineral acids.

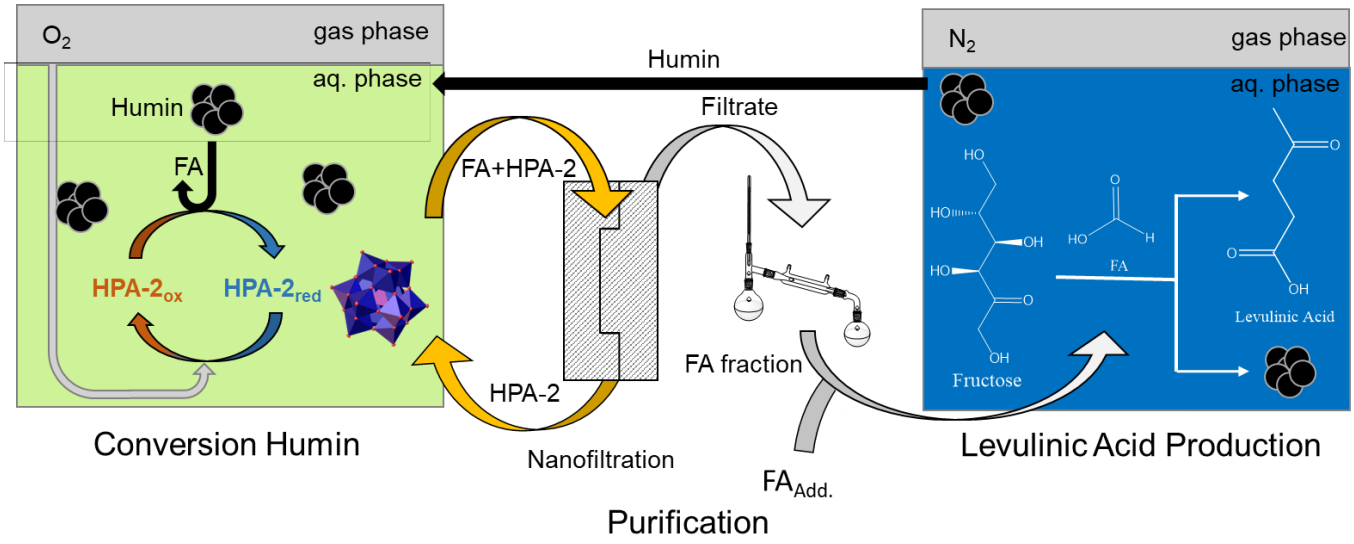

Figure 42: *Cyclic LA production using FA as acidic catalyst. [175]*

During the research for this thesis insights regarding the yields of LA and humins during acid catalyzed carbohydrate conversion were gained using predominantly green catalysts. Low substrate concentrations, low organic solvent contents, low reaction times and high temperatures in combination result in high LA and low humin yields, while being applicable in an industrial setting and transferable to different substrates. Furthermore, the effects of the reaction conditions on the structure of humins, as well as their subsequent valorization through SCO was documented. The usage of partly organic solvents proved to possess an especially big impact on both these properties of humins, with the usage of ethanol resulting in easier to convert humins. Through this, it was also possible to determine, that aliphatic ester- and ether-bonds were a predominant target of the POM catalyst during SCO. Lastly, it was also possible to combine the previous findings in one process, resulting in the conceptualization and implementation of a cyclical process for the synthesis of LA. In this cycle, the humins produced as a by-product of FA catalyzed LA production could be converted into a more FA, which could be used to produce further LA. All in all, the findings presented here could benefit the sustainable, industrial synthesis of LA and thus take a further step towards the complete replacement of fossil raw materials.

8. References

1) A. Behr and T. Seidensticker, Chemistry of Renewables, Springer Berlin Heidelberg (**2020**).

2) J. Houghton, Y. Ding, D. Griggs, M. Noguer, P. van der Linden, X. Dai, M. Maskell, and C. Johnson, in *IPCC – Third Assessment Report* (**2001**).

3) National Academies Press (US), Biobased Industrial Products: Priorities for Research and Commercialization (**2000**).

4) C. Baskar, S. Baskar, and R. S. Dhillon, Biomass Conversion, Springer Berlin Heidelberg (**2012**).

5) B. Kamm, P. R. Gruber, and M. Kamm, in *Ullmann's Encyclopedia of Industrial Chemistry 216*, Wiley (**2005**), pp. 1–38.

6) D. L. Klass. Biomass for Renewable Energy, Fuels and Chemicals, *Academic Press* (**1998**).

7) M. Kaltschmitt, H. Hartmann, and H. Hofbauer, Energie aus Biomasse, Springer Berlin Heidelberg (**2016**).

8) Energy Institute: Statistical Review of World Energy (**2024**).

9) T. Werpy and G. Petersen, Top Value Added Chemicals from Biomass: Volume I -- Results of Screening for Potential Candidates from Sugars and Synthesis Gas (**2004**).

10) T. J. Schwartz, A. R. P. van Heiningen, and M. C. Wheeler. Energy densification of levulinic acid by thermal deoxygenation, *Green Chemistry 12* (**2010**), 8, pp. 1353. https://doi.org/*10.1039/c005067a*.

11) J. Q. Bond, D. M. Alonso, D. Wang, R. M. West, and J. A. Dumesic. Integrated catalytic conversion of gamma-valerolactone to liquid alkenes for transportation fuels, *Science (New York, N.Y.) 327* (**2010**), 5969, pp. 1110–1114. https://doi.org/*10.1126/science.1184362*.

12) F. Kerkel, M. Markiewicz, S. Stolte, E. Müller, and W. Kunz. The green platform molecule gamma-valerolactone – ecotoxicity, biodegradability, solvent properties, and potential applications, *Green Chemistry 23* (**2021**), 8, pp. 2962–2976. https://doi.org/*10.1039/D0GC04353B*.

13) S. Cousinet, A. Ghadban, I. Allaoua, F. Lortie, D. Portinha, E. Drockenmuller, and J.-P. Pascault. Biobased vinyl levulinate as styrene replacement for unsaturated polyester resins, *Journal of Polymer Science Part A: Polymer Chemistry 52* (**2014**), 23, pp. 3356–3364. https://doi.org/*10.1002/pola.27397*.

14) I. Allaoua, B. E. Goi, M. M. Obadia, A. Debuigne, C. Detrembleur, and E. Drockenmuller. (Co)Polymerization of vinyl levulinate by cobalt-mediated radical polymerization and functionalization by ketoxime click chemistry, *Polymer Chemistry 5* (**2014**), 8, pp. 2973–2979. https://doi.org/*10.1039/C3PY01505J*.

15) D. J. Hayes, S. Fitzpatrick, M. H. B. Hayes, and J. R. H. Ross, in *Biorefineries-Industrial Processes and Products*, Wiley (**2005**), pp. 139–164.

16) K. Dussan, B. Girisuta, M. Lopes, J. J. Leahy, and M. H. B. Hayes. Conversion of hemicellulose sugars catalyzed by formic acid: kinetics of the dehydration of D-xylose, L-arabinose, and D-glucose, *ChemSusChem 8* (**2015**), 8, pp. 1411–1428. https://doi.org/*10.1002/cssc.201403328*.

17) X. Li, X. Lu, S. Nie, M. Liang, Z. Yu, B. Duan, J. Yang, R. Xu, L. Lu, and C. Si. Efficient catalytic production of biomass-derived levulinic acid over phosphotungstic acid in deep eutectic solvent, *Industrial Crops and Products 145* (**2020**), pp. 112154. https://doi.org/*10.1016/j.indcrop.2020.112154*.

18) H. Jeong, S.-Y. Park, G.-H. Ryu, J.-H. Choi, J.-H. Kim, W.-S. Choi, S. M. Lee, J. W. Choi, and I.-G. Choi. Catalytic conversion of hemicellulosic sugars derived from biomass to levulinic acid, *Catalysis Communications 117* (**2018**), pp. 19–25. https://doi.org/*10.1016/j.catcom.2018.04.016*.

19) I. Thapa, B. Mullen, A. Saleem, C. Leibig, R. T. Baker, and J. B. Giorgi. Efficient green catalysis for the conversion of fructose to levulinic acid, *Applied Catalysis A: General 539* (**2017**), pp. 70–79. https://doi.org/*10.1016/j.apcata.2017.03.016*.

20) P. P. Upare, J.-W. Yoon, M. Y. Kim, H.-Y. Kang, D. W. Hwang, Y. K. Hwang, H. H. Kung, and J.-S. Chang. Chemical conversion of biomass-derived hexose sugars to levulinic acid over sulfonic acid-functionalized graphene oxide catalysts, *Green Chemistry 15* (**2013**), 10, pp. 2935. https://doi.org/*10.1039/c3gc40353j*.

21) R. Zhang, W. Zhang, J. Jiang, J. Xu, K. Wang, J. Feng, and H. Pan. Catalytic valorization of biomass carbohydrates into levulinic acid/ester by using bifunctional catalysts, *Renewable Energy 221* (**2024**), pp. 119851. https://doi.org/*10.1016/j.renene.2023.119851*.

22) C. J. A. Mota, A. L. de Lima, D. R. Fernandes, and B. P. Pinto, Levulinic acid: A sustainable platform chemical for value-added products, Wiley (**2023**).

23) N. Shi, Q. Liu, H. Cen, R. Ju, X. He, and L. Ma. Formation of humins during degradation of carbohydrates and furfural derivatives in various solvents, *Biomass Conversion and Biorefinery 10* (**2020**), 2, pp. 277–287. https://doi.org/*10.1007/s13399-019-00414-4*.

24) H. Shen, H. Shan, and L. Liu. Evolution Process and Controlled Synthesis of Humins with 5-Hydroxymethylfurfural (HMF) as Model Molecule, *ChemSusChem 13* (**2020**), 3, pp. 513–519. https://doi.org/*10.1002/cssc.201902799*.

25) L. Liu, Biomass-Derived Humins: Formation, Chemistry and Structure, Springer Nature Singapore; Imprint Springer (**2023**).

26) M. V. Morales, K. Góra-Marek, H. Musch, A. Pineda, B. Murray, S. Stefanidis, L. Falco, K. Tarach, E. Ponomareva, J. H. Marsman, and I. Melián-Cabrera. Advanced oxidation process for coke removal: A systematic study of hydrogen peroxide and OH-derived-Fenton radicals of a fouled zeolite, *Applied Catalysis A: General 562* (**2018**), pp. 215–222. https://doi.org/*10.1016/j.apcata.2018.06.008*.

27) T. M. C. Hoang, E. R. H. van Eck, W. P. Bula, J. G. E. Gardeniers, L. Lefferts, and K. Seshan. Humin based by-products from biomass processing as a potential carbonaceous source for synthesis gas production, *Green Chemistry 17* (**2015**), 2, pp. 959–972. https://doi.org/*10.1039/C4GC01324G*.

28) A. Al Ghatta, X. Zhou, G. Casarano, Wilton-Ely, James D. E. T., and J. P. Hallett. Characterization and Valorization of Humins Produced by HMF Degradation in Ionic Liquids: A Valuable Carbonaceous Material for Antimony Removal, *ACS Sustainable Chemistry & Engineering 9* (**2021**), 5, pp. 2212–2223. https://doi.org/*10.1021/acssuschemeng.0c07963*.

29) J. Albert: Chemische Wertschöpfung aus Biomasse mittels selektiver katalytischer Oxidation zu Ameisensäure (FA) - der Erlanger OxFA-Prozess. Dissertation, Friedrich-Alexander-Universität Erlangen-Nürnberg (**2015**).

30) S. G. Maerten, D. Voß, M. A. Liauw, and J. Albert. Selective Catalytic Oxidation of Humins to Low-Chain Carboxylic Acids with Tailor-Made Polyoxometalate Catalysts, *ChemistrySelect 2* (**2017**), 24, pp. 7296–7302. https://doi.org/*10.1002/slct.201701553*.

31) I. van Zandvoort, Y. Wang, C. B. Rasrendra, E. R. H. van Eck, P. C. A. Bruijnincx, H. J. Heeres, and B. M. Weckhuysen. Formation, molecular structure, and morphology of humins in biomass

conversion: influence of feedstock and processing conditions, *ChemSusChem 6* (**2013**), 9, pp. 1745–1758. https://doi.org/*10.1002/cssc.201300332.*

32) I. van Zandvoort, E. J. Koers, M. Weingarth, P. C. A. Bruijnincx, M. Baldus, and B. M. Weckhuysen. Structural characterization of 13 C-enriched humins and alkali-treated 13 C humins by 2D solid-state NMR, *Green Chemistry 17* (**2015**), 8, pp. 4383–4392. https://doi.org/*10.1039/C5GC00327J*.

33) S. K. R. Patil and C. R. F. Lund. Formation and Growth of Humins via Aldol Addition and Condensation during Acid-Catalyzed Conversion of 5-Hydroxymethylfurfural, *Energy & Fuels 25* (**2011**), 10, pp. 4745–4755. https://doi.org/*10.1021/ef2010157*.

34) G. Tsilomelekis, M. J. Orella, Z. Lin, Z. Cheng, W. Zheng, V. Nikolakis, and D. G. Vlachos. Molecular structure, morphology and growth mechanisms and rates of 5-hydroxymethyl furfural (HMF) derived humins, *Green Chemistry 18* (**2016**), 7, pp. 1983–1993. https://doi.org/*10.1039/C5GC01938A*.

35) Y. M. Bar-On, R. Phillips, and R. Milo. The biomass distribution on Earth, *Proceedings of the National Academy of Sciences of the United States of America 115* (**2018**), 25, pp. 6506–6511. https://doi.org/*10.1073/pnas.1711842115*.

36) Y.-Y. Lee, T.-K. Tang, E.-T. Phuah, and O.-M. Lai, Recent Advances in Edible Fats and Oils Technology, Springer Singapore (**2022**).

37) A. E. Atabani and A. S. Da César. Calophyllum inophyllum L. – A prospective non-edible biodiesel feedstock. Study of biodiesel production, properties, fatty acid composition, blending and engine performance, *Renewable and Sustainable Energy Reviews 37* (**2014**), pp. 644–655. https://doi.org/*10.1016/j.rser.2014.05.037*.

38) S. Basu and D. K. Bhattacharyya. Utilization of acid oils in making surface-active compounds by lipase-catalyzed hydrolysis and esterification reactions, *Journal of Surfactants and Detergents 1* (**1998**), 3, pp. 343–344. https://doi.org/*10.1007/s11743-998-0034-2*.

39) O. Kunik, D. Saribekova, G. Lazzara, and G. Cavallaro. Emulsions based on fatty acid from vegetable oils for cosmetics, *Industrial Crops and Products 189* (**2022**), pp. 115776. https://doi.org/*10.1016/j.indcrop.2022.115776*.

40) O. Lamarzelle, G. Hibert, S. Lecommandoux, E. Grau, and H. Cramail. A thioglycerol route to bio-based bis-cyclic carbonates: poly(hydroxyurethane) preparation and post-functionalization, *Polymer Chemistry 8* (**2017**), 22, pp. 3438–3447. https://doi.org/*10.1039/c7py00556c*.

41) B. C. Martin, E. J. Minner, S. L. Wiseman, R. L. Klank, and R. J. Gilbert. Agarose and methylcellulose hydrogel blends for nerve regeneration applications, *Journal of neural engineering 5* (**2008**), 2, pp. 221–231. https://doi.org/*10.1088/1741-2560/5/2/013*.

42) W. Betts, R. K. Dart, A. Ball, and S. Pedlar, in *Biodegradation*, Springer London (**1991**), pp. 139–155.

43) P. Ning, G. Yang, L. Hu, J. Sun, L. Shi, Y. Zhou, Z. Wang, and J. Yang. Recent advances in the valorization of plant biomass, *Biotechnology for biofuels 14* (**2021**), 1, pp. 102. https://doi.org/*10.1186/s13068-021-01949-3*.

44) S. Wang and Z. Luo, GREEN alternative energy resources, volume 1: Pyrolysis of biomass, De Gruyter; Science Press (**2017**).

45) Y. Nishiyama, P. Langan, and H. Chanzy. Crystal structure and hydrogen-bonding system in cellulose Ibeta from synchrotron X-ray and neutron fiber diffraction, *Journal of the American Society 124* (**2002**), 31, pp. 9074–9082. https://doi.org/*10.1021/ja0257319*.

46) A. Ebringerová, Z. Hromádková, and T. Heinze, in *Advances in Polymer Science*: *Polysaccharides I*, Springer-Verlag (**2005**), pp. 1–67.

47) J. Pérez, J. Muñoz-Dorado, T. de La Rubia, and J. Martínez. Biodegradation and biological treatments of cellulose, hemicellulose and lignin: an overview, *International microbiology : the official journal of the Spanish Society for Microbiology 5* (**2002**), 2, pp. 53–63. https://doi.org/*10.1007/s10123-002-0062-3*.

48) D. Sharma and A. Saini, in *Lignocellulosic Ethanol Production from a Biorefinery Perspective*, Springer Singapore (**2020**), pp. 65–109.

49) Sigma-Aldrich, Levulinic acid (**2024**). *https://www.sigmaaldrich.com/DE/en/product/aldrich/l2009* (accessed **07.03.2024**).

50) M. Malaguti. Action des acides étendus sur le sucre, *Compt. Rendus 1* (**1835**), pp. 59–60.

51) G. J. Mulder. Untersuchungen über die Humussubstanzen, *Journal für Praktische Chemie 21* (**1840**), 1, pp. 321–370. https://doi.org/*10.1002/prac.18400210139*.

52) A. F. V. Grote and B. Tollens. Untersuchungen über kohlenhydrate. I. Ueber die bei Einwirkung von Schwefelsäure auf Zucker entstehende Säure (Levulinsäure), *Justus Liebigs Annalen der Chemie 175* (**1875**), 1-2, pp. 181–204.

53) A. F. v. Grote, E. Kehrer, and B. Tollens. Untersuchungen über die Lävulinsäure oder β-Acetopropionsäure. I. Ueber Darstellung und Eigenschaften der Lävulinsäure, *Justus Liebigs Annalen der Chemie 206* (**1881**), 1-2, pp. 207–225. https://doi.org/*10.1002/jlac.18812060111*.

54) R. H. Leonard. Levulinic Acid as a Basic Chemical Raw Material, *Industrial & Engineering Chemistry 48* (**1956**), 8, pp. 1330–1341. https://doi.org/*10.1021/ie50560a033*.

55) L. Farnleitner, H. Stueckler, H. Kaiser, and E. Kloimstein (*CHEMIE LINZ GMBH [AT]*), Process for the preparation of a storage stable levulinic acid, EP0401532 (A1) (**1990**).

56) R. H. Lock and K. Reynolds (*HOWARDS ILFORD LTD*), Process for the manufacture of levulinic acid esters, US2763665 (A) (**1952**).

57) R. Ballini and M. Petrini. Facile and Inexpensive Synthesis of 4-Oxoalkanoic Acids from Primary Nitroalkanes and Acrolein, *Synthesis 1986* (**1986**), 12, pp. 1024–1026. https://doi.org/*10.1055/s-1986-31858*.

58) H. Joshi, B. R. Moser, J. Toler, W. F. Smith, and T. Walker. Ethyl levulinate: A potential bio-based diluent for biodiesel which improves cold flow properties, *Biomass and Bioenergy 35* (**2011**), 7, pp. 3262–3266. https://doi.org/*10.1016/j.biombioe.2011.04.020*.

59) A. Garcia-Ortiz, K. S. Arias, M. J. Climent, A. Corma, and S. Iborra. Transforming Methyl Levulinate into Biosurfactants and Biolubricants by Chemoselective Reductive Etherification with Fatty Alcohols, *ChemSusChem 13* (**2020**), 4, pp. 707–714. https://doi.org/*10.1002/cssc.201903496*.

60) A. Proskouriakoff. Some Salts of Levulinic Acid 1, *Journal of the American Chemical Society 55* (**1933**), 5, pp. 2132–2134. https://doi.org/*10.1021/ja01332a060*.

61) M. Vasavada. Sodium Levulinate and Sodium Lactate Effects on Microbial Growth and Stability of Fresh Pork and Turkey Sausages, *Journal of Muscle Foods 14* (**2003**), 2, pp. 119–129. https://doi.org/*10.1111/j.1745-4573.2003.tb00694.x*.

62) S. Dutta, I. K. M. Yu, D. C. W. Tsang, Z. Su, C. Hu, K. C. W. Wu, A. C. K. Yip, Y. S. Ok, and C. S. Poon. Influence of green solvent on levulinic acid production from lignocellulosic paper waste, *Bioresource technology 298* (**2020**), pp. 122544. https://doi.org/*10.1016/j.biortech.2019.122544*.

63) I. T. Horváth, H. Mehdi, V. Fábos, L. Boda, and L. T. Mika. γ-Valerolactone—a sustainable liquid for energy and carbon-based chemicals, *Green Chemistry 10* (**2008**), 2, pp. 238–242. https://doi.org/*10.1039/B712863K*.

64) A. M. C. F. Castelijns, M. C. C. Janssen, and H. W. L. M. Vaessen (*DSM IP ASSETS BV [NL]*), Process to produce valerolactone from levulinic acid, CA2839137 (A1) (**2012**).

65) M. Sajid, U. Farooq, G. Bary, M. M. Azim, and X. Zhao. Sustainable production of levulinic acid and its derivatives for fuel additives and chemicals: progress, challenges, and prospects, *Green Chemistry 23* (**2021**), 23, pp. 9198–9238. https://doi.org/*10.1039/D1GC02919C*.

66) F. D. Pileidis and M.-M. Titirici. Levulinic Acid Biorefineries: New Challenges for Efficient Utilization of Biomass, *ChemSusChem 9* (**2016**), 6, pp. 562–582. https://doi.org/*10.1002/cssc.201501405*.

67) L. J. Carlson (*RAYONIER INC*), Process for the manufacture of levulinic acid, US3065263 (A) (**1959**).

68) W. W. Moyer (*STALEY MFG CO A E*), Preparation of levulinic acid, US2270328 (A) (**1940**).

69) A. P. Dunlop and P. A. W. Jr (*QUAKER OATS CO*), Process for producing levulinic acid, US2813900 (A) (**1953**).

70) S. W. Fitzpatrick, Final technical report: Commercialization of the Biofine technology for levulinic acid production from paper sludge (**2002**).

71) Green Car Congress. GFBiochemicals starts commercial production of levulinic acid from biomass, *Green Car Congress* (**20.07.2015**). *https://www.greencarcongress.com/2015/07/20150720-gfb.html* (accessed **23.07.2024**).

72) M. Sevilla and A. B. Fuertes. Chemical and structural properties of carbonaceous products obtained by hydrothermal carbonization of saccharides, *Chemistry (Weinheim an der Bergstrasse, Germany) 15* (**2009**), 16, pp. 4195–4203. https://doi.org/*10.1002/chem.200802097*.

73) M. Sevilla and A. B. Fuertes. The production of carbon materials by hydrothermal carbonization of cellulose, *Carbon 47* (**2009**), 9, pp. 2281–2289. https://doi.org/*10.1016/j.carbon.2009.04.026*.

74) I. van Zandvoort, E. R. H. van Eck, P. de Peinder, H. J. Heeres, P. C. A. Bruijnincx, and B. M. Weckhuysen. Full, Reactive Solubilization of Humin Byproducts by Alkaline Treatment and Characterization of the Alkali-Treated Humins Formed, *ACS Sustainable Chemistry & Engineering 3* (**2015**), 3, pp. 533–543. https://doi.org/*10.1021/sc500772w*.

75) S. Liu, Y. Zhu, Y. Liao, H. Wang, Q. Liu, L. Ma, and C. Wang. Advances in understanding the humins: Formation , prevention and application, *Applications in Energy and Combustion Science 10* (**2022**), pp. 100062. https://doi.org/*10.1016/j.jaecs.2022.100062*.

76) Z. Cheng, J. L. Everhart, G. Tsilomelekis, V. Nikolakis, B. Saha, and D. G. Vlachos. Structural analysis of humins formed in the Brønsted acid catalyzed dehydration of fructose, *Green Chemistry 20* (**2018**), 5, pp. 997–1006. https://doi.org/*10.1039/C7GC03054A*.

77) P. Tosi, G. P. M. van Klink, A. Celzard, V. Fierro, L. Vincent, E. de Jong, and A. Mija. Auto-Crosslinked Rigid Foams Derived from Biorefinery Byproducts, *ChemSusChem 11* (**2018**), 16, pp. 2797–2809. https://doi.org/*10.1002/cssc.201800778*.

78) S. Reiche, N. Kowalew, and R. Schlögl. Influence of synthesis pH and oxidative strength of the catalyzing acid on the morphology and chemical structure of hydrothermal carbon,

Chemphyschem : a European journal of chemical physics and physical chemistry 16 (**2015**), 3, pp. 579–587. https://doi.org/*10.1002/cphc.201402834.*

79) X. Hu, C. Lievens, A. Larcher, and C.-Z. Li. Reaction pathways of glucose during esterification: effects of reaction parameters on the formation of humin type polymers, *Bioresource technology 102* (**2011**), 21, pp. 10104–10113. https://doi.org/*10.1016/j.biortech.2011.08.040*.

80) M.-M. Titirici, M. Antonietti, and N. Baccile. Hydrothermal carbon from biomass: a comparison of the local structure from poly- to monosaccharides and pentoses/hexoses, *Green Chemistry 10* (**2008**), 11, pp. 1204. https://doi.org/*10.1039/b807009a*.

81) J. J. Blanksma and G. Egmond. Humin from hydroxymethylfurfuraldehyde, *Recueil des Travaux Chimiques des Pays-Bas 65* (**1946**), 4, pp. 309–310. https://doi.org/*10.1002/recl.19460650410*.

82) I. V. Sumerskii, S. M. Krutov, and M. Y. Zarubin. Humin-like substances formed under the conditions of industrial hydrolysis of wood, *Russian Journal of Applied Chemistry 83* (**2010**), 2, pp. 320–327. https://doi.org/*10.1134/S1070427210020266*.

83) S. K. R. Patil, J. Heltzel, and C. R. F. Lund. Comparison of Structural Features of Humins Formed Catalytically from Glucose, Fructose, and 5-Hydroxymethylfurfuraldehyde, *Energy & Fuels 26* (**2012**), 8, pp. 5281–5293. https://doi.org/*10.1021/ef3007454*.

84) J. Horvat, B. Klaić, B. Metelko, and V. Šunjić. Mechanism of levulinic acid formation, *Tetrahedron Letters 26* (**1985**), 17, pp. 2111–2114. https://doi.org/*10.1016/S0040-4039(00)94793-2*.

85) J. Horvat, B. Klaić, Metelko B., and V. Šunjić. Mechanism of Levulinic Acid Formation in Acid Catalysed Hydrolysis of 2-Hydroxymethylfurane and 5-Hydroxymethylfurane- 2-carhaldehyde, *Croatica Chemica Acta, 59* (**1986**), 2, pp. 429–438.

86) B. Cheng, X. Wang, Q. Lin, X. Zhang, L. Meng, R.-C. Sun, F. Xin, and J. Ren. New Understandings of the Relationship and Initial Formation Mechanism for Pseudo-lignin, Humins, and Acid-Induced Hydrothermal Carbon, *Journal of agricultural and food chemistry 66* (**2018**), 45, pp. 11981–11989. https://doi.org/*10.1021/acs.jafc.8b04754*.

87) V. Maruani, S. Narayanin-Richenapin, E. Framery, and B. Andrioletti. Acidic Hydrothermal Dehydration of d -Glucose into Humins: Identification and Characterization of Intermediates, *ACS Sustainable Chemistry & Engineering 6* (**2018**), 10, pp. 13487–13493. https://doi.org/*10.1021/acssuschemeng.8b03479*.

88) L. Peng, C. Tao, H. Yang, J. Zhang, and H. Liu. Mechanistic insights into the effect of the feed concentration on product formation during acid-catalyzed conversion of glucose in ethanol, *Green Chemistry 24* (**2022**), 13, pp. 5219–5227. https://doi.org/*10.1039/D2GC00300G*.

89) H. Shan, L. Li, W. Bai, and L. Liu. Evolution Process of Humins Derived from Glucose, *ChemistrySelect 7* (**2022**), 22. https://doi.org/*10.1002/slct.202201237*.

90) J. Köchermann, J. Schreiber, and M. Klemm. Conversion of d-Xylose and Hemicellulose in Water/Ethanol Mixtures, *ACS Sustainable Chemistry & Engineering 7* (**2019**), 14, pp. 12323–12330. https://doi.org/*10.1021/acssuschemeng.9b01697*.

91) H. Yang, C. Tao, L. Peng, J. Zhang, L. He, and H. Liu. Reactive and Mechanistic Insights into the Acid-Catalyzed Conversion of Concentrated C 5 /C 6 Sugars in Ethylene Glycol, *ACS Sustainable Chemistry & Engineering 10* (**2022**), 5, pp. 1920–1931. https://doi.org/*10.1021/acssuschemeng.1c07807*.

92) Y. Muranaka, H. Nakagawa, R. Masaki, T. Maki, and K. Mae. Continuous 5-Hydroxymethylfurfural Production from Monosaccharides in a Microreactor, *Industrial & Engineering Chemistry Research 56* (**2017**), 39, pp. 10998–11005. https://doi.org/*10.1021/acs.iecr.7b02017*.

93) L. Faba, D. Garcés, E. Díaz, and S. Ordóñez. Carbon Materials as Phase-Transfer Promoters for Obtaining 5-Hydroxymethylfurfural from Cellulose in a Biphasic System, *ChemSusChem 12* (**2019**), 16, pp. 3769–3777. https://doi.org/*10.1002/cssc.201901264*.

94) N. Shi, Q. Liu, Q. Zhang, T. Wang, and L. Ma. High yield production of 5-hydroxymethylfurfural from cellulose by high concentration of sulfates in biphasic system, *Green Chemistry 15* (**2013**), 7, pp. 1967. https://doi.org/*10.1039/C3GC40667A*.

95) Y. J. Pagán-Torres, T. Wang, J. M. R. Gallo, B. H. Shanks, and J. A. Dumesic. Production of 5-Hydroxymethylfurfural from Glucose Using a Combination of Lewis and Brønsted Acid Catalysts in Water in a Biphasic Reactor with an Alkylphenol Solvent, *ACS Catalysis 2* (**2012**), 6, pp. 930–934. https://doi.org/*10.1021/cs300192z*.

96) Y. Román-Leshkov and J. A. Dumesic. Solvent Effects on Fructose Dehydration to 5-Hydroxymethylfurfural in Biphasic Systems Saturated with Inorganic Salts, *Topics in Catalysis 52* (**2009**), 3, pp. 297–303. https://doi.org/*10.1007/s11244-008-9166-0*.

97) E. Licsandru, M. Gaysinski, and A. Mija. Structural Insights of Humins/Epoxidized Linseed Oil/ Hardener Terpolymerization, *Polymers 12* (**2020**), 7. https://doi.org/*10.3390/polym12071583*.

98) X. Chen, N. Guigo, A. Pizzi, N. Sbirrazzuoli, B. Li, E. Fredon, and C. Gerardin. Ambient Temperature Self-Blowing Tannin-Humins Biofoams, *Polymers 12* (**2020**), 11. https://doi.org/*10.3390/polym12112732*.

99) J.-M. Pin, N. Guigo, A. Mija, L. Vincent, N. Sbirrazzuoli, J. C. van der Waal, and E. de Jong. Valorization of Biorefinery Side-Stream Products: Combination of Humins with Polyfurfuryl Alcohol for Composite Elaboration, *ACS Sustainable Chemistry & Engineering 2* (**2014**), 9, pp. 2182–2190. https://doi.org/*10.1021/sc5003769*.

100) A. Mija, J. C. van der Waal, J.-M. Pin, N. Guigo, and E. de Jong. Humins as promising material for producing sustainable carbohydrate-derived building materials, *Construction and Building Materials 139* (**2017**), pp. 594–601. https://doi.org/*10.1016/j.conbuildmat.2016.11.019*.

101) R. Dinu and A. Mija. Cross-linked polyfuran networks with elastomeric behaviour based on humins biorefinery by-products, *Green Chemistry 21* (**2019**), 23, pp. 6277–6289. https://doi.org/*10.1039/C9GC01813A*.

102) K. Wang, J. Jiang, X. Liang, H. Wu, and J. Xu. Direct Conversion of Cellulose to Levulinic Acid over Multifunctional Sulfonated Humins in Sulfolane–Water Solution, *ACS Sustainable Chemistry & Engineering 6* (**2018**), 11, pp. 15092–15099. https://doi.org/*10.1021/acssuschemeng.8b03558*.

103) S. Kang, G. Zhang, X. Yang, H. Yin, X. Fu, J. Liao, J. Tu, X. Huang, F. G. F. Qin, and Y. Xu. Effects of p -Toluenesulfonic Acid in the Conversion of Glucose for Levulinic Acid and Sulfonated Carbon Production, *Energy & Fuels 31* (**2017**), 3, pp. 2847–2854. https://doi.org/*10.1021/acs.energyfuels.6b02675*.

104) F. Björnerbäck, D. Bernin, and N. Hedin. Microporous Humins Synthesized in Concentrated Sulfuric Acid Using 5-Hydroxymethyl Furfural, *ACS omega 3* (**2018**), 8, pp. 8537–8545. https://doi.org/*10.1021/acsomega.8b01274*.

105) F. Björnerbäck and N. Hedin. Microporous Humins Prepared from Sugars and Bio-Based Polymers in Concentrated Sulfuric Acid, *ACS Sustainable Chemistry & Engineering 7* (**2019**), 1, pp. 1018–1027. https://doi.org/*10.1021/acssuschemeng.8b04658*.

106) T. M. C. Hoang, L. Lefferts, and K. Seshan. Valorization of humin-based byproducts from biomass processing-a route to sustainable hydrogen, *ChemSusChem 6* (**2013**), 9, pp. 1651–1658. https://doi.org/*10.1002/cssc.201300446*.

107) S. Agarwal, D. van Es, and H. J. Heeres. Catalytic pyrolysis of recalcitrant, insoluble humin byproducts from C6 sugar biorefineries, *Journal of Analytical and Applied Pyrolysis 123* (**2017**), pp. 134–143. https://doi.org/*10.1016/j.jaap.2016.12.014*.

108) Y. Wang, S. Agarwal, and H. J. Heeres. Catalytic Liquefaction of Humin Substances from Sugar Biorefineries with Pt/C in 2-Propanol, *ACS Sustainable Chemistry & Engineering 5* (**2017**), 1, pp. 469–480. https://doi.org/*10.1021/acssuschemeng.6b01834*.

109) W. N. Lipscomb. Paratungstate Ion, *Inorganic Chemistry [0020-1669] 4* (**1965**), 132-134.

110) B. Artetxe, L. Ruiz Rubio, J. L. Vilas Vilela, and J. M. Gutiérrez-Zorrilla, Polyoxometalates, Jenny Stanford Publishing (**2022**).

111) M. T. Pope, Inorganic chemistry concepts, Vol. 8: Heteropoly and isopoly oxometalates, Springer (**1983**).

112) M. T. Pope and A. Müller. Polyoxometalate Chemistry: An Old Field with New Dimensions in Several Disciplines, *Angewandte Chemie International Edition in English 30* (**1991**), 1, pp. 34–48. https://doi.org/*10.1002/anie.199100341*.

113) I. Lindqvist. The structure of the hexaniobate ion in 7Na2O· 6Nb2O5· 32H2O, *Arkiv Kemi 5* (**1953**), pp. 247–250.

114) J. F. Keggin. Structure of the molecule of 12-phosphotungstic acid, *Nature 131* (**1933**), 3321, pp. 908–909.

115) L. C. W. Baker and J. S. Figgis. New fundamental type of inorganic complex: hybrid between heteropoly and conventional coordination complexes. Possibilities for geometrical isomerisms in 11-, 12-, 17-, and 18-heteropoly derivatives, *Journal of the American Chemical Society 92* (**1970**), 12, pp. 3794–3797. https://doi.org/*10.1021/ja00715a047*.

116) G. A. Tsigdinos and C. J. Hallada. Molybdovanadophosphoric acids and their salts. I. Investigation of methods of preparation and characterization, *Inorganic Chemistry 7* (**1968**), 3, pp. 437–441. https://doi.org/*10.1021/ic50061a009*.

117) S. A. Malik and T. J. R. Weakley. Heteropolyanions containing two different heteroatoms. Part II. Anions related to 18-tungstodiphosphate, *Journal of the Chemical Society A: Inorganic, Physical, Theoretical* (**1968**), pp. 2647. https://doi.org/*10.1039/J19680002647*.

118) T. Weakley and S. A. Malik. Heteropolyanions containing two different heteroatoms—I, *Journal of Inorganic and Nuclear Chemistry 29* (**1967**), 12, pp. 2935–2944. https://doi.org/*10.1016/0022-1902(67)80126-X*.

119) J.-C. Raabe, T. Esser, F. Jameel, M. Stein, J. Albert, and M. J. Poller. Study on the incorporation of various elements into the Keggin lacunary-type phosphomolybdate [PMo 9 O 34] 9− and subsequent purification of the polyoxometalates by nanofiltration, *Inorganic Chemistry Frontiers 10* (**2023**), 16, pp. 4854–4868. https://doi.org/*10.1039/D3QI00937H*.

120) N. I. Gumerova, E. Al-Sayed, L. Krivosudský, H. Čipčić-Paljetak, D. Verbanac, and A. Rompel. Antibacterial Activity of Polyoxometalates Against Moraxella catarrhalis, *Frontiers in chemistry 6* (**2018**), pp. 336. https://doi.org/*10.3389/fchem.2018.00336*.

121) M. A. Aldamen, J. M. Clemente-Juan, E. Coronado, C. Martí-Gastaldo, and A. Gaita-Ariño. Mononuclear lanthanide single-molecule magnets based on polyoxometalates, *Journal of the American Chemical Society 130* (**2008**), 28, pp. 8874–8875. https://doi.org/*10.1021/ja801659m*.

122) S. Duan, X. Xu, W. Chen, J. Zhi, and F. Li. Grain boundaries passivation of high efficiency and stable perovskite photodetector by polyoxometalate-based composite SiW 11 @ZIF-8, *Polyoxometalates 1* (**2022**), 1, pp. 9140003. https://doi.org/*10.26599/POM.2022.9140003*.

123) S. G. Sarafianos, U. Kortz, M. T. Pope, and M. J. Modak. Mechanism of polyoxometalate-mediated inactivation of DNA polymerases: an analysis with HIV-1 reverse transcriptase indicates specificity for the DNA-binding cleft, *The Biochemical journal 319 (Pt 2)* (**1996**), Pt 2, pp. 619–626. https://doi.org/*10.1042/bj3190619*.

124) J. Zhong, J. Pérez-Ramírez, and N. Yan. Biomass valorisation over polyoxometalate-based catalysts, *Green Chemistry 23* (**2021**), 1, pp. 18–36. https://doi.org/*10.1039/D0GC03190A*.

125) K. Shimizu, H. Furukawa, N. Kobayashi, Y. Itaya, and A. Satsuma. Effects of Brønsted and Lewis acidities on activity and selectivity of heteropolyacid-based catalysts for hydrolysis of cellobiose and cellulose, *Green Chemistry 11* (**2009**), 10, pp. 1627. https://doi.org/*10.1039/b913737h*.

126) W. Deng, Q. Zhang, and Y. Wang. Polyoxometalates as efficient catalysts for transformations of cellulose into platform chemicals, *Dalton transactions (Cambridge, England : 2003) 41* (**2012**), 33, pp. 9817–9831. https://doi.org/*10.1039/c2dt30637a*.

127) C. Fan, H. Guan, H. Zhang, J. Wang, S. Wang, and X. Wang. Conversion of fructose and glucose into 5-hydroxymethylfurfural catalyzed by a solid heteropolyacid salt, *Biomass and Bioenergy 35* (**2011**), 7, pp. 2659–2665. https://doi.org/*10.1016/j.biombioe.2011.03.004*.

128) Y. Song, X. Wang, Y. Qu, C. Huang, Y. Li, and B. Chen. Efficient Dehydration of Fructose to 5-Hydroxy-methylfurfural Catalyzed by Heteropolyacid Salts, *Catalysts 6* (**2016**), 4, pp. 49. https://doi.org/*10.3390/catal6040049*.

129) G. Lv, L. Deng, B. Lu, J. Li, X. Hou, and Y. Yang. Efficient dehydration of fructose into 5-hydroxymethylfurfural in aqueous medium over silica-included heteropolyacids, *Journal of Cleaner Production 142* (**2017**), pp. 2244–2251. https://doi.org/*10.1016/j.jclepro.2016.11.053*.

130) X. Yi, I. Delidovich, Z. Sun, S. Wang, X. Wang, and R. Palkovits. A heteropoly acid ionic crystal containing Cr as an active catalyst for dehydration of monosaccharides to produce 5-HMF in water, *Catalysis Science & Technology 5* (**2015**), 4, pp. 2496–2502. https://doi.org/*10.1039/C4CY01555J*.

131) X. Zhang, X. Zhang, N. Sun, S. Wang, X. Wang, and Z. Jiang. High production of levulinic acid from cellulosic feedstocks being catalyzed by temperature-responsive transition metal substituted heteropolyacids, *Renewable Energy 141* (**2019**), pp. 802–813. https://doi.org/*10.1016/j.renene.2019.04.058*.

132) S.-S. Wang and G.-Y. Yang. Recent advances in polyoxometalate-catalyzed reactions, *Chemical reviews 115* (**2015**), 11, pp. 4893–4962. https://doi.org/*10.1021/cr500390v*.

133) T. Esser, M. Huber, D. Voß, and J. Albert. Development of an efficient downstream process for product separation and catalyst recycling of a homogeneous polyoxometalate catalyst by means

of nanofiltration membranes and design of experiments, *Chemical Engineering Research and Design 185* (**2022**), pp. 37–50. https://doi.org/*10.1016/j.cherd.2022.06.045*.

134) B. Bertleff, J. Claußnitzer, W. Korth, P. Wasserscheid, A. Jess, and J. Albert. Extraction Coupled Oxidative Desulfurization of Fuels to Sulfate and Water-Soluble Sulfur Compounds Using Polyoxometalate Catalysts and Molecular Oxygen, *ACS Sustainable Chemistry & Engineering 5* (**2017**), 5, pp. 4110–4118. https://doi.org/*10.1021/acssuschemeng.7b00087*.

135) A. Bukowski, D. Esau, A. A. Rafat Said, A. Brandt-Talbot, and J. Albert. Combining Cost-Efficient Cellulose and Short-Chain Carboxylic Acid Production: The Polyoxometalate (POM)-Ionosolv Concept, *ChemPlusChem 85* (**2020**), 2, pp. 373–386. https://doi.org/*10.1002/cplu.202000025*.

136) J. Reichert, B. Brunner, A. Jess, P. Wasserscheid, and J. Albert. Biomass oxidation to formic acid in aqueous media using polyoxometalate catalysts – boosting FA selectivity by in-situ extraction, *Energy & Environmental Science 8* (**2015**), 10, pp. 2985–2990. https://doi.org/*10.1039/C5EE01706H*.

137) J. Albert, R. Wölfel, A. Bösmann, and P. Wasserscheid. Selective oxidation of complex, water-insoluble biomass to formic acid using additives as reaction accelerators, *Energy & Environmental Science 5* (**2012**), 7, pp. 7956. https://doi.org/*10.1039/c2ee21428h*.

138) I. V. Kozhevnikov, S. M. Kulikov, and K. I. Matveev. Use of the electrical conductivity method to investigate the acid properties of heteropoly acids in nonaqueous solutions, *Bulletin of the Academy of Sciences of the USSR Division of Chemical Science 29* (**1980**), 10, pp. 1533–1539. https://doi.org/*10.1007/BF00951209*.

139) I. V. Kozhevnikov and K. I. Matveev. Homogeneous catalysts based on heteropoly acids (review), *Applied Catalysis 5* (**1983**), 2, pp. 135–150. https://doi.org/*10.1016/0166-9834(83)80128-6*.

140) K. I. Matveev. Studies on the development of new homogeneous catalysts for ethylene oxidation to acetaldehyde, *Chemischer Informationsdienst 8* (**1977**), 48, no-no.

141) I. V. Kozhevnikov. PMo12−nVnO(3+n)−40 heteropolyanions as catalysts for aerobic oxidation, *Journal of Molecular Catalysis A: Chemical 117* (**1997**), 1-3, pp. 151–158. https://doi.org/*10.1016/S1381-1169(96)00295-6*.

142) R. K. Murmann and K. C. Giese. Mechanism of oxygen-18 exchange between water and the vanadium(V) oxyanion: V10O286-, *Inorganic Chemistry 17* (**1978**), 5, pp. 1160–1166. https://doi.org/*10.1021/ic50183a014*.

143) M. Huber, Extractive-Catalytic Removal of Nitrogenous and Oxygenic Compounds from Fuels with Polyoxometalates and Molecular Oxygen, Staats-und Universitätsbibliothek Hamburg Carl von Ossietzky (**2023**).

144) O. A. Kholdeeva, A. V. Golovin, R. I. Maksimovskaya, and I. V. Kozhevnikov. Oxidation of 2,3,6-trimethylphenol in the presence of molybdovanadophosphoric heteropoly acids, *Journal of Molecular Catalysis 75* (**1992**), 3, pp. 235–244. https://doi.org/*10.1016/0304-5102(92)80128-4*.

145) I. V. Kozhevnikov. Catalysis by Heteropoly Acids and Multicomponent Polyoxometalates in Liquid-Phase Reactions, *Chemical reviews 98* (**1998**), 1, pp. 171–198. https://doi.org/*10.1021/cr960400y*.

146) R. Wölfel: Katalytische Erzeugung von Wasserstoff aus biogenen Rohstoffen. Dissertation, Friedrich-Alexander-Universität Erlangen-Nürnberg (**2011**).

147) A. Boesmann, R. Woelfel, P. Wasserscheid, N. Taccardi, and J. Albert (*JBACH GMBH [DE]*), Method for catalytically producing formic acid, EP2473467 (A1) (**2011**).

148) OxFA GmbH . *https://www.oxfa.eu/* (accessed **01.07.2024**).

149) Shanghai Chemex, What are the Major Uses of Formic Acid in Various Industries? . *https://shanghaichemex.com/what-are-the-major-uses-of-formic-acid-in-various-industries/#:~:text=In%20textiles%2C%20formic%20acid%20is,solution%20when%20washing%20the%20fabric.* (accessed **27.08.2024**).

150) A. Boddien, B. Loges, H. Junge, and M. Beller. Hydrogen generation at ambient conditions: application in fuel cells, *ChemSusChem 1* (**2008**), 8-9, pp. 751–758. https://doi.org/*10.1002/cssc.200800093*.

151) D. Voß, M. Kahl, and J. Albert. Continuous Production of Formic Acid from Biomass in a Three-Phase Liquid–Liquid–Gas Reaction Process, *ACS Sustainable Chemistry & Engineering 8* (**2020**), 28, pp. 10444–10453. https://doi.org/*10.1021/acssuschemeng.0c02426*.

152) S. Ponce, S. Wesinger, D. Ona, D. A. Streitwieser, and J. Albert. Valorization of secondary feedstocks from the agroindustry by selective catalytic oxidation to formic and acetic acid using the OxFA process, *Biomass Conversion and Biorefinery 13* (**2023**), 8, pp. 7199–7206. https://doi.org/*10.1007/s13399-021-01854-7*.

153) S. Maerten: Humine: Bildung und Wertschöpfung. Dissertation, RWTH Aachen University (**2018**).

154) J. Reichert and J. Albert. Detailed Kinetic Investigations on the Selective Oxidation of Biomass to Formic Acid (OxFA Process) Using Model Substrates and Real Biomass, *ACS Sustainable Chemistry & Engineering 5* (**2017**), 8, pp. 7383–7392. https://doi.org/*10.1021/acssuschemeng.7b01723*.

155) D. Voß: Selektive katalytische Umsetzung biogener Rohstoffe zu organischen Säuren unter Einsatz von Polyoxometallat-Katalysatoren. Dissertation, Friedrich-Alexander-Universität Erlangen-Nürnberg (**2020**).

156) J. Albert, D. Lüders, A. Bösmann, D. M. Guldi, and P. Wasserscheid. Spectroscopic and electrochemical characterization of heteropoly acids for their optimized application in selective biomass oxidation to formic acid, *Green Chemistry 16* (**2014**), 1, pp. 226–237. https://doi.org/*10.1039/C3GC41320A*.

157) T. Esser, A. Wassenberg, J.-C. Raabe, D. Voß, and J. Albert. Catalytic Valorization of Humins by Selective Oxidation Using Transition-Metal-Substituted Keggin-Type Polyoxometalate Catalysts, *ACS Sustainable Chemistry & Engineering 12* (**2024**), 1, pp. 543–560. https://doi.org/*10.1021/acssuschemeng.3c06539*.

158) T. Esser, A. Wassenberg, D. Voß, and J. Albert. Selective catalytic oxidation of humins to carboxylic acids using the H4[PVMo11O40] Keggin-type polyoxometalate enhanced by alcohol doping and solubilizer, *Reaction Chemistry & Engineering 9* (**2024**), 7, pp. 1666–1684. https://doi.org/*10.1039/d3re00672g*.

159) Stephanie Maerten, Chiraphat Kumpidet, Dorothea Voß, Anna Bukowski, Peter Wasserscheid, Jakob Albert. Glucose oxidation to formic acid and methyl formate in perfect selectivity .

160) T. Esser, A. Wassenberg, D. Voß, and J. Albert. Novel insights into the recovery and recyclability of homogeneous polyoxometalate catalysts applying an efficient nanofiltration process for the selective catalytic oxidation of humins, *Chemical Engineering Research and Design 209* (**2024**), pp. 311–322. https://doi.org/*10.1016/j.cherd.2024.08.007*.

161) D. C. Montgomery, Design and analysis of experiments, John Wiley & Sons Inc (**2013**).

162) M. J. Anderson and P. J. Whitcomb, DOE simplified: Practical tools for effective experimentation, CRC Press (**2015**).

163) R. A. Fisher, The Design of Experiments, Oliver and Boyd (**1935**).

164) K. Siebertz, D. van Bebber, and T. Hochkirchen, Statistische Versuchsplanung, Springer Berlin Heidelberg (**2017**).

165) Handbook of design and analysis of experiments, Ed. by A. Dean, M. Morris, J. Stufken, and D. R. Bingham, CRC Press Taylor & Francis Group CRC Press is an imprint of the Taylor & Francis Group an informa business, **2015**.

166) Minitab, Response surface central composite and box behnken designs (**2025**). *https://support.minitab.com/en-us/minitab/help-and-how-to/statistical-modeling/doe/supporting-topics/response-surface-designs/response-surface-central-composite-and-box-behnken-designs/* (accessed **21.03.2025**).

167) C. E. Bonferroni, Pubblicazioni del R. Istituto superiore di scienze economiche e commerciali di Firenze: Teoria statistica delle classi e calcolo delle probabilità, Seeber (**1936**).

168) R. H. H. Groenwold, J. J. Goeman, S. Le Cessie, and O. M. Dekkers. Multiple testing: when is many too much?, *European journal of endocrinology 184* (**2021**), 3, E11-E14. https://doi.org/*10.1530/EJE-20-1375*.

169) J.-C. Raabe, J. Aceituno Cruz, J. Albert, and M. J. Poller. Comparative Spectroscopic and Electrochemical Study of V(V)-Substituted Keggin-Type Phosphomolybdates and -Tungstates, *Inorganics 11* (**2023**), 4, pp. 138. https://doi.org/*10.3390/inorganics11040138*.

170) A. Wassenberg, T. Esser, M. J. Poller, and J. Albert. Investigation of the Formation, Characterization, and Oxidative Catalytic Valorization of Humins, *Materials (Basel, Switzerland) 16* (**2023**), 7. https://doi.org/*10.3390/ma16072864*.

171) X. Hu and C.-Z. Li. Levulinic esters from the acid-catalysed reactions of sugars and alcohols as part of a bio-refinery, *Green Chemistry 13* (**2011**), 7, pp. 1676. https://doi.org/*10.1039/c1gc15272f*.

172) D. Jung, P. Körner, and A. Kruse. Kinetic study on the impact of acidity and acid concentration on the formation of 5-hydroxymethylfurfural (HMF), humins, and levulinic acid in the hydrothermal conversion of fructose, *Biomass Conversion and Biorefinery 11* (**2021**), 4, pp. 1155–1170. https://doi.org/*10.1007/s13399-019-00507-0*.

173) B. Girisuta, L. P. B. M. Janssen, and H. J. Heeres. A kinetic study on the decomposition of 5-hydroxymethylfurfural into levulinic acid, *Green Chemistry 8* (**2006**), 8, pp. 701. https://doi.org/*10.1039/b518176c*.

174) A. Wassenberg, T. Esser, M. J. Poller, D. Voß, and J. Albert. Humin-free synthesis of levulinic acid from fructose using heteropolyacid catalysts, *Biofuels, Bioproducts and Biorefining 18* (**2024**), 5, pp. 1585–1597. https://doi.org/*10.1002/bbb.2654*.

175) A. Wassenberg, T. Esser, M. J. Poller, D. Voß, and J. Albert. Valorization of Humins by Cyclic Levulinic Acid Production Using Polyoxometalates and Formic Acid, *ChemSusChem* (**2025**), e202401973. https://doi.org/*10.1002/cssc.202401973*.

9. Appendix

9.1 Hazardous substances

Substance	GHS-Symbol/EUH statements	Hazard statements	Precautionary statements
Acetic acid		226, 314	210, 280, 301+330+331, 303+361+353, 305+351+338
Acetone	 EUH 66	225, 319, 336	210-, 233-, 240-, 241, 242, 305+351+338
Ethanol		225, 319	210, 233, 240, 241, 242, 305+351+338
Formic acid	 EUH 71	226, 302, 331, 314	210, 280, 303+361+353, 304+340+310-, 305+351+338
N_2		280	403
O_2		270, 280	220, 244, 370+376, 403
Para-toluene sulfonic acid monohydrate		315, 319, 335	261, 264, 271, 280, 302-352, 305+351+338
Phosphomolybdic acid		272, 314	220, 280, 305+351+338+310
Phosphotungstic acid		302, 314, 411	260, 264, 270, 273, 280, 301+312, 301+330+331, 303+361+353, 304+340, 305+351+338, 310, 321, 330, 363, 391, 405, 501
Silicotunsgtic acid		314, 315, 319, 335, 412	260, 261, 264, 271, 273, 280, 301+330+331, 302+352, 303+361+353, 304+340, 305+351+338, 310, 312, 321, 332+313, 337+P313, 362, 363, 403+233, 405, 501
Sulfuric acid		290, 314	280, 301+330+331, 303+361+353, 305+351+338+310

9.2 List of figures

9.3 List of tables

10. Supporting Information

10.1.1 Supporting information of publication 1

Supporting information from:

Investigation of the formation, characterization, and oxidative catalytic valorization of humins

André Wassenberg, Tobias Esser, Maximilian J. Poller, Jakob Albert

A. Wassenberg, T. Esser, M.J. Poller, J. Albert, Investigation of the Formation, Characterization, and Oxidative Catalytic Valorization of Humins, Materials (Basel, Switzerland) *16* (**2023**). *https://doi.org/10.3390/ma16072864*.

This document contains 5 equations, 11 tables and 49 figures on 30 pages

Supporting Information

Humin Synthesis

NMR spectra:

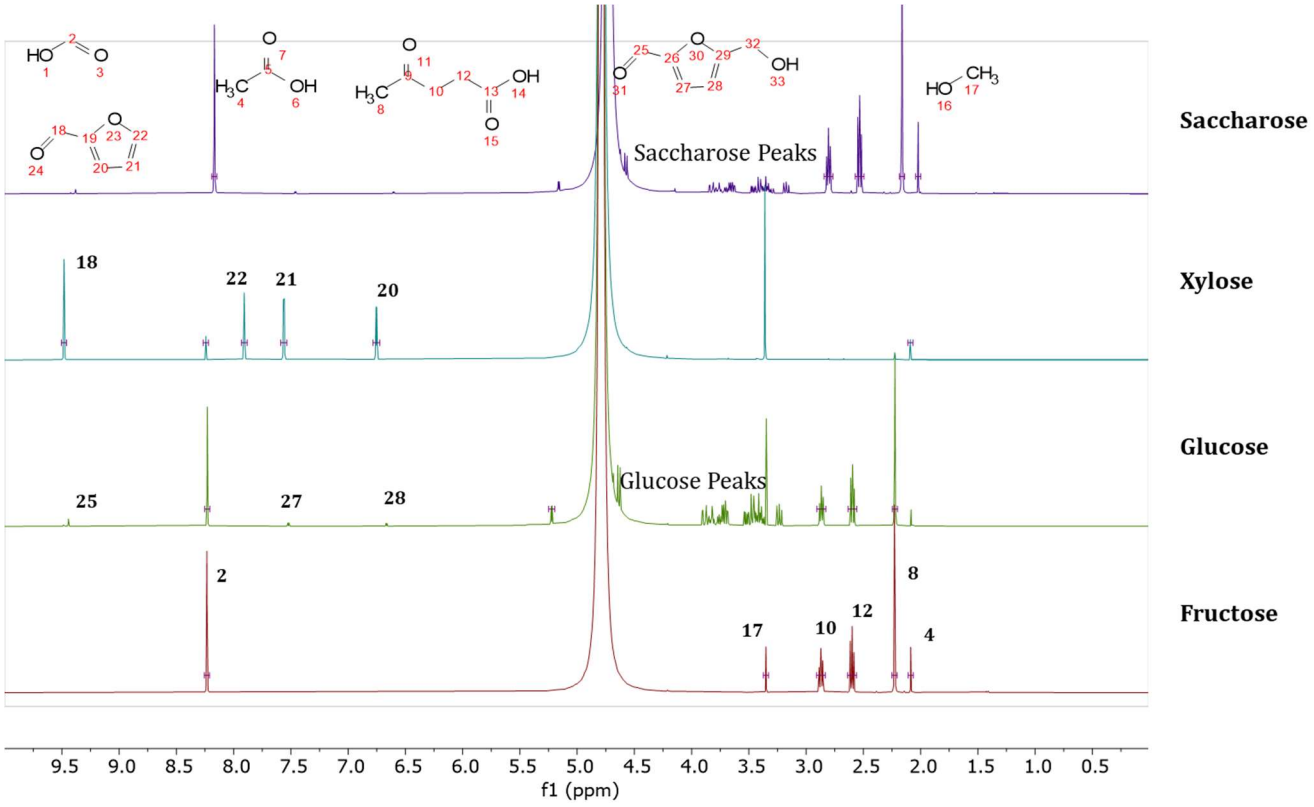

Figure S1: ^{1}H-NMR spectra of humins synthesized in sulfuric acid and water taken in D_2O

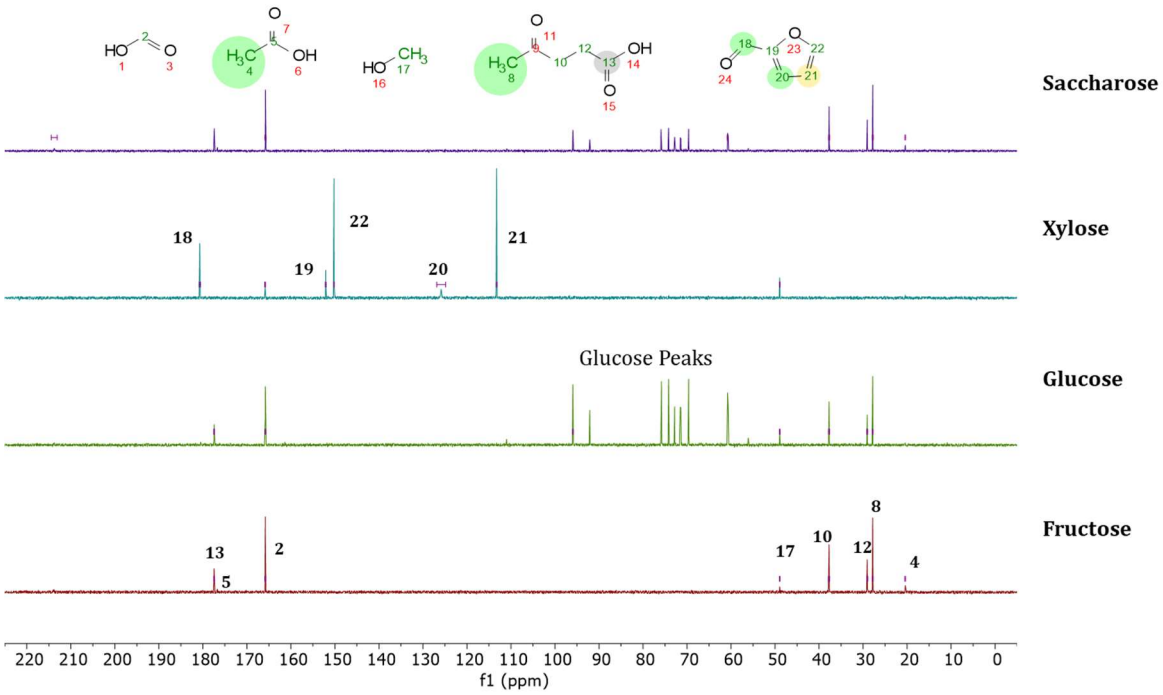

Figure S2: ^{13}C-NMR spectra of humin synthesized in sulfuric acid and water taken in D_2O

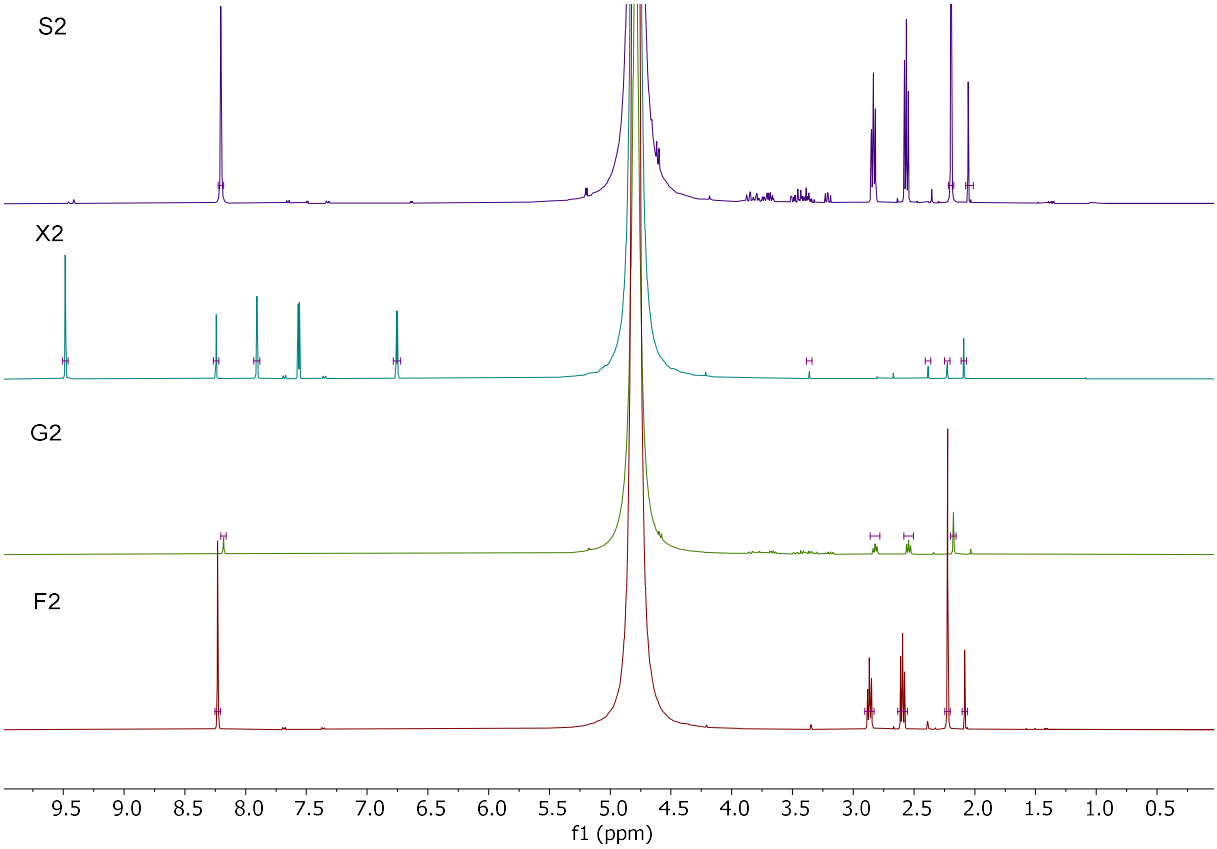

Figure S3:[1]H-NMR spectra of humins synthesized in para toluenesulfonic acid and water taken in D_2O

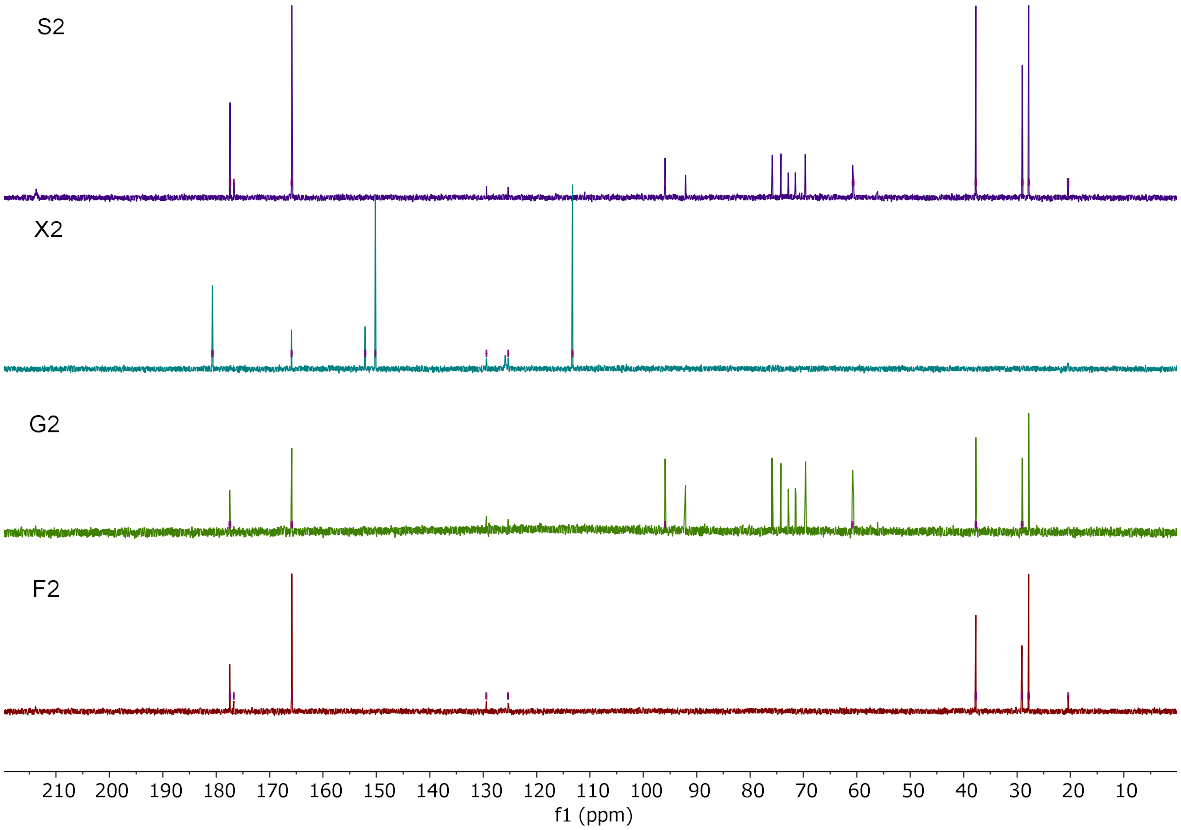

Figure S4: [13]C-NMR spectra of humins synthesized in para toluenesulfonic acid and water taken in D_2O

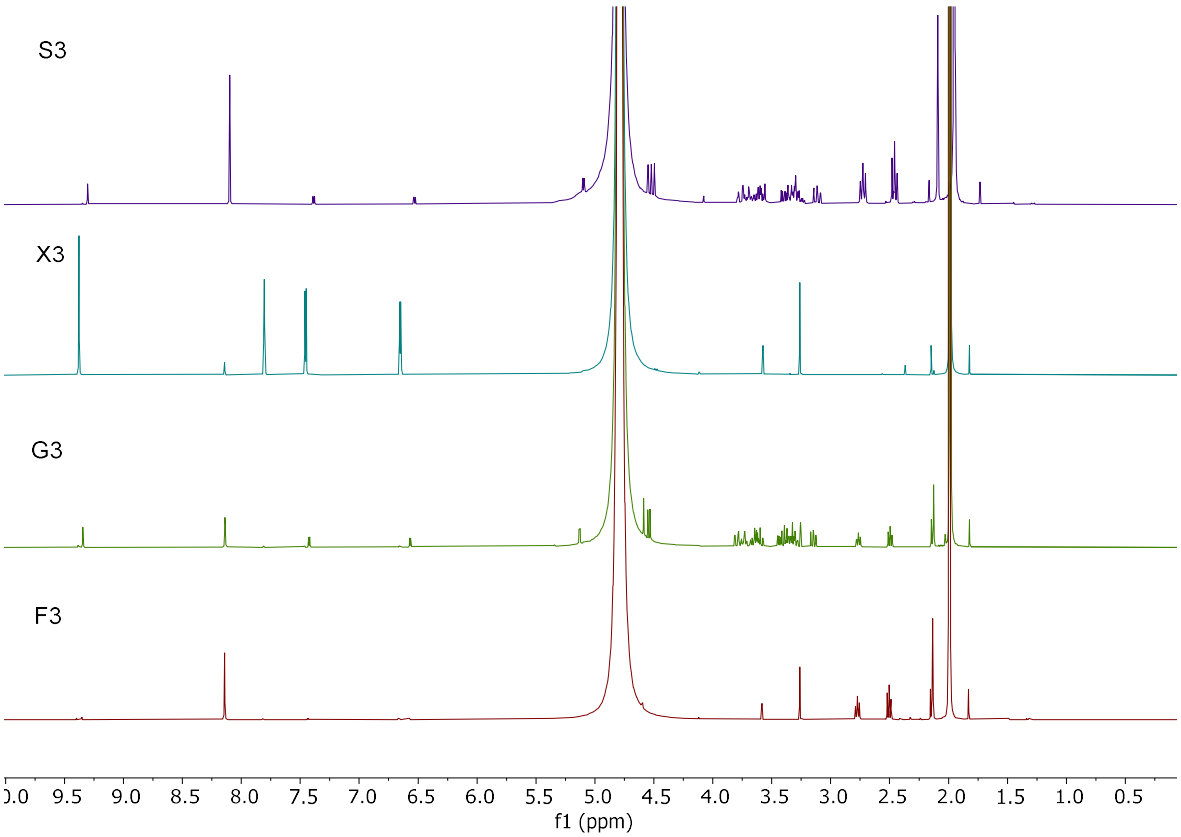

Figure S5: ^{1}H-NMR spectra of humins synthesized in acetic acid and water taken in D_2O

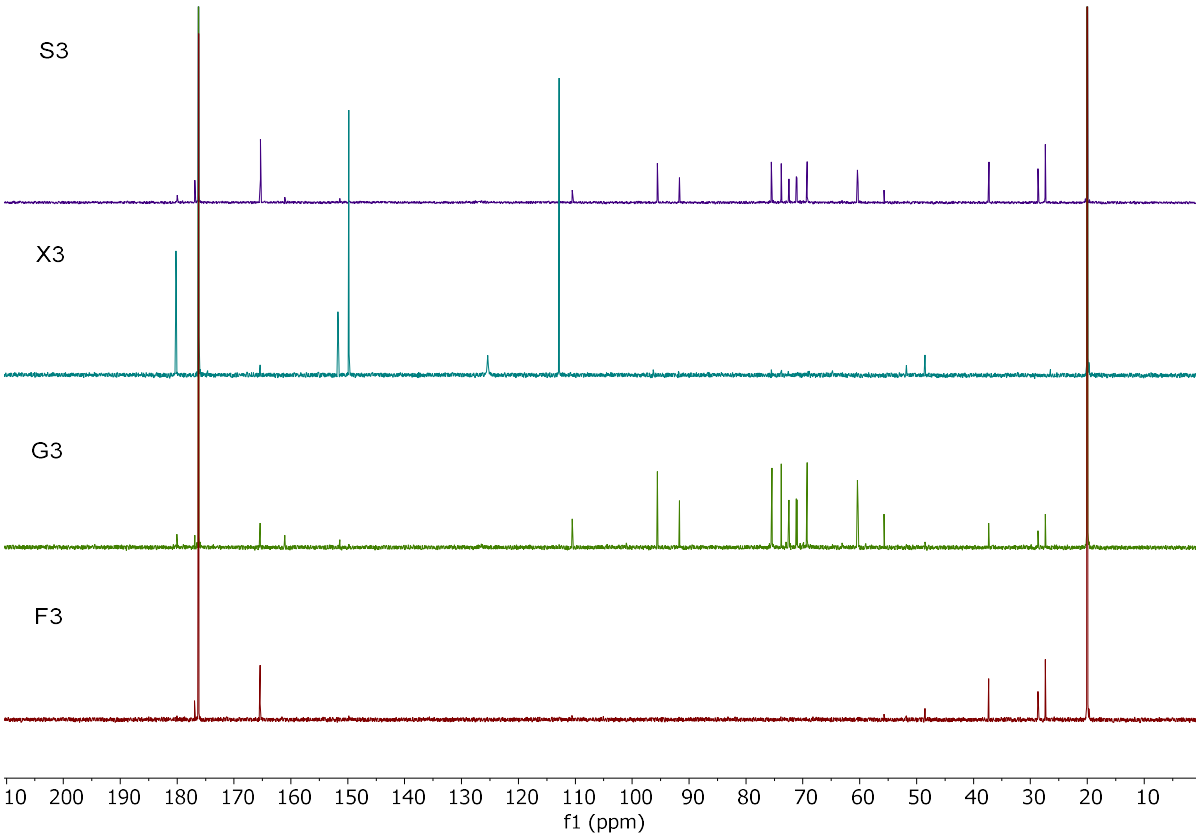

Figure S6: ^{13}C-NMR spectra of humins synthesized in acetic acid and water taken in D_2O

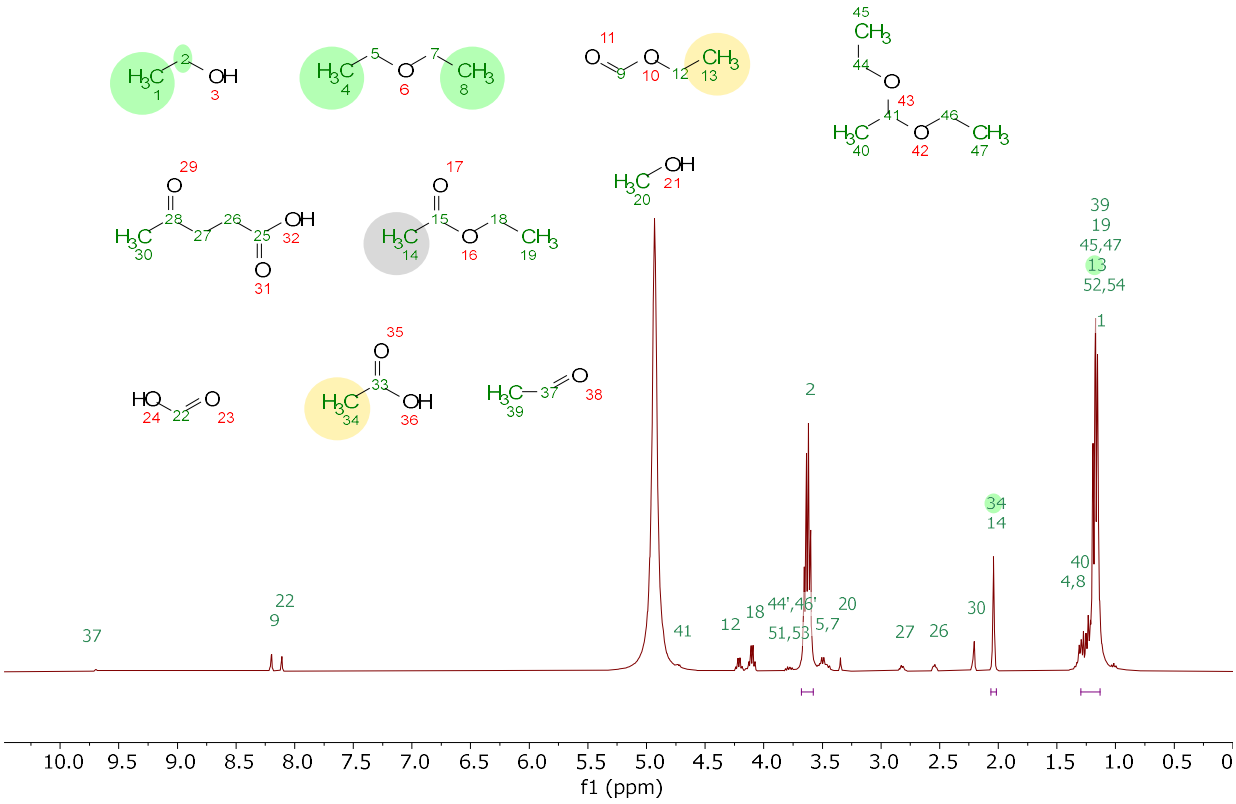

Figure S7:[1]H-NMR spectra of F4 taken in D_2O

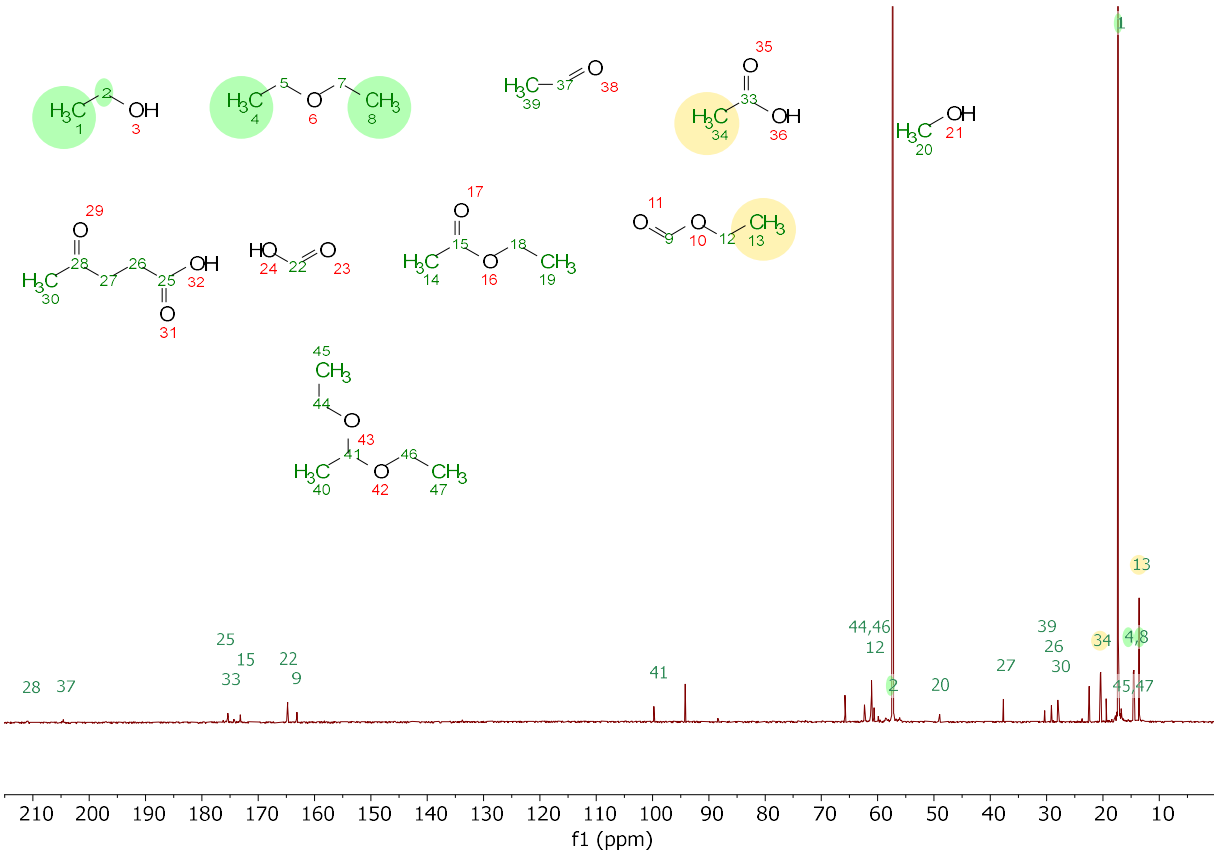

Figure S8: [13]C-NMR spectra of F4 taken in D_2O

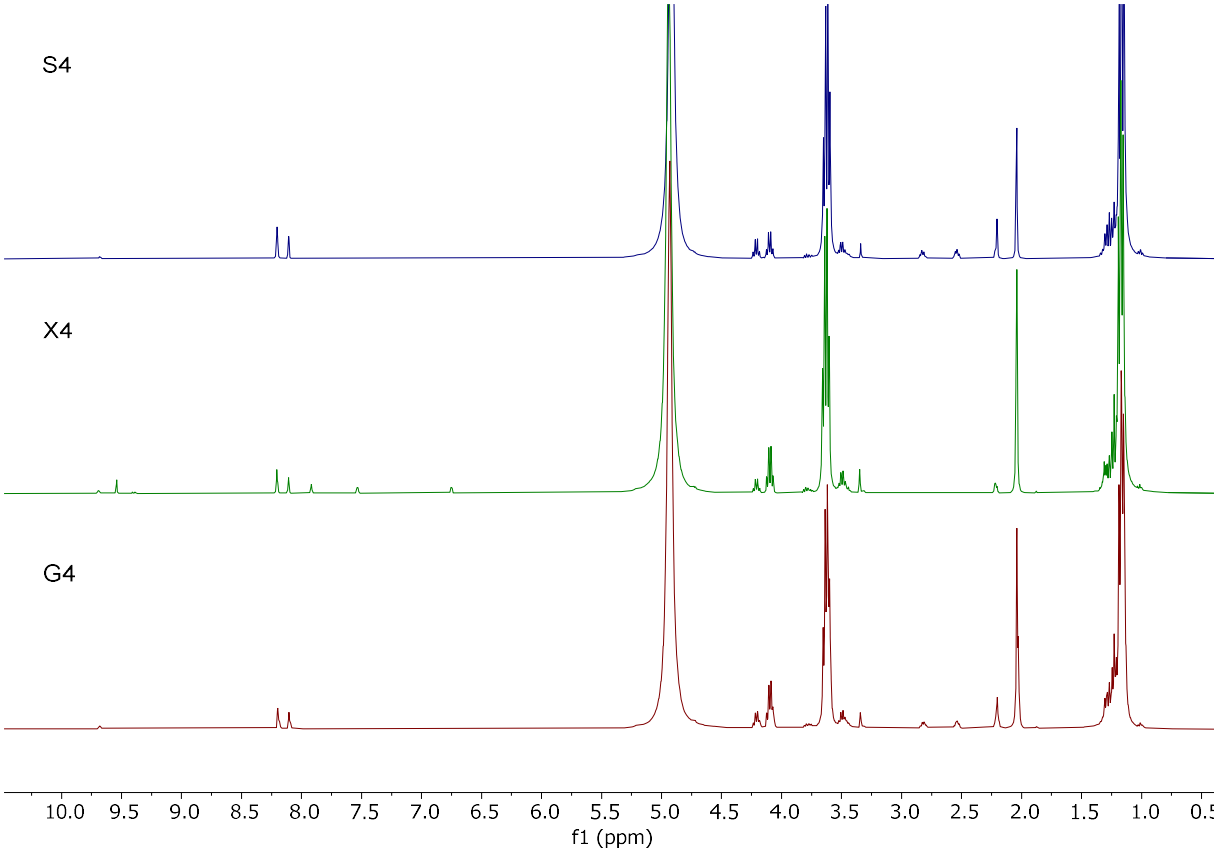

Figure S9:[1]H-NMR spectra of humins synthesized in sulfuric acid and water/ethanol

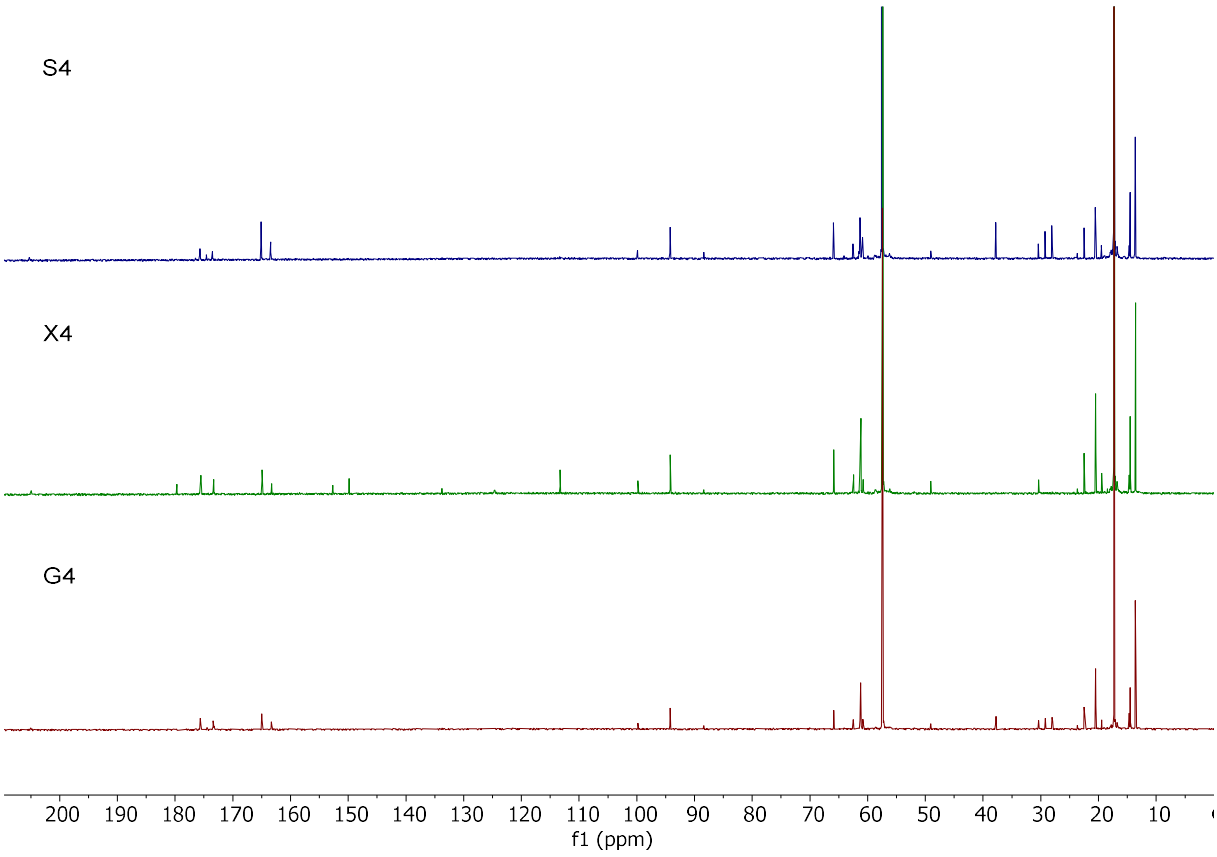

Figure S10: ^{13}C-NMR spectra of humins synthesized in sulfuric acid and water/ethanol taken in D_2O

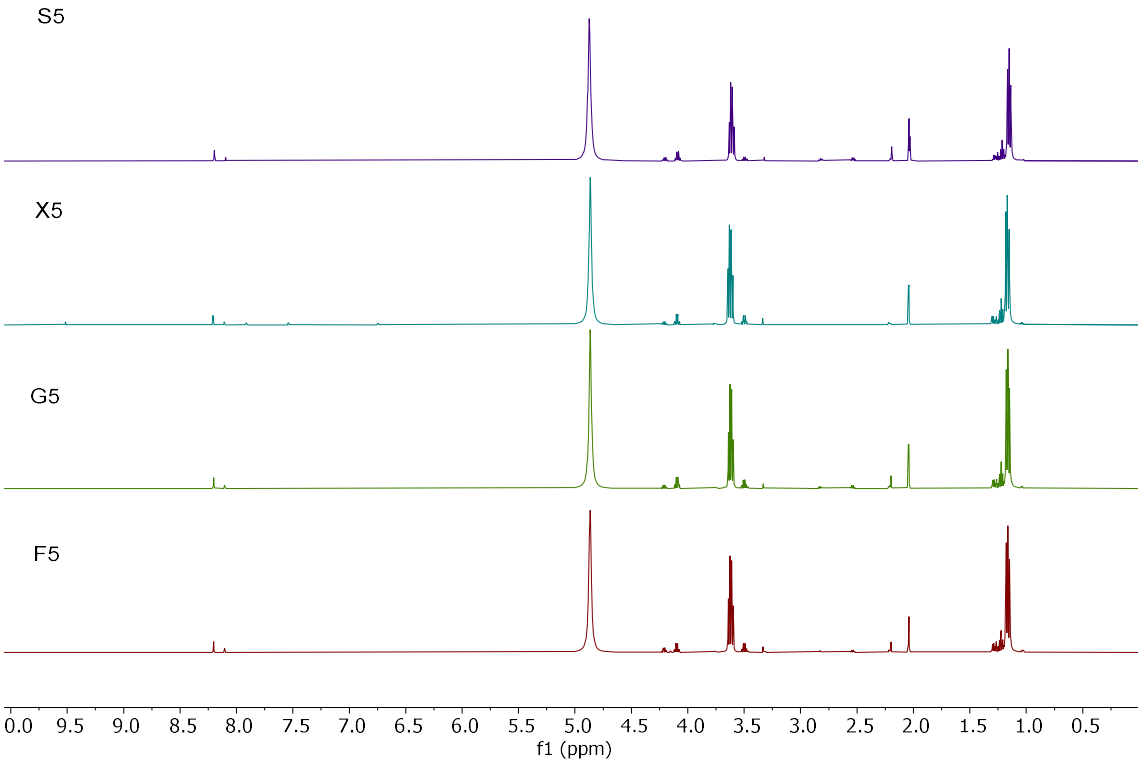

Figure S11:^{1}H-NMR spectra of humins synthesized in para toluene sulfonic acid and water/ethanol taken in D_2O

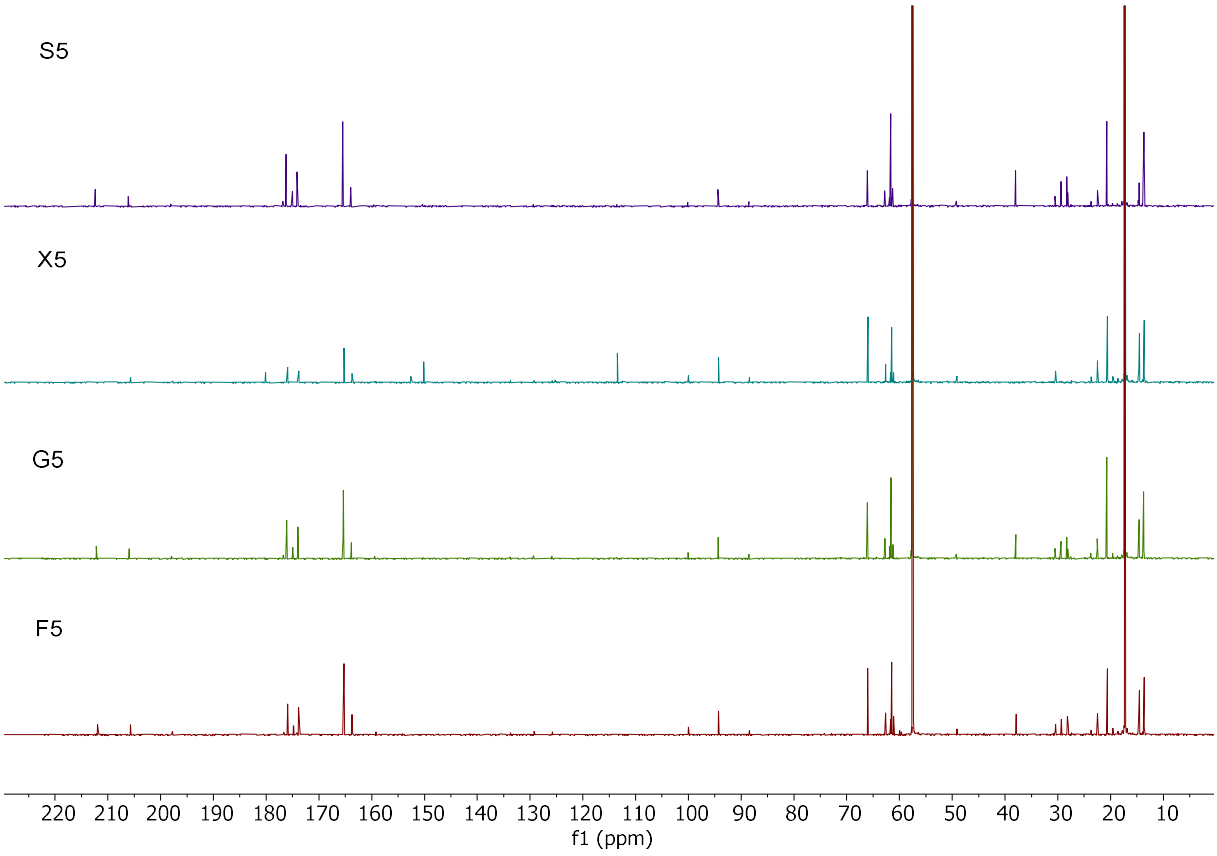

Figure S12: ^{13}C-NMR spectra of humins synthesized in para toluenesulfonic acid and water/ethanol taken in D_2O

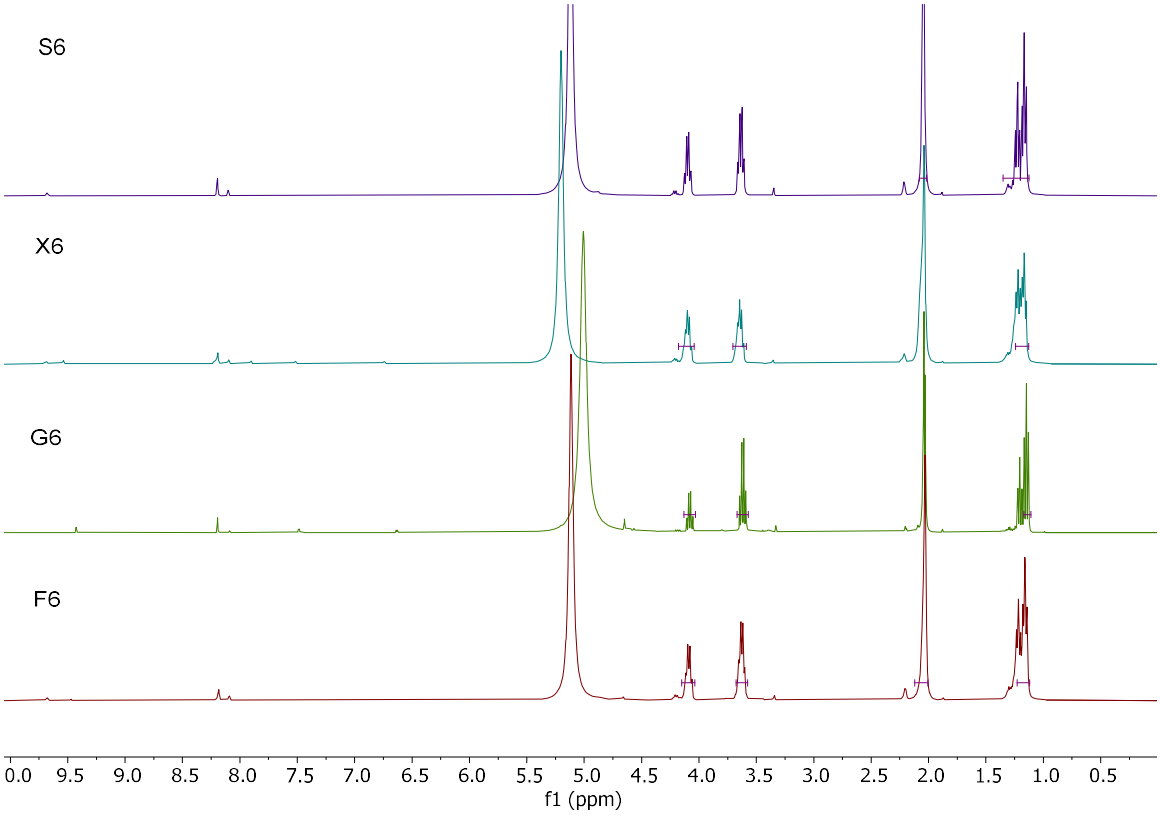

Figure S13:[1]H-NMR spectra of humins synthesized in acetic acid and water/ethanol taken in D_2O

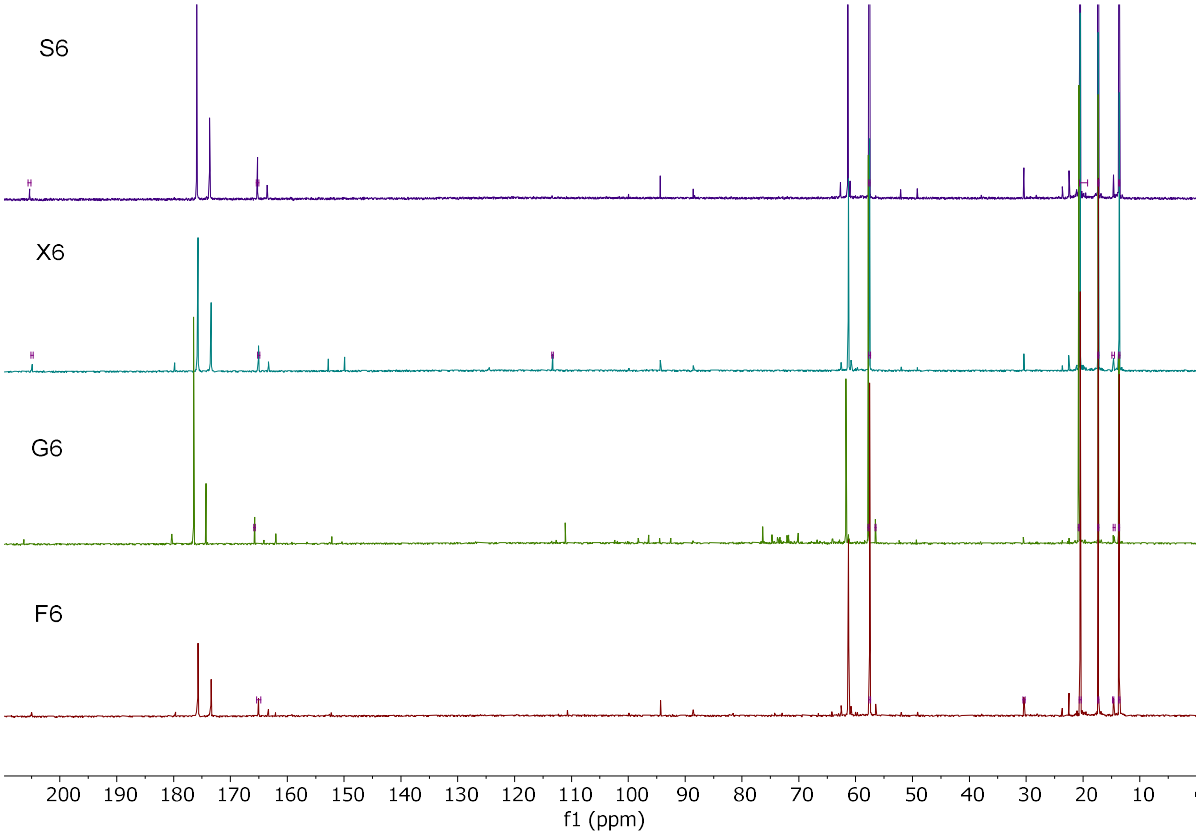

Figure S14: [13]C-NMR spectra of humins synthesized in acetic acid and water/ethanol taken in D_2O

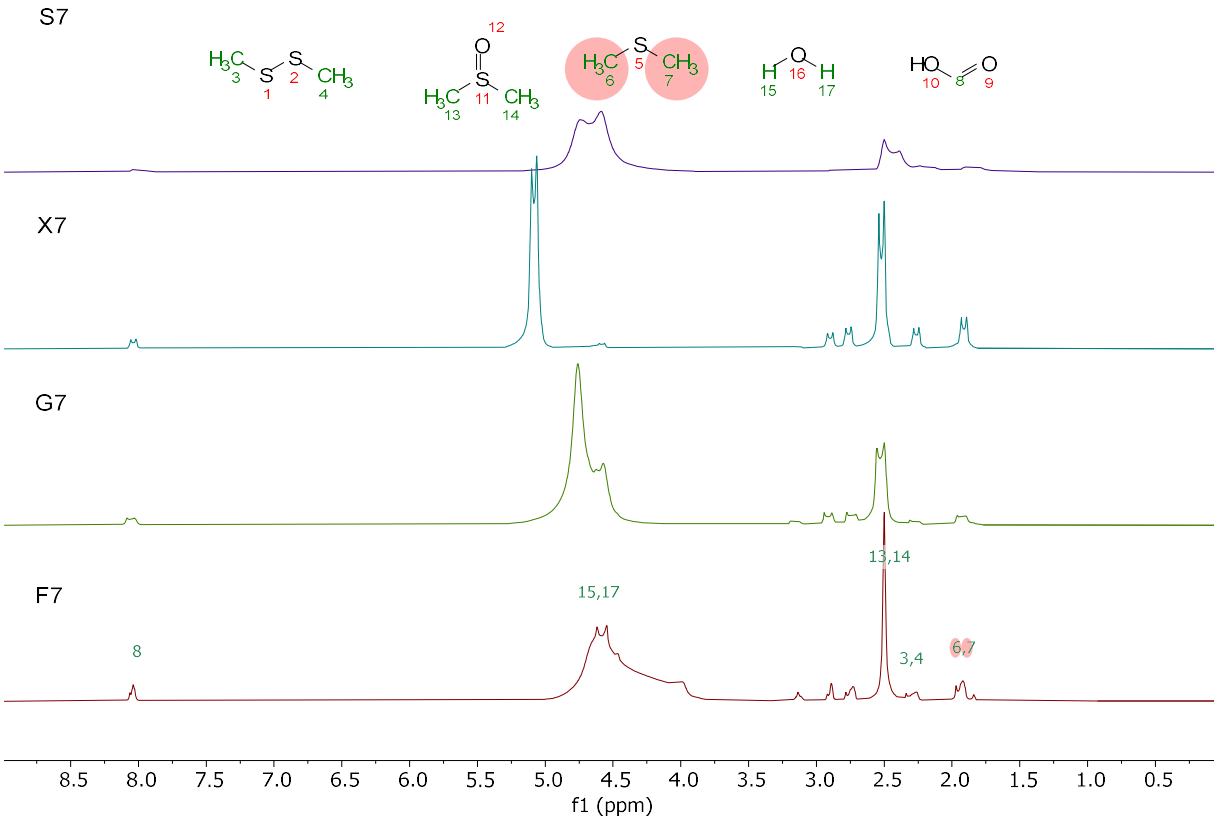

Figure S15:[1]H-NMR spectra of humins synthesized in sulfuric acid and water/dimethyl sulfoxide taken in DMSO-d_6

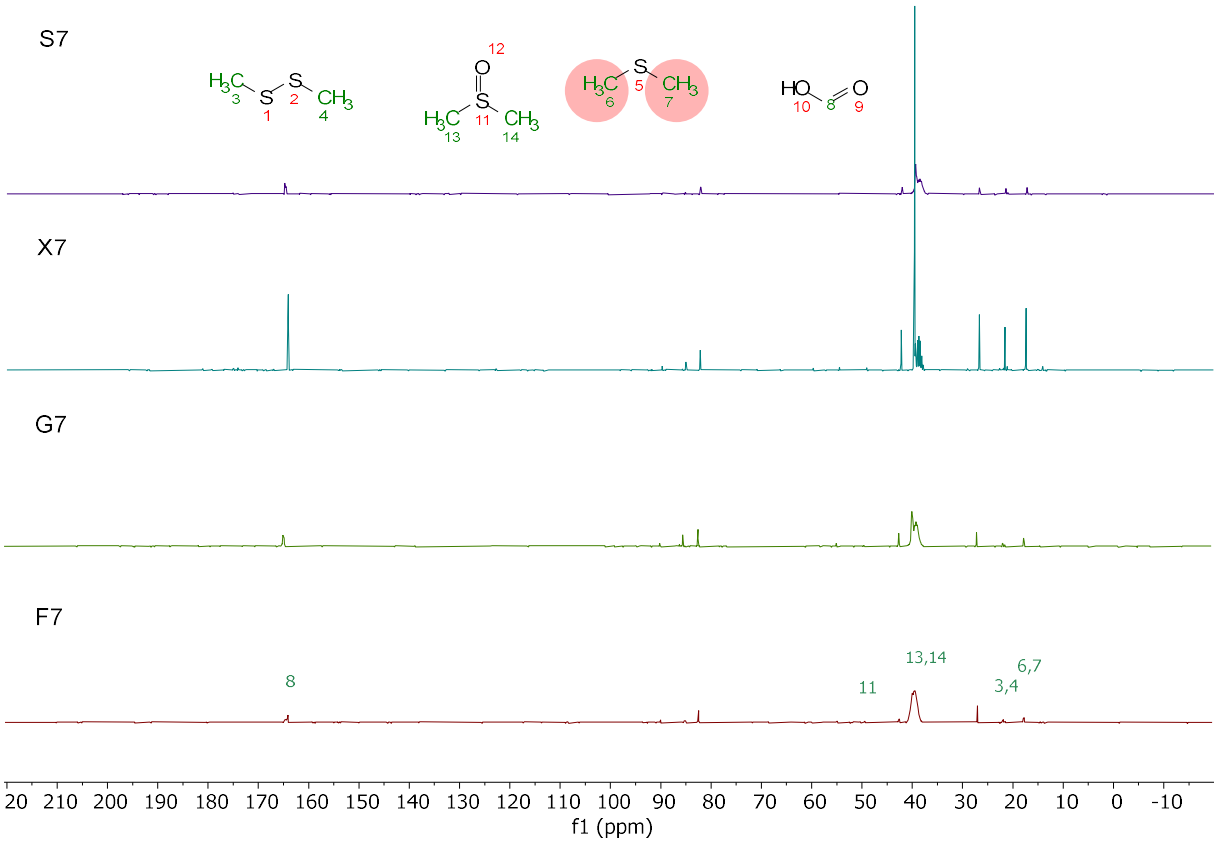

Figure S16: ^{13}C-NMR spectra of humins synthesized in sulfuric acid and water/dimethyl sulfoxide taken in DMSO-d_6

Elemental analysis:

Table S1: Theoretical elemental compositions of sugars used for humin synthesis

Elements	Fructose	Glucose	Xylose	Sucrose
H	6,71	6,71	6,71	6,48
C	40	40	40	42,11
O	53,28	53,28	53,28	51,41
H/C	2,01	2,01	2,01	1,85
O/C	1,00	1,00	1,00	0,92

Table S2: CHSO of humin synthesized in sulfuric acid and water

Elements	F1	G1	X1	S1
H	3.875	4.105	4.01	4.12
C	63.54	63.34	64.66	63.795
O	31.3	31.245	30.425	31.625
S	0	0	0	0
Sum	98.715	98.69	99.095	99.54
H/C	0.73	0.78	0.74	0.77
H/O	0.37	0.37	0.35	0.37

Table S3: CHSO of fructose humins

Elements	F1	F2	F3	F4	F5	F6	F7
H	3.875	3.915	3.7	4.565	4.905	4.165	4.185
C	63.54	62.595	62.985	65.175	67.26	61.7	58.69
O	31.3	32.14	32.225	29.6	26.48	32.78	26.015
S	0	0	0	0	0	0	9.76
Sum	98.715	98.65	98.91	99.34	98.645	98.645	98.65
H/C	0.73	0.75	0.70	0.84	0.88	0.81	0.86
O/C	0.37	0.39	0.38	0.34	0.30	0.40	0.33

Table S4: CHSO of glucose humins

Elements	G1	G2	G3	G4	G5	G6	G7
H	4.11	4.00	3.95	4.83	5.17	3.88	4.12
C	63.34	62.62	62.77	65.87	68.09	59.36	59.00
O	31.25	32.23	32.40	28.34	25.66	34.38	26.85
S	0.00	0.00	0.00	0.00	0.00	0.00	8.99
Sum	98.69	98.84	99.11	99.04	98.91	97.61	98.95
H/C	0.78	0.77	0.76	0.88	0.91	0.78	0.84

O/C	0.37	0.39	0.39	0.32	0.28	0.43	0.34

Table S5: CHSO of xylose humins

Elements	**X1**	**X2**	**X3**	**X4**	**X5**	**X6**	**X7**
H	4.01	3.71	4.01	4.70	4.79	4.03	4.06
C	64.66	63.87	63.92	66.51	68.29	61.42	58.92
O	30.43	31.17	31.24	28.08	25.50	29.26	27.28
S	0.00	0.00	0.00	0.00	0.00	0.00	8.42
Sum	99.10	98.75	99.16	99.28	98.57	98.91	98.66
H/C	0.74	0.70	0.75	0.85	0.84	0.79	0.83
O/C	0.35	0.37	0.37	0.32	0.28	0.36	0.35

Table S6: CHSO of sucrose humins

Elements	**S1**	**S2**	**S3**	**S4**	**S5**	**S6**	**S7**
H	4.12	4.13	3.87	4.50	4.82	3.88	4.27
C	63.80	63.47	62.98	64.77	67.03	59.31	61.19
O	31.63	31.15	32.15	29.86	27.49	34.39	26.54
S	0.00	0.00	0.00	0.00	0.00	0.00	6.64
Sum	99.54	98.74	98.99	99.13	99.34	97.58	98.63
H/C	0.77	0.78	0.74	0.83	0.86	0.79	0.84
O/C	0.37	0.37	0.38	0.35	0.31	0.43	0.33

IR-spectra:

Table S7: Assignment of IR-bands

Wavenumber [cm^{-1}]	**Assignment**
750+795	C-H Out of plane vibration substituted furan ring
965	C-H vibration furan ring
1020	C=C stretch vibration
1090	C-O-C ether vibration
1160+1200	C-O-C deformation vibration furan ring
1295	C-H rocking vibration
1360	C-C framework vibration (furan) C6 sugars
1395	C-C framework vibration (furan) C5 sugars
1420	C=S stretch
1460	C-H aliphatic chain vibration
1510	C=C vibration aromatic double bonds of poly substituted furans
1600	C=C stretch vibration conjugated with carbonyl
1670	C=O carbyonyl, aldehyde vibrations
1700	C=O stretch of acids, aldehydes and ketons
1775	C-S Thioester

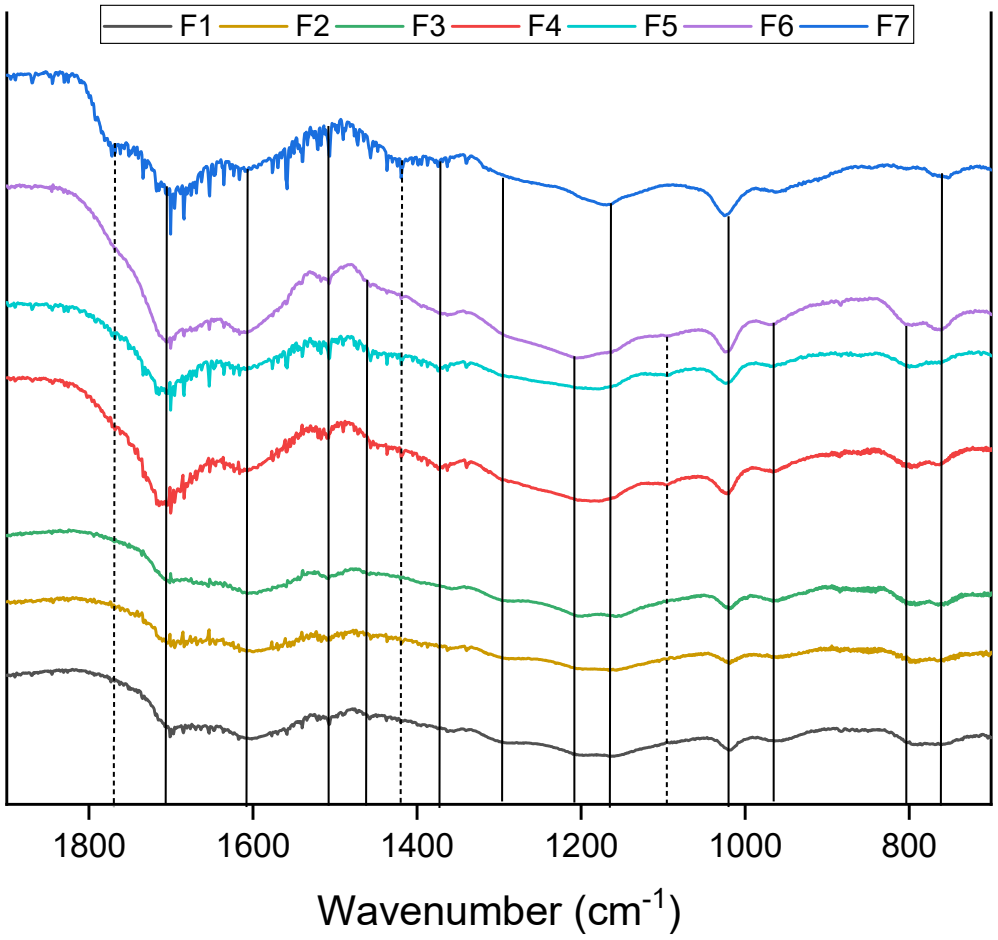

Figure S17: IR spectra of fructose humins

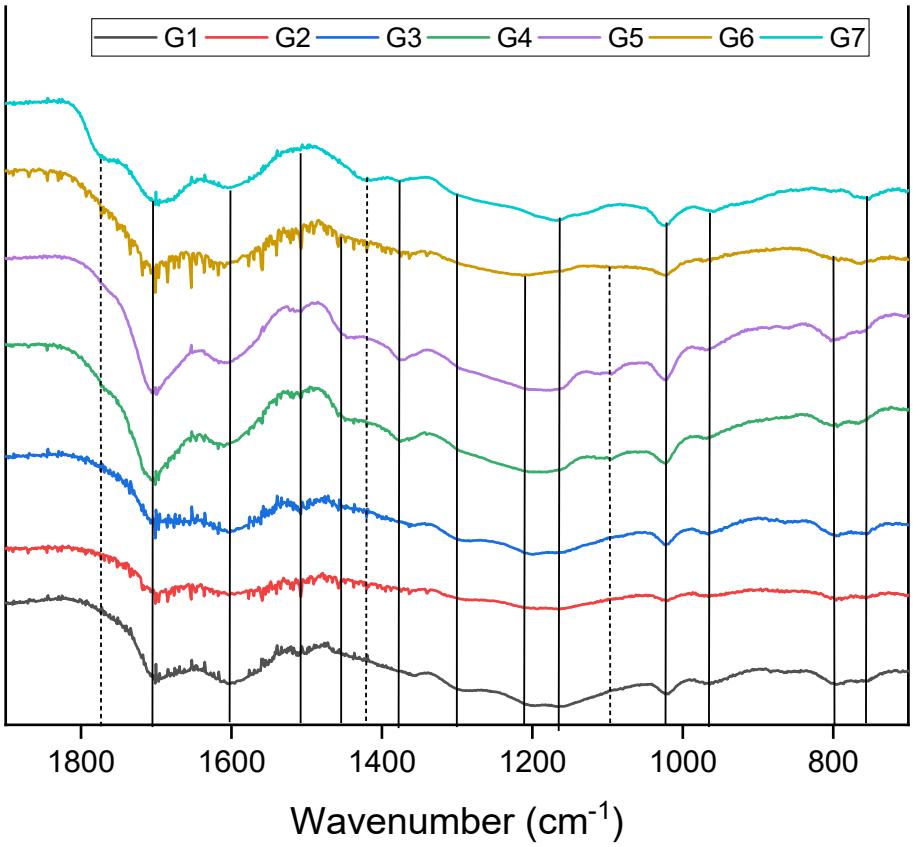

Figure S18: IR spectra of glucose humins

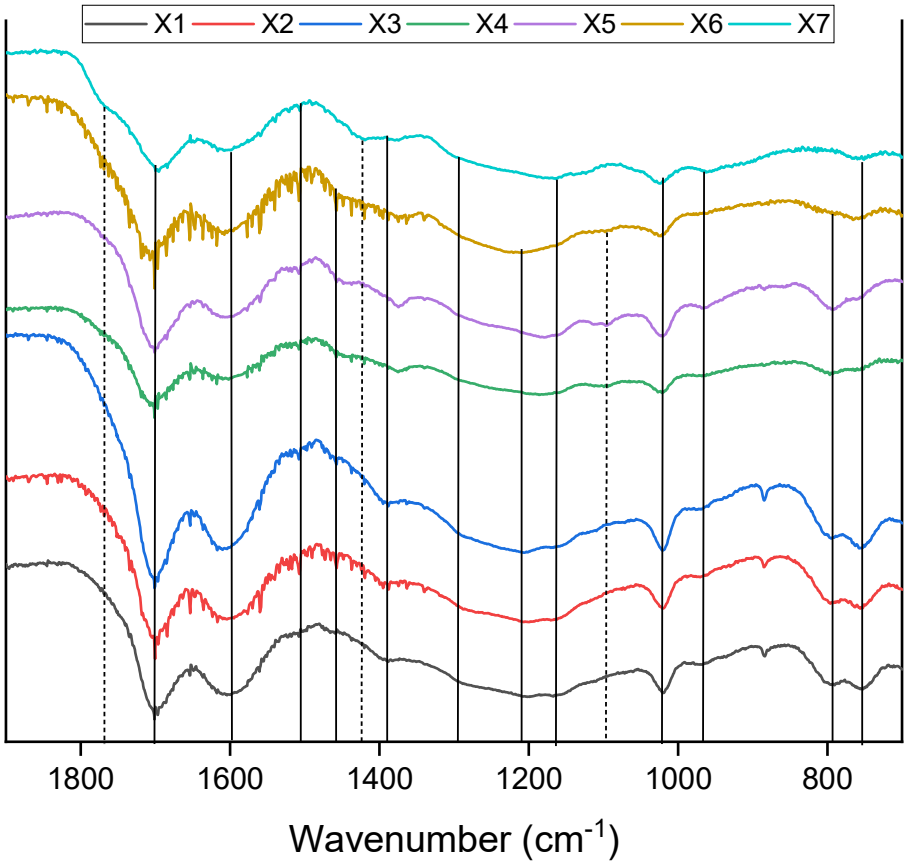

Figure S19: IR spectra of xylose humins

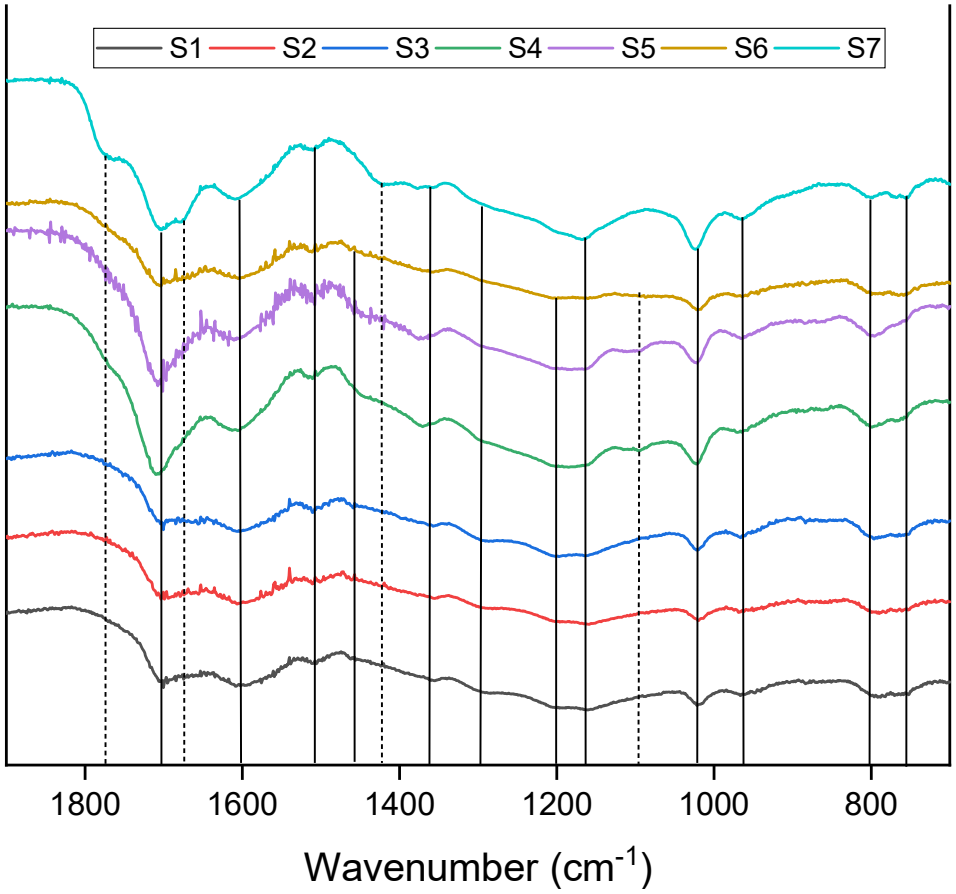

Figure S20: IR spectra of sucrose humins

MALDI-TOF MS spectra:

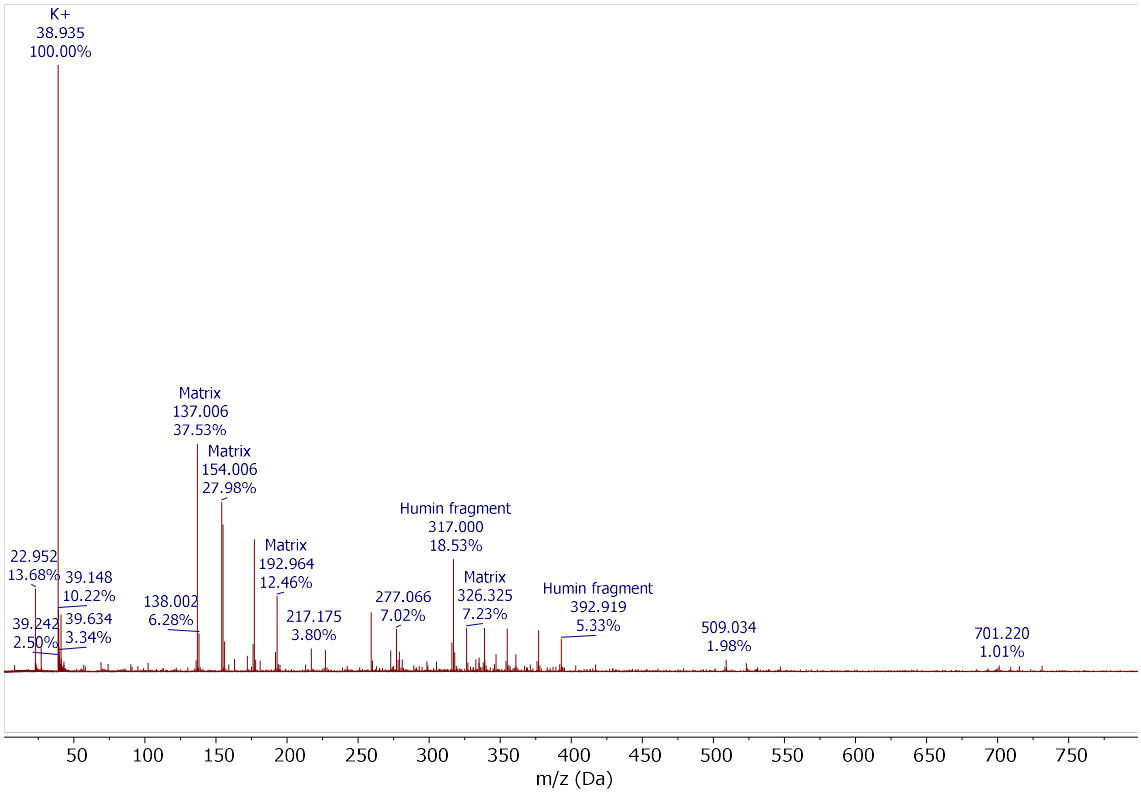

Figure S21: MALDI-TOF-MS spectrum of F1

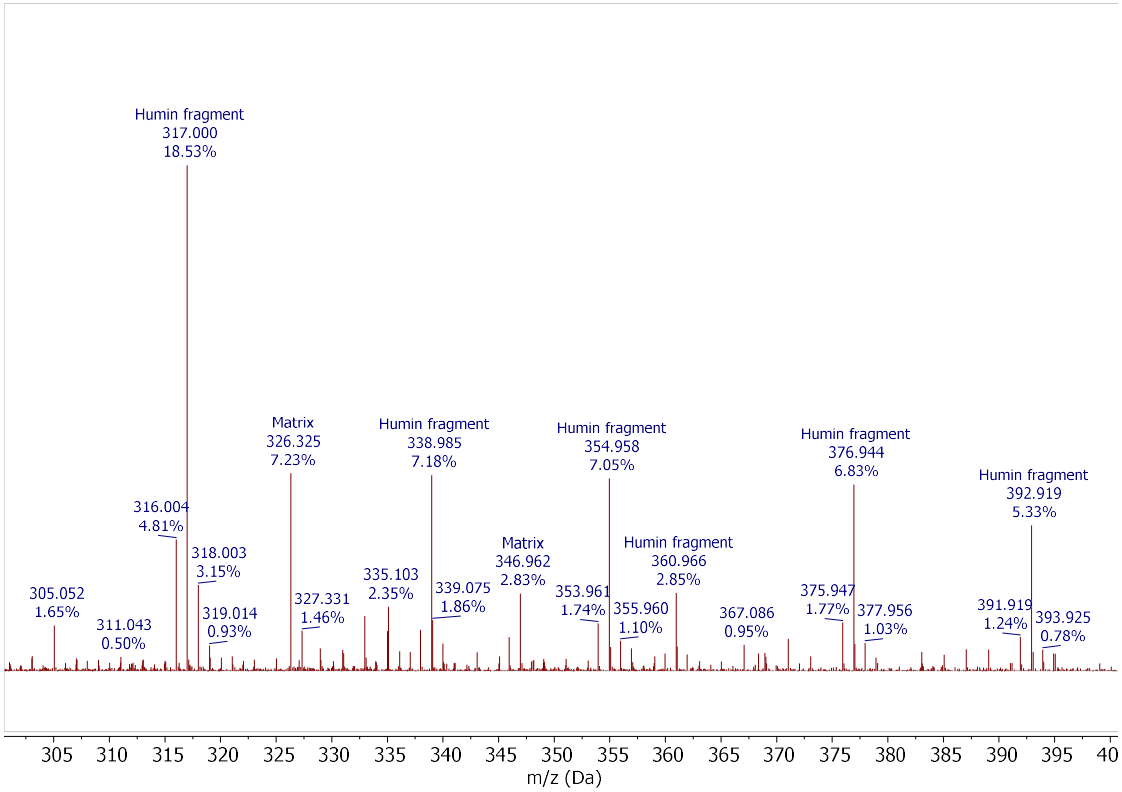

Figure S22: MALDI-TOF-MS spectrum of F1 zoomed in

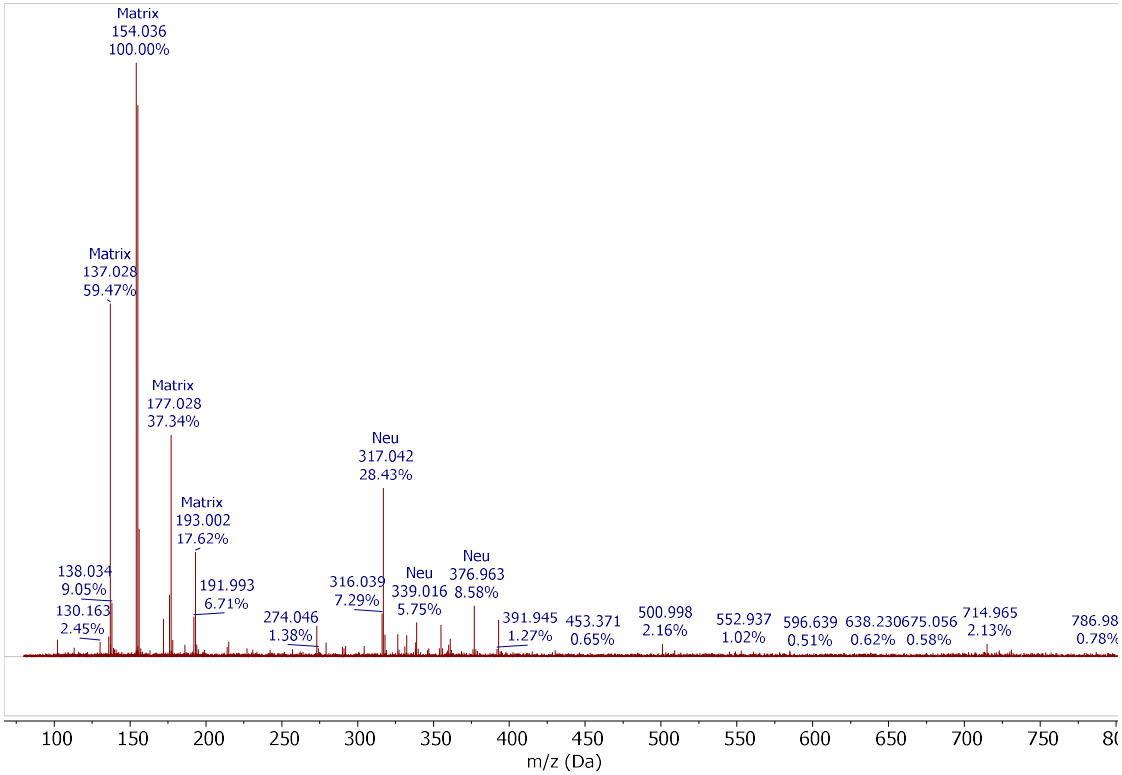

Figure S23: MALDI-TOF-MS spectrum of F2

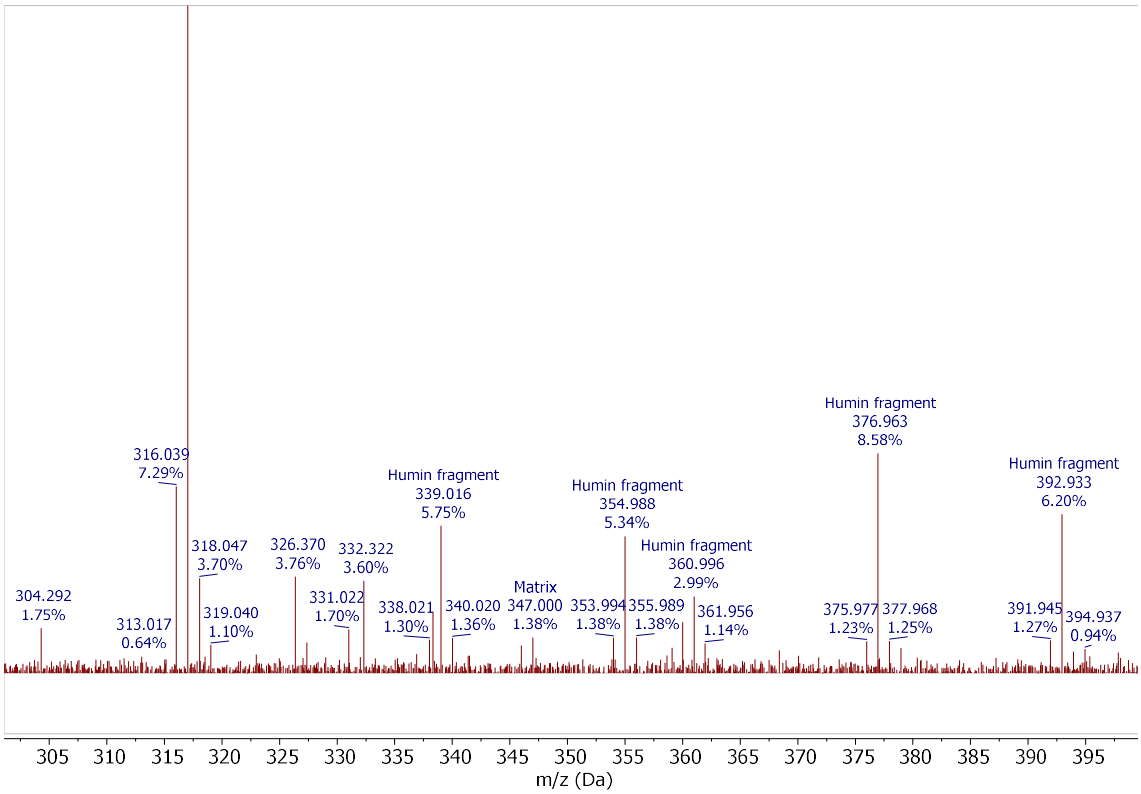

Figure S24: MALDI-TOF-MS spectrum of F2 zoomed in

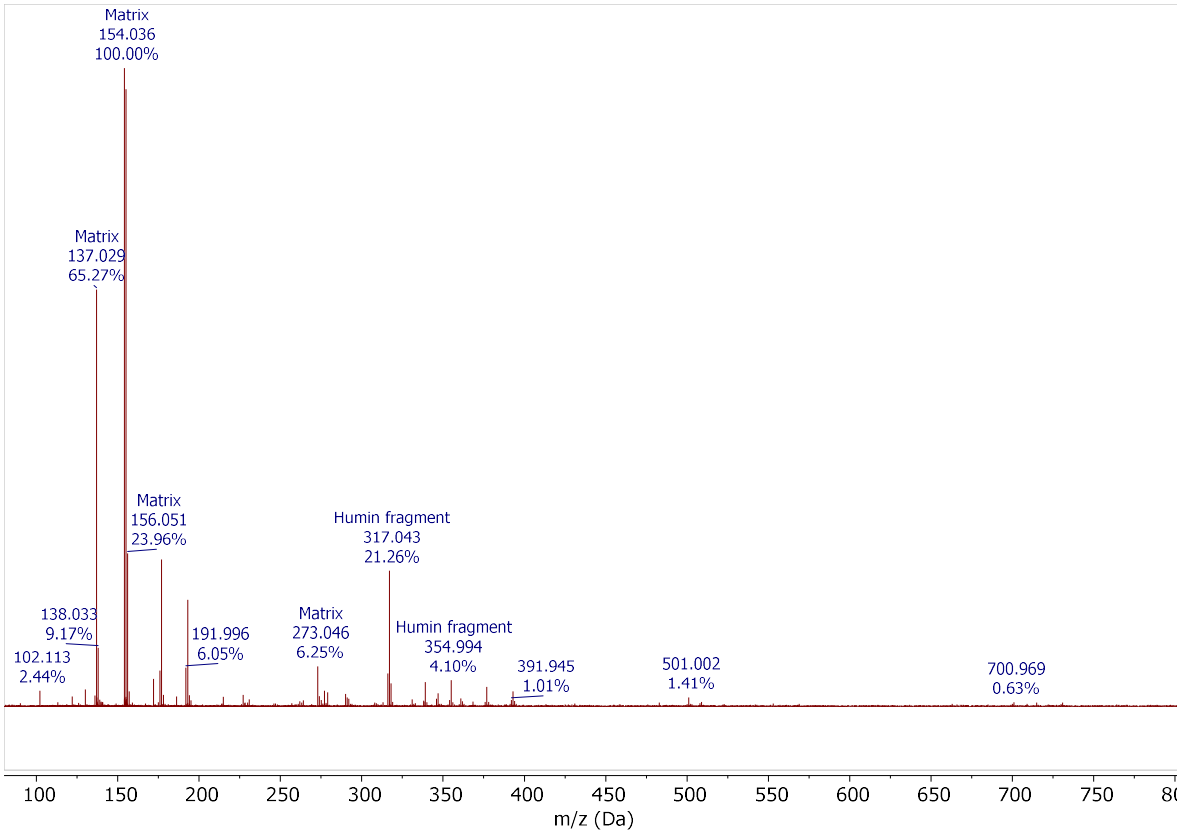

Figure S25: MALDI-TOF-MS spectrum of F3

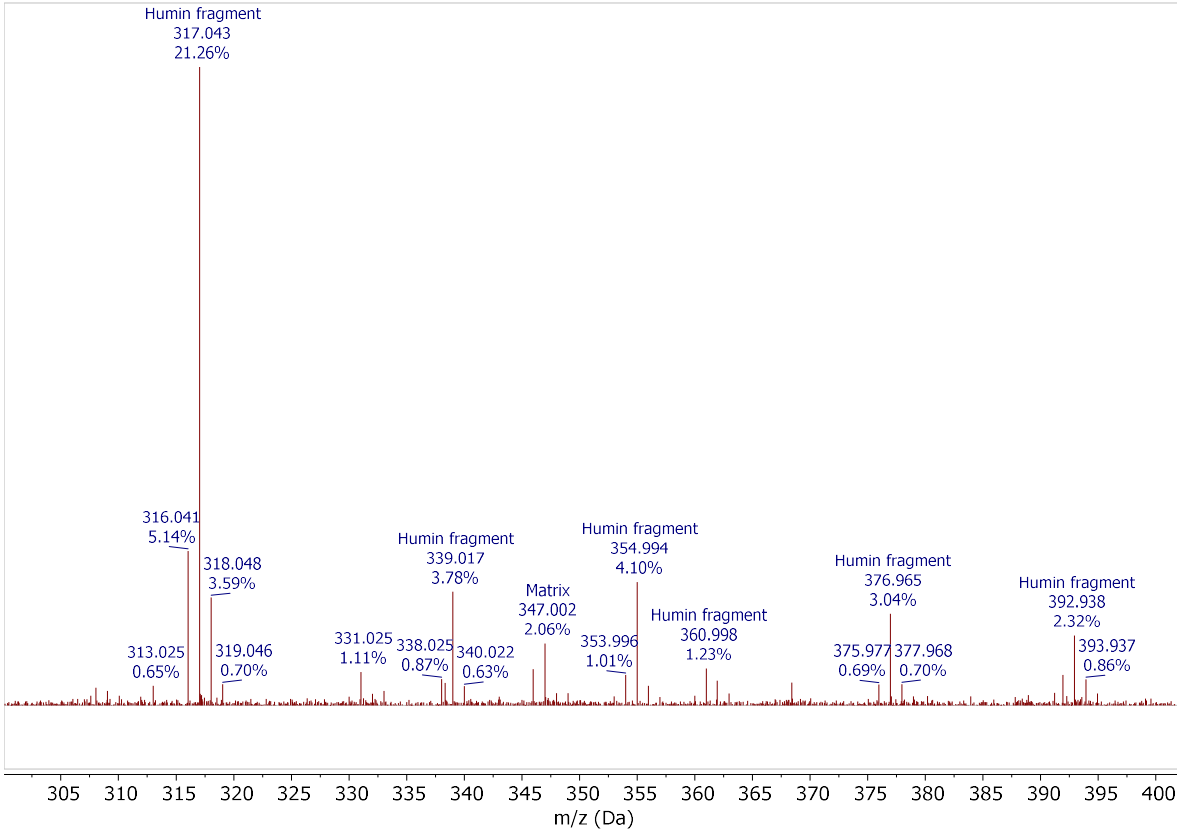

Figure S26: MALDI-TOF-MS spectrum of F3 zoomed in

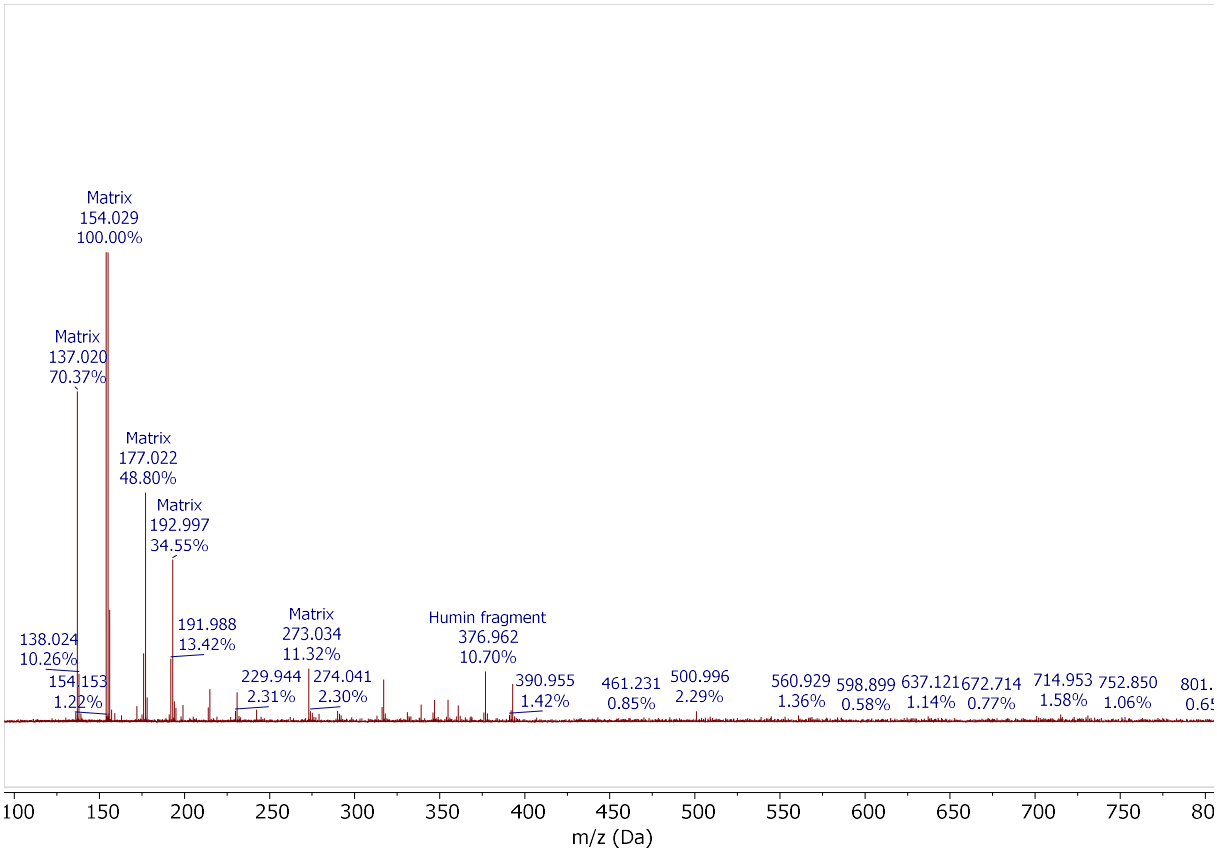

Figure 27: MALDI-TOF-MS spectrum of G1

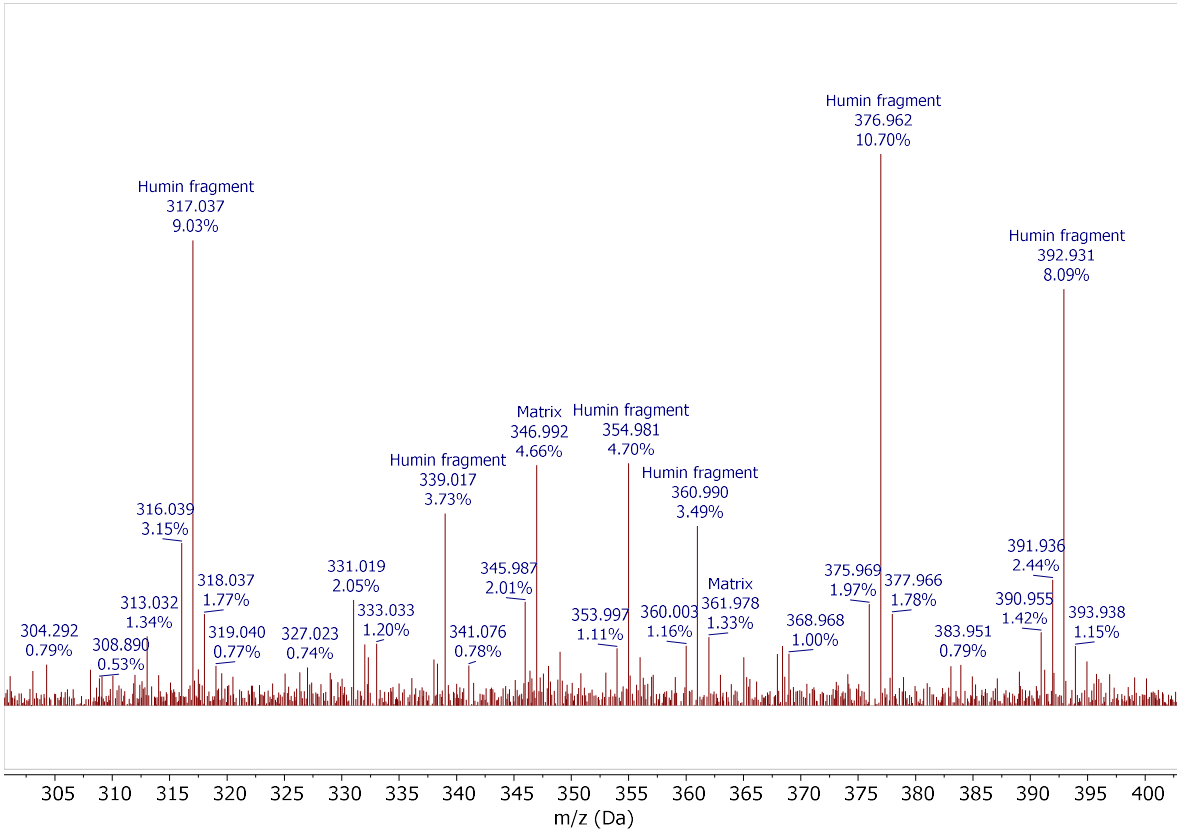

Figure S28: MALDI-TOF-MS spectrum of G1 zoomed in

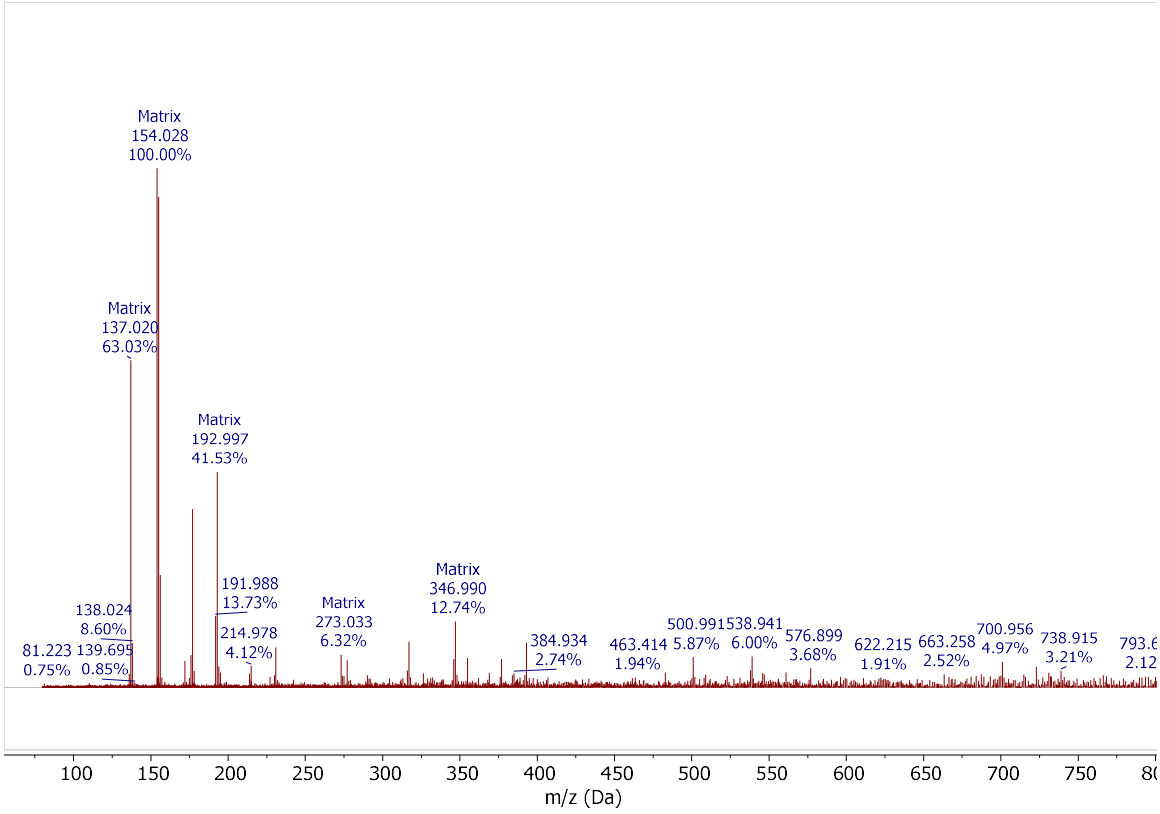

Figure S29: MALDI-TOF-MS spectrum of X1

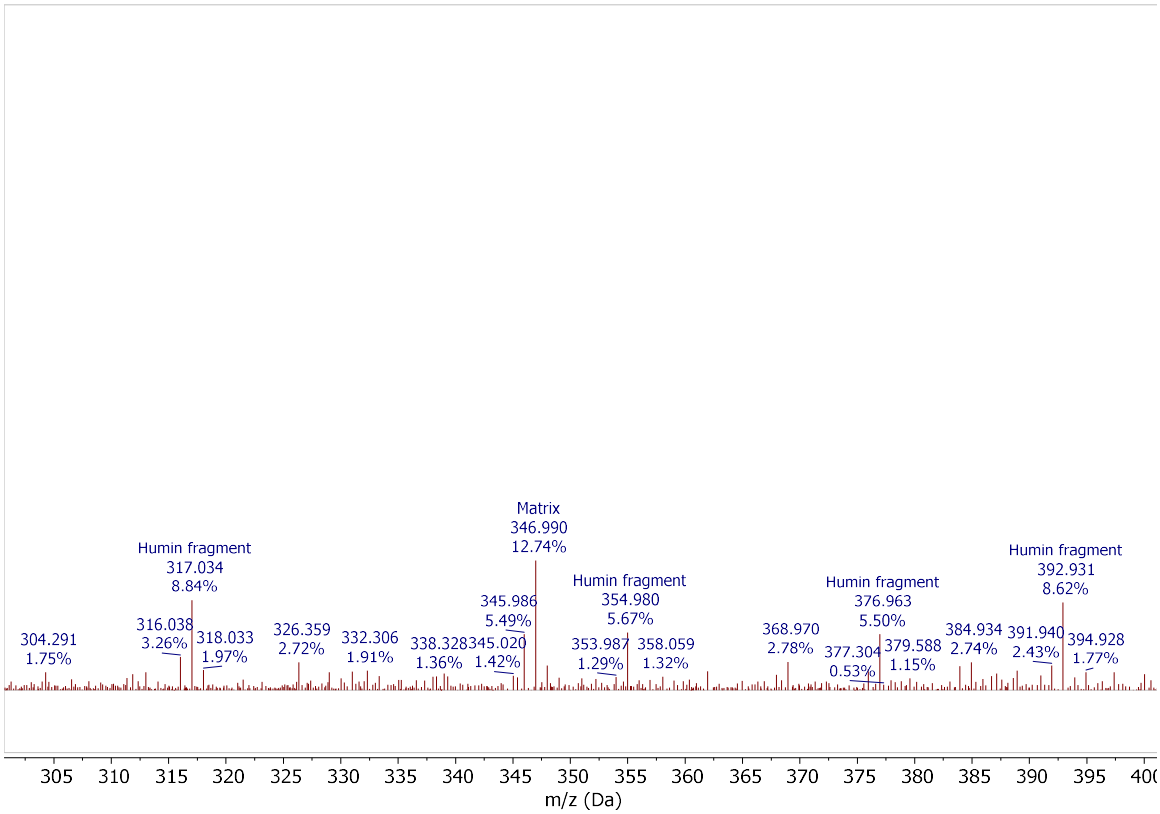

Figure S30: MALDI-TOF-MS spectrum of X1 zoomed in

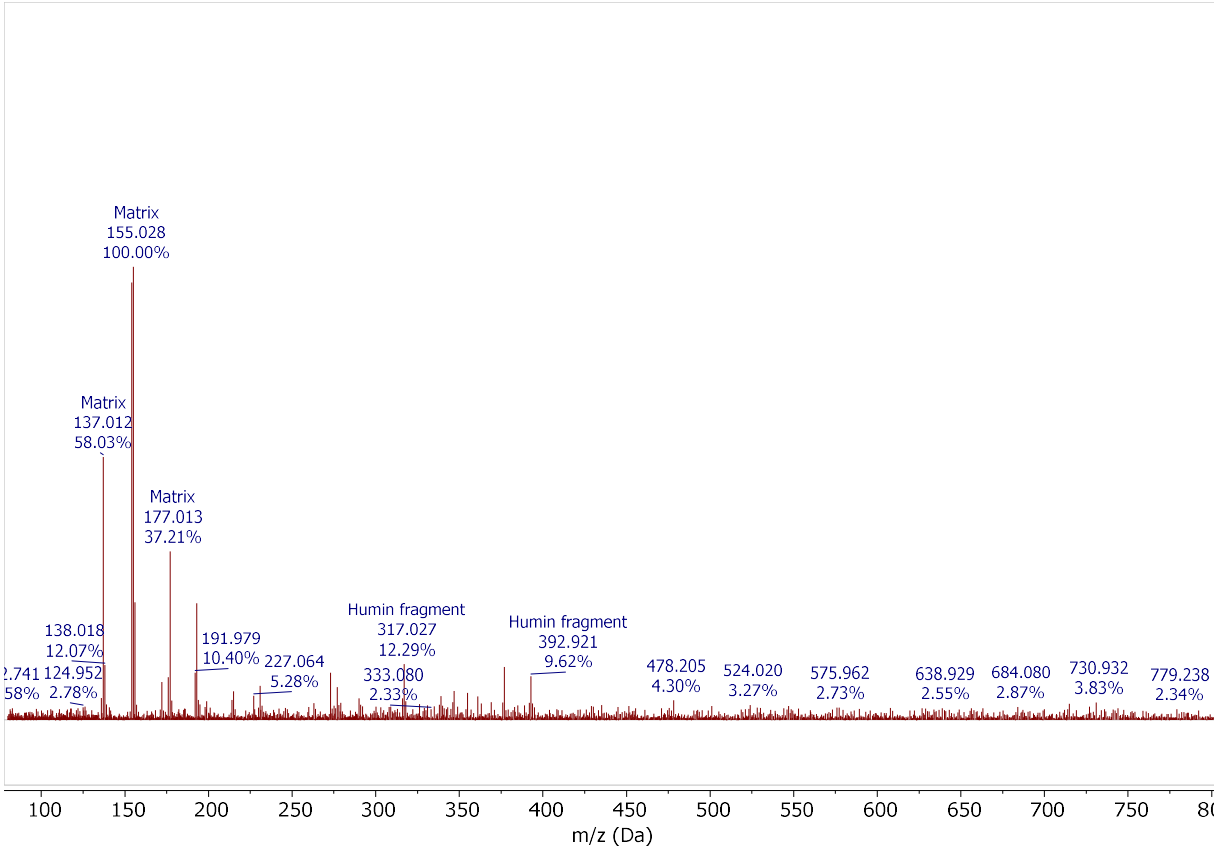

Figure S31: MALDI-TOF-MS spectrum of S1

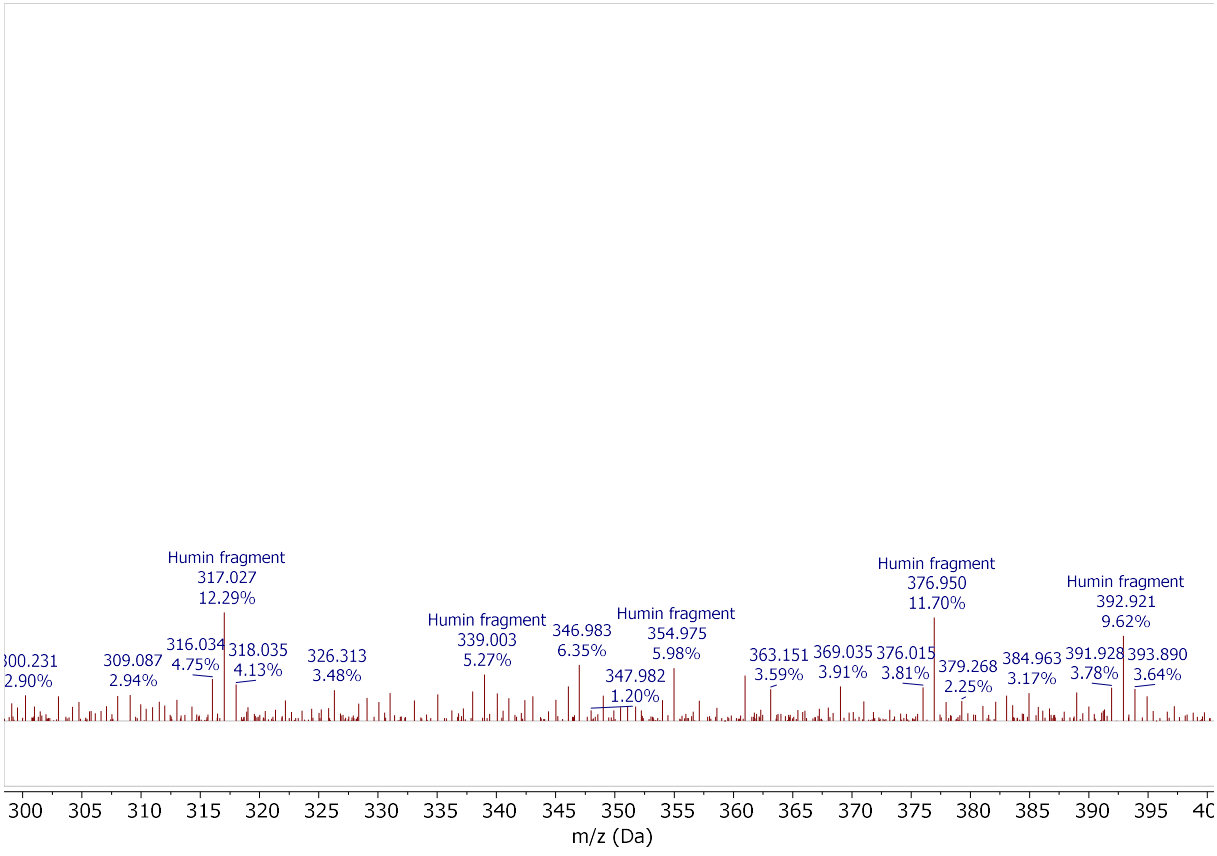

Figure S32: MALDI-TOF-MS spectrum of S1 zoomed in

Electron microscopy

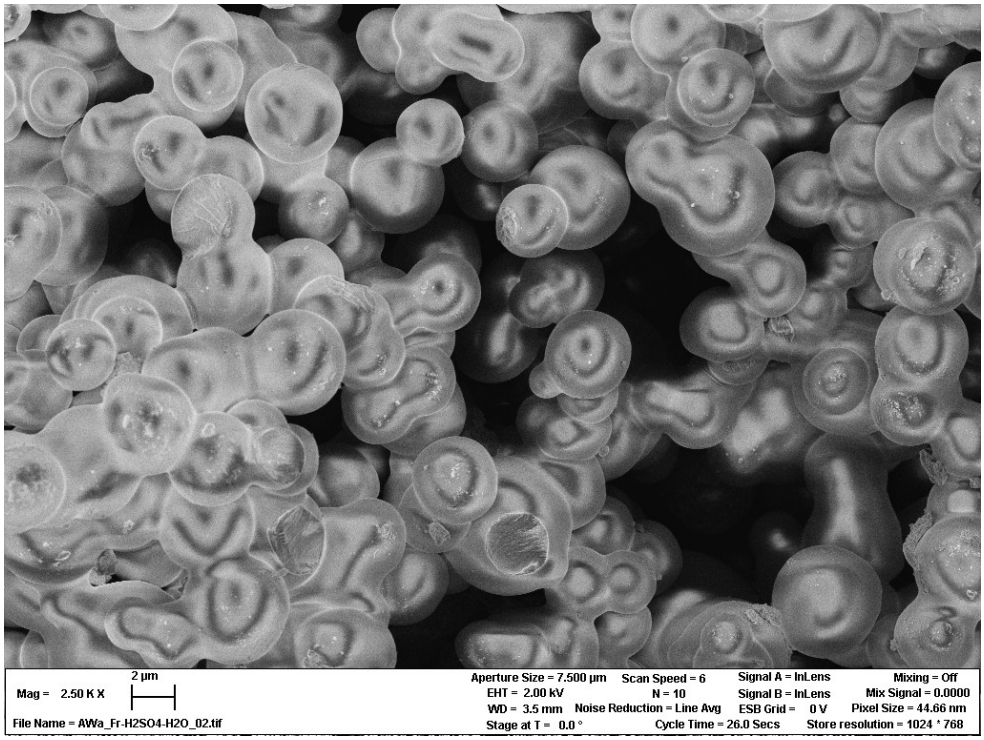

Figure S33: SEM micrograph of F1 zoomed in

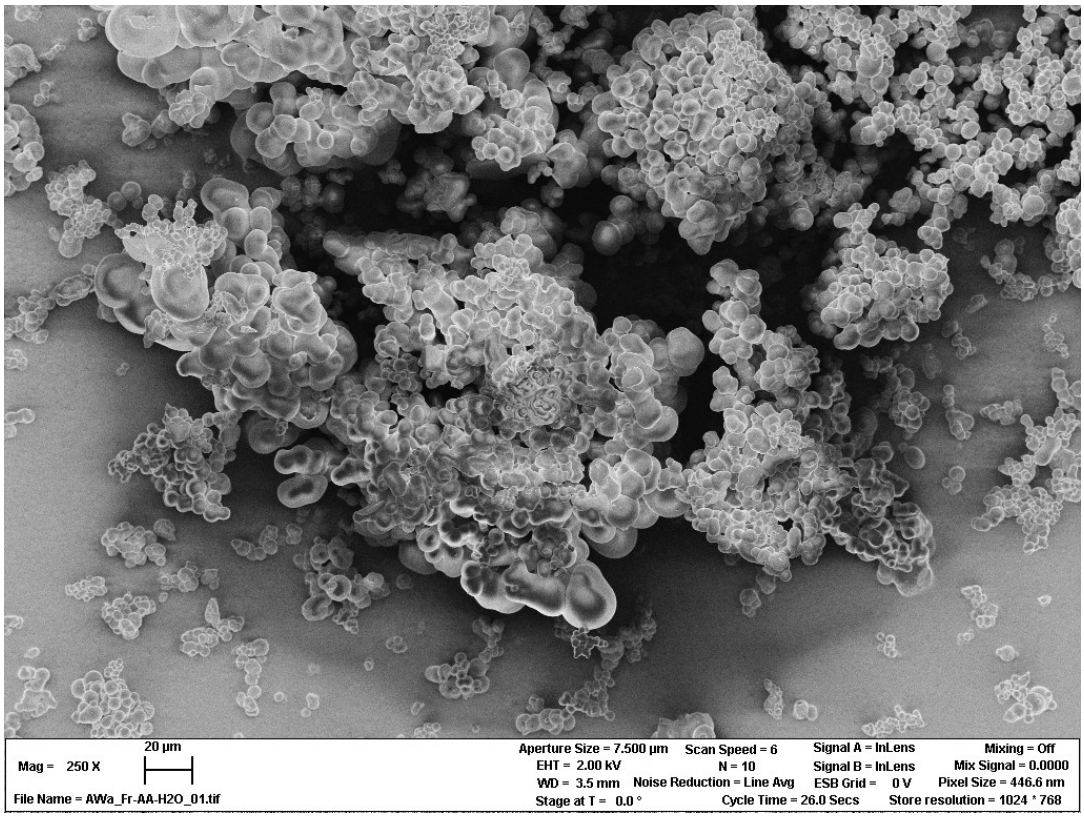

Figure S34: SEM micrograph of F2

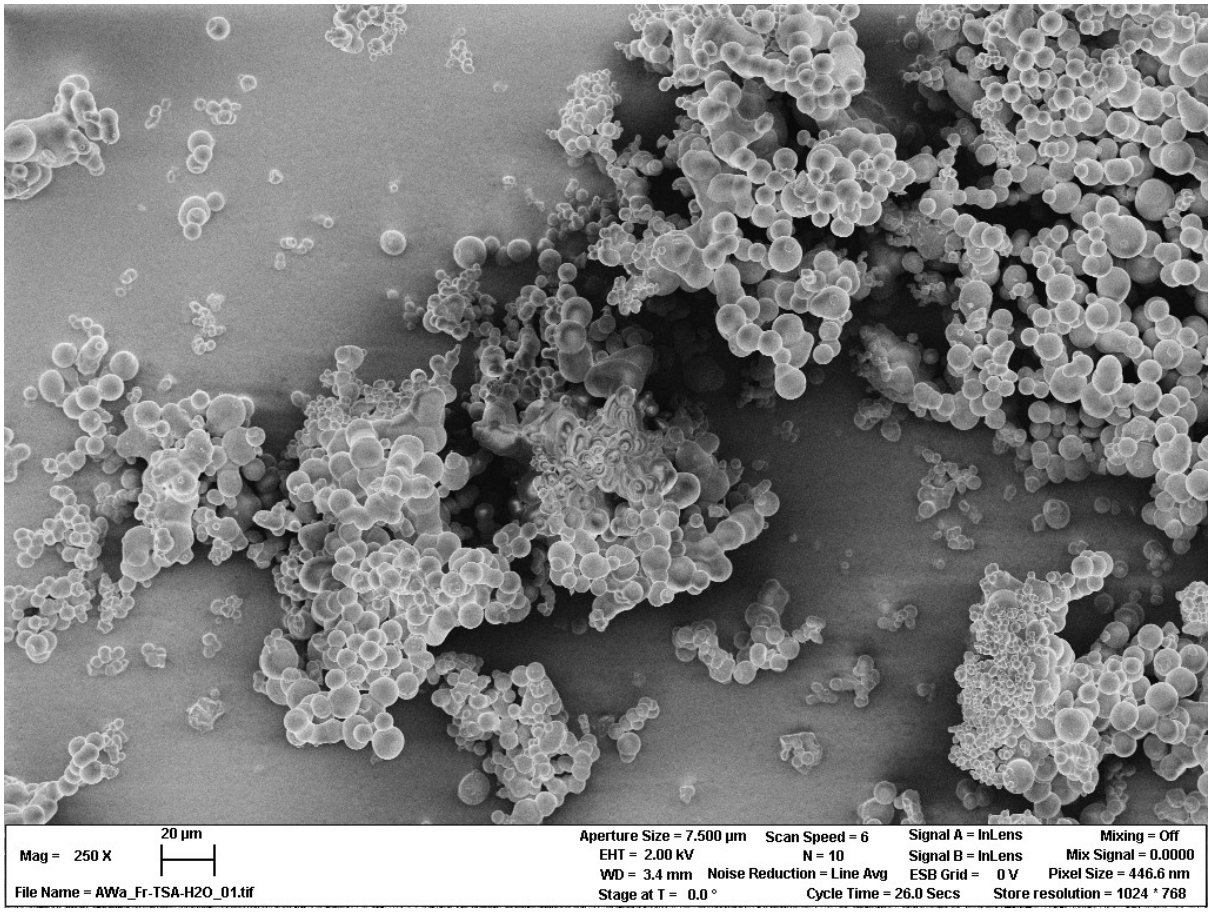

Figure S35: SEM micrograph of F3

Humin conversion

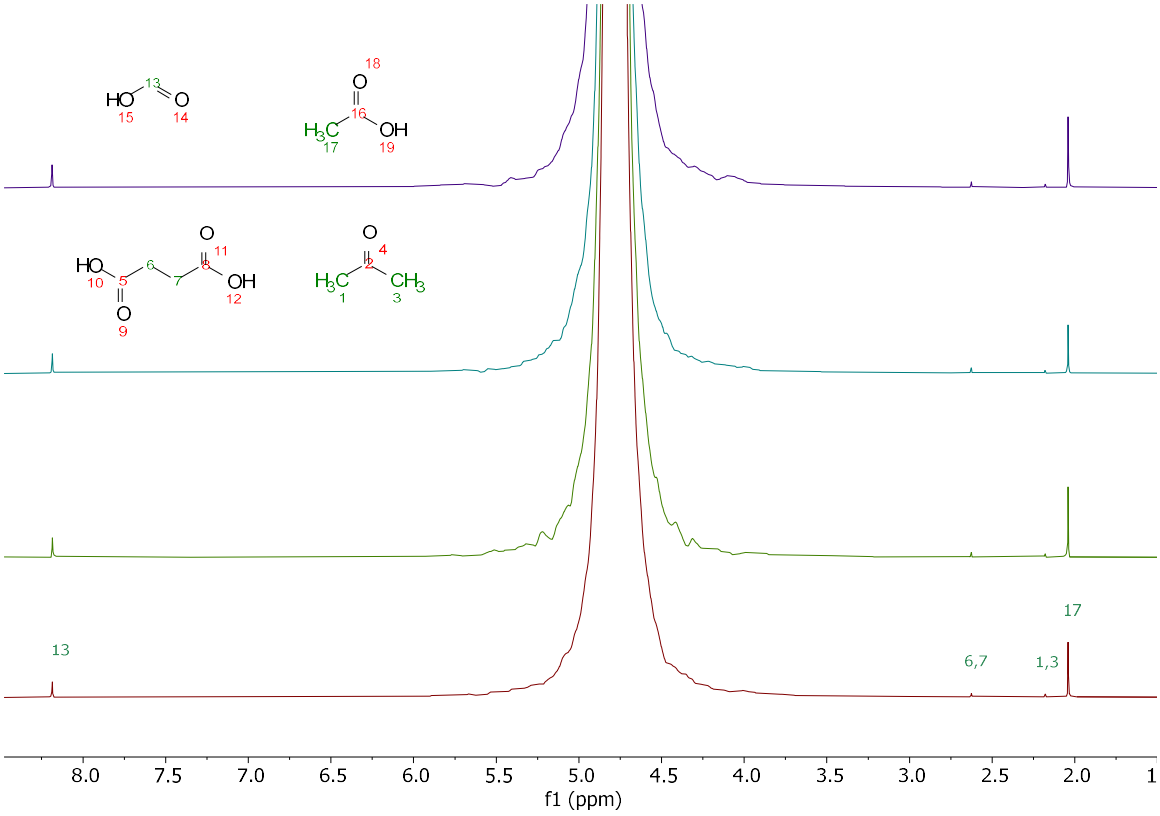

Figure S36: ^{1}H-NMR of the reaction solutions of F1, G1, X1 and S1 after conversion

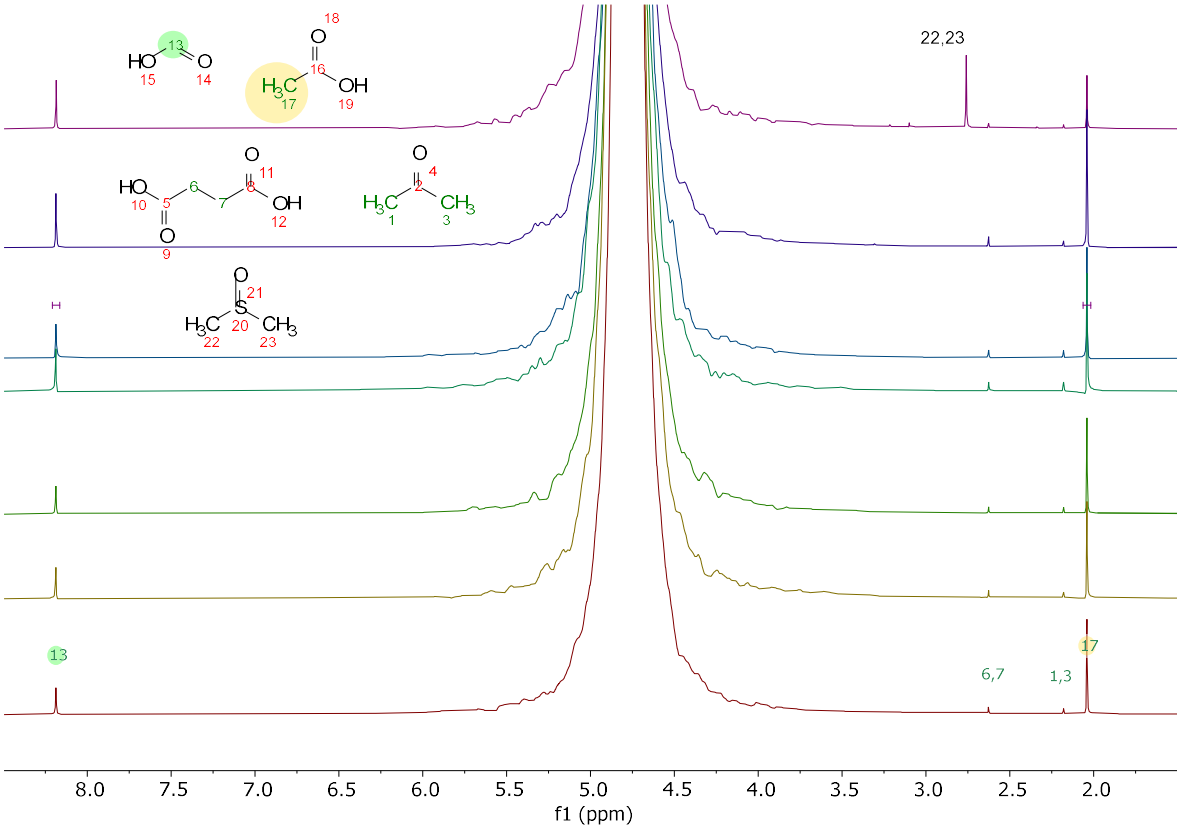

Figure S37: ^{1}H-NMR of the reaction solutions of the fructose humins after conversion

HPLC Analysis

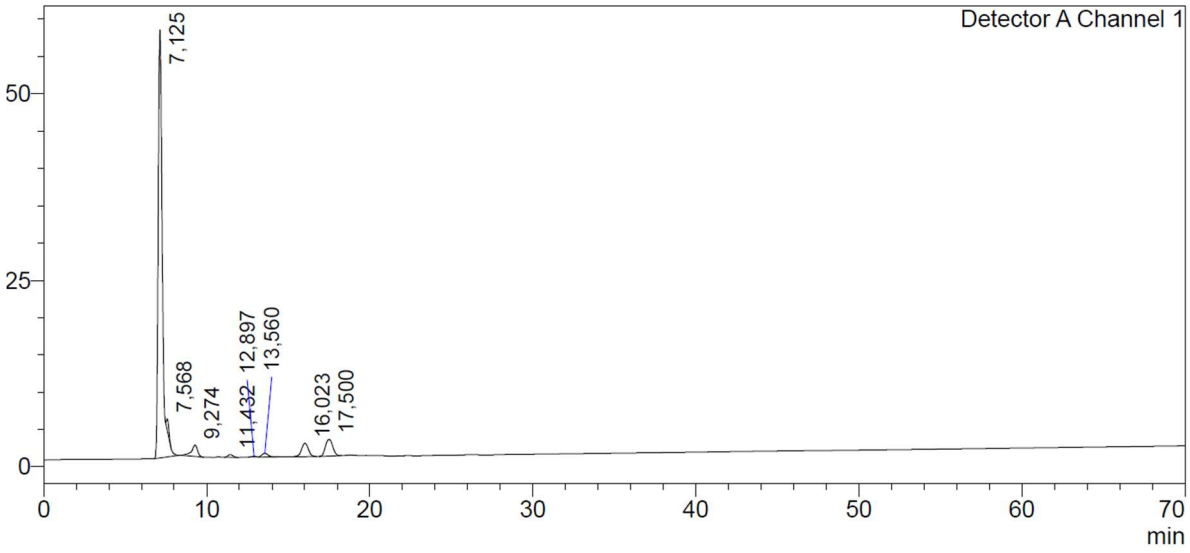

Figure S38: Chromatogram of F1

Table S8: HPLC data of reactions solutions after conversion

	Concentration [mM]		
	Succinic Acid	**Formic Acid**	**Acetic Acid**
F1	1	19	15
F2	1	18	14
F3	1	20	14
F4	1	34	22
F5	1	37	24
F6	1	30	19
F7	1	30	8
G1	1	22	18
X1	1	21	12
S1	1	24	17

Elemental Analysis

Table S9: Product yields and conversion of humins after catalyzed oxidation

	F1	**F2**	**F3**	**F4**	**F5**	**F6**	**F7**	**G1**	**X1**	**S1**
Succinic acid	0.007	0.008	0.008	0.008	0.007	0.008	0.008	0.008	0.008	0.008
Formic acid	0.036	0.040	0.034	0.065	0.055	0.074	0.063	0.043	0.040	0.046
Acetic acid	0.056	0.055	0.053	0.091	0.069	0.095	0.033	0.069	0.045	0.065
DMSO	0.000	0.000	0.000	0.000	0.000	0.000	0.043	0.000	0.000	0.000
CO2	0.388	0.349	0.445	0.382	0.313	0.464	0.158	0.459	0.355	0.469
CO	0.000	0.000	0.004	0.012	0.014	0.009	0.003	0.006	0.006	0.009
Solid residue	0.512	0.548	0.457	0.442	0.542	0.351	0.691	0.415	0.546	0.395
Combined Yield	0.488	0.452	0.543	0.558	0.458	0.649	0.309	0.585	0.454	0.605

Table S10: CHSO of humins synthesized in sulfuric acid and water after catalyzed oxidation

Elements	F1	G1	X1	S1
H	4,17	4,1	4,18	4,135
C	57,63	55,59	58,625	56,61
O	38,2	38,29	34,245	38,245
S	0	0	0	0
Sum	100	97,98	97,05	98,99
H/C	0,87	0,89	0,86	0,88
O/C	0,50	0,52	0,44	0,51

Table S11: CHSO of fructose humins after catalyzed oxidation

Elements	F1	F2	F3	F4	F5	F6	F7
H	4,17	4,02	3,66	4,1	4,835	3,985	3,915
C	57,63	55,58	55,735	56,65	62,79	52,175	54,055
O	38,2	37,25	38,16	36,285	30,66	39,89	33,665
S	0	0	0	0	0	0	5,59
Sum	100	96,85	97,555	97,035	98,285	96,05	97,225
H/C	0,87	0,87	0,79	0,87	0,92	0,92	0,87
O/C	0,50	0,50	0,51	0,48	0,37	0,57	0,47

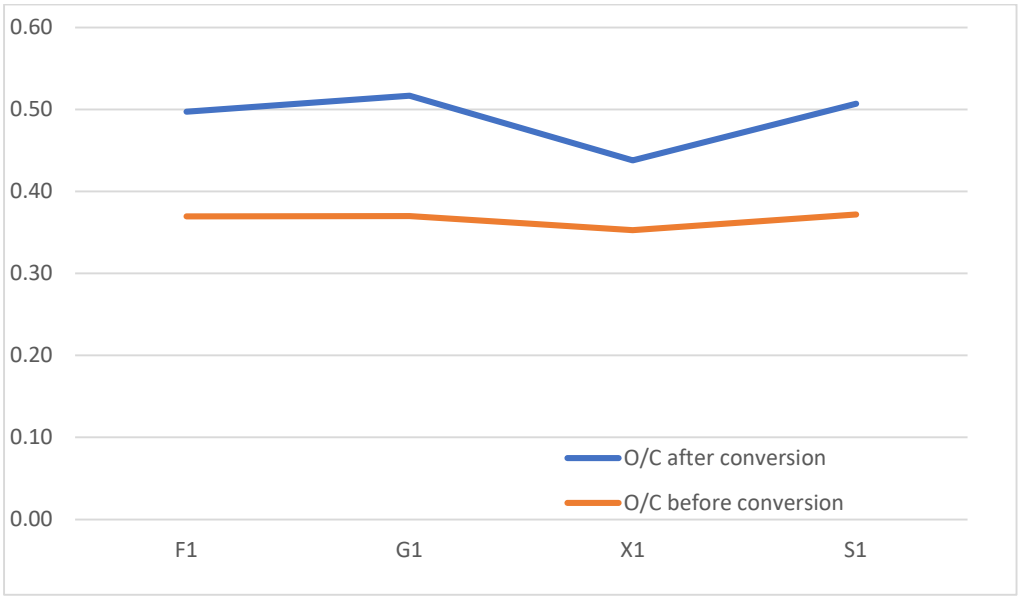

Figure S39: Comparison of O/C ratios before and after catalytic oxidation of humin synthesized in sulfuric acid and water

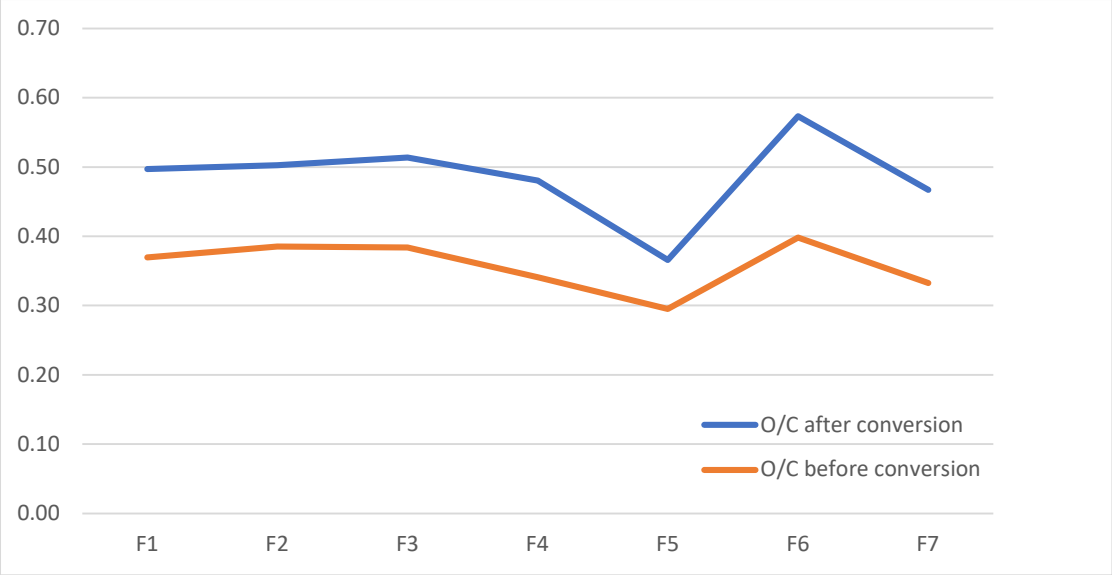

Figure S40: Comparison of O/C ratios before and after catalytic oxidation of fructose humins

IR spectra

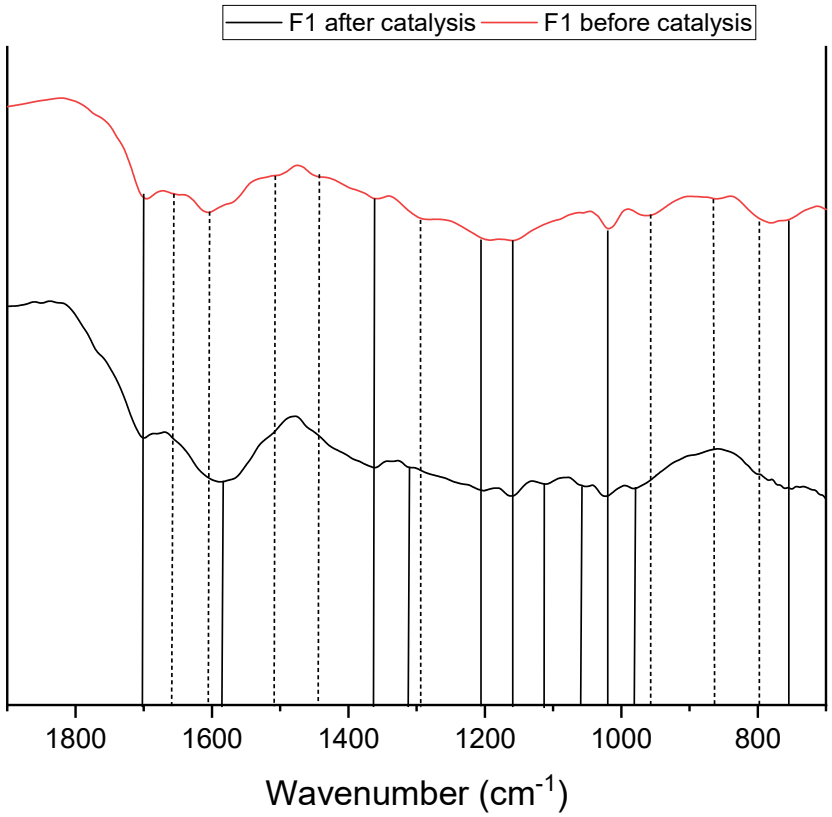

Figure S41: IR-spectrum of F1 before and after the catalysis

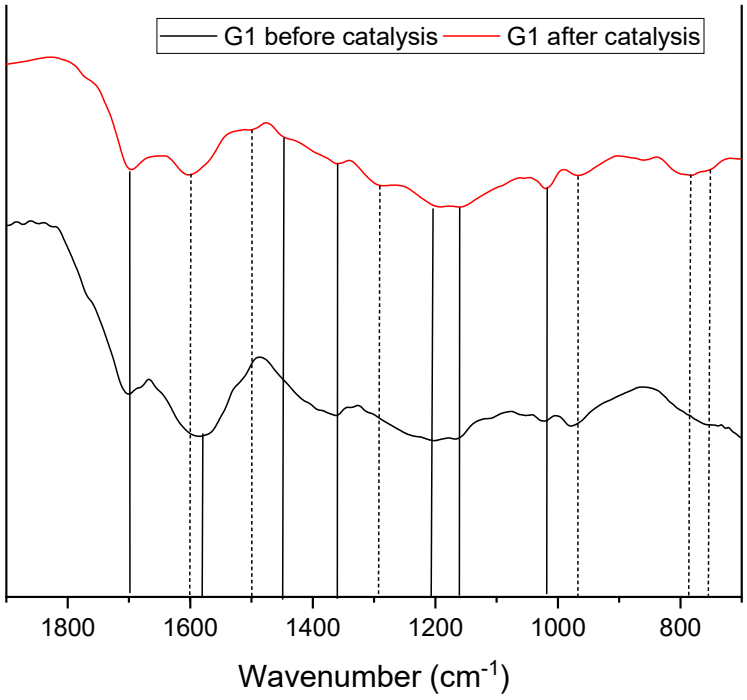

Figure S42: IR-*spectrum of G1 before and after the catalysis*

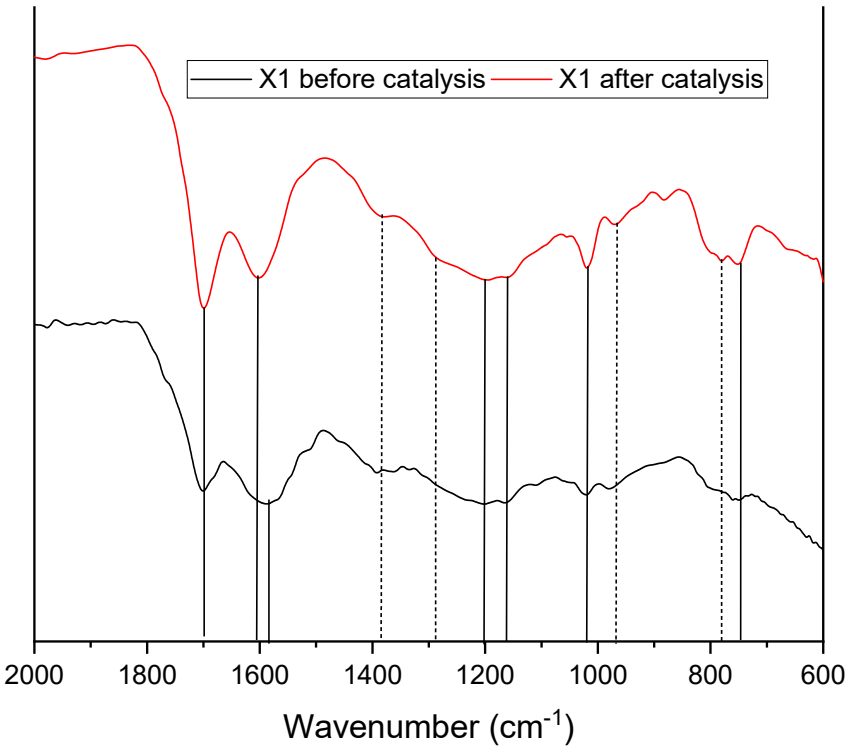

Figure S43: IR-spectrum of X1 before and after the catalysis

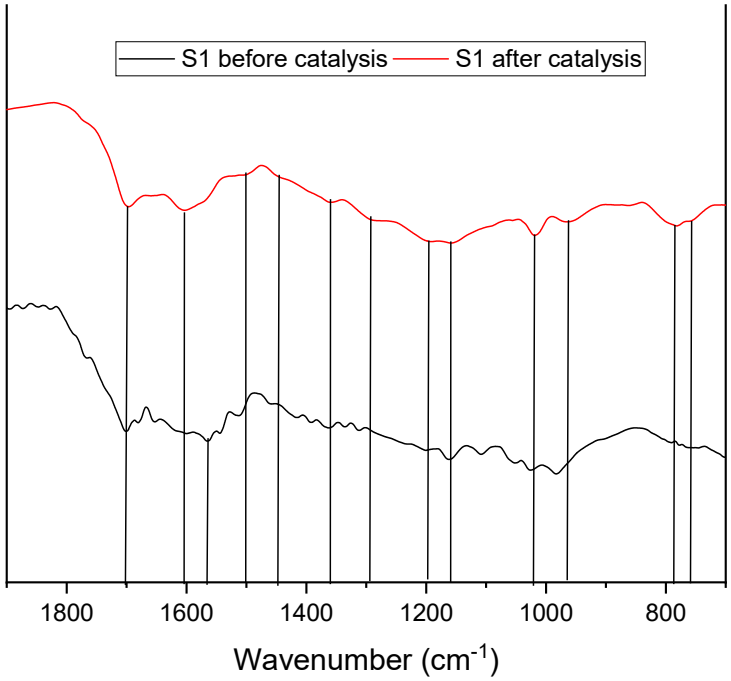

Figure S44: IR-spectrum of S1 before and after the catalysis

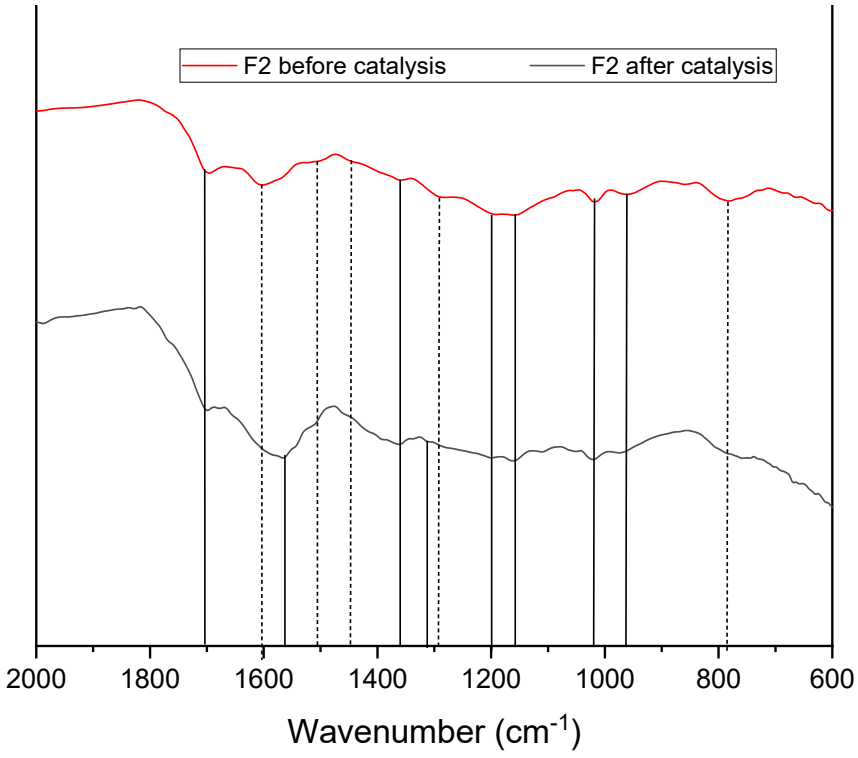

Figure S45: IR-spectrum of F2 before and after the catalysis

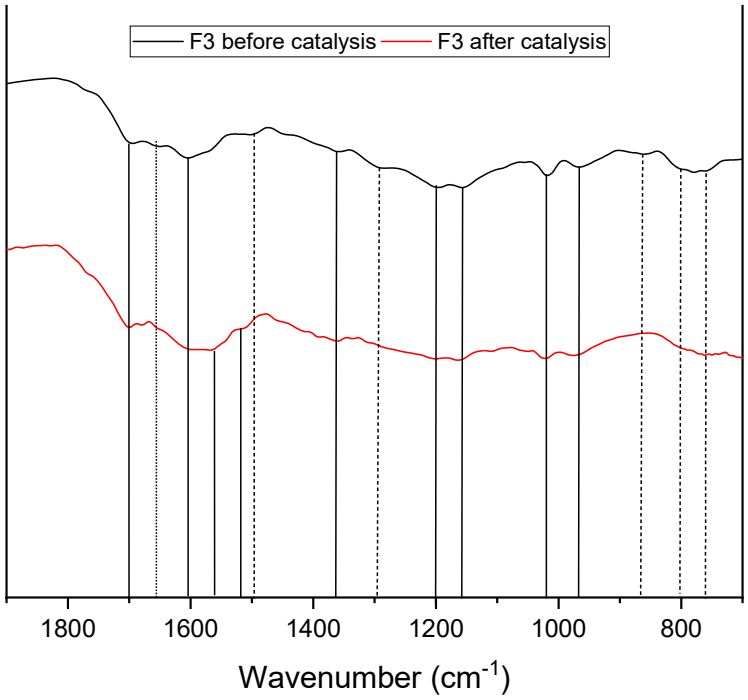

Figure S46: IR-spectrum of F3 before and after the catalysis

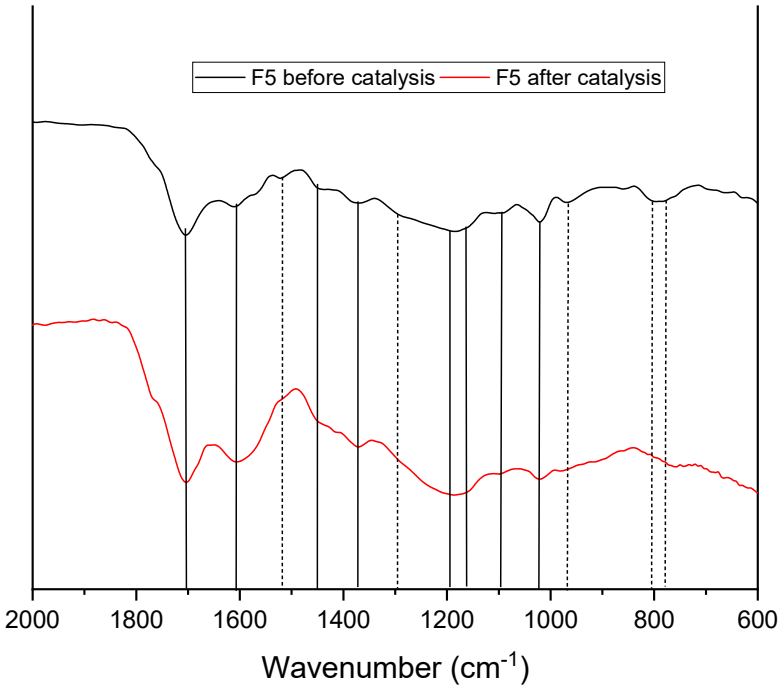

Figure S47: IR-spectrum of F5 before and after the catalysis

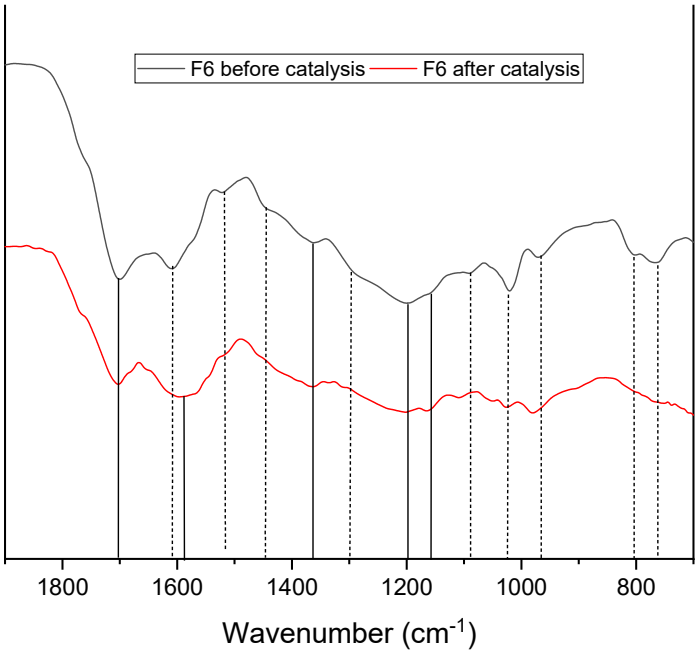

Figure S48: IR-spectrum of F6 before and after the catalysis

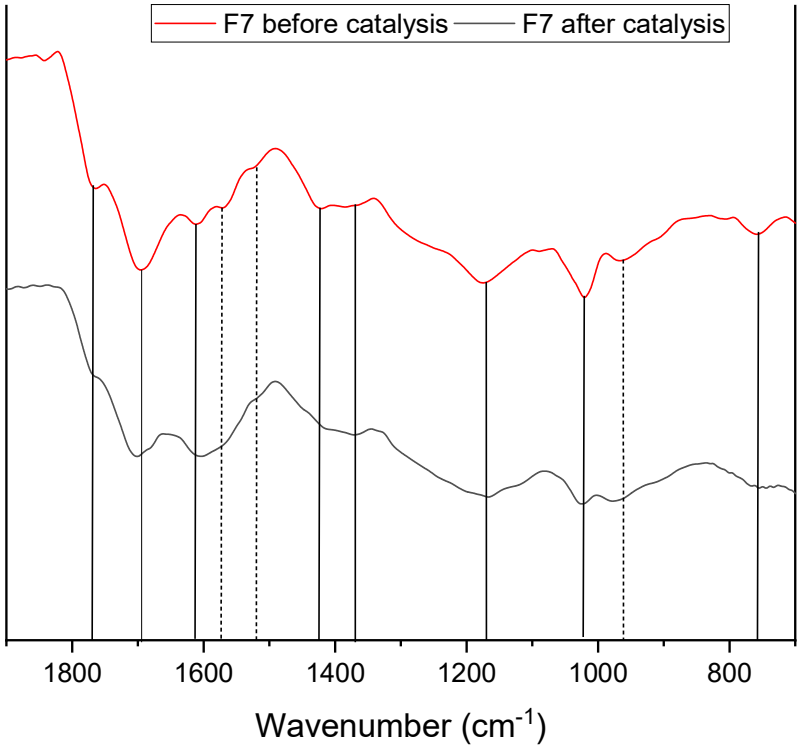

Figure S49: IR-spectrum of F7 before and after the catalysis

Equations used for yield calculations

The conversions of sugars x_i were determined through equation 1:

$$x_i = \frac{c_{i,0} - c_i}{c_{i,0}} * 100 \quad \text{(S1)}$$

With $c_{i,0}$ being the concentration before and c_i the concentration after reaction.

The carbon mass yields of the humin syntheses $Y_{Cmass\%,Hi}$ were calculated using equation 2:

$$Y_{Cmass\%,Hi} = \frac{m_{Hi} * C_{Hi}}{m_{Si} * C_{Si}} * 100 \quad \text{(S2)}$$

With C_{Hi} being the mass percentage of carbon and m_{Hi} the mass of the product humins and m_{Si} and C_{Si} being the respective metrics for the educt sugars.

The yields of the reaction products Pi of humin conversion $Y_{mass,\ Pi}$ were determined with the following equation:

$$Y_{mass,\ Pi} = \frac{m_{Pi}}{m_{Pi,max}} \quad \text{(S3)}$$

With m_{Pi} being the mass of the products and $m_{Pi,max}$ being the maximum possible mass.

m_{Pi} was calculated as the product of the concentration and the molar mass of the reaction product multiplied with the measured density of the reaction solution, to account for deviations in the density through the different densities of the reaction products.

$m_{Pi,max}$ was calculated using equation 4:

$$m_{Pi,max} = \frac{n_{Hi,C} / N_{C,Pi} * M_{Hi}}{m_{Hi} + m_{HPA-5} + m_{H_2O}} \quad \text{(S4)}$$

$N_{C,Pi}$ here is equivalent to the number of carbons contained in the reaction product and $n_{Hi,C}$ is the amount of carbon contained in the humins used for conversion. $n_{Hi,C}$ was determined using equation 5:

$$n_{Hi,C} = \frac{C_{Hi} * m_{Hi}}{M_{Carbon}} \quad \text{(S5)}$$

10.1.2 Supporting information of publication 2

Supporting information from:

Humin-free synthesis of levulinic acid from fructose using heteropolyacid catalysts

André Wassenberg, Tobias Esser, Maximilian J. Poller, Dorothea Voß, Jakob Albert

Wassenberg, T. Esser, M.J. Poller, D. Voß, J. Albert, Humin-free synthesis of levulinic acid from fructose using heteropolyacid catalysts, Biofuels, Bioproducts and Biorefining *18* (**2024**) 1585–1597. *https://doi.org/10.1002/bbb.2654*.

This document contains 4 figures and 4 tables on 7 pages

Supporting Information

Table S1: *DoE factor combinations and results*

Run	acetone [w%]	Temperature [°C]	Time [h]	c(Fructose) [mol/L]	Humin yield [w%]	LA yield [mol%]
1	80	140	3	0,25	16,9%	31,2%
2	0	140	3	0,25	7,7%	56,8%
3	40	140	1	0,25	0,0%	17,2%
4	40	140	5	0,25	18,7%	43,6%
5	40	140	3	0,1	0,0%	45,0%
6	40	140	3	0,4	20,5%	43,3%
7	40	160	1	0,1	0,0%	41,1%
8	40	160	3	0,25	22,2%	52,0%
9	40	160	3	0,25	20,7%	47,6%
10	40	160	5	0,4	29,6%	47,5%
11	40	160	1	0,4	19,8%	48,3%
12	40	160	5	0,1	7,4%	59,1%
13	80	160	3	0,1	7,4%	37,9%
14	0	160	3	0,4	17,4%	60,5%
15	40	160	3	0,25	18,9%	54,3%
16	80	160	3	0,4	45,7%	32,0%
17	40	160	3	0,25	21,9%	51,3%
18	0	160	3	0,1	1,5%	64,0%
19	40	160	3	0,25	19,0%	56,4%
20	80	160	1	0,25	18,0%	38,4%
21	80	160	5	0,25	32,9%	34,4%
22	40	160	3	0,25	18,1%	52,1%
23	0	160	5	0,25	15,4%	60,3%
24	0	160	1	0,25	11,9%	59,3%
25	80	180	3	0,25	40,2%	35,5%
26	0	180	3	0,25	13,9%	60,9%
27	40	180	5	0,25	28,1%	52,3%
28	40	180	1	0,25	15,7%	54,8%
29	40	180	3	0,1	15,5%	63,0%
30	40	180	3	0,4	29,4%	48,0%
31	0	180	1	0,1	1,5%	66,1%
32	80	180	1	0,1	5,9%	47,1%
33	1	180	1	0,1	3,1%	63,9%
34	20	180	1	0,1	5,3%	62,0%

Table S2: *Results of acidic catalyst selection*

	Humin yield [wt%]	LA Yield [mol%]	Conversion [mol%]
HPA0	14.5%	34.7%	95%
Formic Acid	22.6%	36.9%	100%
HPW	18.4%	57.7%	100%
H2SO4	14.2%	57.9%	99%
HSiW	15.7%	60.9%	99%

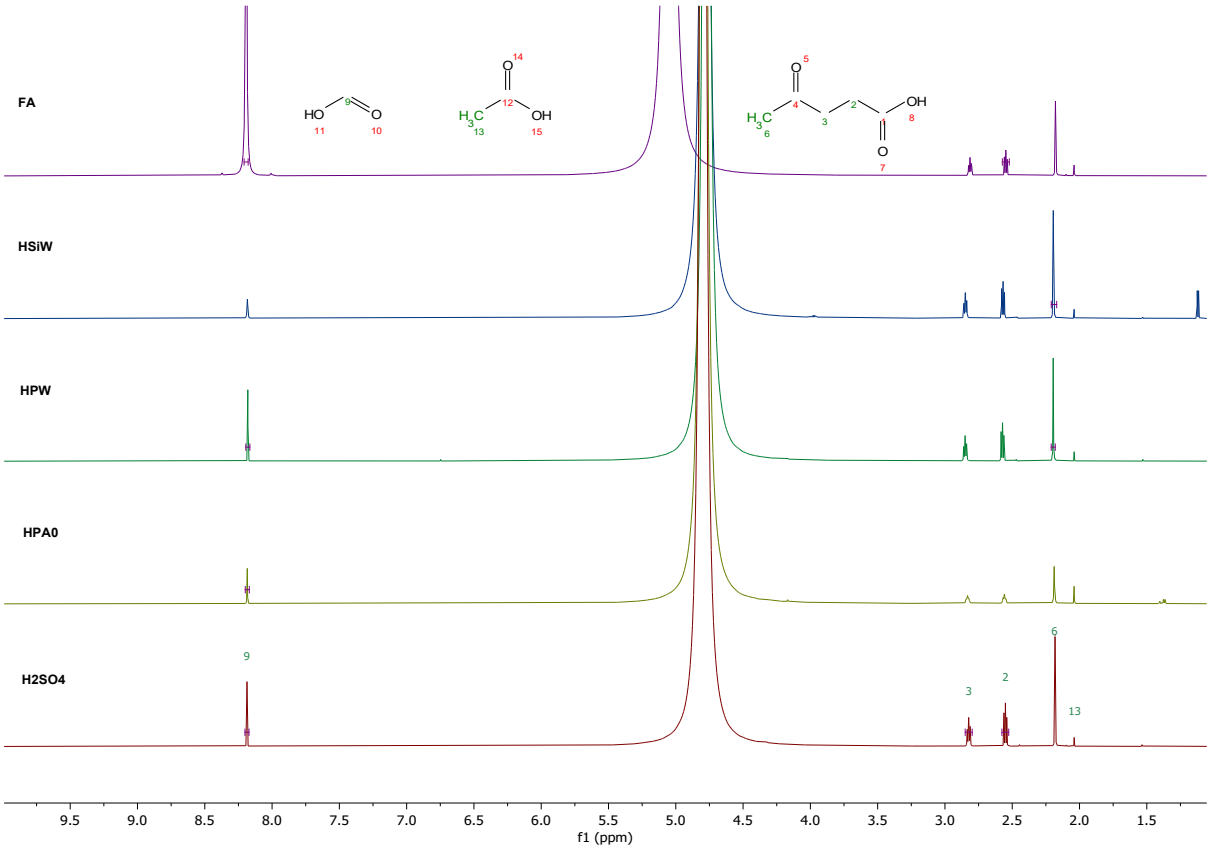

Figure S1: *^{1}H-NMRs of acidic catalyst selection.*

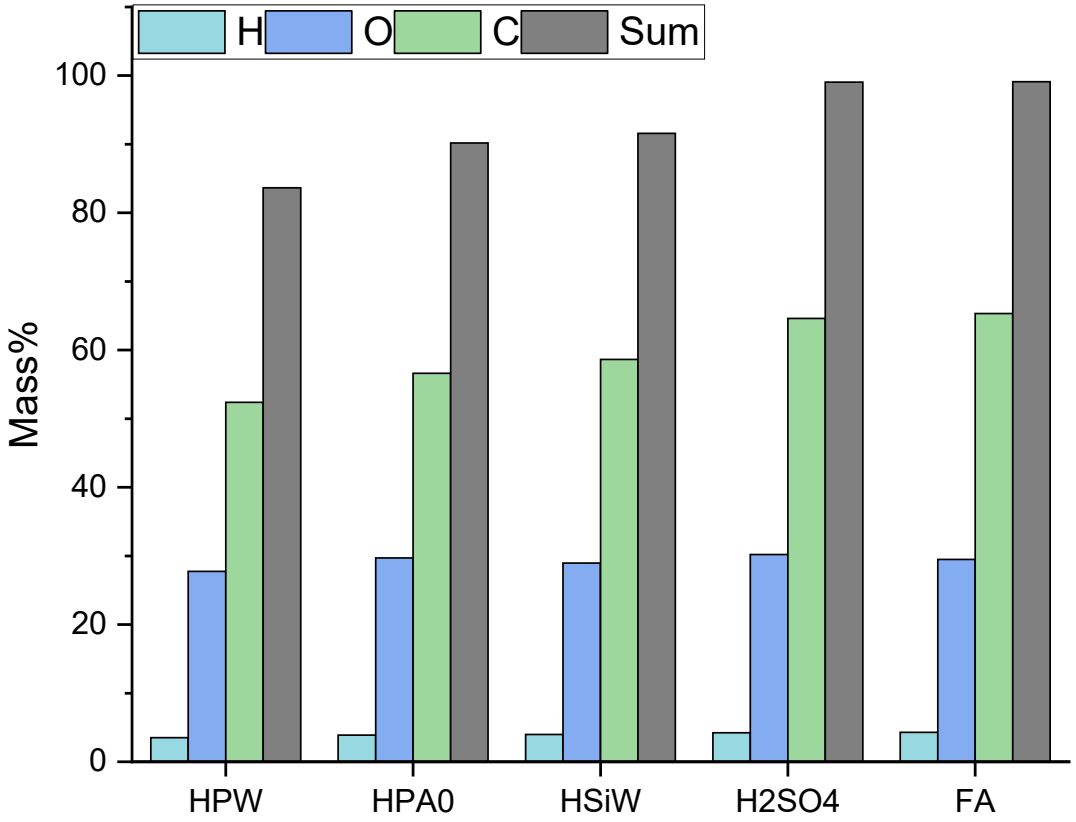

Figure S2: *Elemental analyses of Humins produced during acidic catalyst selection.*

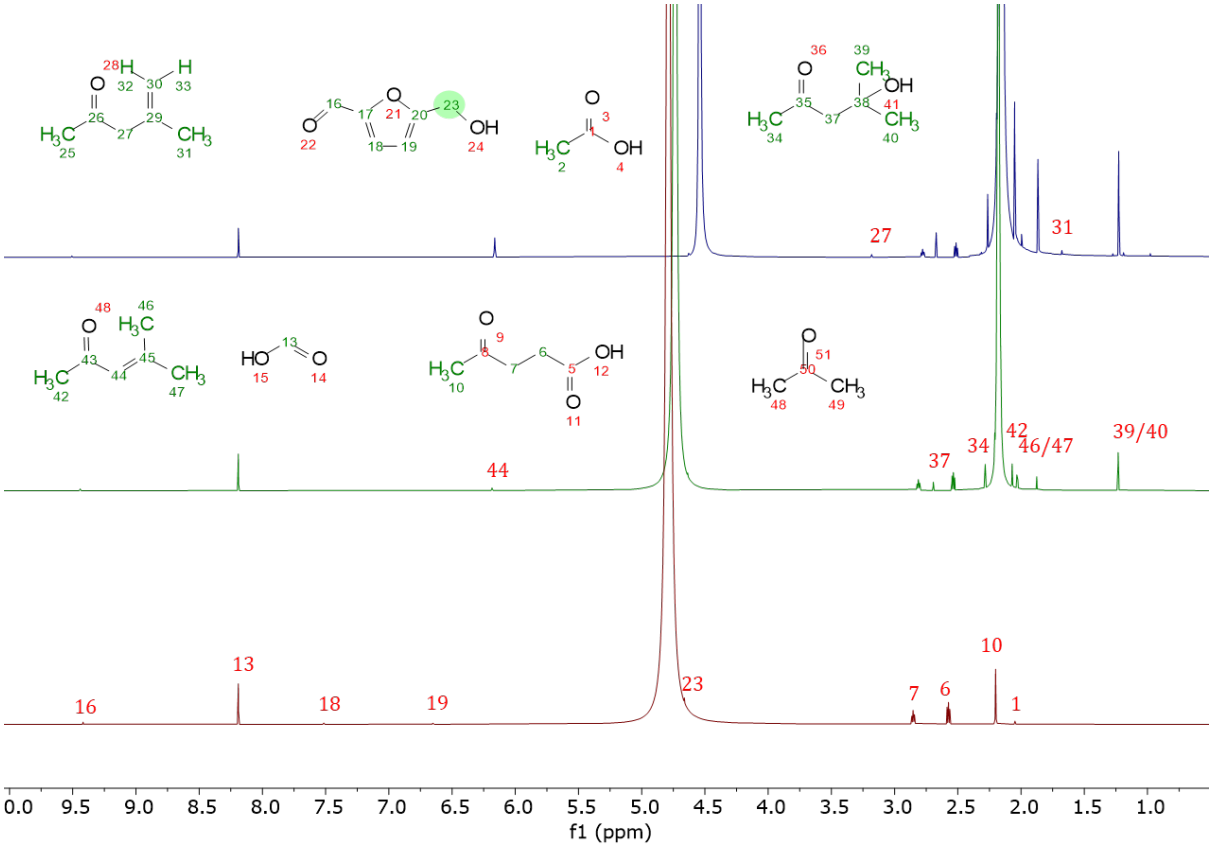

Figure S3: *^{1}H-NMR spectra of DoE runs 2,4 and 1 (From bottom to top).*

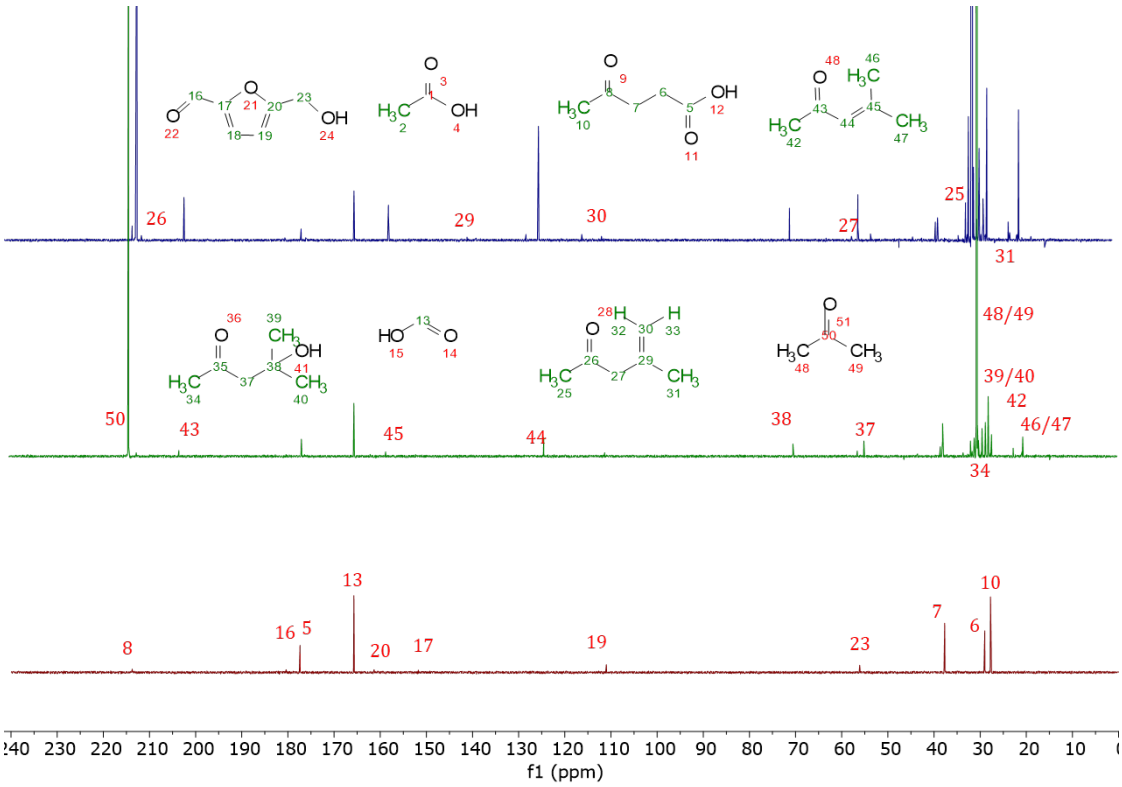

Figure S4: *^{13}C-NMR spectra of DoE runs 2,4 and 1 (From bottom to top).*

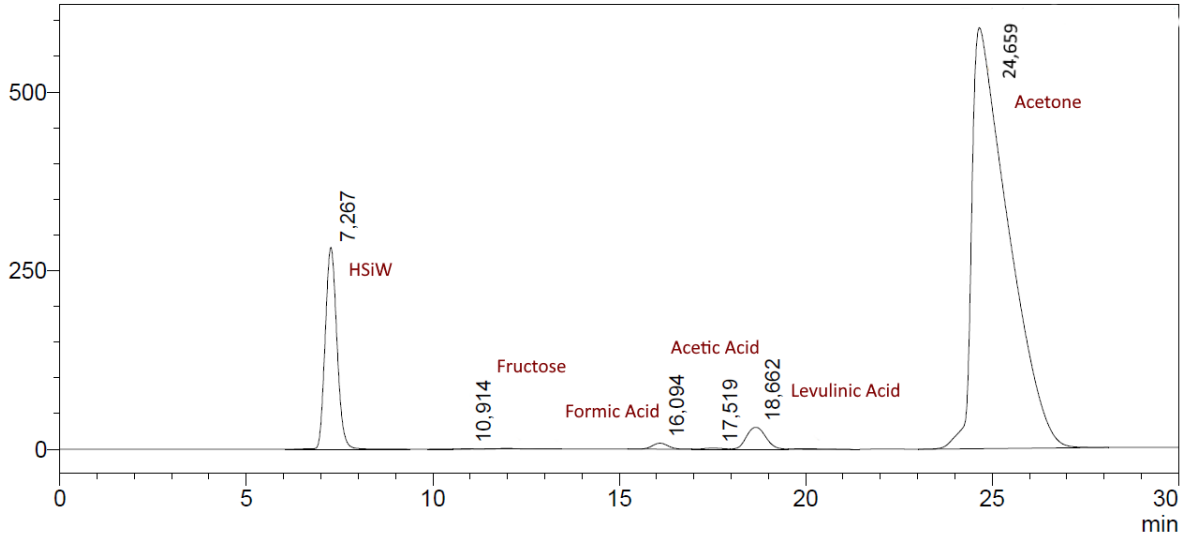

Figure S5: *HPLC Chromatogram of DoE run 1 (140°C; 3 h; 80% Acetone; 0,25 mol/L Fructose)*

Table S3 *Reproduction runs of optimal parameter combination (180°C; 1h; 0% Acetone; 0,1 mol/L Fructose)*

Reaction data	R2	R4	R5	Mean	STDEV
Yield Humin (Mass %)	1,48%	1,48%	2,14%	1,70%	0,31%
Yield Levulinic Acid (Mol %)	66,10%	66,00%	65,80%	65,97%	0,12%

Table S4 *Results of substrate variation at optimal factor combination (180°C; 1h; 0% Acetone; 0,1 mol/L sugar)*

	LA Yield	Furfural Yield	Humin Yield	Conversion
Cellobiose	27.4%	0.0%	0.12%	52%
Glucose	31.0%	0.0%	0.0%	58%
Sucrose	45.2%	0.0%	4.12%	75%
Xylose	0.0%	47.3%	0.54%	94%
Fructose	65.8%	0.0%	2.14%	99%

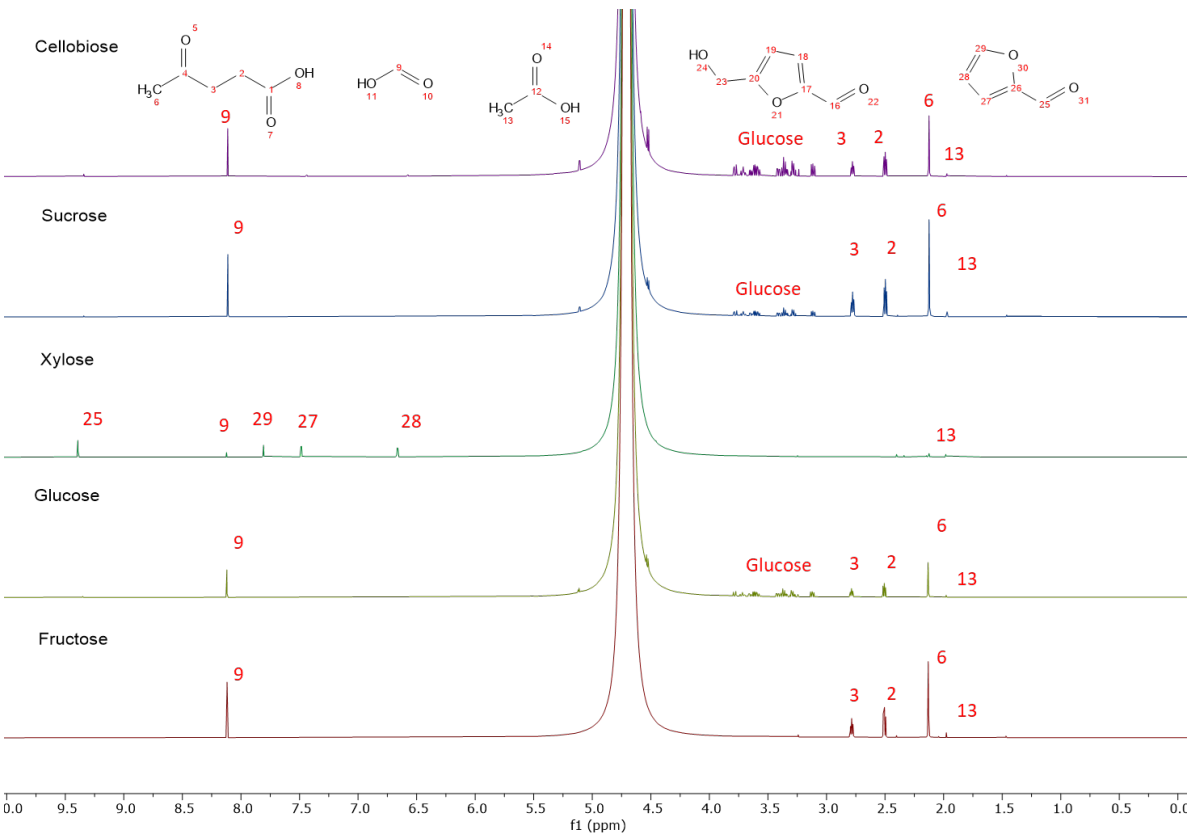

Figure S3 *^{1}H-NMR of substrate variation reactions with optimal parameters (180°C; 1h; 0% acetone; 0,1 mol/L sugar)*

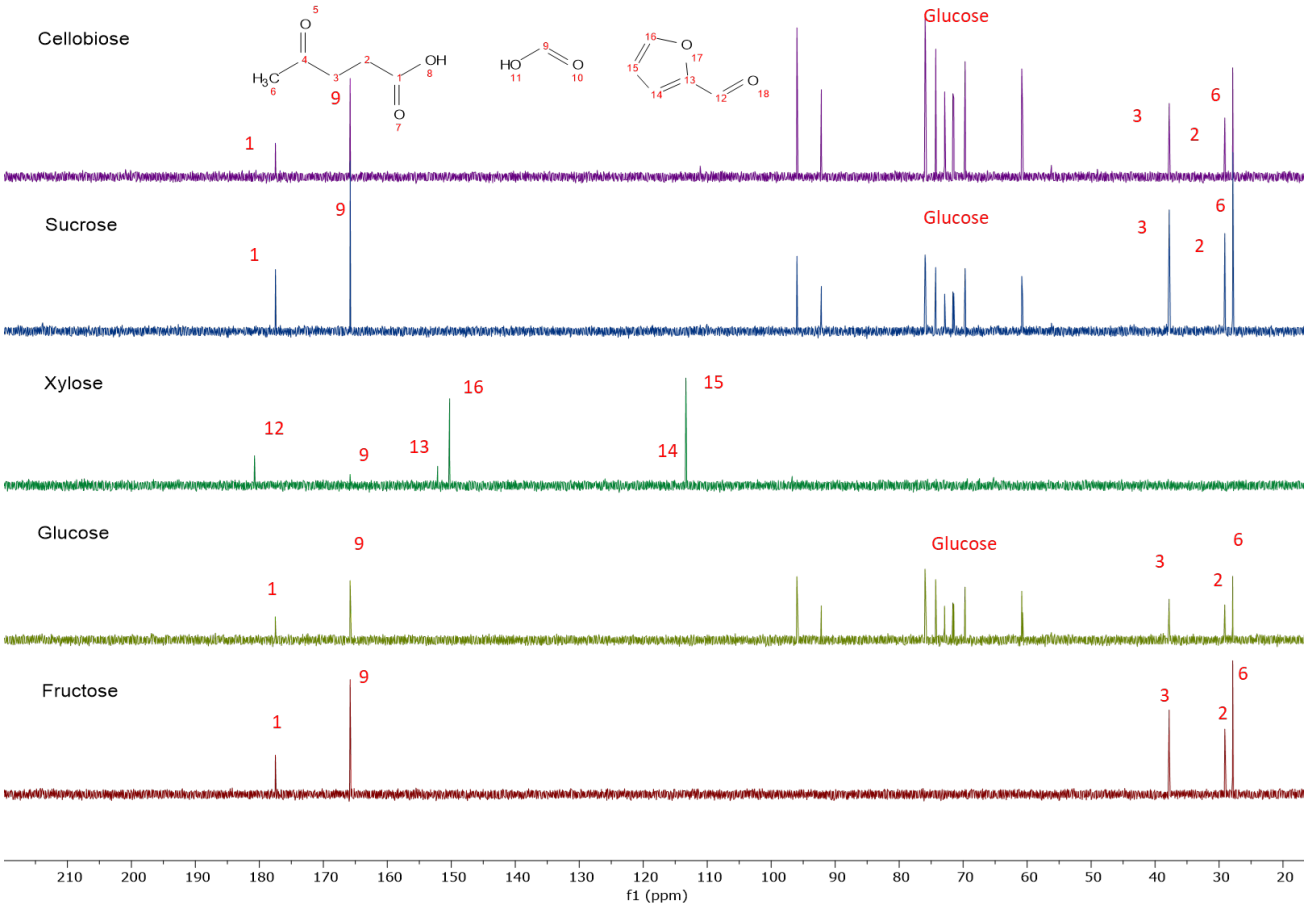

Figure S4: *^{1}H-NMR of substrate variation reactions with optimal parameters (180°C; 1h; 0% acetone; 0,1 mol/L sugar)*

10.1.3 Supporting Information of publication 3

Supporting information from:

Valorization of Humins by Cyclic Levulinic Acid Production Using Polyoxometalates and Formic Acid

André Wassenberg, Tobias Esser, Maximilian J. Poller, Dorothea Voß, Jakob Albert

A. Wassenberg, T. Esser, M.J. Poller, D. Voß, J. Albert, Valorization of Humins by Cyclic Levulinic Acid Production Using Polyoxometalates and Formic Acid, ChemSusChem (**2025**) e202401973. *https://doi.org/10.1002/cssc.202401973*.

This document contains 4 equations, 6 tables and 18 figures on 18 pages.

ChemSusChem

Supporting Information

Valorization of Humins by Cyclic Levulinic Acid Production Using Polyoxometalates and Formic Acid

André Wassenberg, Tobias Esser, Maximilian J. Poller, Dorothea Voß, and Jakob Albert*

Valorization of Humins by Cyclic Levulinic Acid Production Using Polyoxometalates and Formic Acid

Supporting Information

André Wassenberg, Tobias Esser, Maximilian J. Poller, Dorothea Voß, Jakob Albert[*]

Institute for Technical and Macromolecular Chemistry, University of Hamburg, 20146 Hamburg, Germany

* Correspondence: jakob.albert@uni-hamburg.de

Table of Contents

1. Synthesis of humins for SCO experiments

Humin synthesis was carried out applying a modified and upscaled version of the optimal reaction conditions for LA synthesis determined in our previous work [1]. The synthesis was conducted in a 600 mL Hastelloy autoclave under a nitrogen atmosphere, with formic acid as acidic catalyst and a reaction time of 4 h. The reaction solution was stirred (300 rpm), the reaction temperature set to 180 °C, and the pressure increased to 30 bar to prevent evaporation of the solvent. The solid humin contained in the reaction solution was separated from the solution through filtration. The solid residue was subsequently rinsed with water and dried.

Table S1: Humin and LA yields of multiple batches for humin synthesis (180 °C, H_2O, 0.1 mol L^{-1} fructose in 150 mL H_2O, pH = 1 (FA), t = 4 h, p = 30 bar N_2).

	LA yield mol%	Humin yield wt%
LP1	42.0	11.5
LP2	39.0	11.8
LP3	41.0	11.4
Average	40.7	11.5
Standard deviation	1.2	0.2

The yields of humins and LA differ only slightly, which also shows the reproducibility of the reaction. There were also no differences observed in the analysis of the solid and liquid phases (*Figure S1/S2*). For this reason, the three humin batches produced were combined to form humin batch **H** used for the SCO.

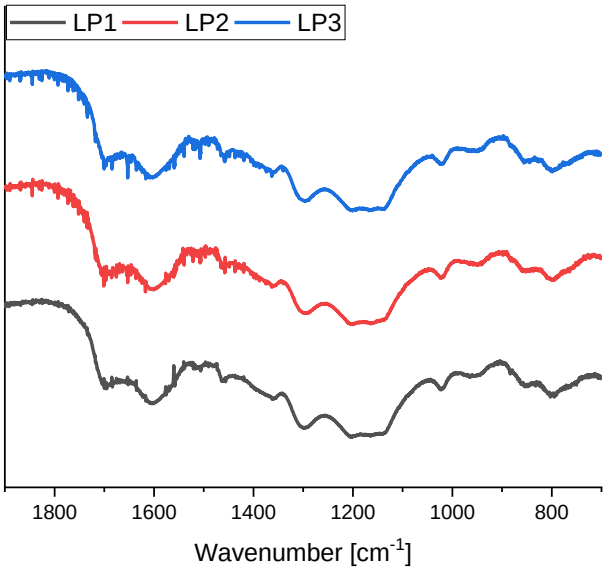

*Figure S1: IR-spectra of fructose humins produced by **LP1**, **LP2** and **LP3** (180°C, 0,1 mol L^{-1} fructose, pH = 1 FA, t = 4h, p=30 bar N_2).*

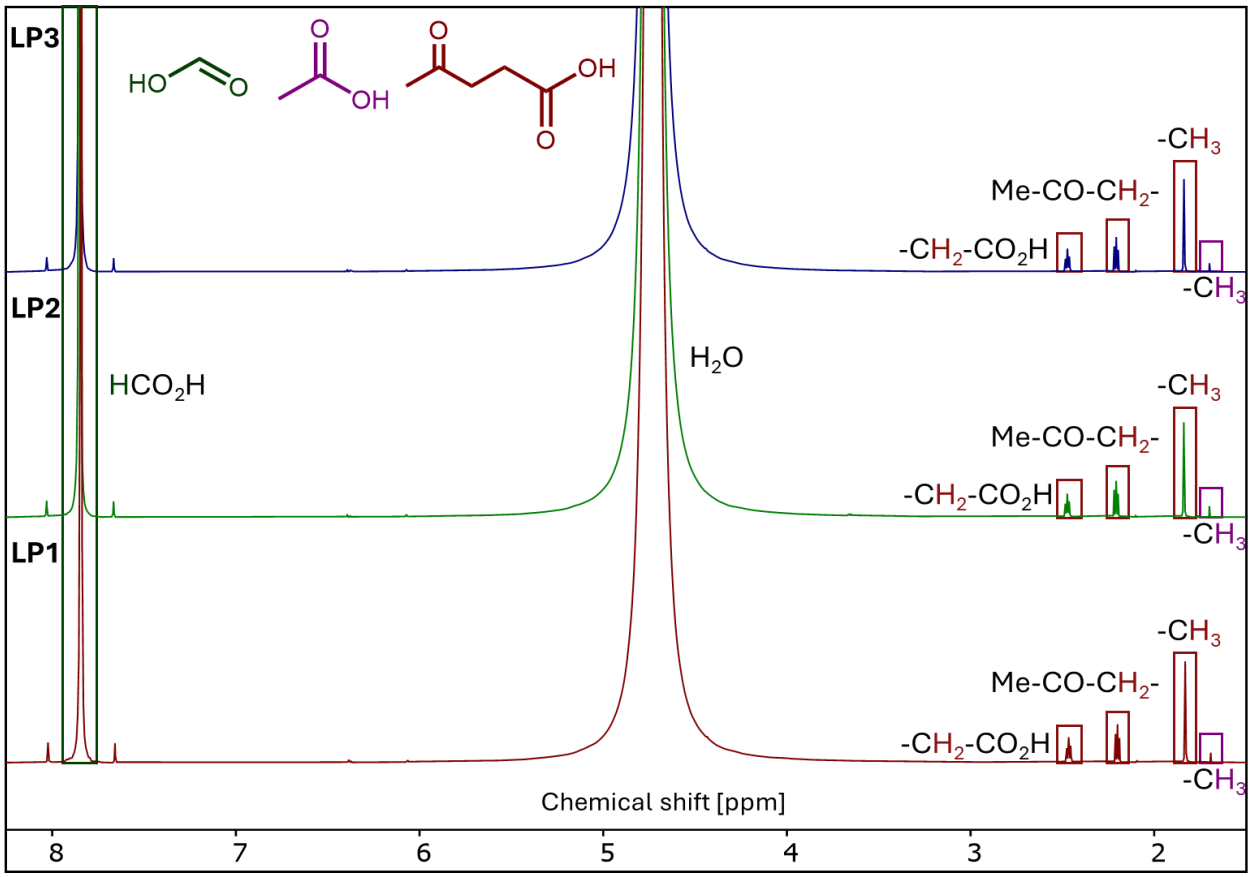

*Figure S2: [1]H-NMR (D_2O) spectra of the liquid phase of **LP1**, **LP2** and **LP3** (180°C, 0.1 mol L^{-1} fructose, pH = 1 FA, t = 4h, p=30 bar N_2).*

2. SCO of humins (CH)

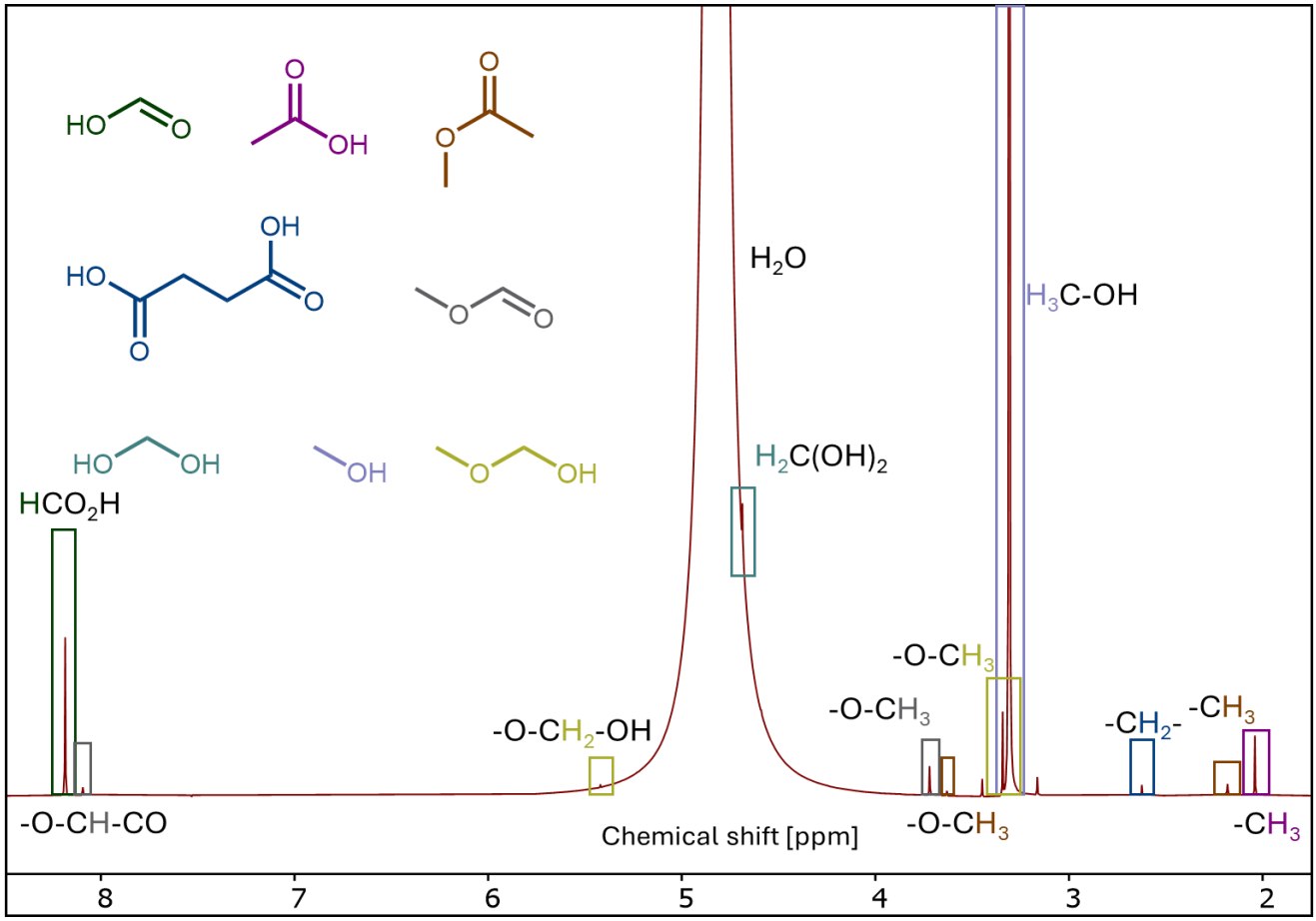

*Figure S3: ^{1}H-NMR of the liquid phase of **CH** (90 °C, 30 h, 1 wt% humin in 5% MeOH/H_2O solution, p = 30 bar O_2, 2.5 wt% HPA-2).*

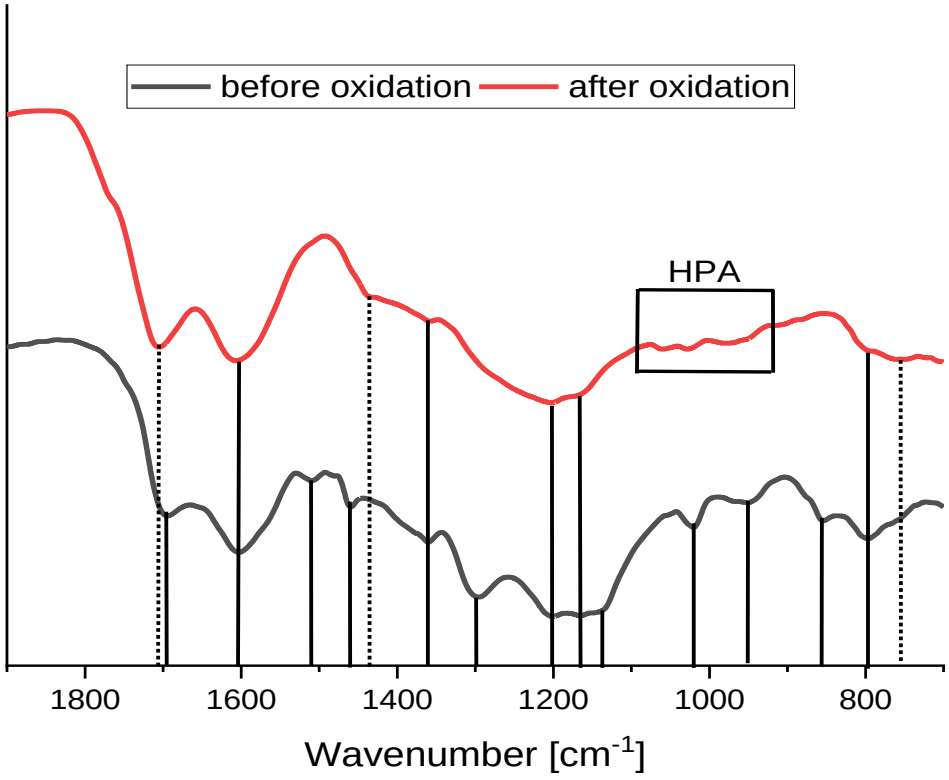

*Figure S4**:** IR-spectra of humine before and after SCO (90°C, 30h, 1 wt% humin in 150 mL 5% MeOH/H_2O solution, p = 30 bar O_2)*

*Table S2: Elemental Analysis of **H** before and after the oxidative conversion (90°C, 30h, 1 wt% Humin in 150 mL 5% MeOH/H_2O solution, p = 30 bar O_2)*

Elemental Analysis	**Before**	**After**
C (w%)	63.1	53.2
H (w%)	4.1	3.9
O (w%)	31.2	39.3
Sum (w%)	98.4	96.4

3. Nanofiltration and distillation

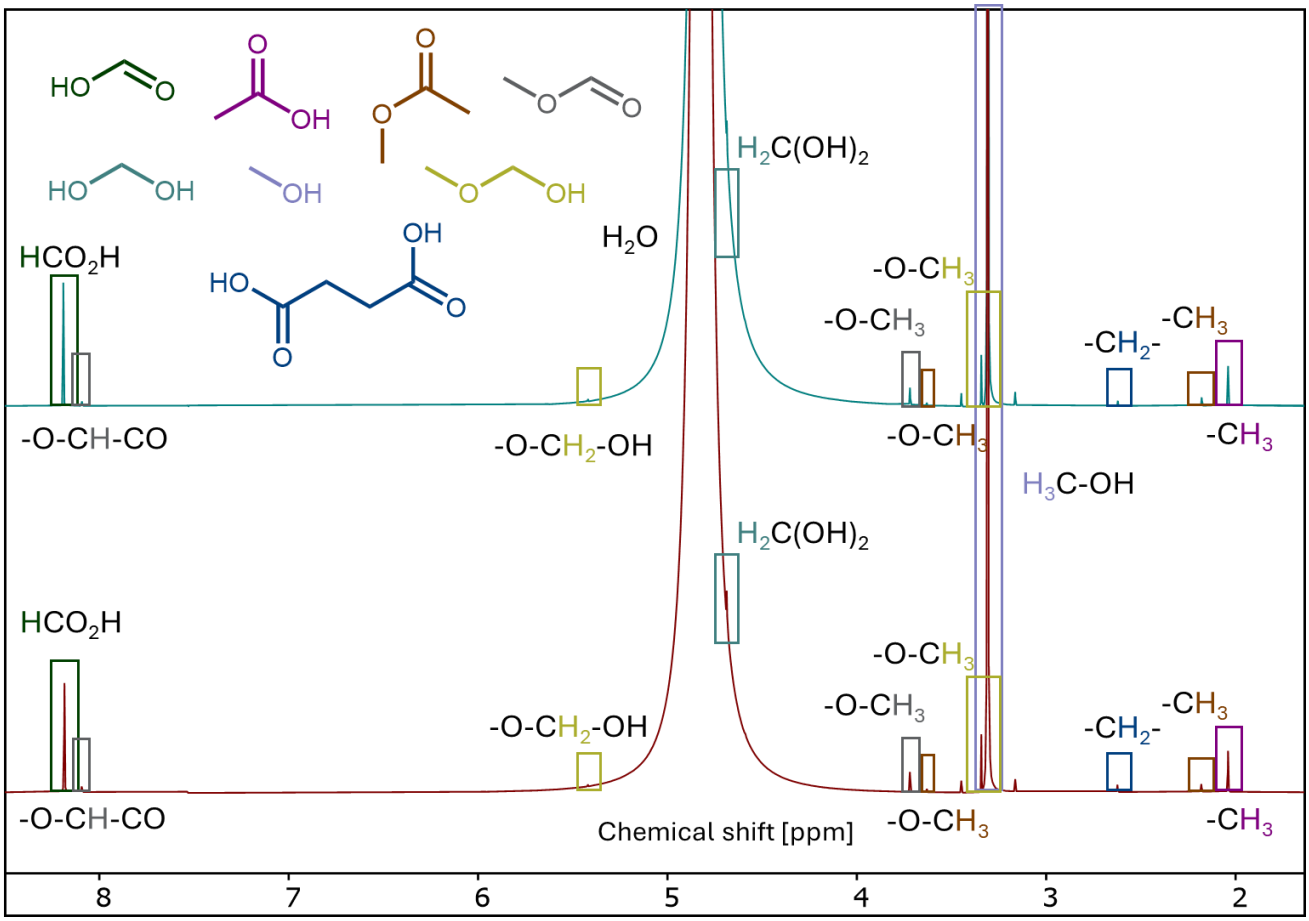

Figure S5: ^{1}H-NMR (D_2O) of the reaction solution of the SCO of humins before (bottom) and after (top) nanofiltration.

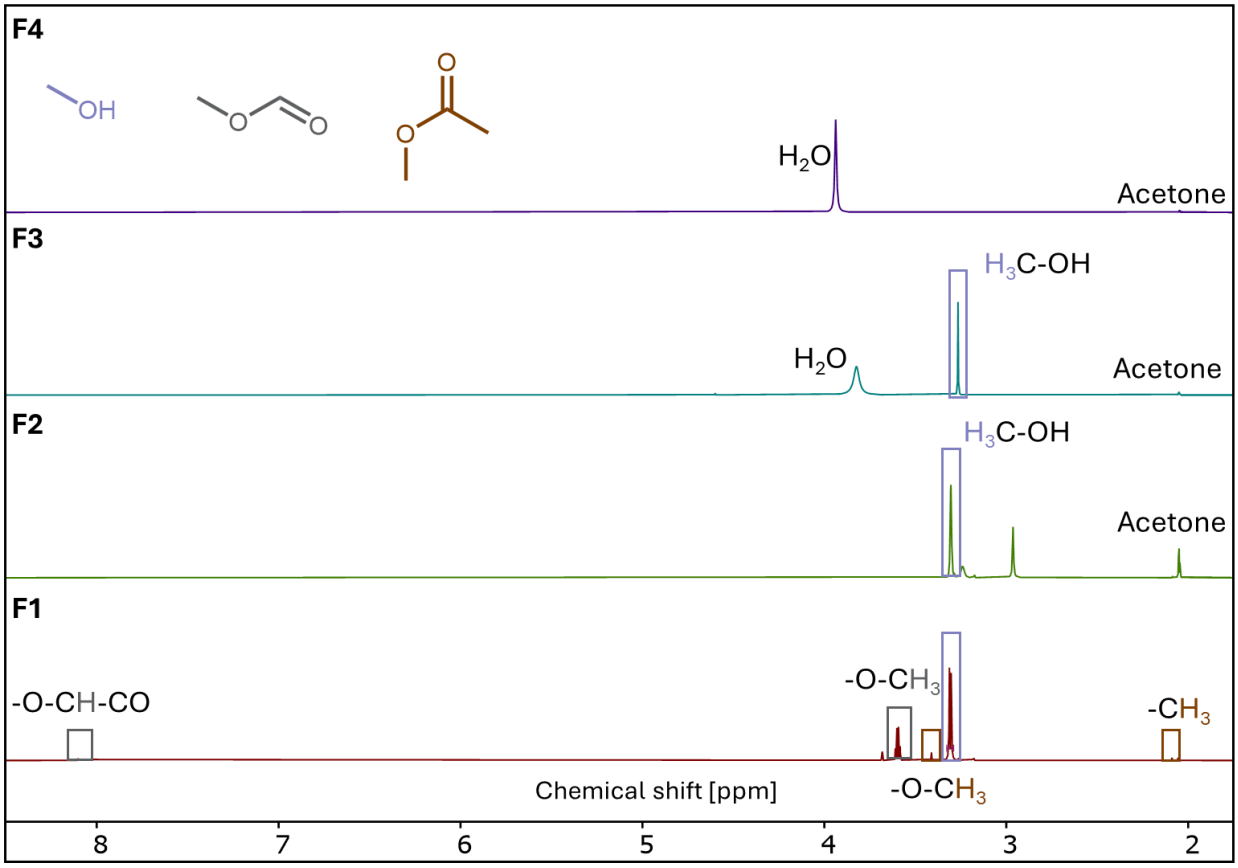

Figure S6: ^{1}H-NMR (Acetone-d_6) spectra of distillation fractions 1-4

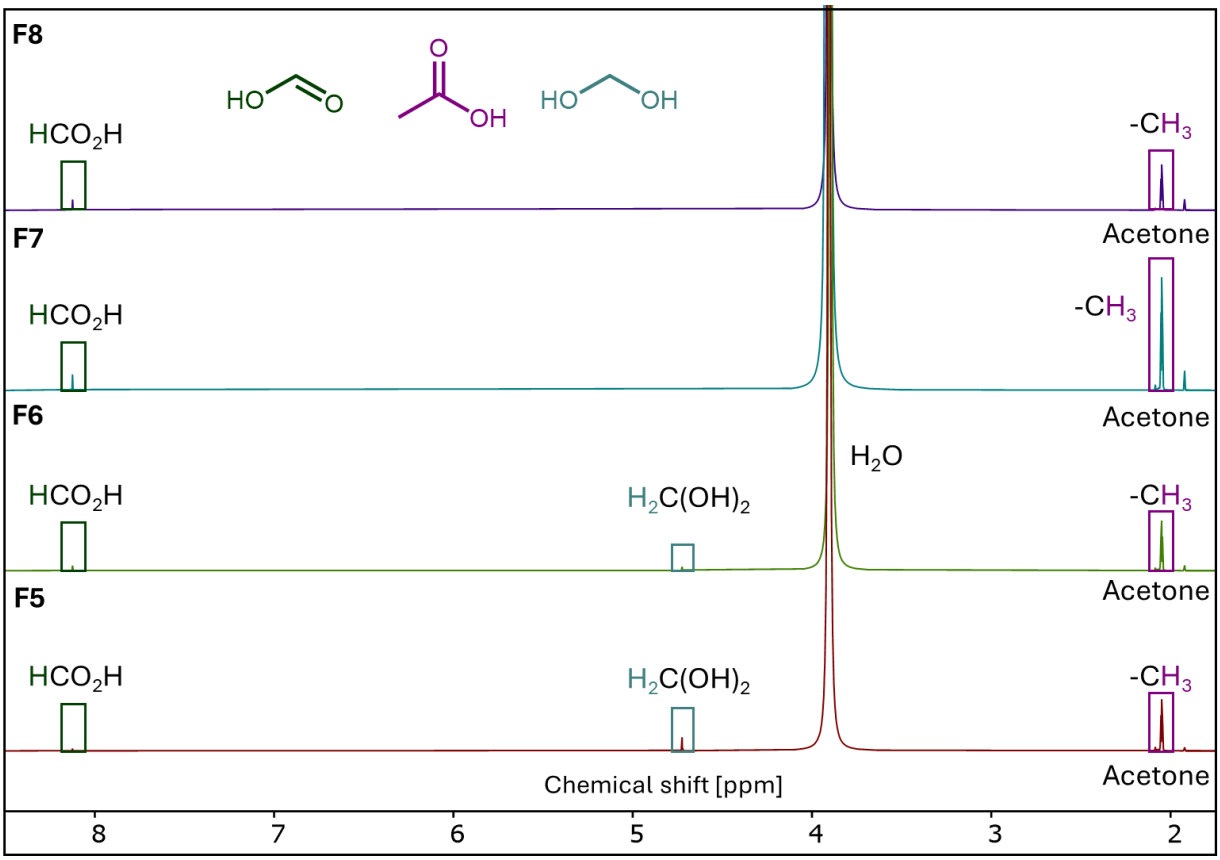

Figure S7: ^{1}H-NMR (Acetone-d_6) of distillation fractions 5-8

4. Levulinic acid production (LP) using FA as organocatalyst

Table S3: Product yields of sugar variation reactions (0.1 mol L^{-1} sugar, 7.5 mL H_2O, pH=1 (FA), 180°C, 1 hour, p = 40 bar N_2).

	Humin (w%)	**HMF (mol%)**	**LA (mol%)**	**Furfural (mol%)**
Fructose	3.70%	7.99%	37.95%	0.00%
Glucose	0.00%	8.96%	8.96%	0.00%
Xylose	0.00%	0.00%	0.00%	58.47%
Sucrose	4.48%	7.46%	22.87%	0.00%
Cellobiose	0.00%	8.45%	7.95%	0.00%

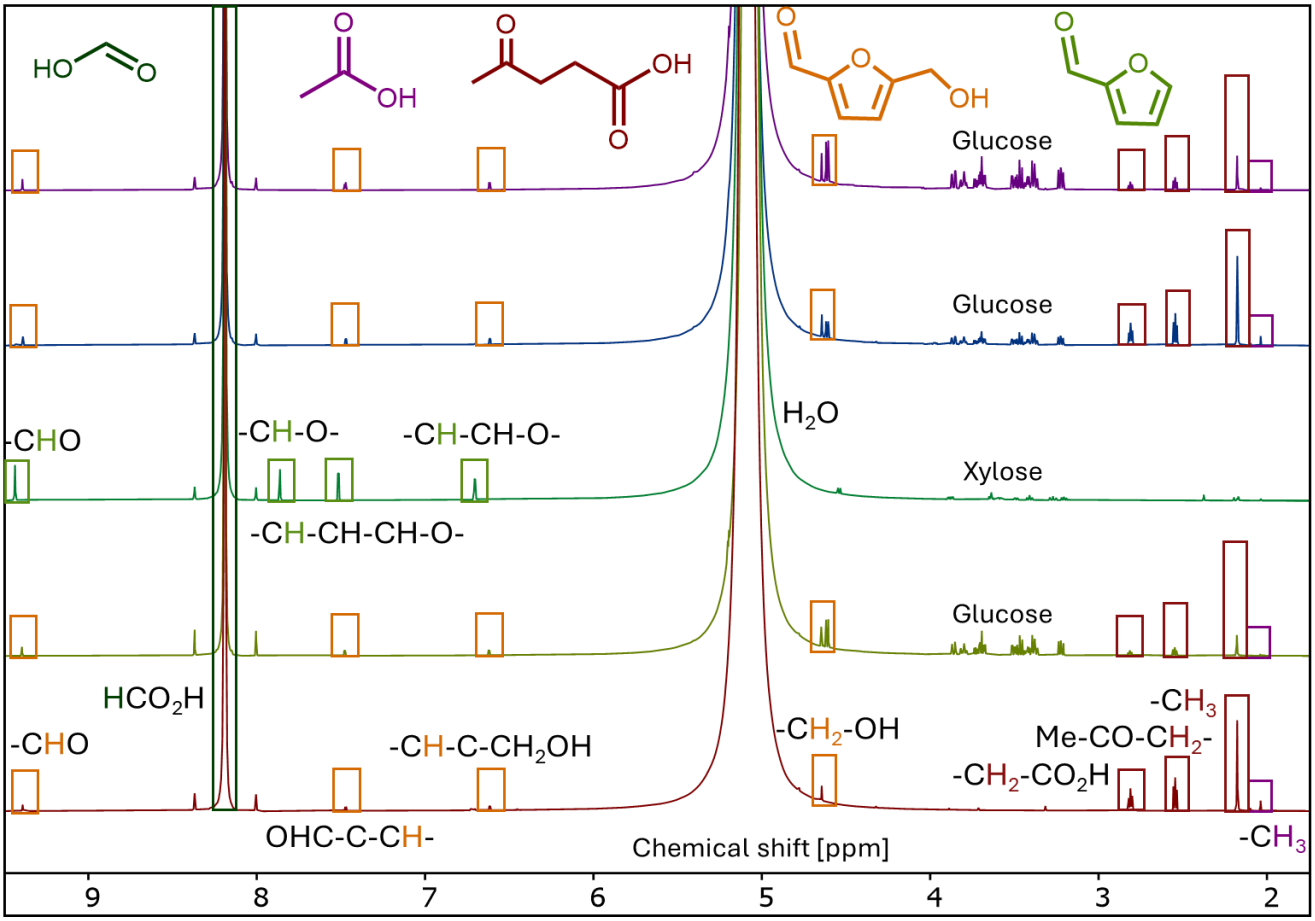

Figure S8: ^{1}H-NMR (D_2O) spectra of sugar variation reactions (from bottom to top: fructose, glucose, xylose, sucrose, cellobiose) (0.1 mol L^{-1} sugar, H_2O, pH=1 (FA), 180°C, 1 hour, p = 40 bar N_2).

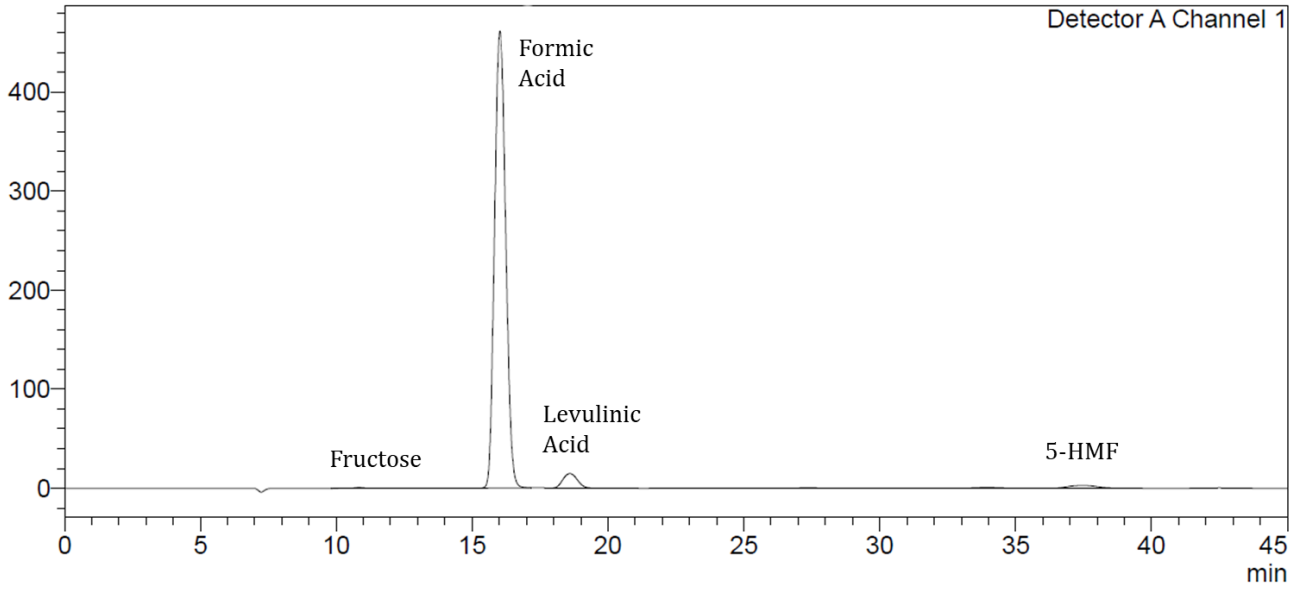

Figure S9: HPLC chromatogram of sugar variation reaction using fructose (0.1 mol L^{-1} fructose, H_2O, pH=1 (FA), 180°C, 1 hour, p = 40 bar N_2)

Table S4: Product yields of LA syntheses from fructose in the 600 mL autoclave for different reaction times (0.1 mol $^{-1}$ fructose, pH = 1 (FA); T= 180°C, p = 30 bar N_2)

Reaction time [h]	**LA yield [mol%]**	**Humin yield [wt%]**
2	31.0%	5.2%
3	41.0%	10.1%
4	42.0%	11.5%
5	40.0%	11.8%

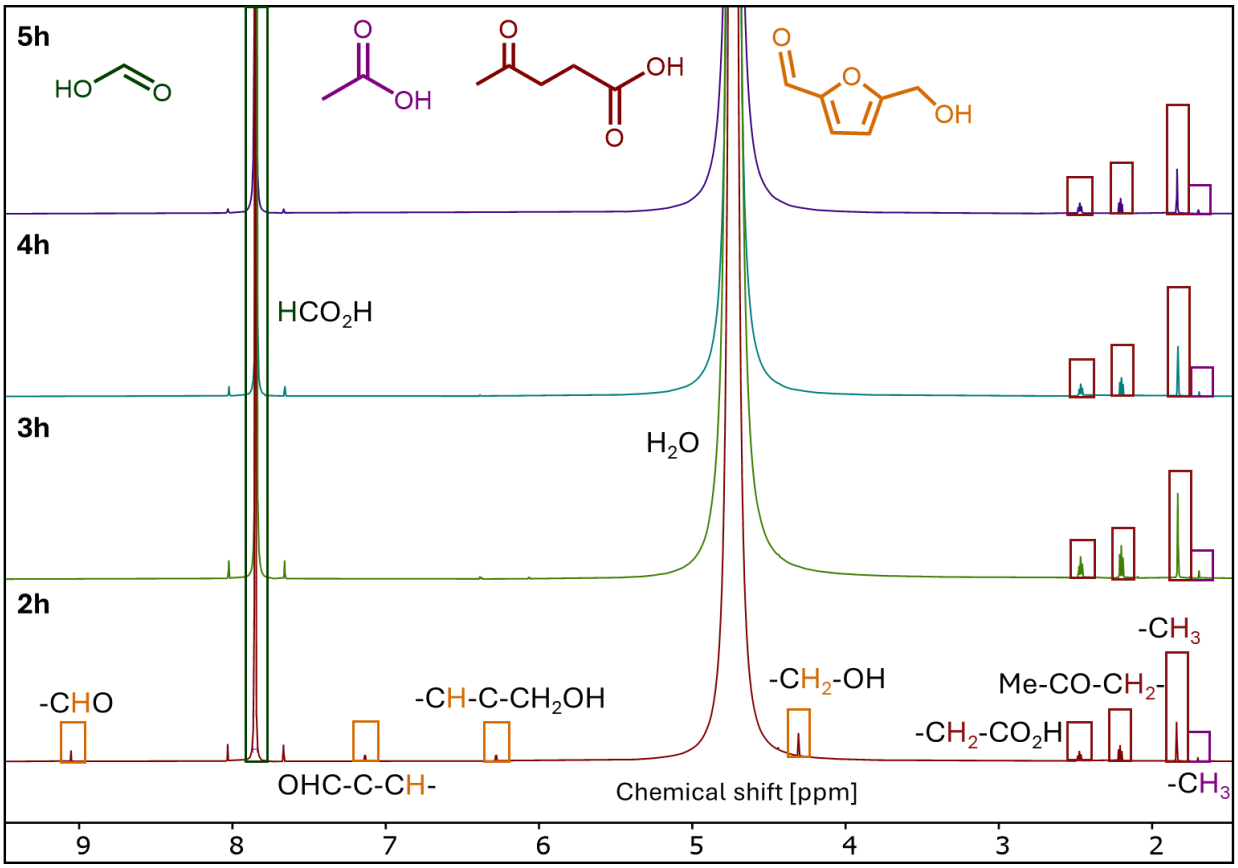

Figure S10: ^{1}H-NMR (D_2O) spectra of fructose conversions in the 600 ml autoclave with different reaction times (from bottom to top: 2,3,4 and 5 hours) (0.1 mol L^{-1} fructose, pH = 1 (FA); T= 180°C, p = 30 bar N_2)

Table S5: Elemental analyses of humins synthesized in the 600 ml autoclave with different reaction times (0.1 mol L^{-1} fructose, pH = 1 (FA); T= 180°C, p = 30 bar N_2).

Elemental Analysis	2h	3h	4h	5h
C (w%)	59.97	61.16	63.12	63.24
H (w%)	3.88	3.93	4.1	4.19
O (w%)	34.27	32.97	31.18	30.57
Sum (w%)	98.11	98.05	98.39	97.99

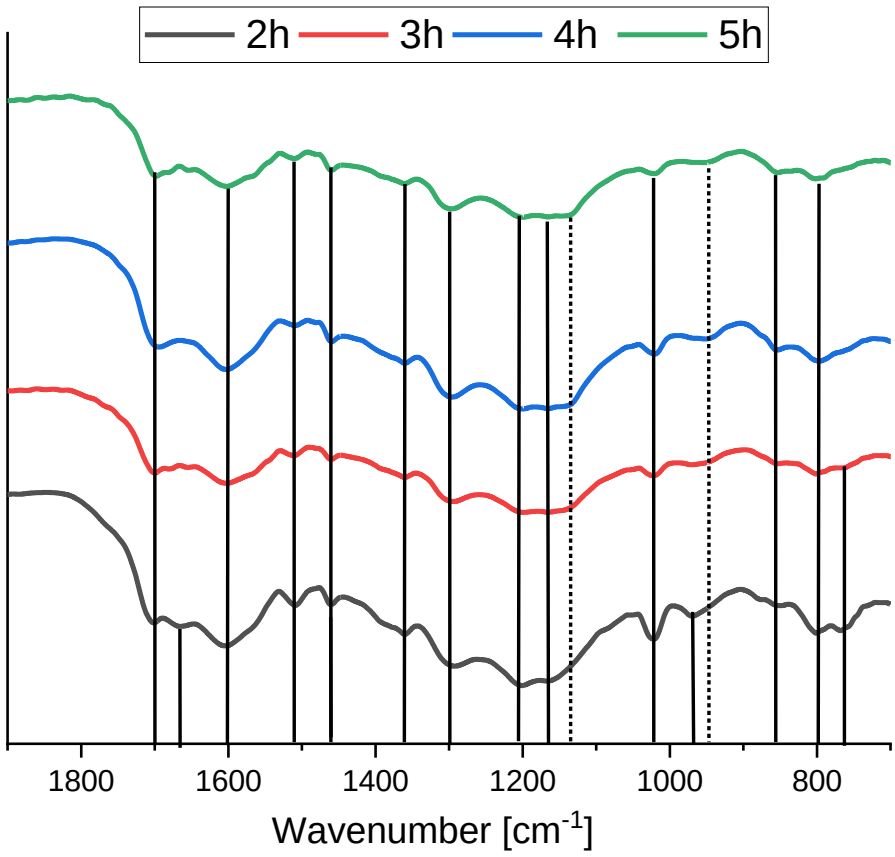

Figure S11: IR spectra of humins synthesized in the 600 ml autoclave with different reaction times (0.1 mol L^{-1} fructose, pH = 1 (FA); T= 180°C, p = 30 bar N_2).

Table S6: Vibrational band assignment of humins in included IR spectra

Wavenumber (cm^{-1})	Assignment
765+800	C-H Out of plane vibration substituted furan ring
855+880	C-H Tri-substituted alkenes
950+970	C-H vibration furan ring
1025	C-O stretch vibration
1085	C-O-C ether vibration
1135+1160+1200	C-O-C deformation vibration furan ring
1300	C-H rocking vibration
1360	C-C framework vibration (furan) C6 sugars
1395	C-C framework vibration (furan) C5 sugars
1460	C-H aliphatic chain vibration
1510	C=C vibration aromatic double bonds of poly substituted furans
1600	C=C stretch vibration conjugated with carbonyl
1670	C=O carbyonyl, aldehyde vibrations
1700	C=O stretch of acids, aldehydes and ketons

5. Cyclic Levulinic acid production (LPC)

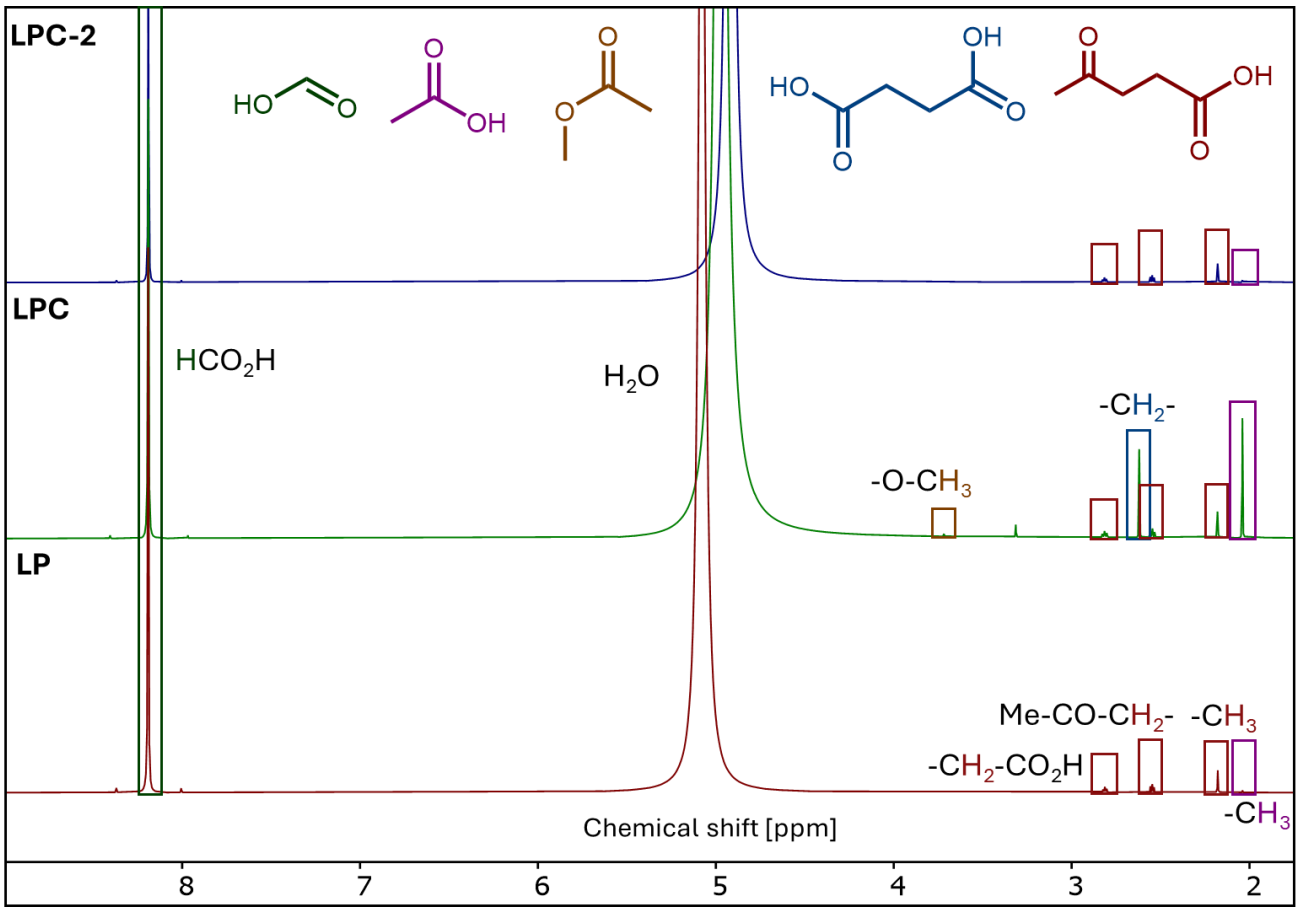

*Figure S12: ^{1}H-NMR (D_2O) comparison of **LP**, **LPC** and **LPC-2** (180°C, 0.1 mol L^{-1} fructose, pH = 1 FA, t = 4 h, p=30 bar N_2).*

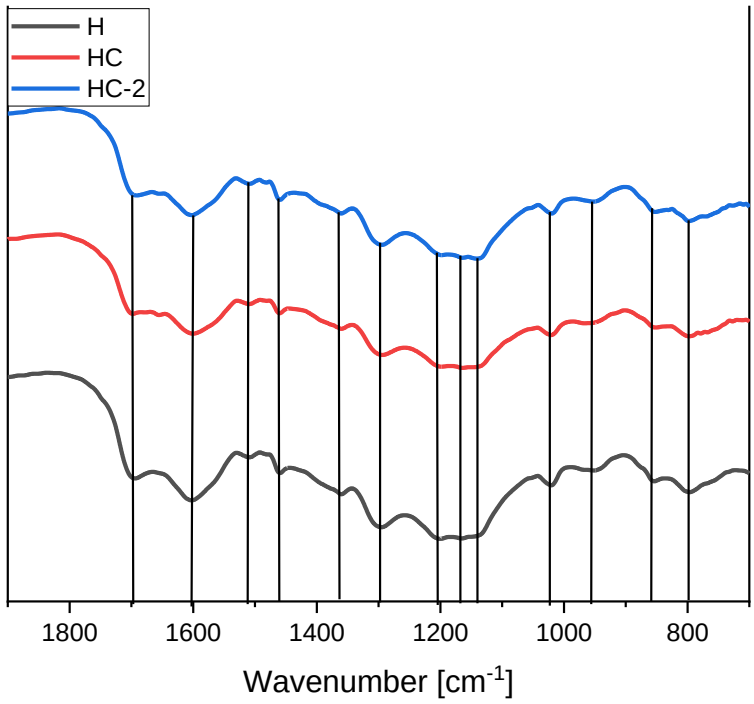

*Figure S13: Comparison of the IR spectra of the humins **H**, **HC** and **HC-2** (180°C, 0.1 mol L^{-1} fructose, pH = 1 FA, t = 4h, p=30 bar N_2).*

6. Characterization of HPA-2

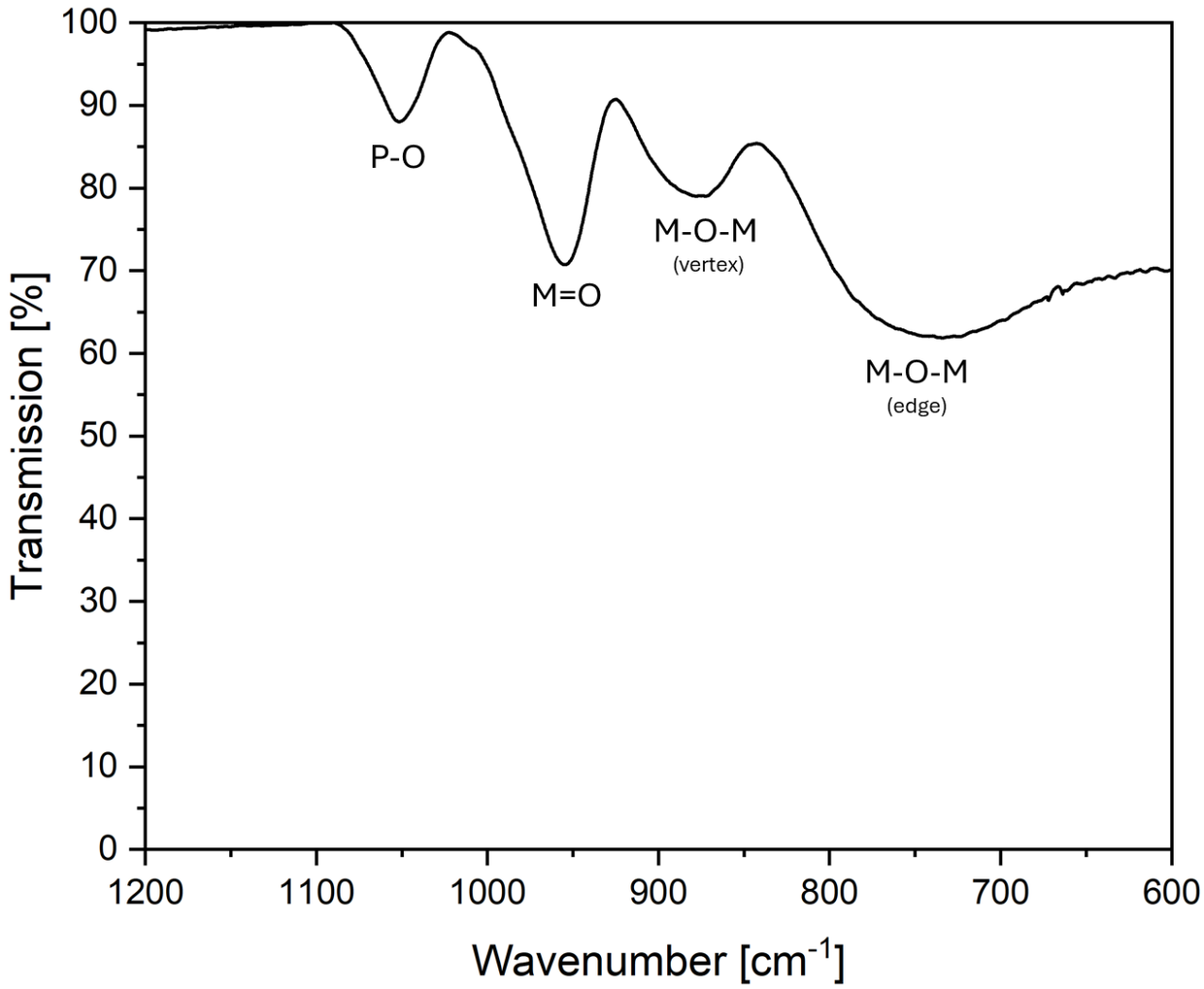

Figure S14: IR-spectrum of the fresh HPA-2 catalyst.

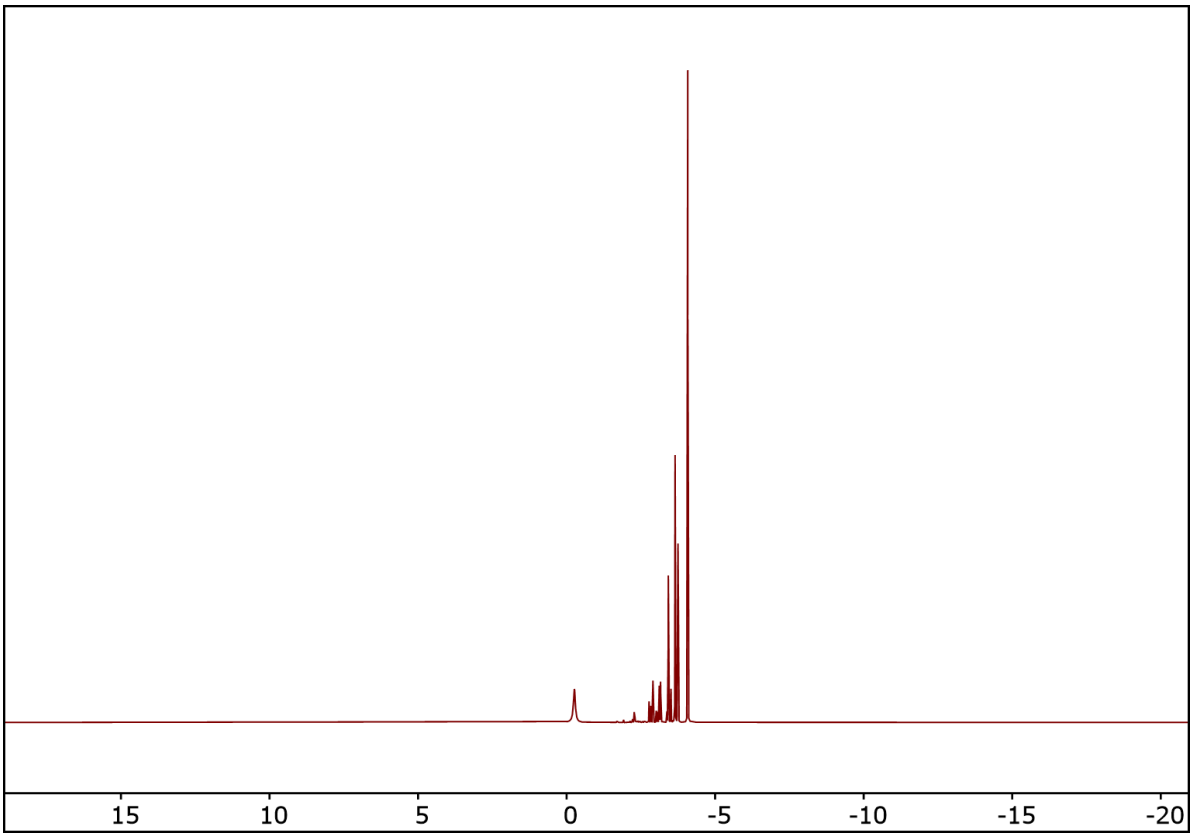

Figure S15: ^{31}P-NMR (Acetone-d_6) of the fresh HPA-2 catalyst.

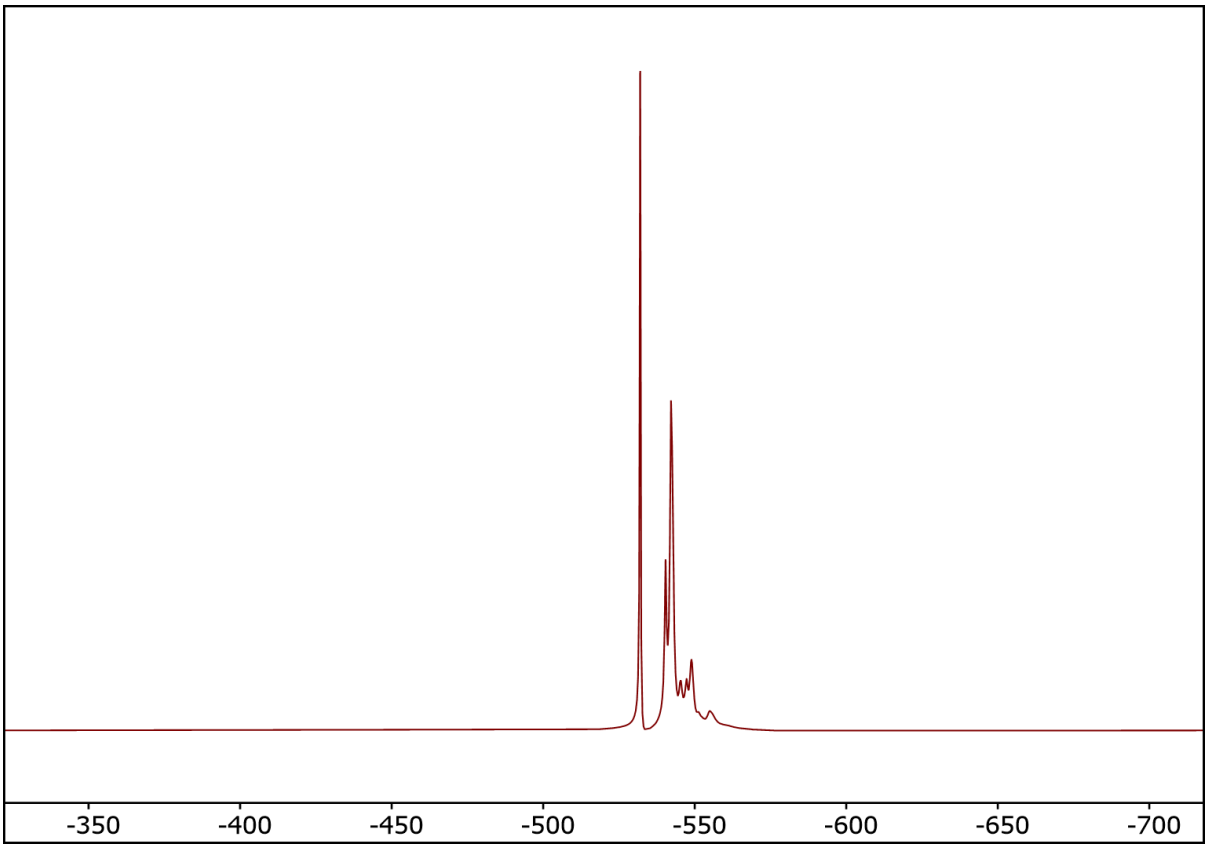

Figure S16: ^{51}V-NMR (Acetone-d_6) of the fresh HPA-2 catalyst.

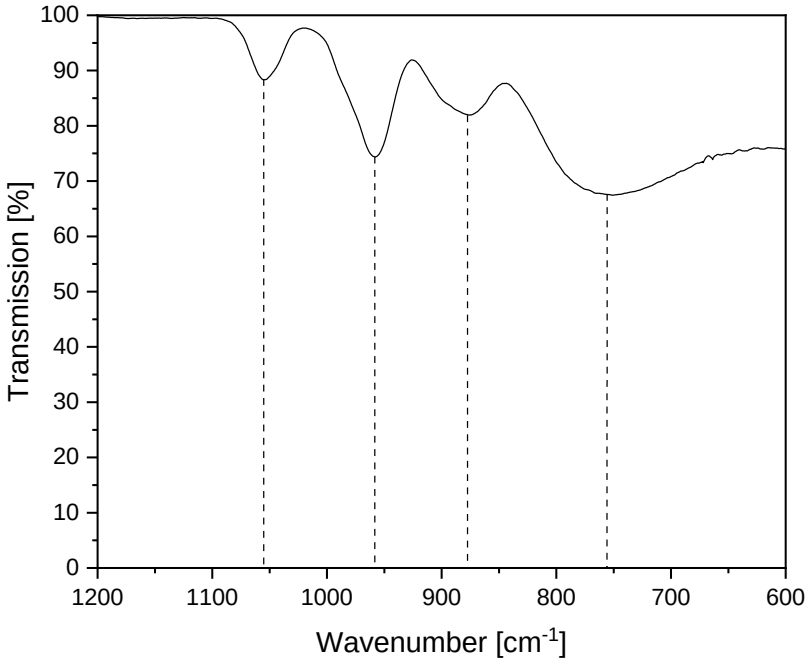

Figure S17: *FT-IR (ATR) spectrum of the used HPA-2-catalyst. Vibration modes: 1055 cm^{-1} (P-O), 958 cm^{-1} (M=O_t), 877 cm^{-1} ((M-O-M)$_{vertex}$), 756 cm^{-1} ((M-O-M)$_{edge}$).*[1]

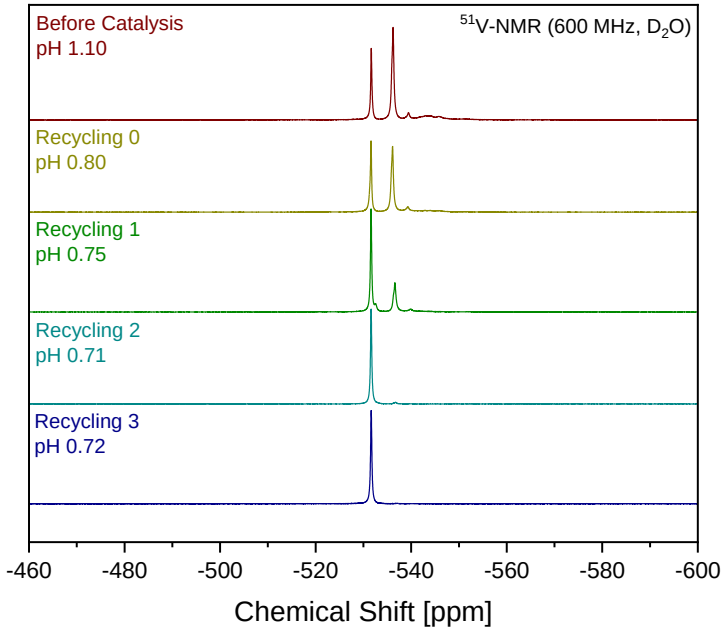

Figure S18**:** *^{51}V-NMR spectra from recycling experiments for SCO of glucose-based humin using HPA-2.*

7. Equations

Sugar conversions x_s were determined through equation S1:

$$x_s = \frac{c_{s,0} - c_s}{c_{s,0}} * 100 \quad \text{(S1)}$$

With $c_{s,0}$ being the concentration before and c_s the concentration after reaction.

The yields Pi of the products of humin conversion CH $Y_{CH,Px}$ were determined with equation S2:

$$Y_{CH,Px} = \frac{m_{Px}}{m_{Px,max}} \quad \text{(S2)}$$

With m_{Px} being the mass of the products and $m_{Px,max}$ being the maximum possible mass.

m_{Px} was determined through the multiplication of the measured density of the reaction solution with the concentration and molar mass of the reaction product. This accounted for deviations in the density through the different densities of the reaction products.

For the calculation of $m_{Px,max}$ equation S3 was used:

$$m_{Px,max} = \frac{n_{H,C}/N_{C,Px} * M_H}{m_H + m_{HPA-2} + m_{H_2O}} \quad \text{(S3)}$$

$N_{C,Px}$ here is equivalent to the number of carbons contained in the reaction product and $n_{H,C}$ is the amount of carbon contained in humin H, which was determined using equation S4:

$$n_{H,C} = \frac{C_H * m_H}{M_C} \quad \text{(S4)}$$

With C_H being the mass percentage of carbon determined by elemental analysis m_H the mass of humin H and M_C being the mass of a carbon atom.

References

[1] A. Wassenberg, T. Esser, M.J. Poller, D. Voß, J. Albert, Humin-free synthesis of levulinic acid from fructose by using heteropolyacid catalysts, Biofuels, Bioproducts and Biorefining 18 (2024). https://doi.org/10.1002/bbb.2654.

Danksagung

Diese Arbeit wurde zwischen Oktober 2020 und September 2023 am Institut der Technischen und Makromolekularen Chemie der Universität Hamburg angefertigt. Ich bedanke mich hiermit schonmal vorab bei allen, die bei der Entstehung dieser Arbeit beteiligt waren.

Zuerst möchte ich mich vor allem bei meinem Doktorvater Prof. Dr.-Ing. Jakob Albert für die Bereitstellung eines interessanten Forschungsthemas und die vielen fachlichen Diskussion bedanken. Ich bedanke mich dabei besonders für die Freiheit, die mir und meinem Projektpartner Tobias Esser bei unserer Forschung am Projekt „DFG Humine“ gelassen wurde und für die Unterstützung bei der Publikation der Ergebnisse dieser Forschung in renommierten Journalen. Die Teilnahme an der „Europa Cat 2023“ Konferenz kurz vor Ende meiner Tätigkeit war ein schöner Abschluss für meine Zeit im AK Albert.

Ich möchte hierbei auch Prof. Dr. Wolfgang Maison herzlichst für die Übernahme des Zweitgutachtens danken, sowie auch der Prüfungskommission bestehend aus Prof. Dr.-Ing. Jakob Albert, Prof Dr. Lisa Vondung als auch Dr. Hackl für die Übernahme der Disputation.

Ich danke auch den wissenschaftlichen Serviceeinrichtungen der Universität Hamburg, besonders dabei der Zentralen Elementanalytik, der NMR-Abteilung, der Elektronenmikroskopie und der Massenspektrometrie, ohne deren Messungen meiner unzähligen Proben meine Promotion nicht möglich gewesen wäre. Mein Dank gilt auch dem Stammpersonal am Institut der TMC, wobei ich mich besonders bei Michael Gröger bedanken, der immer mit Rat und Tat zur Verfügung stand, wenn ich seine Hilfe brauchte.

Des Weiteren möchte ich mich auch herzlichst bei Dr.-Ing Dorothea Voß und Dr. Max Poller bedanken. Doro hatte mit ihrer fürsorglichen Art immer ein offenes Ohr für mich, wenn ich mal nicht weiterwusste, oder generell irgendwelche Fragen hatte. Sie hat mir dabei vor allem geholfen eine technischere Herangehensweise an die wissenschaftlichen Fragestellungen meiner Promotion zu entwickeln. Besonders haben mir auch unsere gemeinsamen Autofahrten in unsere gemeinsame Heimat Neuss gefallen; ich erwische mich immer noch dabei, wie ich beim Fahren über Autobahnen nach Rehen Ausschau halte. Max hat für mich die Rolle, die Doro für mich in den technischen Aspekten meiner Promotion gespielt hat, in den chemischen Aspekten übernommen. Ich kann mich noch gut daran erinnern, wie wir das ein oder andere Mal noch bis spät abends über meine Forschung diskutiert haben und kann mit felsenfester Überzeugung behaupten, dass ohne seinen Input meine Promotion nicht ansatzweise so reibungslos funktioniert hätte. Auch außerhalb der Uni haben wir uns das ein oder andere Mal zum Schwimmen getroffen, wo er mich zu persönlichen Bestleistungen anspornte. Ich danke euch beiden vielmals für eure Unterstützung.

Generell würde ich mich gerne bei allen Kollegen im AK Albert für die schöne Zeit im Labor und außerhalb der Uni bedanken. Ihr habt die drei Jahre meiner Promotion zu einer der besten Perioden meines Lebens gemacht und dafür bin ich euch sehr dankbar. Ich hoffe ich konnte in meiner Tätigkeit als Vergnügungsbeauftragter etwas von dieser Dankbarkeit zeigen. Mein besonderer Dank gilt hier meinen Bürokollegen aus D29: Tobias Esser, Michael Huber und Anne Lichtinger. Tobi war mein Partner im Projekt DFG Humine und ich hätte mir keinen besseren Projektpartner wünschen können. Seine guten Ideen und Erfahrung in technischer Chemie waren unabdingbar für den Erfolg, den wir schlussendlich mit unserem Projekt hatten. Mit seiner disziplinierten und zielorientierten Arbeitsweise war er mir auch ein sehr gutes Vorbild und hat mich dazu motiviert, mich richtig in meine Arbeit reinzuhängen. Aber auch außerhalb der Arbeit haben wir sehr viel Kontakt gepflegt: Tobi, Hubsi

und ich haben waren praktisch von Tag eins an, aufgrund einer gemeinsamen Vorliebe von One Piece und Videospielen unzertrennlich und sind alle seitdem gute Freunde. Hubsi war im Büro ein gewisser Gegenpol gegenüber Tobis zeitweiliger Arbeitswut und sorgte bei uns oft für den notwendigen Freizeitausgleich, womit er auch Tobi das ein oder andere Mal aus der Versenkung holen konnte, wenn dieser zu sehr auf seine Arbeit fokussiert war. Seine lustige lockere bayrische Art hat ihn sehr beliebt im Arbeitskreis gemacht und nachdem er mit seiner Promotion ein Jahr vor uns fertig war, hat einfach etwas im Arbeitskreis gefehlt. Als IT-Beauftragter konnte er uns auch unzählige Male behilflich sein, wenn die Universitätscomputer mal wieder nicht so wollten wie wir es gerne gehabt hätten. Anne Lichtinger war nur sehr kurze Zeit bei uns im Büro, hat sich jedoch in unsere kleine Dreiergruppe nahtlos eingefügt. Unsere One Piece Diskussionen in den Mittagspausen haben sie dabei nicht abgeschreckt, ganz im Gegenteil, sie hat ein reges Interesse an der Materie entwickelt und sich eingebracht, sodass wir heute, drei Jahre später, immer noch in Kontakt stehen und befreundet sind. Aber auch außerhalb meines Büros möchte ich noch ein paar Kollegen danken: Steffanie Wesinger und Jan-Dominik Krüger möchte ich als HPLC-Verantwortlichen danken, dass sie, trotz meiner etwas problematischen Proben, immer zur Verfügung standen, wenn irgendwas nicht stimmte oder Fragen aufkamen. Steffi möchte ich außerdem für die vielen Abende danken, an denen wir in der Stadt feiern waren. Mein Dank gilt außerdem Anne Wesner, die, obgleich ihres Musikgeschmacks, eine hervorragende Laborkollegin war, mit der es nie langweilig wurde. Außerhalb der Arbeit habe ich auch ihre DnD Sessions genossen, auch wenn wir leider viel zu selten zu welchen gekommen sind.

An dieser Stelle möchte ich mich auch nochmal bei Doro, Max, Anne W., Zeljko und meinem kleinen Bruder Tobi für das Korrekturlesen dieser Arbeit, ohne eure Hilfe würde diese sich deutlich schlechter lesen.

Zu guter Letzt gilt mein besonderer Dank natürlich meinen Freunden und meiner Familie in Neuss. Obwohl ich 400 km weit weg gewohnt habe, hatte dies keinen Einfluss auf meine Freundschaften, sodass es sich jedes Mal, wenn ich nach NRW gefahren bin, angefühlt hat, als sei ich nie weggewesen. Mein größtes Dankeschön geht jedoch an meine Familie: Mein etwas zu groß gewachsener, kleiner Bruder Tobias, der gerade auch mitten in seiner Promotion an der HHU in Düsseldorf steckt. Die Möglichkeit jederzeit jemanden auf Abruf zu haben, der eine externe Perspektive auf meine Forschung geben kann war mir eine große Hilfe. Aber auch generell bin ich sehr dankbar ihn zu haben; es ist keine Selbstverständlichkeit, dass Geschwister sich so viele Hobbies teilen, sich so nahestehen und füreinander da sind, auch wenn ich ihn mit meiner Vergesslichkeit manchmal zur Weißglut treibe. Meine Eltern Wolfgang und Bettina, die immer hinter mir standen, auch in den schwierigsten Zeiten. Ich wüsste nicht, wo ich wäre, wenn sie mir nicht die Möglichkeiten zur Selbstverwirklichung und ihre, im Falle meiner Mutter, stille oder, im Falle meines Vaters, lautstarke Unterstützung gegeben hätten. Worte können nicht beschreiben, wie dankbar ich euch dreien bin. Vielen Dank!

Eidesstattliche Versicherung

„Hiermit versichere ich an Eides statt, die vorliegende Dissertationsschrift selbst verfasst und keine anderen als die angegebenen Hilfsmittel und Quellen benutzt zu haben. Sofern im Zuge der Erstellung der vorliegenden Dissertationsschrift generative Künstliche Intelligenz (gKI) basierte elektronische Hilfsmittel verwendet wurden, versichere ich, dass meine eigene Leistung im Vordergrund stand und dass eine vollständige Dokumentation aller verwendeten Hilfsmittel gemäß der Guten wissenschaftlichen Praxis vorliegt. Ich trage die Verantwortung für eventuell durch die gKI generierte fehlerhafte oder verzerrte Inhalte, fehlerhafte Referenzen, Verstöße gegen das Datenschutz- und Urheberrecht oder Plagiate."

André Wassenberg, 08.04.2025

Declaration of oath

"I hereby declare and affirm that this doctoral dissertation is my own work and that I have not used any aids and sources other than those indicated. If electronic resources based on generative artificial intelligence (gAI) were used in the course of writing this dissertation, I confirm that my own work was the main and value-adding contribution, and that complete documentation of all resources used is available in accordance with good scientific practice. I am responsible for any erroneous or distorted content, incorrect references, violations of data protection and copyright law or plagiarism that may have been generated by the gAI."

André Wassenberg, 08.04.2025